



Swansea University
Prifysgol Abertawe



Swansea University E-Theses

Soil water repellency: Comparison between individual particles and bulk properties.

Bayer, Julia

How to cite:

Bayer, Julia (2009) *Soil water repellency: Comparison between individual particles and bulk properties..* thesis, Swansea University.

<http://cronfa.swan.ac.uk/Record/cronfa42689>

Use policy:

This item is brought to you by Swansea University. Any person downloading material is agreeing to abide by the terms of the repository licence: copies of full text items may be used or reproduced in any format or medium, without prior permission for personal research or study, educational or non-commercial purposes only. The copyright for any work remains with the original author unless otherwise specified. The full-text must not be sold in any format or medium without the formal permission of the copyright holder. Permission for multiple reproductions should be obtained from the original author.

Authors are personally responsible for adhering to copyright and publisher restrictions when uploading content to the repository.

Please link to the metadata record in the Swansea University repository, Cronfa (link given in the citation reference above.)

<http://www.swansea.ac.uk/library/researchsupport/ris-support/>



**Swansea University
Prifysgol Abertawe**

**Soil water repellency:
Comparison between individual particles
and bulk properties**

Julia Bayer

2009

**Submitted to the University of Wales in fulfilment of the
requirements for the Degree of Doctor of Philosophy**

ProQuest Number: 10807458

All rights reserved

INFORMATION TO ALL USERS

The quality of this reproduction is dependent upon the quality of the copy submitted.

In the unlikely event that the author did not send a complete manuscript and there are missing pages, these will be noted. Also, if material had to be removed, a note will indicate the deletion.



ProQuest 10807458

Published by ProQuest LLC (2018). Copyright of the Dissertation is held by the Author.

All rights reserved.

This work is protected against unauthorized copying under Title 17, United States Code
Microform Edition © ProQuest LLC.

ProQuest LLC.
789 East Eisenhower Parkway
P.O. Box 1346
Ann Arbor, MI 48106 – 1346



Abstract

Two different methods for probing soil particle surfaces were tested and applied to particles from natural soils to examine soil water repellency arising from organic coatings on their surfaces.

The applicability of laser scanning confocal microscopy to the characterisation of organic soil particle surface coatings was examined. Individual particle fluorescence showed a correlation with organic matter present in the corresponding soil, although not all organic material in soil fluoresces. This indicates that fluorescence could be used to probe soil particle surfaces. Other parameters such as the extent of coverage with fluorescent material, number of fluorescent areas and their size gave no consistent results, but seemed to be strongly dependent on sample origin and possibly factors such as the surface roughness of the particles.

Another new method for investigating soil particle surfaces involved measurement of the height of a water lamella pulled up by an individual particle. Good agreement was found between lamella height and the contact angle of bulk soil materials of various but known water repellencies. Soil samples generally contained particles with a wide distribution of individual water repellencies. However, particles from water repellent soils showed more variation in lamella height than those from wettable soils, indicating a non-uniform distribution of hydrophobic surfaces within soil.

The influence of pH on soil water repellency was examined by changing soil pH using gases rather than liquid reagents. Addition of base led to a decrease in water repellency confirming observations that soils of high pH are seldom water repellent.

Using these methods it was not possible to unravel all the characteristics and effects of organic particle coatings on soil water repellency. However, the results indicate that these coatings, and their chemistry, may not be the only factor involved. Physical properties, such as surface roughness, may interact with the chemistry.

Declaration

This work has not previously been accepted in substance for any degree and is not being concurrently submitted in candidature for any degree.

Signed (candidate): _____

Date: 12/03/2010

Statement 1

This thesis is the result of my own investigations, except where otherwise stated. Other sources are acknowledged by the use of explicit references. A list of references is included.

Signed (candidate): _____

Date: 12/03/2010

Statement 2

I hereby give consent for my thesis, if accepted, to be available for photocopying and for inter-library loan, and for the title and summary to be made available to outside organisations.

Signed (candidate): _____

Date: 12/03/2010

Acknowledgements

There are so many people I would like to thank for the great time I had in Swansea and all the things I learned and achieved. First my thanks go to Rob and Stefan for being such good supervisors. They always had good advice in situations I needed it most and helped me with ideas pointing me in the right direction. Discussions with both of them were always helpful especially during lunch time having coffees together. It was a pleasure to work with them.

I want to thank my colleagues Shuying and Emilia who always had time for discussing problems and ideas. And I owe a special thanks to Shuying for her help with the AFM measurements. We had a great time going to conferences together and having lunch breaks. It was just fun to work with both of them. The dinners they organised once in a while were just fantastic.

I also owe a very big thank you to Sally from the Medical School for all her help with the laser scanning confocal microscope. Without her advice I could not have done a large part of this work. I thank Phil, in Geography, for his help with TOC analysis and the technical staff in the School of Engineering for their help fabricating the various bits and pieces I needed.

I also need to thank the working group of Prof. Schaumann who gave me the opportunity to use some of their equipment. Working with them, especially Dörte, was very productive and led to a joint publication.

A special thanks to all my Swansea friends in and outside University for all the lunch and coffee breaks we shared, the Frisbee playing, the walks and weekend trips, the salsa dancing evenings and all the other special things we did together. Without all these wonderful people my time in Swansea would have never been as fantastic as it was.

I also want to thank my parents who supported me all the time with advice and encouragement and when needed financial support. My thanks goes to my boyfriend Sebastian who was there for me at all times, who flew countless times back and forth between Berlin and Swansea, who spent so much time fixing my Mini. Thanks for his love and support.

And last, but not least I want to thank the **School of Engineering** for the financial support, without it I could not have carried out this work.

Table of contents

CHAPTER 1: INTRODUCTION AND LITERATURE REVIEW	1
1.1 Soils and their role in the environment.....	2
1.2 Soil water repellency.....	3
1.2.1 Definition	3
1.2.2 Occurrence	3
1.2.3 Consequences of soil water repellency	4
1.3 The principle of wetting.....	7
1.4 Measuring soil water repellency	12
1.4.1 Contact angle.....	12
1.4.1.1 Wilhelmy plate method	13
1.4.1.2 Capillary rise and Washburn method.....	14
1.4.1.3 Sessile drop contact angle measurement	16
1.4.2 Molarity of ethanol droplet (MED) test	17
1.4.3 Water drop penetration time (WDPT) test	17
1.5 Influences on soil water repellency.....	19
1.5.1 Temporal and spatial variability.....	19
1.5.2 Influences of soil chemistry	20
1.5.3 Influences of soil physics	26
1.5.4 Influences of soil pH	27
1.5.5 Influences of soil water content	29
1.5.6 Influences of soil biology.....	31
1.5.7 Fire-induced water repellency.....	32
1.6 Remediation strategies.....	33
1.7 Identifying research gaps	35
1.8 Research aims and strategy.....	36
CHAPTER 2: MATERIALS AND METHODS.....	39
2.1 Soil samples	40
2.2 Materials.....	43
2.3 Water repellency measurements.....	44
2.3.1 Water drop penetration time (WDPT) test	44
2.3.2 Contact angle measurement with a sessile drop.....	45
2.4 Soil characteristics	48
2.4.1 pH measurement	48
2.4.2 Total organic carbon (TOC) content	49
2.4.3 Particle size analysis	50
2.4.4 Roughness determination	50
2.4.5 Extraction of organic material using Soxhlet extraction	52
2.4.6 Re-application of extracted material	54
2.4.7 Treatment with acid or base	54
2.4.8 Statistical analysis	55

CHAPTER 3: LASER SCANNING FLUORESCENCE MICROSCOPY (LSCM) ON NATURAL SOIL PARTICLES: METHOD TESTING AND APPLICATION	56
3.1 Introduction.....	57
3.2 Materials and methods	63
3.2.1 Samples and sample preparation.....	63
3.2.2 General LSCM settings.....	64
3.2.3 Emission wavelength distribution	69
3.2.4 Fluorescence coverage	70
3.2.5 Number of fluorescent areas	71
3.2.6 Size of fluorescent areas.....	72
3.2.7 Fluorophore application to soil particles.....	72
3.3 Results from testing LSCM for soil particle investigations.....	75
3.3.1 Removal of organic matter.....	78
3.3.2 Laser and fluorescence stability	79
3.3.3 Image repeatability and reproducibility	81
3.3.4 Emission wavelength distribution	84
3.3.5 Fluorophore application	88
3.4 Discussion of method testing.....	91
3.5 Conclusions of method testing	94
3.6 Application of LSCM to investigations of soil particles: results and discussion	95
3.6.1 Comparison of lasers.....	95
3.6.2 Total fluorescence intensity	96
3.6.2.1 Untreated natural soils.....	96
3.6.2.2 Extracted and cleaned soil samples	105
3.6.3 Distribution of fluorescence	108
3.6.4 Number of fluorescent areas	112
3.6.5 Size of fluorescent areas.....	119
3.6.6 Fluorescence and bulk soil parameters.....	121
3.6.7 Fluorescence spectra	124
3.7 Synthesis	128
3.8 Conclusions.....	132
CHAPTER 4: MEASURING PARTICLE WATER REPELLENCY: DEVELOPMENT OF A "MICRO WILHELMY PLATE METHOD".....	133
4.1 Introduction.....	134
4.2 Materials and methods	136
4.2.1 Samples	136
4.2.2 Bulk contact angle measurement.....	137
4.2.3 Estimation of the proportion of water repellent particles per sample.....	138
4.3 Particle wettability determination using the optical micro Wilhelmy plate method (o- mWPM).....	138
4.3.1 Method	138
4.3.2 Results from o-mWPM	141
4.3.2.1 Lamella height measurements	141
4.3.2.2 Calculation of potential energies	144
4.3.2.3 Reproducibility of measurements	148

4.4	Particle wettability determination using the gravimetric micro Wilhelmy plate method (g-mWPM).....	149
4.4.1	Method	149
4.4.2	Results of the g-mWPM.....	153
4.5	Discussion and comparison of o-mWPM and g-mWPM	154
4.6	Application of the o-mWPM to soil particles	157
4.6.1	Results.....	157
4.6.1.1	Lamella height measurement of natural soil particles	157
4.6.1.2	Comparison of particles before and after coating with a hydrophobic agent.....	159
4.7	Relative amount of hydrophobic and hydrophilic particles per bulk sample.....	161
4.8	Discussion	162
4.9	Conclusions.....	165
CHAPTER 5: EFFECTS OF ARTIFICIALLY INDUCED CHANGES IN PH ON SOIL WATER REPELLENCY		167
5.1	Introduction.....	168
5.2	Methods	169
5.2.1	pH increase.....	170
5.2.2	pH decrease	171
5.3	Results.....	173
5.3.1	pH reaction to acid and base	173
5.3.2	Changes in wettability.....	176
5.3.3	Re-evaluation after three months	179
5.4	Discussion	181
5.5	Conclusions.....	186
CHAPTER 6: ATOMIC FORCE MICROSCOPY (AFM) INVESTIGATIONS OF PH ADJUSTED SOIL PARTICLES		188
6.1	Introduction.....	189
6.2	Method.....	194
6.3	Results and discussion	195
6.4	Conclusions.....	200

CHAPTER 7: SYNTHESIS AND CONCLUSIONS.....	202
7.1 Introduction.....	203
7.2 Bulk soil water repellency measurements.....	204
7.3 Comparison of particle properties and bulk soil measures.....	210
7.4 Comparison of different particle properties.....	214
7.5 Summary	217
BIBLIOGRAPHY	224
APPENDIX A.....	240
APPENDIX B.....	249
APPENDIX C.....	253

List of figures

Figure 1-1: Forces experienced by molecules within the liquid body and at the surface.	7
Figure 1-2: Complete and partial wetting of a smooth solid surface (adapted from Schwuger, 1996).	9
Figure 1-3: Liquid droplet on a rough solid surface including air gaps.	10
Figure 1-4: Principle of the Wilhelmy plate method for contact angle measurement.	13
Figure 1-5: a) different possibilities of binding of amphiphilic molecules to the mineral surface, rendering the surface hydrophobic b) different possible binding mechanisms of organics to the mineral surface apart from electrovalence: (1) hydrogen bonding, (2) complex formation, (3) or van der Waals dipole – dipole interactions.	24
Figure 1-6: Model of organic material arrangement on mineral surface depending on organic carbon content (from Ellerbrock et al., 2005).	25
Figure 1-7: Research strategy: The two central questions are coloured in green and pink and investigations used to clarify them are framed in the corresponding colour. Dotted arrows indicate some of the primary aims of this work.	38
Figure 2-1: Soxhlet apparatus (adapted from http://www.rsc.org/chemistryworld/Issues/2007/September/ClassicKitSoxhletExtractor.asp)	52
Figure 3-1: Principle of a confocal microscope (adapted from Wolf, 1997).	58
Figure 3-2: Jablonski-diagram of fluorescence emission (adapted from http://icecube.berkeley.edu/~bramall/work/astrobiology/fluorescence.htm).	59
Figure 3-3: Visible light spectrum from 380 nm (violet) to 750 nm (red) (adapted from http://de.wikipedia.org/wiki/Lichtspektrum).	60
Figure 3-4: Sample preparation. a) for individual particles and b) for multi-particle specimens of at least two layers (only used in method application).	64
Figure 3-5: a) Laser settings for the He/Ne-laser at 100 % output intensity as used for all images. b) Laser settings for the Ar-laser as used for imaging at 3 % and 82 % output intensity.	66
Figure 3-6: a) z-stack projection of soil particle b) selected background (automatically detected after choosing a background pixel) in red for coverage determination.	70
Figure 3-7: a) Selected image background b) fluorescent regions highlighted for N_F determination.	71
Figure 3-8: Maximum emission and absorption wavelengths. Based on Haughland (2005).	73
Figure 3-9: Images of a particle from soil sample NL2 obtained using illumination at various excitation wavelengths.	76
Figure 3-10: Images of particles from samples UK1 (a and b) and AU2 (c and d) excited with an Ar-laser at 3 % output intensity (a and c) and a He/Ne-laser with output intensity of 100 % (b and d).	77
Figure 3-11: Background auto-fluorescence of natural and oxidised particles with a) Ar laser, 3 %, and b) He/Ne-laser, 100 %.	78
Figure 3-12: The proportion (%) of the maximum fluorescence of one focal plane over 10 minutes for a) standard control slide and, b) soil particle (NL2).	79
Figure 3-13: Proportion (%) of f_{cum} as a function of time for a particle from soil sample NL2, for irradiation with Ar-laser at 3 %, using various objective lenses.	81
Figure 3-14: a) Fluorescent intensity $f_{cum,z}$ as a function of depth (μm) and, b) integral fluorescence I_I for 5 imaging cycles, using irradiation with the Ar laser at 3 %.	82
Figure 3-15: Fluorescence intensity I_I of individual particles imaged with Ar-laser at 3 % on day 1 and one week later on day 8.	83
Figure 3-16: Overlay images of fluorescence from various emission wavebands (meta-channels) shown in (false) colour code (emission wavelengths are associated with colour of that wavelength), with main filter HFT 406/514.	84
Figure 3-17: Series of images of increasing emission wavebands λ_E (top left to bottom right) with $\lambda_E = (417, 427, 438, \dots, 748)$ of particle from sample AU1. The filter HFT 405/514 was used.	85
Figure 3-18: A) Series of images of increasing emission wavebands λ_E (top left to bottom right) with $\lambda_E = (417, 427, 438, \dots, 748)$ of a particle from sample AU1, filter NT 80/20. B) Overlay images of fluorescence from various emission wavebands shown in (false) colour code, using the filter NT80/20.	86
Figure 3-19: Colour coded overlays of wavelength distributions of a) and b) particles from GK2 and c) and d) of particles from PT2.	87

Figure 3-20: Colour coded overlays of wavelength distributions of particles from sample NL1 after a) acid washing, b) IPA/NH ₃ extraction, c) base washing and, d) thermal oxidation.....	88
Figure 3-21: NL2 particle after labelling with	89
Figure 3-22: Particles from soil sample NL1 dyed with Nile red.....	90
Figure 3-23: Mean I_f of all soil samples (individual particles) measured by He/Ne-laser vs Ar-laser.....	95
Figure 3-24: Mean I_f of individual particles vs TOC of bulk samples for a) all samples and b) excluding NL1 and GK2.....	97
Figure 3-25: Mean I_f/A of individual particles (I_f/A calculated for each particle) vs TOC of bulk samples for a) several samples and b) NL1 excluded.	98
Figure 3-26: Mean I_f/V_S vs TOC. I_f imaged with Ar-laser a) for samples AU, NL, PT and UK b) for samples AU and NL, and c) for samples PT and UK.	99
Figure 3-27: Mean I_f of bulk samples vs TOC for a) all samples, and b) without NL1 and GK2.....	100
Figure 3-28: Mean I_f of individual particles vs TOC by sample origins and imaged with the Ar-laser for a) samples NL and PT, b) NL samples excluding NL1, c) UK and GK samples, and d) AU samples.....	102
Figure 3-29: Mean I_f of multi-particle specimens vs TOC by sample origins and imaged with the Ar-laser for a) NL and PT samples, b) NL samples excluding NL1, c) UK and GK samples, and d) AU samples.	103
Figure 3-30: Mean of original particles, single extractions with IPA/NH ₃ , acid washing and NaOH washing and reapplication of extracted material to the extracted particles. All I_f were imaged with the Ar-laser.	105
Figure 3-31: Mean C_F vs mean I_f of single particles drawn from natural soil samples AU, NL, UK and PT.	109
Figure 3-32: C_F vs I_f of individual particles imaged with Ar-laser. Errors were assumed to be no more than 10% of the value as a rough estimate.	110
Figure 3-33: C_F of original, extracted and re-applied samples AU2, NL1 and UK1.	111
Figure 3-34: Mean N_F vs mean I_f . Error bars represent the standard error, imaged with both Ar- and He/Ne-lasers.....	113
Figure 3-35: N_F vs I_f of individual particles from a) AU, b) NL, c) PT and d) UK samples. Error bars (partly within the limits of the symbols) represent maximum assumed error of 10 % per particle.	114
Figure 3-36: N_F of original, extracted and re-applied samples AU2, NL1 and UK1. Error bars represent standard errors.....	115
Figure 3-37: Possibilities of redistribution of fluorescing organic matter after re-application of the extracted material, with light grey circles representing particles and small dark circles organic matter molecules/aggregates	116
Figure 3-38: Mean N_F vs C_F values of original, extracted and re-applied samples from AU, NL and UK. Arrows represent the sequence of extraction and re-application.	117
Figure 3-39: Mean N_F vs mean C_F for AU, NL, UK, PT samples. Error bars represent standard errors.....	118
Figure 3-40: a_F vs mean I_f . Dashed lines represent category limits (small/medium at 1.5, medium/large at 2.5) and error bars represent the standard error.....	120
Figure 3-41: a) Mean C_F , b) mean a_F , c) mean I_f and d) mean N_F of single particle images vs CA for various samples using an Ar-laser.	122
Figure 3-42: Average baseline normalized emission spectra of five particles from UK, NL and PT samples imaged with LSM meta-mode.....	125
Figure 3-43: a) Spectra of individual regions on selected particles from samples PT1, PT2, UK1, GK2, AU1 and, b) colour coded images of these particles.....	127
Figure 4-1: Diagram of a) approach of particle to water surface and, b) retraction of particle with water lamella attached.....	139
Figure 4-2: Determination of co-ordinates of the liquid surface just before the lamella breaks.	140
Figure 4-3: a) θ of bulk material vs height of water lamella and, b) θ of bulk material vs lamella height normalized by particle diameter.	143
Figure 4-4: Distribution width for each sample given as box plots.....	144
Figure 4-5: Integrals of right hand side data vs left hand side data for all samples based on the integration procedures and geometric elements used for integration.	145
Figure 4-6: Mean E_{pot} vs h of sample GL.....	146

Figure 4-7: a) Mean E_{pot} and b) mean E_{pot}/d of individual particles vs contact angle of the material on a flat surface.	147
Figure 4-8: Set-up for SCAT21 tensiometer (DataPhysics) with a single particle glued to a microscopy glass slide.	149
Figure 4-9: Typical weight vs distance curve for a spherical particle: A) at increasing distance from liquid surface, B) at maximum force/ maximum weight of water pulled up by sample, and C) thinning liquid lamella reduces the force pulling on the particle.	152
Figure 4-10: a) position of sample (p) relative to liquid surface vs contact angle θ on a smooth surface and b) p normalized by wetted length (L) vs θ . Error bars equal standard error.	153
Figure 4-11: Mean lamella heights determined by tensiometer vs goniometer.	155
Figure 4-12: Box plots of the distribution of h , h/d and h/L of various soil samples. The dashed line represents the arithmetic mean, the solid horizontal line the median and x outliers.	158
Figure 4-13: Lamella height h of original and hydrophobized samples.	160
Figure 5-1: Experimental setup for gaseous NH_3 addition.	171
Figure 5-2: Experimental set-up for gaseous HCl addition.	172
Figure 5-3: pH vs amount of gaseous HCl or NH_3 added to soil samples a) UK samples, b) NL samples, and c) AU samples.	175
Figure 5-4: WDPT vs pH after treatment with gaseous HCl and NH_3 of all samples. Open symbols represent original values. UK samples are shown in two graphs for better resolution (different scales of WDPT).	177
Figure 5-5: WDPT vs pH after treatment with gaseous HCl and NH_3 of the German samples (TW, TR, BW, BR). Open symbols represent original values.	178
Figure 5-6: pH vs amount of NH_3 added to the sample directly after the treatment (black symbols) and 3 months later (open symbols). Errors bars for pH are within the symbol limits.	179
Figure 5-7: WDPT vs amount of NH_3 added to the sample directly after the treatment (black symbols) and 3 months later (open symbols).	180
Figure 6-1: a) Schematic overview of AFM operation (from Bowen et al., 1997), and b) SEM image of an AFM tip.	189
Figure 6-2: Schematic representation of the deflection-distance curve (from Noel et al., 2004).	191
Figure 6-3: a) and c) AFM topography images and b) and d) phase angle images of sample NL1 and UK1 particle surfaces (provided by Dr. Shuying Cheng).	196
Figure 6-4: Adhesion force distribution on particles from sample a) UK1, b) UK1 with increased pH after treatment with gaseous NH_3 , and c) UK1 after treatment with gaseous HCl	197
Figure 6-5: Adhesion force distribution on particles from sample a) NL1 and b) NL1 with increased pH after treatment with gaseous NH_3	198
Figure 7-1: log WDPT vs contact angle of all samples. Minimum logWDPT values were taken as being 0.1 s.	205
Figure 7-2: WDPT as measured in 2001 and 2006. Values from 2001 are given as the upper limit of the corresponding WDPT category (cf. chapter 2).	208
Figure 7-3: Particle arrays containing a) wettable (brown) and some strongly hydrophobic grains (red) and b) only grains with a uniform, slightly hydrophobic surface (pink).	210
Figure 7-4: Predicted vs measured contact angle.	212
Figure 7-5: Contact angle vs micro roughness (as measured by AFM on $5 \times 5 \mu m^2$), dotted and dashed lines indicating different influence factors on the bulk wettability.	214
Figure 7-6: a) I_t , b) C_F and c) N_F of single individual particles vs h determined by mWPM.	215

List of tables

Table 1-1: Wettability classification for soils after Bisdom et al. (1993).....	18
Table 2-1: Sample names, origins, vegetation cover, sampling details and mean particle size and width of size distribution. Sample names with suffix C indicate wettable (control) samples (data from Llewellyn, 2004; Mainwaring, 2004).....	41
Table 2-2: Materials and chemicals used, supplier and chemical grades or other details.	43
Table 2-3: WDPT classes, sub-categories and repellency rating. Upper limits of these were used as $WDPT_{2001}$ values.	44
Table 2-4: WDPT values measured in 2001 close to sampling date ($WDPT_{2001}$) and values obtained in 2006/2007 ($WDPT_{2006}$), initial and mean contact angles on unsieved samples and the $< 150 \mu\text{m}$ sieve fraction (sv). Errors are the standard errors calculated from replicate samples.	47
Table 2-5: pH values determined with distilled water (¹) and 0.01 M CaCl_2 solution (²). Errors are the standard deviation calculated from three replicate samples.....	48
Table 2-6: TOC of samples in g kg^{-1}	50
Table 2-7: Average roughness (R_a) determined by AFM for area of $1 \times 1 \mu\text{m}^2$ (R_1) and $5 \times 5 \mu\text{m}^2$ (R_{25}). Errors are the standard deviation calculated from replicate samples.	51
Table 2-8: TOC, WDPT and CA_i after single extraction, acid washing and re-application of extract.....	53
Table 2-9: TOC and CA_i of sequentially extracted sample NL1.....	54
Table 3-1: Number of pixels at various intensities (0-255) obtained from fluorescence of an optical plane of a particle from soil NL2.....	68
Table 3-2: Excitation wavelength λ_E , output intensity, pinhole size, filters and beam splitter settings for different fluorescent dyes.	74
Table 3-3: Mean I_f of sample NL2 imaged with different settings according to dye (see methods section), without dye application and after dye application.....	89
Table 3-4: Mean I_f imaged with He/Ne-laser of original, extracted, acid washed and re-applied particles.	106
Table 3-5: Sequential extraction of sample NL1 with water, IPA/ NH_3 , NaOH; mean I_f	107
Table 3-6: Mean roughness R_{25} of original, extracted and re-applied samples NL1, AU1 and UK1, measured with AFM on $5 \times 5 \mu\text{m}^2$ areas. Errors are given as standard deviation.	117
Table 3-7: Water repellency (measured as WDPT and CA) and mean I_f of samples AU2, NL1 and UK1 after different treatments.	123
Table 4-1: Contact angle of bulk materials (measured on single layers) and smooth surfaces of glass and Fabsil TM coated glass.....	137
Table 4-2: Lamella breakpoint (p) calculated from different immersion depths for materials GL, DIA and GLwr for five particles per material using three repetitions for each immersion depth.....	150
Table 4-3: Absolute and relative mean reductions of h after coating with Fabsil TM	159
Table 4-4: Fluorescence, mean size and mean surface area of floating and non-floating particles.	161
Table 6-1: pH, WDPT and TOC of NL1 before and after treatment with gaseous NH_3 and HCl.....	195

Abbreviations and symbols

AFM	Atomic force microscopy
BET	Brunnauer, Emmett and Teller
CA	Contact angle
DOM	Dissolved organic matter
DRIFT	Diffuse reflectance infrared Fourier transformation
EFM	Electrostatic force microscopy
ESEM	Environmental scanning electron microscopy
EDX or EDS	Energy dispersive X-ray spectroscopy
FA	Fulvic acid
FT-IR	Fourier transformation infrared
g-mWPM	Gravimetric micro Wilhelmy plate method
HA	Humic acid
LSCM	Laser scanning confocal microscopy
MRI	Magnetic resonance imaging
mWPM	Micro Wilhelmy plate method
NOM	Natural organic matter
o-mWPM	Optical micro Wilhelmy plate method
PSPD	Position-sensitive-photo-diode
SEM	Scanning electron microscopy
SOM	Soil organic matter
TEM	Transmission electron microscopy
TC	Total carbon
TOC	Total organic carbon
RH	Relative humidity
WDPT	Water drop penetration time
WPM	Wilhelmy plate method
WR	Water repellency
XRD	X-ray diffraction
XRF	X-ray fluorescence

A	Area [m ²]
a_F	Size of fluorescent areas
C_F	Fluorescence coverage [%]
d	Diameter [m] or [mm]
E	Energy [J]
f_a	Absolute frequency of pixels of a certain intensity
$f_{cum,z}$	Cumulative frequency of intensity per optical slide z
F	Force [N]
g	Gravitational constant [m ⁻³ kg ⁻¹ s ⁻²]
γ	Surface tension [J m ⁻²] or [N m ⁻¹]; with subscripts lg: liquid gas, sl: solid-liquid, sg: solid - gas
h	Height [m] or [mm]
I_a	Absolute fluorescence intensity, values between 0 and 255
$I_{I,0}$	Integrated intensity of z-stack
I_I	z-stack intensity scaled by factor 10 ⁻⁵
k_{tip}	Tip constant [N m ⁻¹]
l	Length [m] or [mm]
L	Wetted perimeter [mm]
m	Mass [kg]
N_F	Number of fluorescent areas
r	Radius [m] or [mm] / correlation coefficient
R	Roughness [nm]
V	Volume [m ³]
W	Work [J]
κ^{-1}	Capillary length [m]
λ	Wavelength [m]
η	Viscosity [N s m ⁻²]
p	Lamella breakpoint [mm]
θ	Contact angle [°]
ρ	Density [kg m ⁻³]
σ	Standard deviation

Chapter 1
Introduction and literature review

1.1 Soils and their role in the environment

Soils are defined as the top layer of loose material formed from weathered rock and other minerals with organic material in various states of decay. It is confined by rocks at the base and the atmosphere, and possibly vegetation cover, at the top (Wild, 1993; Scheffer et al., 2002).

While some other parts of our ecosystem are visible and their importance thus more obvious soils are often neglected within concerns about environmental issues despite their important regulatory functions within global and regional ecosystems. Soils are a storage and filter medium for water. Nitrogen and carbon cycles are partly controlled by soil organisms, e.g. atmospheric nitrogen fixation is restricted to special soil fungi (*Mycorrhiza*) living in symbiosis with plant roots (Wild, 1993); organic matter is decomposed by soil organisms thus transforming “dead” organic matter back into the building blocks of life. Soils also form the habitat for plants and animals, especially decomposers and microorganisms. They are the base for agriculture and therefore the base of modern life. Additionally, soils can be an archive of landscape history. Both natural and cultural history is conserved in soils: soil profiles, for example, can give information about the climate during their formation, and also preserve fossils and man-made objects (Scheffer et al., 2002).

The investigation and understanding of soil processes and disturbances to them is important to preserve soil quality. This study concerns aspects of the variability in natural soil water repellency on the individual soil particle scale.

1.2 Soil water repellency

1.2.1 Definition

Soils are often thought to wet instantly when in contact with water due to capillary forces, porosity and gravity. However, it is commonly observed that there is a significant delay in the penetration of water into the soil surface, during which water may evaporate leading to reduction or complete elimination of its uptake. Soils are then called water repellent or hydrophobic (e.g. Wallis et al., 1992).

In this work the term water repellent is used for natural soils and the term hydrophobic is reserved for chemical substances, and for materials rendered water repellent by treatment with such chemicals. The many methods available to determine the strength and persistence of water repellency (WR) are described in detail in chapter 2. The strength of water repellency is here defined as the initial degree of water repellency, i.e. measured as contact angle between solid and liquid. The persistence is defined as the time it takes for the water repellency to break down during contact with water (Doerr, 1998; Regalado et al., 2009).

1.2.2 Occurrence

Water repellency was identified for the first time in the late 19th century in relation to fairy rings (DeBano, 2000b). Fairy rings are circles of poor grass growth or fungal growth within a perfectly healthy grass area (e.g. Albrecht et al., 2001). The 1960s brought a renewed interest in the wetting behaviour of soils and the amount of published work greatly increased. Since then soil water repellency has seen increasing attention in scientific investigations (DeBano, 2000b).

Early studies reporting water repellency were conducted on soils under arid or semi-arid climates like Australia (e.g. Bond, 1964; Gilmour, 1968; DeBano, 1969b), southern USA (e.g. Adams et al., 1970; Cahn, 1977; Berens, 1989) and Spain (e.g. Diaz-Fierros Viqueira, 1977). However, later work has shown that water repellency is not restricted to these climatic conditions (Doerr et al., 2000a; Jaramillo et al., 2000) and is also found under humid climates. Regions under investigations have been the Netherlands (Hendrickx et al., 1988; Bisdorn et al., 1993; Dekker et al., 1996a), the UK (e.g. York et al., 2000), Sweden (e.g. Berglund et al., 1996) and

Germany (e.g. Capriel et al., 1995; Ellerbrock et al., 2005; Hurraß et al., 2006) to just mention a few.

Soil water repellency is mostly associated with sandy soils (e.g. Roberts et al., 1971; McGhie et al., 1980; Hurraß et al., 2006) but has also been found in soils with high clay contents (e.g. Dekker et al., 1996a). Factors influencing soil water repellency that have been widely investigated are vegetation type (e.g. DeBano, 1969a; McGhie et al., 1981; Scott, 2000), organic matter content (e.g. Taumer et al., 2005 ; Wallis et al., 1990) and composition (e.g. Roberts et al., 1972; Capriel et al., 1995; Llewellyn et al., 2004), the soil water content (e.g. Dekker et al., 1994) and soil pH (e.g. Wallis et al., 1992; Karnok et al., 1993; Steenhuis et al., 2001). Apart from research on naturally occurring soil water repellency, very detailed research has been conducted on fire-induced water repellency (e.g. DeBano et al., 1970; DeBano, 2000a; Robichaud, 2000). Additionally, soil water repellency can be found following contamination of soils with hydrophobic materials such as crude oil (e.g. Roy et al., 1998; Roy et al., 2003; Buczko et al., 2006) or after irrigation of soils with waste water (e.g. Wallach et al., 2005; Graber et al., 2006).

Further details on the most important factors influencing soil water repellency and environmental problems arising from it are presented in section 1.5.

1.2.3 Consequences of soil water repellency

The occurrence of water repellency in soils, although a natural phenomenon, has multiple and, in some cases, serious implications. One of the main direct consequences is reduced water infiltration into the affected soil (e.g. Doerr et al., 2000a). Many studies have been conducted on the influence of soil water repellency on infiltration rates, including modelling of the reduced and uneven infiltration in water repellent soils (e.g. Witter et al., 1991; Clothier et al., 2000; Ritsema et al., 2000; Wang et al., 2000). An early example is the study by DeBano (1971), who found that infiltration rates were 25 times lower in a water repellent soil compared with the same soil rendered wettable by intense heating.

Reduced water infiltration into soil can lead to increased overland flow (e.g. Leighton-Boyce et al., 2007; Jordan et al., 2008), which tends to accumulate and pond in local depressions on the surface (e.g. Jordan et al., 2008). In combination with steep slopes and heavy rainfall events, this can increase the risk for flooding (Contreras et al., 2008). Increased overland flow enhances the risk of soil erosion (e.g. Keizer et al., 2005), especially after wildfires when the protecting plant cover has been removed (e.g. Varela et al., 2005). However, quantifying the direct influence of water repellency on water erosion especially after fires is difficult as other factors influence erosion (Benito et al., 2003; Shakesby et al., 1993; Benda et al., 2003). Despite these problems two studies on Dutch dune sands were able to identify, quantify and model the impact of water repellency on water erosion in this environment (Jungerius et al., 1989; Witter et al., 1991).

When water infiltration occurs into water repellent soil, it is mostly uneven and localized at zones with the lowest water repellency or along macropores, particularly below small depressions where water collects and gravity aids infiltration. Water can then flow quickly through the water repellent zone down to deeper layers of wettable subsoil or directly into the aquifer bypassing the unsaturated zone (e.g. Van Dam et al., 1990; Hendrickx et al., 1993; Ritsema et al., 2000; Clothier et al., 2008). The unsaturated zone provides capacity to filter water and buffer the transport of agricultural or other chemicals deposited on the surface. Bypassing of this zone by large quantities of water or solute can not only lead to inefficient use of the applied chemicals, but also to the direct transfer of nutrients or pollutants into water storage areas, ground water or surface reservoirs (Van Dam et al., 1990; Hendrickx et al., 1993; Scanlon et al., 1997; Bauters et al., 1998; Horn et al., 2000; Hallett et al., 2001; Clothier et al., 2008). The bypassing often occurs through macropores. These may be formed by a variety of mechanisms, such as action by soil fauna (e.g. earthworms), channels remaining when plant roots decay, or when soil cracks due to drying or along boundaries of different material. Macropores and preferential pathways are not restricted to water repellent soils and occur more generally in soils. They are effective in inhibiting a homogeneous distribution of soil water content (Scheffer et al., 2002). This can affect plant growth, especially in agricultural systems, relying on even distribution of irrigation water (Das et al., 1972; Blackwell, 2000; Clothier et al., 2008).

The vegetation cover over water repellent soils is often poorer than over wettable soils (Jungerius et al., 1989). This is due to uneven moisture distribution and can make them more prone to wind erosion. The period during which water repellent top soils are dry is longer than for wettable soils. This further increases the risk of wind erosion in the former (Doerr et al., 2000b). Soil water repellency, therefore, can indirectly increase wind erosion of soils.

Despite these detrimental effects of water repellency, some benefits can also be found. For example, the evaporation rate in water repellent soils was found to be 15 to 35 % lower than in a similar wettable soil (DeBano, 1969a). This could serve as an advantage for certain plant species adapted to arid and semi-arid conditions or those that may create water repellent soil conditions themselves, like pines and eucalyptus (e.g. Blackwell, 2000). However, a direct correlation between vegetation cover and soil water repellency is not proven. Less evaporation and increased preferential flow through the water repellent top layer into deeper soil layers could also conserve water within these deeper layers and thus favour deep-rooted plants (DeBano, 1969b).

Under normal circumstances water evaporates quickly in arid environments, but having a water repellent surface means surface runoff is enhanced and the water can then be stored in reservoirs. Therefore, water repellent soils could be used for water harvesting in such climates (DeBano, 1969b; DeBano, 1981).

Additionally, it was shown that subcritical water repellency (contact angles between 0° and 90° , Hallett et al., 2001; Hallett et al., 2004; Lamparter et al., 2006) can increase the pore structure stability and, therefore, soil stability may increase (Hallett et al., 2001). This can be used for engineering purposes e.g. in road base construction. Unfortunately soils normally are not water repellent in areas where it would be useful for these kind of applications; therefore soils have to be artificially rendered water repellent (DeBano, 1969b).

1.3 The principle of wetting

In order to understand soil water repellency it is necessary to understand the physical background of the wetting process.

Any contact area between two different materials is called an interface. Technically a surface only exists in a vacuum, but both terms are commonly used interchangeably. Three interfaces are involved in the wetting process: liquid – gas (lg), liquid – solid (sl) and solid – gas (sg).

The force acting at the surface of a liquid, causing the liquid to minimise its surface area is called its surface tension (γ). Surface tension is caused by the “desire” of a liquid to expose the smallest possible surface: within the body of a liquid phase, molecules interact with neighbouring molecules in all directions and, therefore, the net time-averaged force of attraction such a molecule is experiencing equals zero. A molecule at the surface with no neighbouring molecules beyond the surface to counteract the attractive forces from molecules inside the liquid experiences a net attraction towards the liquid (Figure 1-1). Therefore, liquids tend to minimize their free energy and surface area (de Gennes, 1988).

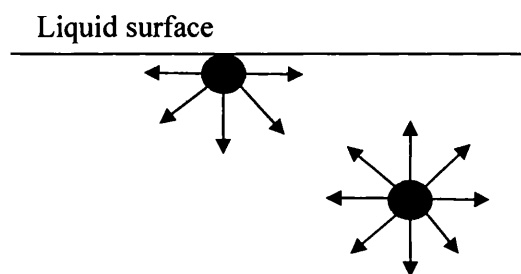


Figure 1-1: Forces experienced by molecules within the liquid body and at the surface.

The intermolecular forces involved in the surface tension are mainly short range, such as dispersion forces and hydrogen bonding (Garbassi et al., 1998). In order to

overcome these forces and increase the surface area (by dA) of a liquid work (δW) is required.

$$\delta W = \gamma \cdot dA \quad (1-1)$$

The surface tension or surface free energy, can thus be defined as “the energy that must be supplied to increase the surface area by one unit” or as “a force [...] in the plane of the surface directed toward the liquid” (de Gennes et al., 2004, p. 4 and 5, respectively). Depending on the definition, two different ways of expressing the unit for the surface tension are given: J m^{-2} or N m^{-1} , respectively. Although the definitions of surface free energy or surface tension are based on observations made in liquids any surface has this characteristic property.

A liquid has to overcome the solid surface tension in order to wet a solid surface. Complete wetting will only happen if the liquid acquires a lower energy state. Zisman (1964) developed the model of the critical surface tension γ_c stating that for a given solid surface a surface tension exists below which liquids will wet the solid and above which the solid will not be wetted completely. Hence, the wetting of surfaces with a high surface energy is easier than of a surface with low surface energy.

The process of total wetting is described by the Young equation (Young, 1855):

$$\gamma_{sg} \leq \gamma_{sl} + \gamma_{lg} \quad (1-2)$$

where γ_{sg} is the surface tension at the solid – gas interface, γ_{sl} the one at the solid-liquid surface and γ_{lg} the one at the liquid – gas interface. If this equation does not apply, the liquid will not spread instantly over the solid surface, but will form an angle at the three phase interface – the so called contact angle θ and equation (1-2) becomes:

$$\gamma_{sg} = \gamma_{sl} + \gamma_{lg} \cos \theta \quad (1-3)$$

Both types of wetting are shown in Figure 1-2. Although the Young equation illustrates the relationship between surface energies it neglects other influences on the wetting process such as gravity, surface impurities and surface roughness.

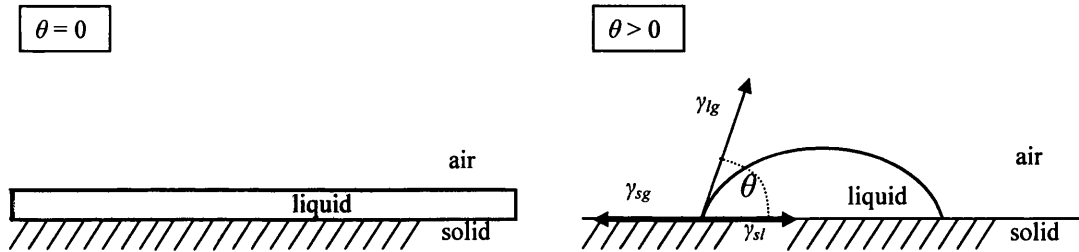


Figure 1-2: Complete and partial wetting of a smooth solid surface (adapted from Schwuger, 1996).

The contact angle formed at the three phase interface depends on the properties of the phases involved. γ_{lg} can be measured directly, but the term $\gamma_{sg} - \gamma_{sl}$ is not measurable on its own so that the measurement of the contact angle has to be used in order to describe the relationship between solid and liquid phases. On a flat surface, a contact angle $> 90^\circ$ is an indicator for a hydrophobic (i.e. non-wetting) surface. Contact angles of $< 90^\circ$ indicate partially wetting surfaces and only that of 0° indicates a totally wetted surface (Garbassi et al., 1998).

So far the description of wetting refers to a smooth solid non-porous surface. When surface heterogeneities, roughness and the influence of gravity are considered the description of wetting becomes much more involved (McHale et al., 2005).

In order to describe the influence of a rough chemically homogeneous surface where the liquid is in contact with the solid at all points a correction factor r can be introduced to the Young equation, equation (1-3) (e.g. Wenzel, 1949; Hiemenz, 1977). The equation is such that with increasing roughness θ_r increases when the

contact angle of the corresponding smooth surface is larger than 90° and θ_r decreases when the smooth contact angle is lower than 90° .

$$r \cdot \gamma_{lg} \cos \theta_r = \gamma_{sg} - \gamma_{sl} \quad (1-4)$$

However, if a surface is rough, air gaps may exist between the contact points of the liquid with the solid surface (Figure 1-3). A water droplet in contact with a mixed solid-air interface only contacts the solid interface itself in some areas, the rest of the contact area consists of air; this is called the Cassie-Baxter state (Cassie et al., 1945; Shirtcliffe et al., 2006; Koc et al., 2008). As the interfacial tension between air and water is very high, the water-air contact angle is $\theta = 180^\circ$, water will not easily wet such surfaces.

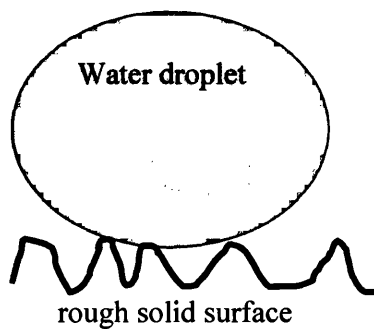


Figure 1-3: Liquid droplet on a rough solid surface including air gaps.

In such cases, the critical condition for wetting on rough solid-air interfaces may not be found at 90° contact angle, but at much lower values (Shirtcliffe et al., 2006), which is referred to as subcritical wetting (Hallett et al., 2001; Lamparter et al., 2006). Shirtcliffe et al. (2006) considered a closed pack of spheres as a rough model for hydrophobic soils and calculated a critical contact angle for wetting of 50.73° . This value was confirmed by contact angle measurements on beds of hydrophobic beads.

However, the model holds true only for particles with gaps smaller than the capillary length (κ^{-1}) of the liquid, otherwise the liquid is not able to bridge the gaps between

particles. In the case of water this is 2.7 mm as determined by equation (1-5) (McHale et al., 2007).

$$\kappa^{-1} = \sqrt{\frac{\gamma_{lg}}{\Delta\rho g}} \quad (1-5)$$

where $\Delta\rho$ is the difference in density between liquid and gas (i.e. in the case of water and air, the liquid density) and g the gravitational constant.

When dealing with partially wettable or non-wettable surfaces the influence of gravity on the shape of the droplet should also be examined as this influences the observed contact angle. Gravity can be neglected for all droplets with a smaller footprint than 1/10 of the capillary length of the liquid (McHale et al., 2007). In order to ensure water infiltration driven solely by the surface free energy it is, therefore, necessary to use small volumes of liquid for contact angle determination (Shirtcliffe et al., 2006).

The description of the wetting process thus far was described as a static process and involves no infiltration of liquid into the pores of a particulate medium such as soil. The infiltration process into a rough porous medium can only occur if the contact angle is smaller than the critical value. This critical value is often given as $> 90^\circ$ (Drummond et al., 2004), but may be well below that at around 50° (Shirtcliffe et al., 2006). If it is larger than the critical value the surface is water repellent and the water will sit on top of the solid-air surface. In order to wet a water repellent surface it is necessary to change the properties of that surface or the liquid (Hiemenz, 1977), which may happen on various time scales of seconds to hours in soils (e.g. Ma'shum et al., 1985; Roy et al., 2002, cf. section 1.4). This process can be measured using other methods or time dependent contact angle measurements (Diehl et al., 2007).

The contact angle or any other time independent method measured directly or shortly after liquid application (i.e. water), thus characterises an initial state of the sample surface, i.e. it can be defined as the severity of its water repellency (Zavala et al., 2009). The process of the breakdown of the contact angle with time and the following water penetration describes the persistence of water repellency (Doerr, 1998). This can be measured by water drop penetration time (section 1.4.3).

The contact angle is a commonly used method to describe surface wettability and is also often applied in soil water repellency research. As described above the measurement of the contact angles on bulk soil samples involves various problems and results may deviate strongly from the contact angle an individual soil particle surface would form with water solely due to its surface properties.

Details for the measurement of contact angle are given in section 1.4.1.

1.4 Measuring soil water repellency

To be able to compare different soils and classify their wettability, standard methods are necessary and, ideally, one standard procedure that allows comparison of different investigations is desirable. Although much research has focused on soil water repellency no universally accepted standard procedure exists and different techniques are employed to determine soil wettability. Unfortunately results from these different techniques are not easy to compare. While some measure the severity of water repellency namely the contact angle methods (Zavala et al., 2009) others represent the persistence of soil water repellency (Doerr, 1998; Regalado et al., 2009). The following section introduces commonly used techniques and discusses their relative merits and disadvantages.

1.4.1 Contact angle

The contact angle, formed at the three phase interface, is described in the simplest of cases by Young's equation (see section 1.3); wettable surfaces are generally characterized by a contact angle smaller than 90° and water repellent ones by those greater than 90° (e.g. King, 1981; Garbassi et al., 1998). On smooth surfaces the contact angle can be determined very easily by optical methods. This is more difficult on rough and porous media (Wallis et al., 1992) so that other methods have been developed. Three of these methods are commonly used to measure contact angles in porous media and are described in detail below.

1.4.1.1 Wilhelmy plate method

Normally the Wilhelmy plate method is used to measure surface tensions of liquids (Richter et al., 2006). For this measurement one would use a plate fully wettable by the liquid of interest in order to have a contact angle of 0° . If the solid is not completely wetted by the liquid a situation as depicted in Figure 1-4 occurs.

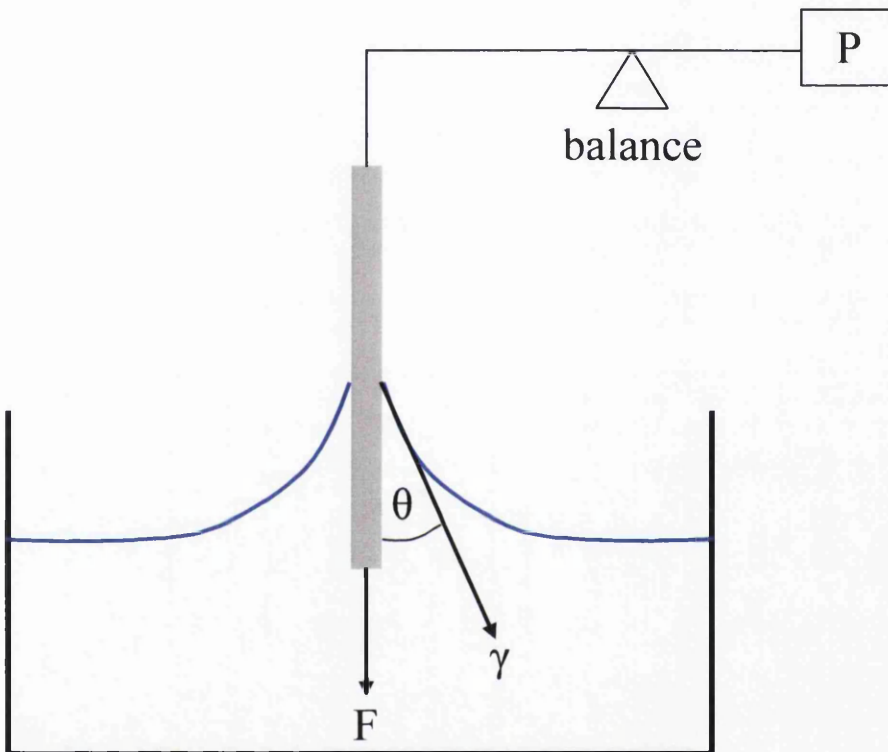


Figure 1-4: Principle of the Wilhelmy plate method for contact angle measurement.

A lamella is formed between liquid and plate. The angle θ which the lamella forms with the plate is the contact angle between solid and liquid and is determined by the material, wetted length of the material, immersion depth and the surface tension of the liquid. A plate is useful for these measurements due to its simple geometry which provides for ready evaluation of the wetted length. When immersing the plate into liquid, the force F acting on it changes and this change is determined by (Kvitek, 2002):

$$\Delta F = -\rho g(dhl) + 2(l+d)\gamma_{lg} \cos\theta = \Delta mg \quad (1-6)$$

where $-\rho g(dhl)$ represents the upthrust acting on the plate and $2(l+d)$ the wetted length. Apart from $\cos\theta$ all variables are measurable so that $\cos\theta$ can be evaluated from:

$$\cos\theta = \frac{\Delta mg + \rho g(dhl)}{2(l+d)\gamma_{lg}} \quad (1-7)$$

Soil samples are normally prepared for this method by completely coating a glass microscope slide with sample material using double sided adhesive tape (Bachmann et al., 2003; Woche et al., 2005). This glass slide is then used instead of the Wilhelmy plate and immersed into water. It is a quick and simple method if the equipment is available, but also has a big disadvantage when it comes to dealing with porous media in general. The exact geometry of the plate has to be known in order to calculate the contact angle correctly. When using soil coated plates, the true circumference of the sample is not known due to its roughness, so that accurate contact angle determination with this method can be difficult for very rough samples. Thus, sieving into very narrow particle size fractions prior to analysis is advisable (Bachmann et al., 2003; Woche et al., 2005).

1.4.1.2 Capillary rise and Washburn method

Measurement techniques based on the principle of capillary rise are indirect methods for determining contact angles, but are limited to wettable material as the liquid needs to actually rise up in the porous medium. If the medium is not wettable no infiltration of liquid will occur (Letey et al., 1962; Letey, 1969; Schwuger, 1996).

A glass tube with a glass frit at the bottom is filled with material and lowered into water or any other liquid of interest and the amount of liquid infiltrating the medium within a certain time period is measured. The amount of liquid taken up is determined by the capillary pressure pulling liquid up and the weight of liquid, i.e. gravimetric force, pulling the liquid down. This mechanical force equilibrium is determined by equation (1-8) with the force exerted by the capillary pressure on the

left hand side and weight force of the liquid column on the right hand side. This equation is not only valid for a single capillary but also for a bundle of capillaries in parallel. This is assumed to be equivalent to the situation in porous media, although e.g. the tortuosity of the capillaries is neglected.

$$2r\pi(\gamma_{sg} - \gamma_{sl}) = \pi r^2 \rho g h_{\max} \quad (1-8)$$

with r – radius of the capillary bundle and h_{\max} – capillary rise.

From that equation the maximum capillary rise can be determined as

$$h_{\max} = \frac{2(\gamma_{sg} - \gamma_{sl})}{r\rho g} \quad (1-9)$$

Substituting equation (1-3) in (1-9) provides a connection between maximum capillary rise and contact angle:

$$h_{\max} = \frac{2\gamma_{lg} \cos \theta}{r\rho g} \quad (1-10)$$

In this equation all variables apart from r and θ are measurable. If r can be calculated independently the contact angle θ can be determined. It is commonly assumed that ethanol or hexane wet any porous medium completely and instantly, therefore reducing θ to zero, so that r can be calculated. Assuming further that the capillary radius is similar for two sub-samples the contact angle can be calculated after repeating the experiment with water. Therefore, identical packing of the two sub-samples has to be achieved.

For this experiment a certain, always identical, time period is chosen. For example, Letey et al (1962) used a 24 h period for the soil in order to reach an equilibrium state.

A similar approach is the so-called Washburn method, which is also based on the principle of capillary rise, but exploits the kinetics of liquid capillary rise: the weight change of the system per time unit is measured. The height of capillary rise is described by the Washburn equation (Schwuger, 1996):

$$h = \sqrt{\frac{\gamma_{lg} r \cos \theta}{2\eta}} \cdot t \quad (1-11)$$

where t is the time for capillary rise and η the viscosity of the liquid.

However, equation (1-12) is only valid for a single capillary. For a bundle of capillaries it is expressed as:

$$h = \frac{V}{A} = \frac{m/\rho}{r^2 \pi h n} \quad (1-12)$$

where V is the total volume of the capillary bundle, A the cross section of the capillary bundle, m the liquid mass and n the number of capillaries.

Combining equations (1-11) and (1-12) and solving for $\cos \theta$ we get:

$$\cos \theta = \frac{m^2}{t} \cdot C \cdot \frac{2\eta}{\gamma_{lg} \pi^2 \rho^2} \quad (1-13)$$

where C is a material constant

$$C = \frac{1}{r^5 n^2} \quad (1-14)$$

This again can be determined using a reference measurement from ethanol or hexane. The advantage of the Washburn method over the capillary rise method is that results can be obtained rapidly. However, more sophisticated apparatus and data processing are needed to compute the contact angle.

1.4.1.3 Sessile drop contact angle measurement

The direct method of contact angle measurement is optical. Although this is more difficult than it would be for a smooth surface, contact angle measurements were adapted to measurements of soil water repellency (Bachmann et al., 2000a; Bachmann et al., 2000b). The physical and mathematical background for these measurement techniques is described in detail in section 1.3.

In order to be able to measure initial contact angles (within the first 10 seconds after droplet application) optically over the full range of wettable and water repellent samples, fixation of a single layer on a glass slide is necessary to inhibit infiltration.

Contact angles may be determined manually from images of a liquid droplet, usually water, obtained using a camera (e.g. Diehl et al., 2007) or directly using a microscope fitted with a goniometric scale (e.g. Bachmann et al., 2000b).

1.4.2 Molarity of ethanol droplet (MED) test

The MED test is a simple and indirect method to quantify soil water repellency. It can be carried out in the field due to its easy and straight forward nature.

The test is based on Zisman's concept of the critical surface tension (γ_c) which states that liquids with low surface tension wet a surface better than liquids with a high surface tension. Solids with a high surface tension are wetted easier than solids with a low surface tension and so a critical liquid surface tension exists below which a liquid wets a solid of a given surface tension (Zisman, 1964; Schwuger, 1996).

The MED test involves placing droplets of aqueous ethanol, of various concentrations, on the soil. From the drop with the lowest ethanol concentration that enters the sample after a prescribed time period (1 – 10 s depending on the study) the molarity of ethanol is recorded as the MED. The concentration of ethanol may be adjusted to provide various intervals in γ so that estimates of γ_c may be refined as considered necessary. Pure ethanol has a very low surface tension of 22.39 mN m⁻¹ at 20 °C and, therefore, wets practically every solid instantly; a sample that is only wetted by pure ethanol is classified as extremely hydrophobic.

1.4.3 Water drop penetration time (WDPT) test

The WDPT test is based on the breakdown of the water repellency and the reduced infiltration rate of water into water repellent soils. This is measured by the time required for a droplet of water, placed on the sample surface, to infiltrate completely (Letey, 1969). The WDPT is more a measure of the persistence of soil water

repellency than its severity because it measures the breakdown of water repellency of the specimen in contact with the water droplet (Wallis et al., 1992; Doerr, 1998; Regalado et al., 2009). The fact that the water does not penetrate instantly means the solid – liquid contact angle is greater than a critical value (calculated to be $\sim 50^\circ$, Shirtcliffe et al., 2006) and the net soil surface energy must be lower than that of the water droplet which is 72.8 mN m^{-1} at 20°C (e.g. Doerr, 1998; Letey et al., 2000). The surface tension of water and evaporation rate are functions of temperature. This also explains why the WDPT test is highly dependent on environmental factors such as temperature and relative humidity (Doerr, 1998).

After the initial contact of the solid surface with water the contact angle decreases until the water droplet finally infiltrates the soil. The longer this process takes the higher the persistence of the water repellency. WDPT measurements can be made in the field. Some studies, however, indicate that the WDPT test might only be sensitive in a narrow range of contact angles around 90° (King, 1981; Bachmann et al., 2000b).

Soils are often classified into different categories of wettability based on the WDPT measurements. Not all publications use the same classification system, but the one introduced by Bisdom et al. (1993) is commonly used in its original or modified form (Table 1-1).

Table 1-1: Wettability classification for soils after Bisdom et al. (1993).

WDPT [s]	Classification
< 5	Wettable
5 – 60	slightly water repellent
60 – 600	strongly water repellent
600 – 3600	severely water repellent
> 3600	extremely water repellent

While the definition of various wettability classes may be useful for scientific purposes as it allows differentiation between samples and changes in wettability, they might be less relevant in terms of environmental considerations. However, a

general definition of environmental implications is difficult as some of the classes may be only relevant for certain conditions, others under all conditions: e.g. in cases of heavy rainfall events in combination with poor vegetation cover the definition of the <5 s limit for wettable soils may be much too long as the high impact velocity of water droplets may already cause erosion whereas plant coverage would prevent it.

King et al. (1981) found a logarithmic relationship between MED and water drop penetration time (WDPT) values, but only for highly water repellent soils as other studies have found no correlations between these methods for samples in the moderate water repellency range (e.g. Doerr, 1998).

1.5 Influences on soil water repellency

1.5.1 Temporal and spatial variability

Soil water repellency shows temporal variations in both the long and short term as well as spatial variations on different scales. Many publications examined influences on these variations and identified possible factors.

In some environments very small scale spatial variations ($\sim 10^{-3}$ m) have been found (Dekker et al., 1996b; Taumer et al., 2005; Hurraß et al., 2006). Water content was identified as one of the main factors in the appearance of water repellency, but it is unclear as to what may cause such small scale differences in this property (see Section 1.5.5). It is also unclear whether water content changes are the cause of water repellency or resulting from it. Other special variations occur within the soil profile. Water repellent layers are often found just beneath the organic horizon but also in deeper layers indicating that spatial variations in repellency occur both vertically as well as horizontally (e.g. Doerr et al., 1996; Leighton-Boyce et al., 2007; Rodriguez-Alleres et al., 2007a).

During summer months with high temperature, an increased water repellency can be found for some sites (e.g. Dekker et al., 2001; Hubbert et al., 2005; Leighton-Boyce et al., 2005; Taumer et al., 2005; Hurraß et al., 2006; Buczko et al., 2007; Keizer et

al., 2007; Lemmnitz et al., 2008). Apart from this seasonal variation, some sites show changes in water repellency over periods of ~3 days and 2 weeks (e.g. Keizer et al., 2007). Buzko et al. (2007) suggested that both long term seasonal and short term variations can be explained by a complex interplay between water availability (i.e. rainfall) and temperature.

Temporal changes in water repellency were also related to the crop cycle: Keizer et al. (2007) investigated the temporal variations of water repellency during a crop cycle for different plant species, but could only find a clear pattern for maize. Before planting the soil was wettable, showed increased water repellency before harvest and returned to a wettable state afterwards. Variations of the average soil moisture content, during the crop cycle, did not themselves account for the changes in repellency.

1.5.2 Influences of soil chemistry

The influence of soil organic matter (SOM) and with that its chemistry is still widely discussed. Many studies so far have been investigating the influence of SOM, but no overall relation was found.

It is widely agreed that hydrophobic and/or amphiphilic substances are responsible for the occurrence of soil water repellency. These materials can either be present in the soil as part of soil particle coatings or as particulate organic matter (e.g. van't Woudt, 1959; DeBano, 1981; Harper et al., 1994; Franco et al., 1995). Hydrophobic material can be introduced to the soil through decomposition of plant material such as roots or leaves, microbial and fungal decomposition products or exudates and plant root exudates (DeBano, 1981; Bisdorf et al., 1993; Franco et al., 2000a) (for more details see section 1.5.6).

The amount of soil organic matter, measured mostly as total organic carbon (TOC) content, has been investigated with respect to soil water repellency. Assuming that organic matter is the critical factor for the development of water repellency the amount of organic material may be correlated to its severity. While some researchers found positive correlations between TOC and water repellency (Wallis et al., 1990;

McKissock et al., 2003; Taumer et al., 2005) some did not find correlations at all (Jungerius et al., 1989; Doerr et al., 2006). Amongst others, DeBano (1969a), Bisdom et al. (1993) and, more recently Doerr et al. (2006) showed that even soils with a very low TOC content can be water repellent. Soils with TOC of only 0.1 % were found to be water repellent while others with > 5 % were less repellent or wettable. In general it can be said that only very little hydrophobic material needs to be present in a soil in order to render the whole soil water repellent, thus explaining the often poor correlation between TOC and soil water repellency (Wallis et al., 1992). Therefore, it was suggested that rather the nature of organic material, i.e. the chemical structure, rather than the amount was responsible for water repellency (Wallis et al., 1992). Capriel et al. (1995) found a positive correlation between the amount of CH groups in arable soil and the water repellent character of the soil organic matter using diffuse reflectance infrared Fourier transformation DRIFT analysis of the samples. Additionally, they found that sandy soils contain relatively more alkyl C and less carbohydrates and proteins than clay soils. This suggests a more hydrophobic nature of organic matter in sandy soils and could explain the more prevalent occurrence of water repellency in sands (Capriel et al., 1995). However, Doerr et al. (2005b) could not verify the relationship between CH groups and water repellency in samples of different origin and texture, neither could Hurraß and Schaumann (2006) find such correlations, for samples from two urban locations, using Fourier transformation infrared FT-IR spectroscopy.

One group of substances often referred to in the context of soil water repellency are humic substances (DeBano, 1981; Bisdom et al., 1993). These have amphiphilic character and thus could be potentially hydrophobic. Specifically, polyacidic humic acids, which are commonly present in soils, are known to form hydrophobic films and also are very stable in soils (Graber et al., 2009). Nevertheless, the group of humic substances is a variable mixture of different materials, leaving much room for closer investigations of specific SOM components that might have an influence on water repellency.

Many investigations have been conducted in order to obtain more information about the specific organic compounds involved in the development of water repellency (e.g. Ma'shum et al., 1985; Franco et al., 1995; Horne et al., 2000; Mainwaring,

2004). No standard procedure has so far been established to investigate soil organic matter composition. Most procedures require an extraction prior to using instrumental analysis techniques. Numerous different extraction techniques and different extraction solvents combined with numerous types of analytical techniques have so far been used. One of the most common techniques is that of Soxhlet extraction, sometimes in combination with a sequential extraction procedure. The Soxhlet technique allows an intensive extraction with a continuous reflux of solvent, whereas sequential extraction uses various solvents in sequence and distinguishes between SOM components on the basis of relative affinity of soil and solvent (Lewandowski et al., 1997) and allows detection of changes in wettability after each extraction step.

In combination with these or other extraction techniques a variety of solvents has been used. One of the more commonly used solvents is an isopropanol–aqueous ammonia mixture (7:3 v:v), because it removes large amounts of organic material and renders soil wettable (e.g. Ma'shum et al., 1988; Franco et al., 2000a; Horne et al., 2000; Litvina et al., 2003; Doerr et al., 2004; Mainwaring et al., 2004; Morley et al., 2005); other solvents used are hot and cold water (Roberts et al., 1972; McGhie et al., 1980; Horne et al., 2000), chloroform (Roberts et al., 1972; McGhie et al., 1980; Franco et al., 2000a), ethanol (e.g. Roberts et al., 1972), acetone (e.g. Roberts et al., 1972), methanol (e.g. Roy et al., 1999) and strong oxidising agents e.g. hydrochloric acid (Roberts et al., 1972) or hydrogen peroxide (Bisdorf et al., 1993).

Many types of characterization can be used for identification of components in the extract. Frequent use has been made of infrared spectroscopy (e.g. Ma'shum et al., 1988), nuclear magnetic resonance spectroscopy (e.g. Kögel-Knabner, 1997) and gas chromatography coupled to mass spectrometry (GC-MS) (e.g. Horne et al., 2000).

Much of the research into the chemical causes of water repellency in the last decades has been devoted to identification of specific substances, leading to the general acceptance that several substance groups are relevant to soil water repellency: aliphatic hydrocarbons and fatty acids (e.g. Franco et al., 2000a; Horne et al., 2000), especially long chain fatty acids (e.g. Ma'shum et al., 1988; Graber et al., 2009); long

chain carboxylic acids, amides, alkanes, aldehydes and ketones (Mainwaring et al., 2004; Morley et al., 2005).

Although both bulk particulate organic matter and soil particle coatings have been identified as potentially inducing water repellency, Horne and McIntosh (2003) argue that if free particulate organic matter within the soil determined the water repellency there should be some kind of correlation with TOC, total lipid extract or any lipid fraction. Such correlations are generally not found. The determining factor for the wettability of particle coatings, however, should only be the amount of hydrophobic material within the outermost layer which would be poorly reflected in the TOC content (Horne et al., 2003). Therefore, hydrophobic particle coatings are more likely to influence water repellency than bulk organic material at least in soil where no correlation between TOC and water repellency exists.

Doerr et al. (2005b) found that extracts from both water repellent and wettable samples were able to induce water repellency in an acid washed sand. This suggests that the mere presence of hydrophobic substances in the soil is not sufficient to render a soil water repellent. Other factors are clearly involved in the phenomenon of water repellency.

One conceptual model explaining this observation is to consider the role of amphiphilic substances like fatty acids in the expression of water repellency. Although generally not hydrophobic, they can render a surface hydrophobic due to their orientation on that surface (Ma'shum et al., 1985; Horne et al., 2000; Ellerbrock et al., 2005; Hurraß et al., 2006). Bozer et al. (1969) suggested that the hydrophilic end of an amphiphilic molecule binds to hydrophilic soil mineral particle surface and thus the hydrophobic tail sticks out into the inter-particle pore space (see Figure 1-5a). Mineral surfaces are mostly negatively charged (e.g. clay), but some can also be positive (e.g. Al_2O_3 surfaces at $\text{pH} < 8$), which then influences the adsorption of organic amphiphilic molecules. These can be both negatively (anionic surfactants) and positively (cationic surfactants) charged.

Although the ionic bond is only one possible mechanism for organic material to bind to the mineral surface, it could account for some of the observed phenomena related to water repellency, like changes in severity with time. However, the possible

mechanisms for binding of organics to the mineral surface are manifold. Some of them are shown in Figure 1-5b: hydrogen bonding (1), complex formation (2) or van der Waals dipole – dipole interactions (3).

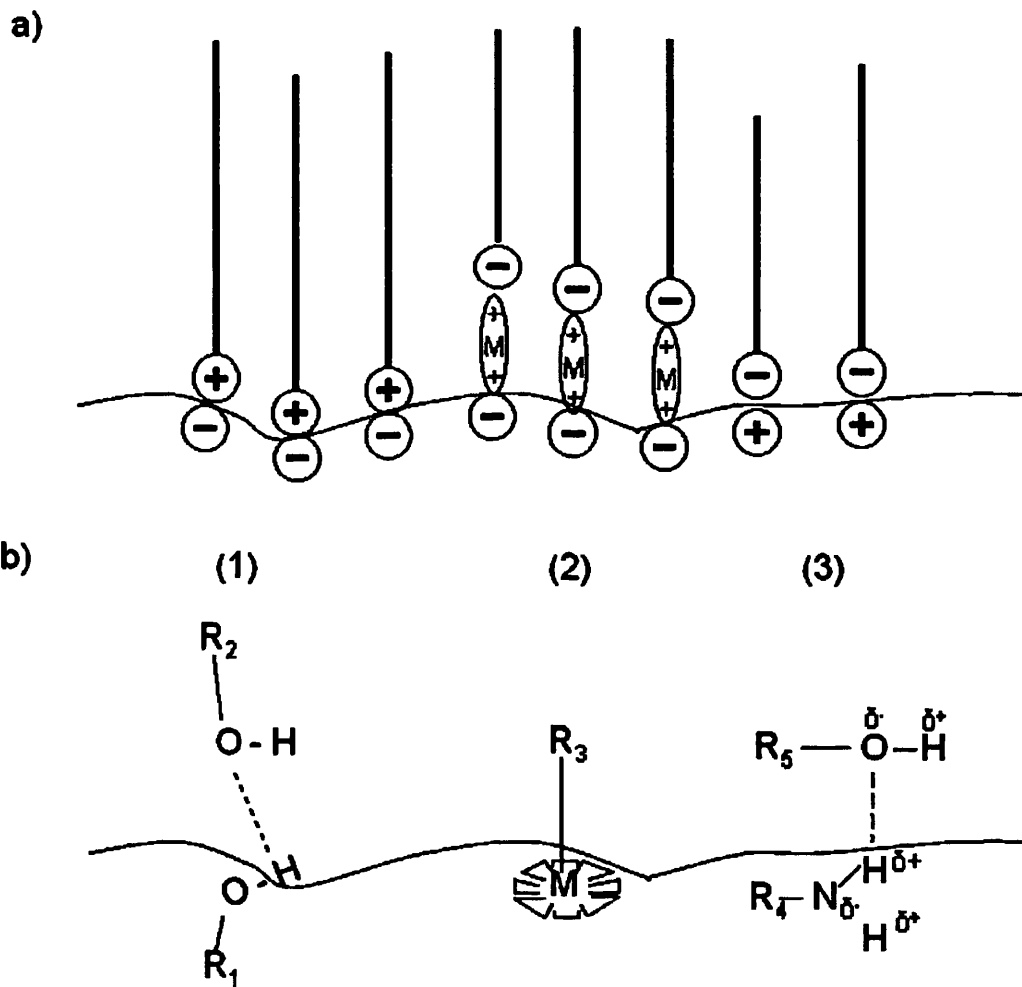


Figure 1-5: a) different possibilities of binding of amphiphilic molecules to the mineral surface, rendering the surface hydrophobic b) different possible binding mechanisms of organics to the mineral surface apart from electrovalence: (1) hydrogen bonding, (2) complex formation, (3) or van der Waals dipole – dipole interactions.

Ellerbrock et al. (2005) further considered the so called ‘effectiveness’ of SOM for the expression of water repellency. They suggest that depending on the weight ratio of organic matter to mineral matrix, the organic material has a disposition to induce water repellency or not. In their model, a low ratio of TOC to mineral matrix means

hydrophilic groups are orientated towards hydrophilic mineral surface and hydrophobic groups are pointing outwards, rendering the soil water repellent. With increasing ratio of TOC to mineral surface, more organic material is present per mineral surface area, forcing the molecules into a more upright position due to space restrictions exposing more hydrophilic groups and resulting in a wettable soil. At very high organic matter contents, and in the presence of multivalent cations, a second layer of organics could form exposing the non-polar molecular “backbone” in the pore space (Ellerbrock et al., 2005). This model is shown in Figure 1-6. However, although the relative surface area of the mineral and the ability of the available SOM to cover the surface are likely to be involved in the expression of water repellency, its relevance is difficult to quantify.

Whereas most models do not specify any substance class Graber et al. (2009) postulated that the only substance class able to account for all of their observations were divalent long chain fatty acid salts arranged in monolayers on the particle surface. They found fatty acids of molecular weights between 242 and 283 g mol⁻¹.

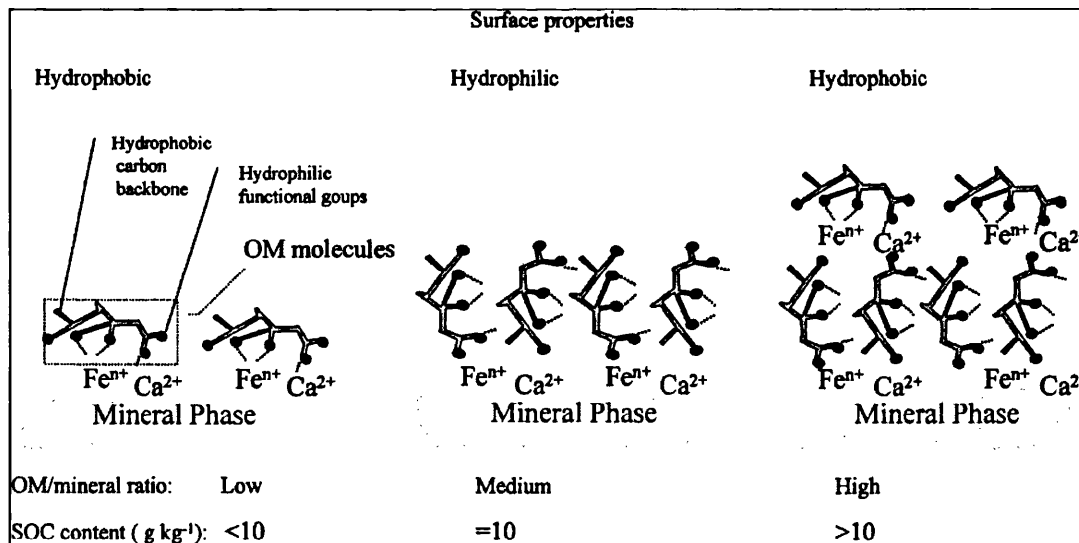


Figure 1-6: Model of organic material arrangement on mineral surface depending on organic carbon content (from Ellerbrock et al., 2005).

Most models assume a static state of organic matter in an often dynamically changing soil system. Depending on external circumstances such as water content, temperature or soil pH, the conformation of the organic matter may change (Ma'shum et al., 1985; Roy et al., 2000). These changes could be very slow (occurring over timescales of days, weeks or years) or also might happen within minutes or hours during the actual wetting process (Ma'shum et al., 1985; Roy et al., 2000; Bayer et al., 2007; Diehl et al., 2007). Furthermore, the nature of the kinetic process which is described by either a chemical or a physical rate-limiting step may be influenced by the soil itself (Diehl et al., 2007).

The existing models that explain and to some degree allow prediction of the occurrence and development of water repellency are useful. However, they are based on very limited evidence. Most models are derived using evidence gained from changing bulk soil properties or soil extraction procedures. Those using aggressive solvents (Roy et al., 1999), however, can modify organic molecules and disrupt any extended networks adsorbed on soil surfaces. Models based on the assumption that the conformation of organic matter on particle surfaces is relevant, lack evidence which cannot easily be provided by methods of bulk soil investigation. The direct investigation of SOM in its natural state in soil samples, especially on soil particle surfaces in relation to the wettability of the surface is, therefore, necessary in order to verify the models. However, research on that size scale so far has been neglected in soil water repellency research.

1.5.3 Influences of soil physics

When soil water repellency was first discovered it was associated with sandy soils. Most research, to this day, is focused on such soils. DeBano (1981) found that water repellency was most likely to occur in sandy soils with a clay content below 10 %. Other studies also came to the conclusion that water repellency is mainly caused by the coarse fraction (Roberts et al., 1971; McGhie et al., 1981; Crockford et al., 1991). This was explained by the lower specific surface area of coarser material and, thus, a higher coverage with organic material at the same level of organic matter content in comparison with a clay-bearing soil.

However, water repellency is not restricted to sandy soils (e.g. McGhie et al., 1980; Wallis et al., 1992). McGhie and Posner (1980) argued that clay soils might be water repellent when hydrophobic material covers clay aggregates whose internal surfaces are not readily available to distribute organic adsorbates. Later studies, however, did not support this argument as they found the highest water repellency within the smallest size fraction (< 0.05 mm) (Bisdorn et al., 1993; Doerr et al., 1996; de Jonge et al., 1999; Mataix-Solera et al., 2004; Rodriguez-Alleres et al., 2007b). Doerr et al. (1996) suggested that very fine organic particulate material within this size fraction may be responsible for water repellency rather than organic adsorbates.

The direct investigation of individual soil particle properties may help differentiation between the pure physical effect of bulk soil roughness inducing or amplifying soil water repellency and real properties of the soil particle surfaces (section 1.5.2). Investigations on the individual particle scale so far have been neglected and need to be addressed.

1.5.4 Influences of soil pH

It is generally accepted that soil pH may have an influence on soil water repellency although the correlation between pH and water repellency still remains inconclusive (Wallis et al., 1992). Soil wettability was often increased after addition of lime, which increases the pH (e.g. van't Woudt, 1959; Blackwell, 1996) or after the addition of sodium hydroxide to localized dry spots on golf greens (Karnok et al., 1993). Some systematic studies on pH and water repellency found water repellent soils were more likely to have a lower pH than wettable soils. Roberts and Carbon (1971) found this connection for sandy soils from south-western Australia, Steenhuis et al. (2001) for more than 3000 garden and agricultural samples from New York State and Hurraß and Schaumann (2006) for 46 samples from inner city parkland in Berlin. However, Hurraß and Schaumann (2006) did not find a significant correlation between pH and water repellency for a former sewage field in Berlin. Although water repellency occurs in calcareous forest soils with a generally very narrow range of pH, a tendency for water repellent areas to have lower pH than wettable areas was found within this environment (Mataix-Solera et al., 2007).

The influence of pH on soil wettability has been related to the state of functional groups and the ratio of dissolved to particulate organic matter (Tschapek, 1984; Babejova, 2001). At low pH relatively more humic acids (HA) are present in a soil than fulvic acids (FA). As fulvic acids are soluble over a wide pH range while humic acids are soluble only at high pH, fulvic acids are readily leached. The addition of HA to soil samples has been shown to increase their water repellency. A higher ratio of HA to FA may favour water repellency (Tschapek, 1984; Babejova, 2001). Stable humic acid complexes were identified as an important contributing factor for water repellency in some sandy soils (Roberts et al., 1972). Although HA are not completely hydrophobic, they are thought to act similarly to amphiphilic molecules and orient the non-polar groups into soil pore space and render it water repellent (Tschapek, 1984).

The local agent for reducing soil pH could be fungal exudates (Lin et al., 2006). This reduction could lead to the precipitation of FA and HA within these regions and so be responsible for the resulting water repellency. In a study of water repellency in Taiwan the contact angle of FA and HA extracts was found to be higher the lower the pH of the extract was, so that the pH might be an indicator for the hydrophobic potential of the organic matter (*ibid*). However other studies did not find increased fungal growth within the water repellent areas of the soil (e.g. Hurraß et al., 2006; Bayer et al., 2007).

In a different approach to clarify the influence of pH on soil water repellency Bayer and Schaumann (2007) increased soil pH artificially by addition of NaOH to soil samples. The water repellency in some samples increased with slightly increased pH, but decreased dramatically at $\text{pH} > 9$. The increased water repellency at slightly increased pH was explained by the stretching of organic molecules after a first deprotonation of functional groups which in turn could lead to a mutual repulsion of these groups (Deo et al., 2005) and a consequent stretching of the molecules exposing hydrophobic parts to the pore space. With even higher pH this effect is overcompensated by the increasing polarity of the organic matter. At pH 4 only 31 % of carboxylic groups in humic acids are deprotonated whereas at pH 7 most are dissociated (Terashima et al., 2004).

A recent study on the influence of pH, multivalent cations and their interplay developed a model based on the behaviour of fatty acid salts in monolayers. With high pH and only in the presence of Ca^{2+} the water repellency of their samples increased with increasing pH. This was explained by the complexation of undissociated free fatty acids and the mineral surface via Ca^{2+} bridges leading to a higher density of fatty acids on the mineral surface increasing the water repellency of said surface (Graber et al., 2009). Although these mechanisms may be of relevance for soil water repellency the model has to be considered carefully, as it is based on the behaviour of pure components within a monolayer. Soil organic matter is composed of various different substances so that the formation of continuous monolayers is unlikely. The addition of Ca^{2+} was only locally and for short time periods. Any long term changes in water repellency (more than several hours) are not accounted for in the model.

All models for the influence of pH on soil water repellency are based on the molecular scale, but validation, at this scale, has yet to be made.

1.5.5 Influences of soil water content

Water repellent conditions in soils are generally associated with low soil water content and wettable conditions with higher water contents (e.g. Leighton-Boyce et al., 2005; Ziogas et al., 2005) with a transition region dividing the two states, sometimes referred to as critical water content or transition region (e.g. Dekker et al., 2001). Most soils become wettable eventually after prolonged contact with water. Bringing wettable and water repellent samples from one location to a similar water content often adjusts their wettability to a similar level (e.g. de Jonge et al., 1999; Dekker et al., 2001). Some soils, however, do not show this adaptation and keep their differences even after adjustment to similarly high moisture levels (e.g. Hurraß et al., 2006; Bayer et al., 2007).

Measuring wettability on dried samples is often referred to as the ‘potential water repellency’ in contrast to the term ‘actual water repellency’ used for measurements under field conditions (e.g. Dekker et al., 2001). As the water repellency development is not predictable upon drying, the term is not particularly useful as it

does not reliably predict observed increases and decreases in water repellency (e.g. Rodriguez-Alleres et al., 2007a).

Different drying conditions or regimes (e.g. variations in temperature; oven drying or freeze drying) have been found to lead to a variety of outcomes where water repellency had been induced in some soils (e.g. Dekker et al., 2001) and destroyed in others (Ziogas et al., 2005).

Other studies found a complex relationship between water content and sample wettability: some samples had a maximum in water repellency at low water contents, but at water contents below 1 % after oven drying were wettable again (de Jonge et al., 1999; Goebel et al., 2004; Bayer et al., 2007). This decrease in water repellency was found for some sandy samples even after air drying (Doerr et al., 2006). This behaviour could be explained by the absence of adsorbed water molecules on particle surfaces at very low water contents, resulting in high energy surfaces with a great affinity for water molecules resulting in a wettable soil (Derjaguin et al., 1986; Vogler, 1998). The decrease of water repellency at very low water contents following drying could also be connected to conformational changes in the surface layer of the organics (Wallis et al., 1990). With increasing water content, a water film is formed on the particle surface, reducing the surface free energy of the solid. It does not behave like free water until a critical film thickness is reached and, therefore, wettability may be reduced. Above this critical water content the water film shows properties of free water and may render the sample wettable again (Clifford, 1975; Zettlemoyer et al., 1975; Goebel et al., 2004).

In general the heating regime seems to influence the resulting wettability of the partially or fully dried sample. The drying temperature itself seems to have a significant influence probably due to the different energy fluxes into the soil providing different opportunities for conformational changes to occur (e.g. Dekker et al., 1998; Bayer et al., 2007).

If the water content is changed by increasing the relative humidity, an unexpected increase in water repellency is often observed even for previously wettable samples (e.g. Jex et al., 1985; Hubbell, 1988). This was often explained by factors not directly related to the water content, but the increased growth of fungi and actinomycetes under these favourable conditions (Savage et al., 1972; Jex et al., 1985; Hallett,

2002). A different explanation was given by Doerr et al. (2000a) who suggested that the high mobility of water vapour allows the molecules to penetrate into the pores, increase the water content of the soil and disrupt hydrophobic bonds at the mineral surface with the release of enthalpy of condensation, but would not increase the wettability at the soil surface.

Investigating conformational changes in SOM due to water content changes *in situ* is difficult. However, this is necessary for validation of the models, in order to relate such changes e.g. to consequences for pollutant adsorption which is highly dependent on the state of the organic matter (e.g. Gaillardon, 1996; Altfelder et al., 1999; Johnson et al., 1999).

1.5.6 Influences of soil biology

Data from various soils suggest that the vegetation may influence their wettability. Plants with very waxy leaves, like different species of the *Pinus* and *Eucalyptus* families, are supposed to induce water repellency in soils when leaves are decomposed and waxes and oils are incorporated into the soil (Imeson et al., 1992; Ferreira et al., 2000; Scott, 2000; Mataix-Solera et al., 2007; Rodriguez-Alleres et al., 2007a). Other plant families commonly associated with soil water repellency are various shrubs (Verheijen et al., 2007) or dune grass (Jungerius et al., 1989). Whole plant families are often associated with water repellency (e.g. Eucalyptus: Garkaklis et al., 2000; Scott, 2000, pine: Robichaud, 2000; Scott, 2000 and coniferous trees: van't Woudt, 1959). The severity of induced water repellency can vary with the species (Verheijen et al., 2007). Plants may also contribute to soil water repellency via root exudates and/or their products of decomposition (Dekker et al., 1996c; Doerr et al., 1998). Hydrophobic root exudates of some plants may serve to reduce water evaporation rates and so provide an advantage of location over other plant species (Hallett et al., 2001).

Fungi and microorganisms have both been implicated to play a role in soil water repellency. Bacteria are mostly associated with decomposition of organics and, so, may be responsible for the production of low molecular mass hydrophobic substances. They also might use hydrophobic biofilms as part of a survival strategy

in order to store water and nutrients or to attach to certain surfaces. Schaumann et al. (2007) found that bacterial biofilms can affect mineral and soil surface wettability, depending on the bacterial species. *α-Proteobacterium* and *Variovorax paradoxus* proved to render a soil water repellent in a laboratory experiment. More generally Feeney et al. (2006) investigated bacterial respiration rates with respect to soil water repellency and established a connection between increased respiration and increased water repellency.

Fungal biomass was directly linked to the severity of water repellency in some studies (e.g. Bond, 1964; White et al., 2000; Hallett, 2002). Either the fungi themselves or their metabolic products could be responsible for development of water repellency. Investigations on so-called fairy rings also often found a connection between the circular zones of water repellency in turf grass soils. These rings of poor turf grass quality and high water repellency often show an increased fungal colonization (e.g. Fidanza et al., 2007). Other studies suggest that exudates of filamentous fungi change local pH and induce a very localized water repellency (Lin et al., 2006). Strong water repellency was developed in soils following storage at moderate temperatures and of high relative humidity (RH) conditions suitable for rapid growth of fungi (Savage et al., 1972; Jex et al., 1985; Hallett, 2002). However, not all studies could find clear relationships between fungal biomass and water repellency.

1.5.7 Fire-induced water repellency

Many studies have been conducted on the influence of fires on soil water repellency. Wildfires have no consistent effect on the occurrence or severity of water repellency. Fire was noted to induce or enhance water repellency in wettable soils (DeBano, 2000a), but also to decrease pre-existing repellency (Giovannini et al., 1983; Spaeth et al., 2007) or have little to no effect on pre-existing water repellency when soil temperatures remained below the temperature at which organics are sufficiently altered (Doerr et al., 1996).

These differences are largely attributed to the temperature reached in the soil and its duration, which in turn depend on fuel characteristics, the fire temperature and

duration, and soil texture and moisture (DeBano et al., 1976; DeBano, 1981; Wallis et al., 1992; Robichaud et al., 2000; Pierson et al., 2008).

On some sites the surface soil layer showed no or low water repellency following fires whereas deeper layers developed a more severe water repellency (e.g. Letey, 2001). High temperatures at the surface vaporize and combust all organic material and thus leave the soil wettable (DeBano, 2000a). The volatile organic material is translocated along the temperature gradient downwards into the soil into a region of sufficiently low temperature for organic material to condense. Organic matter may accumulate in this region and water repellency is often induced. This might be a temporary or permanent feature of the affected soil (Savage et al., 1972; DeBano et al., 1976; Doerr et al., 2000b; Pierson et al., 2008).

1.6 Remediation strategies

Where water repellency has detrimental implications, a number of different remediation strategies may be applied.

In any agricultural system a relatively simple way of avoiding the occurrence of soil water repellency is irrigation. If the soil water content is maintained above the critical water content at which soil water repellency may occur it will not develop (Cisar et al., 2000). As this critical water content is generally not known and irrigation needs to be very even and above this level, it is only an option for regions with high water availability or on high value soil systems such as golf greens (Wallis et al., 1992; Cisar et al., 2000). At highly managed systems like golf course turf, grasses are easily affected by uneven wetting and can develop localized dry spots (Cisar et al., 2000; Kostka, 2000). Wetting agents have been used to improve irrigation and efficiency of use of water (Kostka, 2000; Dekker et al., 2005; Roper, 2006). These, however, are expensive and must be used repeatedly as they are biodegradable. Their use is problematic as their decomposition products may be phytotoxic (e.g. Miyamoto et al., 1978; DeBano, 2000a). This narrows their applicability to highly managed systems such as golf greens. Wetting agents normally reduce the surface tension of the irrigation water and so facilitate the

wetting process (see also section 1.3). On reaching the soil most modern wetting agents adsorb to the particle surfaces and create a temporarily wettable surface (Kostka, 2000). Cationic surfactants and non-ionic surfactants are commonly used (Miyamoto et al., 1978; Sunderman, 1983; Kostka, 2000).

Other strategies to reduce or remove water repellency involve the use of wax-degrading bacteria (Roper, 2004; Roper, 2005; Roper, 2006). Schaumann et al. (2007), for example, showed that some bacteria (*Bacillus sphaericus*) have the potential to render a soil hydrophilic. Although these methods have so far been tested mainly in the laboratory they might prove useful for wider application. However, the problem at the field scale is often that other nutrients may be available which are easier to metabolize than the organics responsible for the water repellency. On the contrary, microbial activity itself might create hydrophobic material counteracting the positive effects of decomposition (e.g. Franco et al., 2000b; Hallett, 2002)

The addition of lime has been shown to have positive effects for soil wettability, but as often huge amounts are needed (100 t ha^{-1}) it only seems applicable if lime is available on site or close by (Roper, 2006). However, even a limited addition of 1 to 5 t ha^{-1} may help to improve wettability as it helps to increase the population of wax-degrading bacteria (Roper, 2005; Roper, 2006). The reason for the positive effect of lime addition may also lie in the changes to soil texture by the addition of a fine particle fraction, thus, increasing the wettable surface area of the soil and through increasing the soil pH (Blackwell, 2000).

Increasing the surface area of the soil through the addition of clay to sandy soils has proven to be a successful strategy in reducing water repellency (Ma'shum et al., 1988; Blackwell, 2000; Ismail et al., 2007). It is a very safe strategy as no chemicals or non-native microorganisms are added to the soil system and can have a long term effect especially in areas with a clay subsoil where the clay is readily available (Ward et al., 1993). In such soils, ploughing and tillage can improve wettability greatly by incorporating the clay from the subsoil into the upper layers (Harper et al., 2000). The addition of kaolinite was found to be successful was found to be effective in reducing water repellency. The kaolinite covered the sand grains, and only 1-3 % was needed to reduce the severity of soil water repellency (McGhie et al., 1981;

Ward et al., 1993). Additionally, clay has improved the general soil quality by increasing water storage capacity, nutrient availability and reducing the risk of wind erosion (e.g. Bisdom et al., 1993; Blackwell, 2000).

Ploughing and tillage alone can also reduce water repellency in the upper layers by diluting the water repellent material with wettable soil from deeper layers (Roberts et al., 1972). Nevertheless, ploughing in general might bring other problems like an increased potential for wind erosion through decreasing soil stability (Wallis et al., 1992) and the destruction of microorganism communities potentially disturbing the whole soil structure (Hallett, 2002).

1.7 Identifying research gaps

The review provided above, highlights that for most findings reported in the literature about soil water repellency, there is some other work which does not support such findings. There always seems to be contradictory evidence available from field studies. No common basis for explaining the occurrence of water repellency has so far been established despite significant research effort.

Water repellency affects soil at a range of scales. At the individual particle scale (0.063 – 2 mm), soil water repellency is relevant to the interactions between sub-microscopic and microscopic soil components. It may influence the retention of soil organisms and macromolecules and a localised ability to interact with any water available. This in turn may influence the stability and strength of soil aggregates at the scale of $\sim 10^{-3}$ m. At this scale water repellency may influence the participation of individual aggregates in the retention and storage of water and its transport in inter-aggregate pore space. In the locality of an individual plant, inter-aggregate behaviour may influence plant growth and this in turn may modify aspects of local soil structure (and water repellency). At the scale of 1×10^1 m and above, soil water repellency may influence soil behaviour in response to precipitation such as surface run-off, ponding or infiltration.

Although the problem occurs at all size scales, many theoretical approaches and models explain the manifestation of soil water repellency on a molecular level, i.e. the sub-microscopic scale of soil component behaviour, but evidence at these scales is mainly based on evidence from bulk soil material. This evidence, however, does not provide direct information about the distribution and orientation of the organic materials at smaller scales. Little work has focused on the pore or particle scale and soil water repellency at the scale of individual soil particles and/or where individual soil conditions are adjusted with minimal disturbance to others (Doerr et al., 2007).

One of the main problems in soil water repellency research seems to be the difference between the occurrence of soil water repellency on all kind of scales and the model explanations of the mechanisms behind it on a purely molecular scale, but without any direct evidence. Therefore, the development of new research tools or the application of research tools from other research areas (biological investigations, materials science etc.) on a nano- to micrometer scale is necessary for the validation of the models predicting or explaining soil water repellency.

1.8 Research aims and strategy

This study addresses the scaling problem by developing and employing new methods as well as adapting methods from other research fields for the non-invasive investigation of soil particle surfaces on a micro- to nano-scale with respect to soil water repellency.

Data obtained by these methods are compared with those determined from common methods for bulk soil investigations in order to validate the findings. A particular focus, hereby, is made on identifying the mechanisms responsible for changes in and the occurrence of soil water repellency. Attempts are also made to induce changes in soil or particle properties and to determine the consequent changes in water repellency. This helps to identify mechanisms in a direct ‘action to reaction’ situation.

Central research questions:

1. What are the mechanisms behind water repellency?
2. What is the nature of soil water repellency?

The primary aims of the research were, therefore, to:

1. develop new methods for nano- to micrometer scale investigations of individual soil particles;
2. evaluate the new methods for their use in soil water repellency investigations by comparing them to data obtained from bulk soil investigations;
3. induce artificial changes in the water repellency of samples in order to elucidate the mechanisms involved;
4. use the data for validating existing models of water repellency or suggesting new mechanisms for soil water repellency.

Research approach:

1. Evaluation and application of Laser Scanning Confocal Microscopy (LSCM) for soil particle surface characterisation.
2. Development of a method to investigate individual soil particle wettability.
3. Inducing changes to the surface properties of soil particles and investigating these changes at the macroscopic and microscopic scales, such as the extraction of organic material and the change of soil pH.
4. Applying Atomic Force Microscopy (AFM) – a method only recently applied in soil research – and cross-correlation with results from LSCM and other investigations.
5. Cross-correlations of data obtained from the application of these methods.

Figure 1-7 provides an overview of the research strategy for this work chosen to achieve these aims, and a very brief outline of the following chapters. Specific details of each topic are presented in individual chapters.

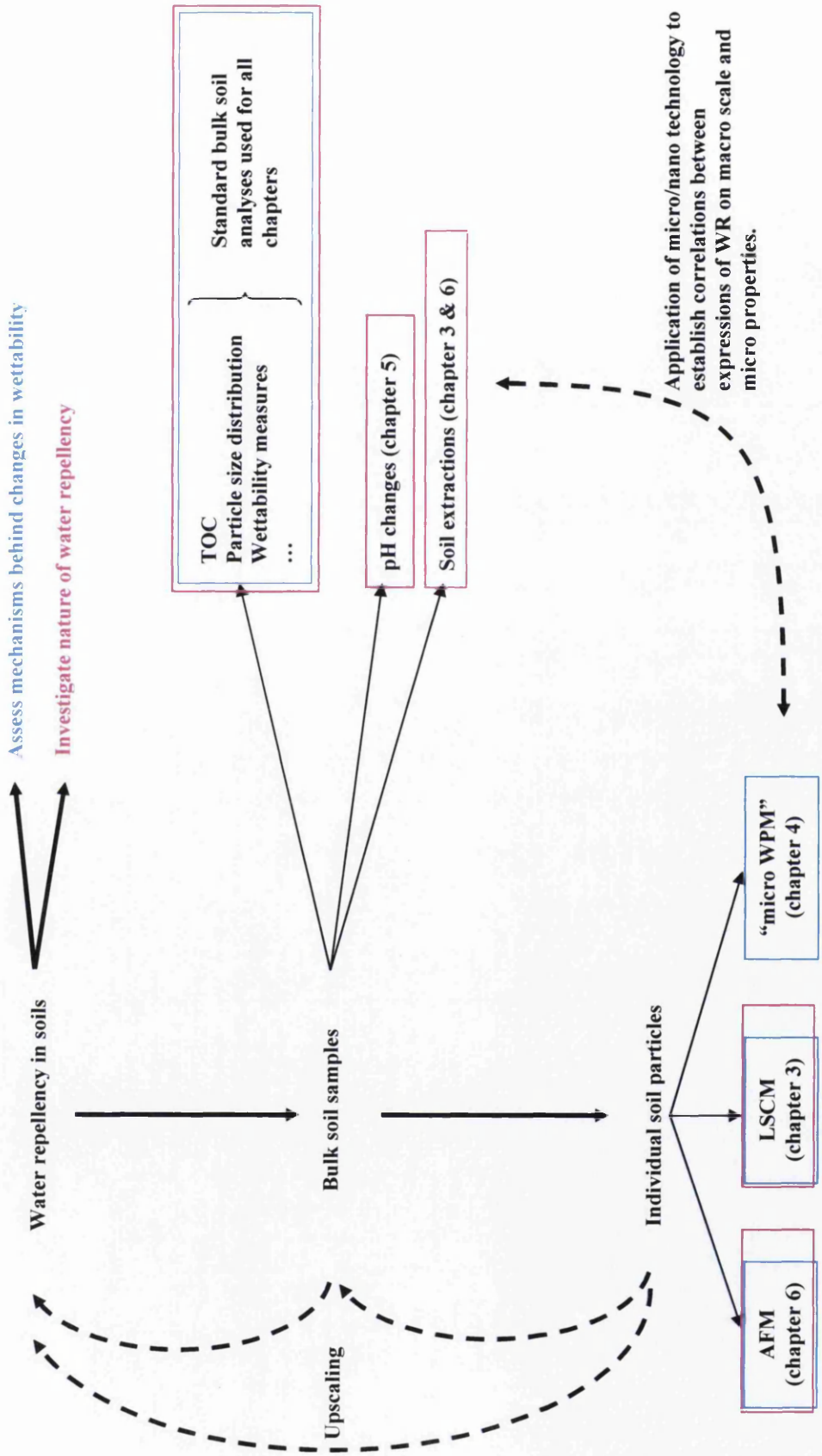


Figure 1-7: Research strategy: The two central questions are coloured in green and pink and investigations used to clarify them are framed in the corresponding colour. Dotted arrows indicate some of the primary aims of this work.

Chapter 2
Materials and methods

2.1 Soil samples

Soil sample material was taken from a sample pool collected between October 1999 and May 2001 for a European Fifth Framework project entitled “Water Repellent Soils”. These samples were chosen because they had been the focus of a number of investigations, providing valuable background information. Sample codes, origin and selected characteristics are given in Table 2-1. Results from investigations of the samples used in this thesis can be found e.g. in Doerr et al. (2002), Doerr et al. (2005a), Doerr et al. (2005b), Morley et al. (2005), Douglas et al. (2007).

All samples are sandy soils from various origins, climates and with different vegetation cover from five different countries. Sampling sites in Portugal (PT) and Australia (AU) exhibit a Mediterranean-type climate with long dry periods during the summer, whereas the sites in the Netherlands (NL) and the United Kingdom (UK) exhibit an oceanic humid-temperate climate with rainfall throughout the year. The sampling sites in Greece (GK) are also under a temperate climate, but with a pronounced dry summer season.

Apart from the NL samples, which were taken from a single soil profile, samples were taken from the upper 20 cm of the soil (Table 2-1). Originally, each sample set of each country included two or three water repellent samples and one wettable control sample (see Table 2-1). Wettable control samples (suffix ‘C’) were taken as close as possible to the sites of the water repellent soils to eliminate in so far as possible variations in soil type and land use. In the case of the Dutch samples NL, the wettable sample (NLC) was taken from 40 cm depth. Unfortunately, insufficient wettable soil material GKC was available for comprehensive investigation in this study.

Table 2-1: Sample names, origins, vegetation cover, sampling details and mean particle size and width of size distribution. Sample names with suffix C indicate wettable (control) samples (data from Llewellyn, 2004; Mainwaring, 2004).

Sample name	Country	Region	Site Location	Latitude/Longitude (UTM coordinates)	Vegetation Type	Sampled Depth [cm]	Mean Diameter & Distribution Width [mm]
AU1	Australia	Naracoorte	Pine Views	36°26'S, 140°40'E	Paddock	0-10	0.25; 0.16
AU2	Australia	Naracoorte	Pine Views	36°26'S, 140°40'E	Paddock	0-10	0.29; 0.23
AUC	Australia	Naracoorte	Myome	36°30'S, 140°42'E	Paddock	0-10	0.24; 0.14
AU7*	Australia	Naracoorte	Prydham	36°38'S, 140°42'E	Paddock	0-10	n.d.
GK1	Greece	Thrace	Dialambi Rodopi	41°07'N, 25°07'W	Permanent pasture	0-12	0.45; 0.32
GK2	Greece	Thrace	Mitriko Rodopi	40°57'N, 20°19'W	Permanent pasture	0-5	0.47; 0.24
GK3	Greece	Thrace	Abdera Xanthi	40°56'N, 24°59'W	Dune herbs & grasses	0-19	0.35; 0.14
NL1	Netherlands	Zuid Holland	Ouddorp	51°48'N, 3°54'E	Grass & moss	0-10	0.27; 0.22
NL2	Netherlands	Zuid Holland	Ouddorp	51°48'N, 3°54'E	Grass & moss	10-20	0.23; 0.10
NL3	Netherlands	Zuid Holland	Ouddorp	51°48'N, 3°54'E	Grass & moss	20-30	0.22; 0.08
NLC	Netherlands	Zuid Holland	Ouddorp	51°48'N, 3°54'E	Grass & moss	30-40	0.22; 0.07
PT1	Portugal	Aveiro	Gafanha do Areão	40°32'N, 8°46'W	Cabbage	0-10	0.57; 0.23
PT2	Portugal	Aveiro	Caldeiras	40°19'N, 8°46'W	Eucalyptus ¹	0-10	0.46; 0.16
PT3	Portugal	Aveiro	Berlingas	40°20'N, 8°47'W	Pine ²	0-10	0.47; 0.16
PTC	Portugal	Aveiro	Berlingas	40°20'N, 8°47'W	Pine ²	0-10	0.50; 0.17
UK1	UK	Gower	Nicholaston Dunes	51°35'N, 4°06'W	Dune herbs & grasses	0-5	0.33; 0.08
UK2	UK	Gower	Pennard Golf Course	51°35'N, 4°06'W	Turf grass	0-5	0.30; 0.08
UKC	UK	Gower	Nicholaston Dunes	51°35'N, 4°06'W	Un-vegetated	0-5	0.39; 0.12

*Used only for pH change experiment (chapter 5)

¹*Eucalyptus globulus*, ²*Pinus pinaster*.

Samples were dried at 20 °C in an oven and then stored in a laboratory environment at room temperature.

Samples were passed through a 2 mm sieve. All material apart from some organic debris passed through the sieve so that the composition was essentially unchanged. All samples are medium-textured sands (0.22-0.70 mm) with a clay content below 0.1 %.

Representative sub-samples (~15 g) were obtained from bulk sample material following the use of the coning and quartering method (Lewandowski et al., 1997). These were sufficient for multi-particle analysis. Where required, individual particles were selected from a small amount (~15 mg) of one of these sprinkled on a microscopy glass slide. Particles were picked randomly using the heat-sealed tip of a glass pipette.

Further details on sample preparation and specimens for LSCM investigations and the micro Wilhelmy plate technique are given in the corresponding sections.

2.2 Materials

All chemicals and materials used, and their suppliers, are given in Table 2-2.

Table 2-2: Materials and chemicals used, supplier and chemical grades or other details.

Material	Supplier	Details, Grade
5-Carboxy-fluorescein diacetate <i>N</i> -succinimidyl ester	BioChemika	for fluorescence, ~95 %
Acid washed sand	Fluka	quartz, purum p.a.
Acrylic polymer beads	Imperial Chemical Industries Ltd., UK	brand name Diakon mean diameter 270 μm
Ammonia	Fisher Scientific Ltd., UK	0.88 S.G., 35 %
Anglin' glue™	Fisherman's choice, UK	-
Fabsil™	Grangers, UK	silicone-based water proofing
Fluorescein 5(6)-isothiocyanate (FITC)	Sigma, UK	~90 %
Glass beads	unknown source	mean diameter 120 μm
Glass beads	unknown source	mean diameter 270 μm
Glass micro-fibre extraction thimbles	Whatman, UK	internal diameter 30 mm external length 100 mm
Hydrochloric acid	Fisher Scientific Ltd.	1.18 S.G., 36 %
Isopropanol	Acros Organics	
Methanol	Fisher Scientific Ltd.	
Microscope glass slides	Menzel, Germany	-
Microscope cover slips	Menzel, Germany	22 × 22 mm, thickness 0.16 – 0.19 mm
Microscope cover slips	Menzel, Germany	22 × 22 mm, thickness 0.08 – 0.12 mm
Nitric acid	Fisher Scientific Ltd., UK	70 %
Nile Red	BioChemika	for fluorescence, ~98 %
Oxalic acid	Aldrich	99 %
Potassium hydroxide	Fisher Scientific Ltd., UK	0.1 M
Rhodamine B	Sigma, UK	~95 %

Water, prepared by deionisation and reverse osmosis ($5.5 < \text{pH} < 6.7$, specific conductivity $< 2 \mu\text{S}$) was used throughout unless stated otherwise.

2.3 Water repellency measurements

Water repellency measurements were performed using two methods. Water drop penetration time (WDPT) was measured according to Letey (1969) and contact angles (CA) were measured with the sessile drop method (Bachmann et al., 2000a). These two were chosen to represent different classifications of water repellency: the WDPT test being a measure of the persistence of water repellency (Doerr, 1998; Regalado et al., 2009) whereas CA is a measure of its severity (Zavala et al., 2009).

2.3.1 Water drop penetration time (WDPT) test

Samples (5-10 g) were placed in a plastic weighing dish. The surface was smoothed gently using a spatula. Samples were equilibrated at 20 °C and a RH ~50 % for 24 h in order to minimise effects from local variations in atmospheric conditions. Three to five droplets of water (~40 µl) were placed carefully from a height of less than 5 mm on the sample surface from a pipette and the time required for their complete infiltration recorded. The number of droplets was adjusted to the available area of sample surface, with a minimum of three per sample. Mean WDPT values were rounded to the nearest 5, 10 or 100 seconds, for values <100 s, <1000 s or >1000 s, respectively. Measurements made in 2001 (WDPT₂₀₀₁) were grouped into sub-categories (Table 2-3) and the value given (Table 2-4) is the upper limit of the corresponding sub-class of WDPT.

Table 2-3: WDPT classes, sub-categories and repellency rating. Upper limits of these were used as WDPT₂₀₀₁ values.

WDPT Classes (s)	≤5	10	30	60	180	300	600	900	3600	18000	> 18000
Sub-category	1	2	3	4	5	6	7	8	9	10	11
Repellency Rating	Wettable	Slight		Strong			Severe		Extreme		

Table 2-4 shows WDPT originally measured in 2001 (Llewellyn, 2004; Mainwaring, 2004) and values obtained in the present work 2006/2007 together with the water repellency rating according to Bisdom et al. (1993) (see section 1.4.3). Significant differences between the two measurements were found. These are discussed in chapter 7.

2.3.2 Contact angle measurement with a sessile drop

Specimens were prepared by sprinkling the sample on to a glass microscope slide whose surface was covered in double-sided adhesive tape. The glass slide was then tapped gently against the bench top to remove loose material.

Contact angles of bulk materials were measured using a goniometer (Easydrop DSA100, Krüss GmbH, Hamburg, Germany; software DSA Version 1.900.14). A droplet of water ($\sim 15 \mu\text{l}$) was placed on the sample surface, using a software-controlled stepper-motor-driven syringe and images of it were recorded by camera at 1.67 frames per second for a total of 60 s. The contact angle was then calculated using the software. This fits a function to the drop profile and uses it to find the tangent at the three phase contact point, from which the contact angle is determined. In order to minimize the effect of gravity, an ellipsoid shape is used.

Two contact angles were determined (Table 2-4): i) the initial contact (CA_i) angle which was calculated from the first image after the droplet was placed on the surface and ii) the average contact angle (CA_{mean}) determined from 10 images obtained at 5 s intervals during the period 7 – 60 s (Bachmann et al., 2000a).

In order to remove the effects of variations in particle size between samples (cf. Table 2-1), additional CA measurements were carried out on sieved samples ($sv < 150 \mu\text{m}$; see Table 2-4)

Although differences were found between initial and mean contact angles, the general trend was similar for both measures. Therefore, only the mean contact angle (following Bachmann et al., 2000a) is used in this study.

No significant differences were found between the contact angles of the unsieved samples and the fraction $< 150 \mu\text{m}$. In the following the contact angle of the unsieved samples is used.

Table 2-4: WDPT values measured in 2001 close to sampling date (WDPT₂₀₀₁) and values obtained in 2006/2007 (WDPT₂₀₀₆), initial and mean contact angles on unsieved samples and the < 150 µm sieve fraction (sv). Errors are the standard errors calculated from replicate samples.

sample	WDPT ₂₀₀₁ [s]	WR ₂₀₀₁ classification*	WDPT ₂₀₀₆ [s]	WR ₂₀₀₆ classification*	CA _i [°]	CA _{mean} [°]	CA _{i,sv} [°]	CA _{mean,sv} [°]
AU1	3600	Severe	160	Strong	110 ± 1	93 ± 2	107 ± 1	91 ± 1
AU2	180	Strong	0	Wettable	97 ± 1	81 ± 3	96 ± 2	82 ± 3
AUC	< 5	Wettable	800	Severe	116 ± 3	104 ± 2	113 ± 1	103 ± 1
AU7**	3600	Severe	430	Strong	n.d.	n.d.	n.d.	n.d.
GK1	600	Strong	40	Slight	105 ± 3	85 ± 2	104 ± 2	88 ± 2
GK2	600	Strong	140	Strong	108 ± 2	95 ± 3	111 ± 2	98 ± 1
GK3	180	Strong	0	Wettable	86 ± 3	72 ± 2	93 ± 2	80 ± 2
NL1	180	Strong	4800	Extreme	118 ± 2	107 ± 2	117 ± 1	98 ± 1
NL2	3600	Severe	2400	Severe	111 ± 2	102 ± 1	108 ± 2	98 ± 1
NL3	18000	Extreme	470	Strong	110 ± 3	97 ± 2	106 ± 1	97 ± 1
NLC	< 5	Wettable	< 5	Wettable	89 ± 1	82 ± 1	88 ± 2	84 ± 1
PT1	180	Strong	0	Wettable	86 ± 3	63 ± 1	93 ± 1	70 ± 1
PT2	18000	Extreme	250	Strong	108 ± 3	101 ± 3	113 ± 1	103 ± 2
PT3	60	Slight	0	Wettable	82 ± 4	73 ± 3	91 ± 1	81 ± 1
PTC	< 5	Wettable	0	Wettable	69 ± 1	60 ± 3	87 ± 2	79 ± 2
UK1	900	Severe	> 18000	Extreme	113 ± 1	105 ± 1	111 ± 1	106 ± 1
UK2	300	Strong	30	Slight	92 ± 3	81 ± 1	93 ± 3	86 ± 2
UKC	< 5	Wettable	0	Wettable	36 ± 1	30 ± 2	42 ± 1	28 ± 6

* According to Bisdom et al., 1993.

** Used only for pH change experiment (chapter 5).

2.4 Soil characteristics

2.4.1 pH measurement

Soil pH was measured using a pH meter (pH/mV/temperature meter, Fisher Scientific Ltd., UK) with temperature compensation, following a standard procedure. This involved using 12 g of soil and 25 ml of 0.01 M aqueous CaCl₂ solution (DIN ISO 10390). Where possible these amounts were used. However, where there was a restricted availability of sample material, the quantities used were reduced to 5 g soil sample and 11 ml solution. The suspension was shaken ensuring total wetting of the sample and then left for one hour. After stirring once more, the material was left to settle and the pH of the supernatant liquid was measured.

Llewellyn (2004) determined the sample pH using distilled water. Sample AU7 was not used in that study.

Table 2-5: pH values determined with distilled water (¹) and 0.01 M CaCl₂ solution (²). Errors are the standard deviation calculated from three replicate samples.

Sample code	pH ¹ determined in 2001	pH ² determined in 2006
AU1	5.2 (±0.6)	4.8 (±0.4)
AU2	5.1 (±0.6)	4.4 (±0.5)
AUC	6.8 (±1.5)	5.1 (±0.7)
AU7*	n.d.	5.2 (±0.7)
NL1	4.4 (±0.4)	4.7 (±0.3)
NL2	5.4 (±0.4)	3.9 (±0.3)
NL3	4.7 (±0.6)	3.9 (±0.5)
NLC	4.1 (±0.3)	4.1 (±0.2)
GK1	5.4 (±0.7)	n.d.**
GK2	4.8 (±0.4)	n.d.**
GK3	4.1 (±0.3)	n.d.**
PT1	6.3 (±0.6)	n.d.**
PT2	4.4 (±0.7)	n.d.**
PT3	4.7 (±0.8)	n.d.**
PTC	4.2 (±0.4)	n.d.**
UK1	5.3 (±0.4)	4.2 (±0.6)
UK2	4.4 (±0.6)	4.5 (±0.3)
UKC	6.0 (±0.7)	7.0 (±0.5)

* Used only for pH change experiment (chapter 5).

** Not determined, as not enough sample material was available.

Sample pHs originally determined using distilled water (Llewellyn, 2004) rarely agree precisely with those determined using CaCl_2 in the present work. This may be the effect of the solvent as CaCl_2 is specifically used in order to mimic the soil suspension and to exclude the influence of ions other than H^+ by adding Ca^{2+} (Schlichtling et al., 1995). However, significant differences, in relation to the error in pH are rare.

2.4.2 Total organic carbon (TOC) content

Total organic carbon (TOC) was determined using a Skalar Primacs^{SC} Solid Sample TC Analyser connected to an oxygen supply, a balance and a PC. The latter allows complete control of the apparatus. The apparatus was calibrated using oxalic acid (25, 50, 75 and 100 mg). Depending on the anticipated carbon content, between 20 mg and 1.5 g of material was weighed into quartz containers. Material was pre-ground to improve combustion using a ceramic mortar. Samples were then placed in the instrument and heated to 1050 °C for seven minutes. As samples were carbonate free, total carbon (TC) was used as a measure of TOC. Samples were oxidized or decomposed in the presence of pure O_2 into CO_2 . The amount of CO_2 was measured with an IR detector at a wavelength of 4.2 μm and TC content calculated from the calibration using oxalic acid.

Table 2-6: TOC of samples in g kg⁻¹

sample	TOC [g kg ⁻¹]
AU1	11.7 ± 1.0
AU2	14.4 ± 0.5
AUC	2.2 ± 0.4
GK1	10.4 ± 0.2
GK2	21.2 ± 0.8
GK3	6.2 ± 0.7
NL1	36.2 ± 2.9
NL2	5.9 ± 0.3
NL3	0.8 ± 0.2
NLC	none detected
PT1	6.3 ± 0.1
PT2	10.3 ± 1.5
PT3	0.6 ± 0.4
PTC	0.1 ± 0.2
UK1	11.4 ± 2.7
UK2	7.8 ± 1.0
UKC	3.1 ± 0.6

Some particles were recovered from the instrument following TOC analysis as these were assumed to be free of organic material and are here referred to as ‘oxidised’.

2.4.3 Particle size analysis

Particle size measurements were obtained from Mainwaring (2004). A *Malvern Lasersizer 2000* and *Beckmann Coulter LS 230 Particle Size Analyzer* (Dry Powder Module) were used for analysis. The mean particle diameter values for the samples were calculated based on particle diameter and assuming that particles were spherical and non-porous (Table 2-1).

2.4.4 Roughness determination

Individual particles were glued to a glass microscope slide using double sided adhesive tape. Roughness (R) of individual particle surfaces was determined by atomic force microscopy from topographical images (in air at 20 °C, RH 40 ± 5 %) using a Dimension 3100 scanning probe microscope in tapping mode (Digital

Instrument, Inc., Santa Barbara, CA). Probes with a spring constant of 42 N m^{-1} and nominal tip radius of 5 nm were used for imaging areas of $1 \mu\text{m}^2$ and $25 \mu\text{m}^2$ at a scan rate of 1 Hz . All imaging parameters were kept constant for comparability. In total between 10 and 15 images were taken per sample so that results given are average R values. Mean roughness (R_a) values are shown in Table 2-7 with the standard deviation (values partly from Cheng et al., 2008 and courtesy of Dr Shuying Cheng). The mean roughness was determined as:

$$R_a = \frac{1}{n} \sum_{i=1}^n |y_i| \quad (2-1)$$

where n is the number of observations and y_i the deviation from the mean.

Table 2-7: Average roughness (R_a) determined by AFM for area of $1 \times 1 \mu\text{m}^2$ (R_1) and $5 \times 5 \mu\text{m}^2$ (R_{25}). Errors are the standard errors calculated from replicate samples.

sample	R_1 [nm] ($1 \times 1 \mu\text{m}^2$)	R_{25} [nm] ($5 \times 5 \mu\text{m}^2$)
AU1	13.2 ± 3.2	53.3 ± 13.9
AU2	14.4 ± 2.5	61.5 ± 13.4
AUC	14.9 ± 2.8	54.9 ± 18.0
GK1	14.3 ± 2.9	70.1 ± 12.0
GK2	8.4 ± 1.5	40.7 ± 5.8
GK3	15.9 ± 4.4	71.3 ± 22.4
NL1	8.5 ± 0.3	46.5 ± 6.8
NL2	14.3 ± 6.8	63.8 ± 8.6
NL3	10.8 ± 1.8	67.1 ± 7.6
NLC	16.3 ± 4.5	79.1 ± 13.1
PT1	25.6 ± 6.4	60.3 ± 19.1
PT2	12.9 ± 2.4	82.3 ± 26.7
PT3	26.1 ± 5.7	77.8 ± 10.4
PTC	11.6 ± 0.7	54.4 ± 7.9
UK1	13.9 ± 2.8	98.4 ± 22.3
UK2	20.9 ± 3.9	58.3 ± 8.6
UKC	15.5 ± 2.2	53.5 ± 5.2

2.4.5 Extraction of organic material using Soxhlet extraction

Soil samples were extracted for 24 h using a Soxhlet apparatus. Single and sequential extraction procedures were carried out. The Soxhlet apparatus (capacity 5 L) allows intensive extraction. A diagram is shown in Figure 2-1.

Soil samples (40 g) were pre-wetted with the solvent mixture for 15 min prior to refluxing. Single extractions involved one litre of isopropanol : aqueous ammonia (7:3) (IPA/NH₃) mixture in contact with the samples (AU2, NL1 and UK1). Samples were placed in a Whatman glass microfibre extraction thimble (30 mm internal diameter, 100 mm external length) and an isomantle was used as heat source.

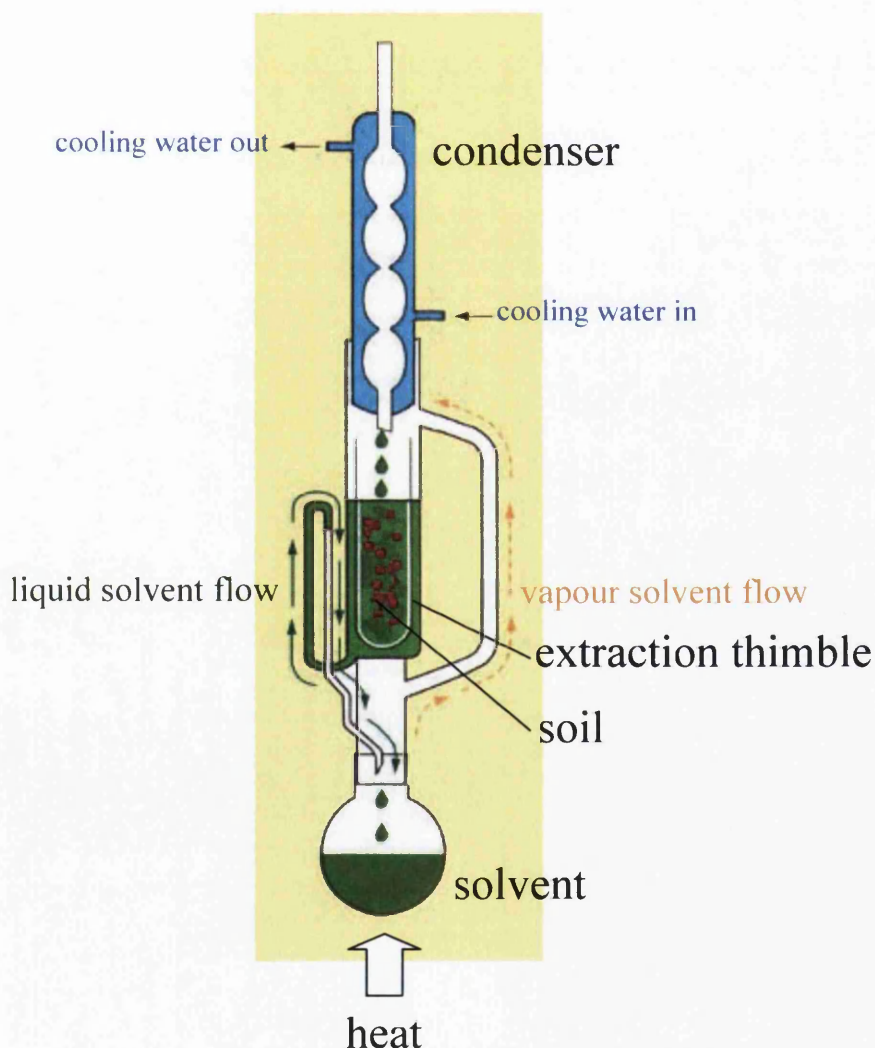


Figure 2-1: Soxhlet apparatus (adapted from <http://www.rsc.org/chemistryworld/Issues/2007/September/ClassicKitSoxhletExtractor.asp>)

The extracted soils were cooled and dried at room temperature (~20 °C). Water repellency measurements and TOC contents of the samples after extraction are shown in Table 2-8.

Samples in their native condition are termed “original”, those that have been extracted are termed “extracted” and those “extracted” to which their extracts have been quantitatively re-applied are termed “re-applied” (see section 2.4.6).

Table 2-8: TOC, WDPT and CA_i after single extraction, acid washing and re-application of extract.

	Pre-extracted	IPA/NH ₃	Acid washed	Re-applied
TOC [g kg⁻¹]				
AU2	11.7	3.8	n.a.	7.1
NL1	36.2	12.6	n.a.	12.4
UK1	11.4	3.0	n.a.	3.6
WDPT [s]				
AU2	10	1-5	<1	7
NL1	1320	1-5	<1	47
UK1	1600	1-5	<1	37
CA_i [°]				
NL	112 ± 4	87 ± 4	64 ± 4	128 ± 6
AU	95 ± 3	72 ± 3	64 ± 3	85 ± 3
UK	106 ± 4	82 ± 2	58 ± 5	108 ± 2

The procedure for sequential extractions follows the one described above for single extractions, but different solvents were used on the same sample in series. The first extraction step involved chloroform, the second IPA/NH₃, followed by washing with deionised water and finally aqueous NaOH (0.01 M). Data for chloroform are not shown here as the sample following the first step was not used further (no data for single extractions was available as chloroform was only used in sequential extractions).

Table 2-9: TOC and CA_i of sequentially extracted sample NL1.

	<i>Pre-extracted</i>	<i>IPA/NH₃</i>	<i>Water</i>	<i>NaOH</i>
TOC [g kg ⁻¹]	36.2	1.32	0.74	0.04
CA _i [°]	112 ± 4	93 ± 3	70 ± 10	68 ± 5

2.4.6 Re-application of extracted material

The extracts were re-applied to the extracted soil samples by rotary evaporation at 45 °C, in order to examine (i) whether the substances isolated from the soils using Soxhlet extraction are capable of causing water repellency, and (ii) how soil particle surfaces are affected by this re-application. The extracted solutions were directly applied to the extracted soil after cooling. 25 % of the extract solution was added to 25 % of the extracted soil sample. Water repellency measurements and TOC values are shown in Table 2-8.

2.4.7 Treatment with acid or base

Treating the samples with acid was used in order to remove organics, especially organic coatings on soil particle surfaces and in the case of purchased clean sand to remove impurities. The purchased sand was termed acid washed sand (AWS) only after this procedure. Acid treatment consisted of heating the sample (~10 g) in HNO₃ (70 %) at 130 °C for 4 hours. The samples were then rinsed with deionised water until the natural pH of water was reached. All acid washed samples were dried at room temperature (~20 °C). For simplification this treatment is referred to as “acid washing” in the following.

In some cases additional base washing was used in order to remove organics that may not be dissolvable at low pH (e.g. humic acids). Base washing consisted of shaking the sample (~20 g) in NaOH (~100 ml, 0.1 M) for 24 hours, then rinsing with water until the natural pH of water was reached.

When samples were subjected to both procedures, acid washing was performed first.

Samples subjected to this treatment are referred to as “acid-washed” (AW) or “base-washed” (BW). If procedures are combined samples are termed AW+BW.

Water repellency measurements and TOC values are shown in Table 2-8 and Table 2-9.

2.4.8 Statistical analysis

All error bars and values given are based on the standard error (SE) calculated from the standard variation (σ) unless stated otherwise.

$$SE = \frac{\sigma}{\sqrt{n}} \quad (2-1)$$

where n is the number of observations.

In the following, where results are referred to as “significant”, a statistical analysis was conducted at the significance level of $\alpha = 0.05$ unless stated otherwise. For testing whether two means (M_1 and M_2) have the same value, t-tests were used and the t-variable calculated from:

$$t = \frac{M_1 - M_2}{\sqrt{\frac{\sigma_1^2}{n_1} + \frac{\sigma_2^2}{n_2}}} \quad (2-2)$$

If the calculated t value is higher than the critical t_α value, the null hypothesis ($M_1 = M_2$) is rejected at the appropriate significance level α .

Chapter 3

Laser scanning fluorescence microscopy (LSCM)

on natural soil particles:

method testing and application

3.1 Introduction

In the following chapter the applicability of laser scanning confocal microscopy (LSCM) to the investigation of soil particle surfaces is tested and subsequently applied to a broad range of natural soil samples.

The confocal microscope was invented in 1955 by M. Minsky (US Patent #3013467, 1957). The resolution of a confocal microscope is much higher compared to a normal light microscope. Instead of illuminating the whole sample, the light is focused on one spot in one thin optical plane and then scanned over the whole sample (see below for a more detailed description). At that time a conventional (incoherent) light source was used for sample illumination. In 1979 a laser scanning confocal microscope (LSCM) was developed (Wilkinson, 1998). The wide application of the technique was initiated in the 1990s with the development of powerful and stable lasers as well as computers that were able to deal rapidly with the large quantities of data produced. LSCM fluorescence imaging is now a widely used microscopic technique in biological applications such as identification of biochemical processes in living cells and neural networks (Hibbs, 2004).

In contrast to a normal light microscope, the light source, i.e. laser, in a scanning confocal microscope is passed through a pinhole and reflected from a dichroic mirror through the objective and focused on one point within the specimen (see Figure 3-1). The fluorescence emitted from the specimen at this point, which has a longer wavelength than the incident excitation light, is passed back through the objective. It is separated from the reflected and scattered light, which is not associated with the point of excitation, by the dichroic mirror and passed through a second pinhole. The light is then collected by a photomultiplier. A scan head moves the point of excitation/imaging over the surface of the specimen and so builds an image out of individual points. Several optical planes can be imaged in this way (by changing the focus) and finally a 3D image can be formed by combination from the planes, a so called z-stack (Minsky, 1988; Wilson, 1993; Wolf, 1997; Atkins, 1998; Hibbs, 2004).

By imaging point by point, no contrast or resolution is lost at the edges of the field of view and the digital imaging process allows image enhancements after the data collection (Wilson, 1993).

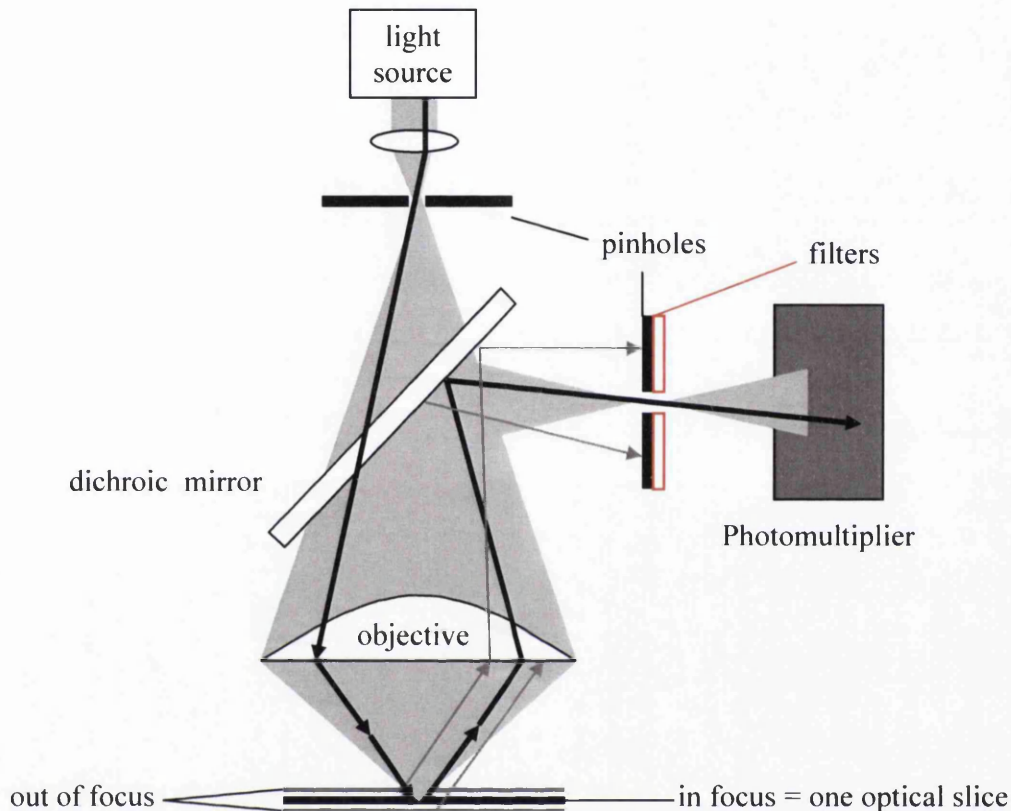


Figure 3-1: Principle of a confocal microscope (adapted from Wolf, 1997).

Fluorescence is the emission of light of a longer wavelength (λ_F) after excitation with light of shorter wavelength (λ_E). The process of fluorescence is schematically depicted in Figure 3-2, the so called Jablonski-diagram (Wilson, 1993). An electron is moved into an excited state through the absorption of light (stage 1 in Figure 3-2). Every electron has several possible excited states and which of them is reached is dependent on the energy input during excitation. The excited state is not stable and the electron will lose energy in small quantities moving through all possible states until it reaches the lowest excited state which is semi-stable (2 in Figure 3-2). This is

called the transient state. The electron then falls back into the ground state, losing the remaining energy in the form of light emission. Due to the energy loss during the transient state the emitted light has a lower energy than the excitation light and, therefore, a longer wavelength (3 in Figure 3-2). The wavelength shift of the emitted light to longer λ_F is called the Stokes shift (*ibid*).

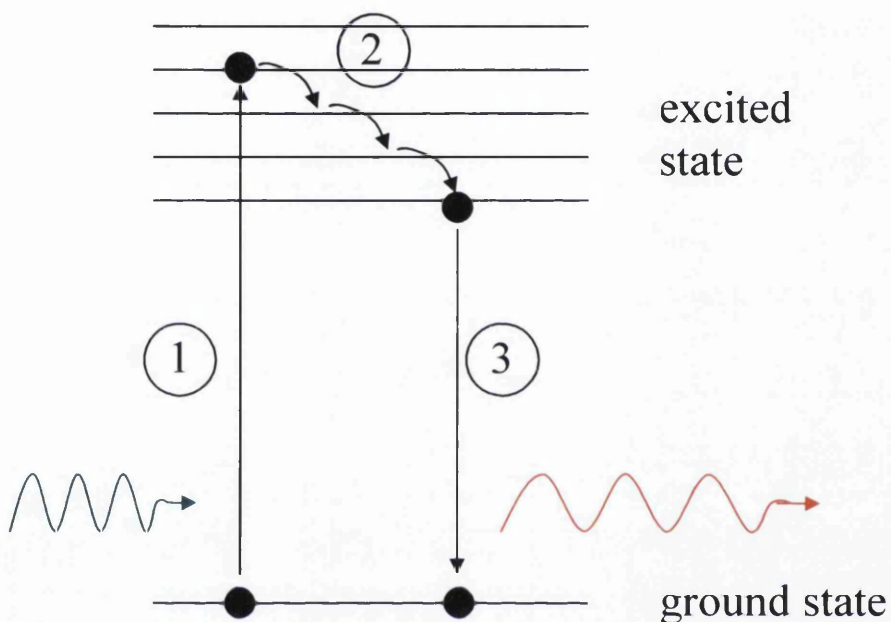


Figure 3-2: Jablonski-diagram of fluorescence emission (adapted from <http://icecube.berkeley.edu/~bramall/work/astrobiology/fluorescence.htm>).

In theory, a molecule can go through this cycle indefinitely, but a high intensity of excitation can destroy or partly disrupt the molecule by overheating it (Hibbs, 2004). The molecule may then not fluoresce anymore. This process is called photo-bleaching (*ibid*).

The spectrum of molecular fluorescence emission is within the visible light range, which makes it very easy to use for imaging purposes.

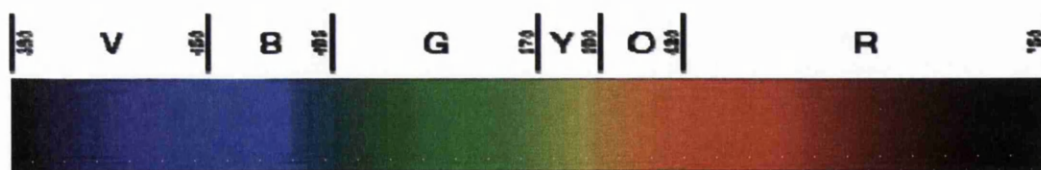


Figure 3-3: Visible light spectrum from 380 nm (violet) to 750 nm (red) (adapted from <http://de.wikipedia.org/wiki/Lichtspektrum>).

Many natural materials have the ability to fluoresce. Commonly all molecules with large conjugated π -electron systems or double bonds can fluoresce as the ground and lowest excitation state are relatively close in these systems so that the energy input required for excitation is modest. Such π -bonding occurs mainly between elements of the second period like C, O and N (Riedel, 1999).

In contrast to the spontaneous occurrence of fluorescence in molecules, the so-called auto-fluorescence, special fluorophores also can be introduced. These fluoresce when bound to target molecules. Ideal fluorophores do not fluoresce in the unbound state or at least change the wavelength of fluorescence after binding.

Fluorescence spectroscopy has been applied to investigate humic matter extracts from aquatic and soil environments. The technique does not provide detailed structural information due to the heterogeneity of humic matter, but can be used for comparison of humic matter from different origins and for distinguishing between fulvic acid (FA) and humic acid (HA) (Ewald et al., 1983). Although fluorescence only accounts for a part of the organic matter it can be of considerable interest as it can be measured non-destructively and under ambient conditions (Alberts et al., 2004).

The mostly widely used excitation wavelength is 340 nm emission and emission wavelengths are captured between 240 and 600 nm. It is assumed that if the wavelengths of the emission maxima of humic substances are similar, then also their condensed structures are similar and they have a similar molecular weight (Bayer et al., 2002).

HA extracted from soil shows a low intensity emission profile with a broad maximum at 510 nm. This is typical for systems with a high degree of conjugation, e.g. condensed aromatic ring and unsaturated bond systems, and the presence of electron withdrawing groups like carbonyl and carboxyl species (Chen et al., 2002).

It is known that aquatic FA have a lower maximum emission wavelength than HA, which is associated with the reduced proportion of aromatic structures, a lower molecular weight and the presence of electron donating groups like hydroxyls and methoxyls (Chen et al., 2003; Alberts et al., 2004).

The fluorescence intensity of FA is higher than that of HA: although the higher molecular weight of the latter means that probably more conjugated systems are present the large molecules also tend to re-absorb the fluorescent light (Alberts et al., 2004). Also, HA with a low degree of humification show stronger fluorescence than those with a high degree of humification (Bayer et al., 2002).

Apart from decreasing with increasing molecular weight of the compounds, the fluorescence intensity also is lower for solutions with lower pH and increasing ionic strength (Chen et al., 2003). It is known that spectra of aromatic compounds with basic or acidic functional groups are pH sensitive. An increase in ionization of phenolic hydroxyls with increase in pH causes a decrease in particle association and leads to decoiling of macromolecular structures, e.g. the disruption of inter- and intramolecular hydrogen bonds. This lowers the molecular weight of the compounds and increases fluorescence intensity. However, the pH did not influence the maximum emission between 350 and 450 nm (Chen et al., 2003).

However, commonly used fluorescence spectroscopy can only be applied to liquid samples and gives no information about spatial fluorescence distribution. The LSCM, however, is able to image solid samples and no extraction procedures are necessary. The high spatial resolution allows specimen fluorescence to be mapped (Hibbs, 2004).

Literature on soil water repellency suggests that apart from the chemical nature of organic material present in soils, the conformation and distribution of organic

material might be of importance for the expression of water repellency (e.g. Doerr et al., 2000a; Ellerbrock et al., 2004). Particle coverage with fluorescent material may give insight into relationships between particle coverage and water repellency or other relevant parameters.

LSCM imaging of soil samples was, therefore, chosen here as one promising method to gain information about organic matter distribution and possibly structural information from the organic matter on the individual particle scale. Detailed examination of fluorescence may help to gain information about distribution of organic matter as well as structural information as only certain organic matter fractions will exhibit fluorescence. The LSCM additionally gives the possibility of fluorescence spectral analysis. However, this is not very detailed as it does not work continuously, but only captures separate wavebands.

In order to investigate soil particles with LSCM, the general applicability of the method was tested, and the reproducibility and repeatability of quantitative fluorescence measurements was evaluated. This is described in the first part of this chapter. The second part of the chapter is concerned with the application of the method to various different soil samples. Therefore, various parameters were selected and analysed: the amount of total fluorescence on a particle and within a multi-particle specimen was used as a simple quantitative measure. Additionally, several qualitative measures, such as coverage of the particle with fluorescing material, the size and number of fluorescent areas on the particle surface were investigated. These were investigated with respect to bulk soil properties like soil water repellency, as the distribution of organic matter on soil particle surfaces has repeatedly been suggested to have an impact on soil water repellency.

3.2 *Materials and methods*

The process of scanning the laser over the selected area, exciting the sample and collecting the resulting fluorescence emission is here referred to as ‘imaging’, irrespective of whether or not the data were used to produce an image of the specimen or to quantify aspects of its fluorescence.

3.2.1 *Samples and sample preparation*

Individual soil particles (~100 – 300 μm) were randomly picked, from a selection drawn from the bulk soil sample, and glued to a microscope cover slip ($22 \times 22 \text{ mm}^2$ and thickness 0.19 – 0.23 mm) using waterproof cyanoacrylate adhesive (Anglin’ glue, Fishermans choiceTM). Depending on further use of the particles, either one particle or a row of several particles was immobilized in this way. A second thinner coverslip ($22 \times 22 \text{ mm}^2$, thickness 0.08 – 0.12 mm) was equipped with two thin strips of acetate sheet along two edges of the same face. This was used as removable cover for the particle-bearing slip. The two acetate strips served as spacers of sufficient thickness to ensure that the particles did not touch the removable cover (see Figure 3-4a). This setup was necessary in order to protect the particles from contacting the immersion oil used as coating for the objective lens of the LSCM instrument. Particles were imaged through this thinner cover slip to preserve the specimen, intact, for re-examination following further treatment or storage.

At least two layers of particles evenly distributed over the glass base of a specimen tray so that it appeared to be completely opaque were used to image the fluorescence of bulk (multi-particle) specimens (see Figure 3-4b).

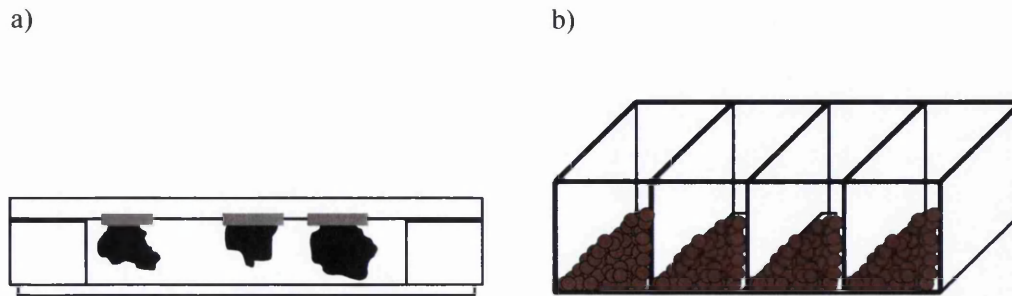


Figure 3-4: Sample preparation. a) for individual particles and b) for multi-particle specimens of at least two layers (only used in method application).

Soil samples NL2 and NLC, AWS, Lecithin coated AWS and the standard prepared slide #3 (FluoCells® mouse kidney section with Alexa Fluor® 488 WGA, Alexa Fluor® 568 phalloidin, DAPI, from Invitrogen) were used for method testing. For details on the samples refer to chapter 2, table 2-2. For all other experiments various samples were used which are also described in chapter 2, table 2-2, and the relevant sections in this chapter, including extracted soil samples and such samples to which the previously extracted material was re-applied quantitatively (which are referred to as “re-applied” samples, cf. chapter 2).

3.2.2 General LSCM settings

Examinations were performed using a LSM 510meta (Carl Zeiss, Jena, Germany) and the proprietary LSM 510 software. Samples were irradiated with light from a He/Ne-laser ($\lambda_E = 543$ nm) and an Ar-laser ($\lambda_E = 488$ nm). The He/Ne-laser was used at 100 % output (1 mW) and the Ar-laser at 3 % and 82 % of its maximum output (30 mW). The manufacturer recommends use of the He/Ne-laser at 50-100 % and of the Ar-laser at 1-3 % output. The 82 % output was used for comparison and possible improvement in auto-fluorescence imaging of soil samples.

The instrument parameters and settings like contrast, pinhole opening, resolution and number of scans were partly adjusted by trial and error, for both the He/Ne-laser and the Ar-laser and are shown in Figure 3-5a and b, respectively. They were chosen in order to reach an optimum compromise between image quality and acquisition time. These settings were then used for acquisition of all subsequent images of auto-fluorescence from soil particles.

In addition, a transmitted light monochrome image of each particle was captured using light from an Hg discharge lamp (the so called ChD-channel on this type of microscope) in order to obtain information about the general shape and size of the particle. From this type of image it is possible to determine the surface area of the planar projection of the particle, using the software for calculating the surface area from the outline of the particle. This outline can be selected manually.

Inspection of images and data obtained by excitation of particles selected from soil sample NL2 were used to determine optimum instrumental parameters for comparison of images and data obtained from particles from various sources. This sample provides particles with mean diameters of ~ 0.27 μm and the entire particle was captured within the frame of the image. The sample has a TOC content of 5.9 g kg^{-1} which is in the midrange of those studied.

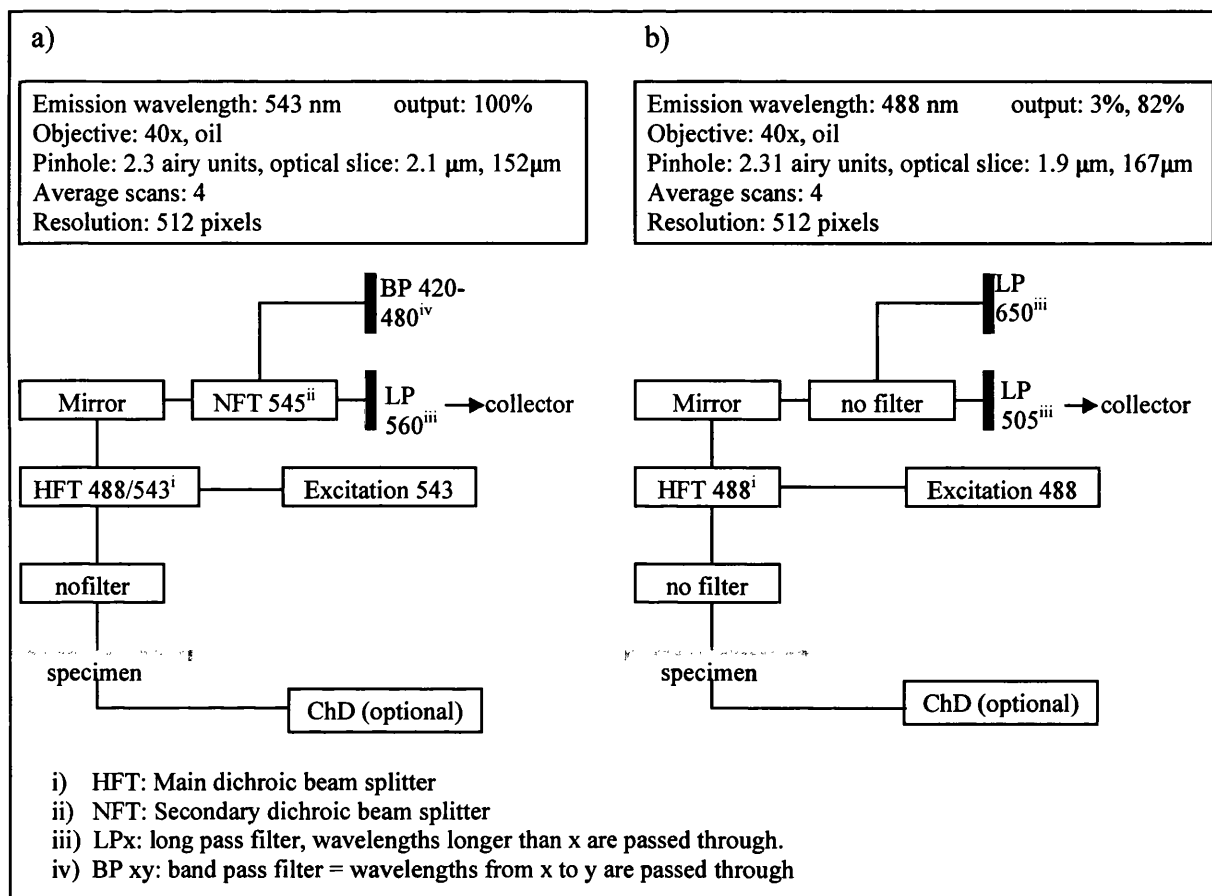


Figure 3-5: a) Laser settings for the He/Ne-laser at 100 % output intensity as used for all images.
 b) Laser settings for the Ar-laser as used for imaging at 3 % and 82 % output intensity.

Fluorescent images were obtained by scanning the laser across the plane of the particle close to the objective (the top, depth defined as 0) and then moving the plane of focus in 20 to 25 equally spaced optical slices z_i towards the particle bearing cover slip (depth z). These images were then assembled into a 3D projection using the associated software. Intensity data, obtained for each optical slice, were exported in ASCII format for further calculation.

Intensity data were provided in the form of the number of pixels per image. This is the frequency (f_a), with a certain absolute intensity (I_a) in the range of 0 to 255 for a monochrome image at 8 bit resolution from black to white (an example of such an array is given in Table 3-1). The cumulative frequency or fluorescence intensity per optical slice ($f_{cum,z}$) was then calculated:

$$f_{cum,z} = \sum f_a \cdot I_a \text{ with } I_a = (0, 1, 2, \dots, 255) \quad (3-1)$$

Table 3-1: Number of pixels at various intensities (0-255) obtained from fluorescence of an optical plane of a particle from soil NL2.

I_n	f_n	I_n cont.	f_n	I_n cont.	f_n	I_n cont.	f_n	I_n cont.	f_n
0	528972	52	735	104	151	156	46	208	32
1	86588	53	737	105	156	157	48	209	23
2	53674	54	675	106	156	158	43	210	34
3	41246	55	657	107	118	159	50	211	27
4	33848	56	640	108	133	160	47	212	25
5	28522	57	602	109	136	161	58	213	19
6	24648	58	564	110	165	162	40	214	17
7	21262	59	566	111	121	163	42	215	28
8	19063	60	515	112	128	164	42	216	21
9	16468	61	524	113	126	165	53	217	27
10	14736	62	502	114	117	166	40	218	17
11	13037	63	561	115	113	167	39	219	22
12	11907	64	473	116	116	168	42	220	22
13	10809	65	460	117	123	169	44	221	24
14	9674	66	446	118	105	170	36	222	28
15	8756	67	422	119	104	171	38	223	22
16	8026	68	410	120	90	172	43	224	21
17	7251	69	390	121	94	173	41	225	20
18	6825	70	396	122	112	174	35	226	17
19	6119	71	374	123	90	175	36	227	19
20	5523	72	359	124	82	176	41	228	21
21	5129	73	344	125	85	177	39	229	19
22	4844	74	337	126	102	178	34	230	13
23	4333	75	329	127	90	179	27	231	24
24	4032	76	299	128	85	180	35	232	24
25	3701	77	310	129	96	181	31	233	11
26	3355	78	291	130	98	182	27	234	19
27	3266	79	292	131	71	183	27	235	17
28	2960	80	293	132	91	184	25	236	21
29	2662	81	253	133	91	185	30	237	16
30	2558	82	275	134	76	186	28	238	21
31	2334	83	245	135	88	187	40	239	18
32	2233	84	235	136	63	188	34	240	16
33	2097	85	227	137	72	189	45	241	17
34	1902	86	242	138	68	190	31	242	10
35	1826	87	223	139	67	191	17	243	15
36	1732	88	224	140	55	192	26	244	11
37	1642	89	219	141	83	193	32	245	12
38	1581	90	229	142	50	194	23	246	18
39	1400	91	207	143	75	195	33	247	16
40	1339	92	238	144	68	196	27	248	18
41	1282	93	190	145	64	197	29	249	13
42	1193	94	183	146	54	198	26	250	12
43	1106	95	171	147	54	199	22	251	10
44	1038	96	157	148	78	200	34	252	12
45	1041	97	216	149	68	201	25	253	12
46	1005	98	178	150	60	202	23	254	15
47	913	99	158	151	52	203	24	255	230
48	883	100	156	152	47	204	20		
49	860	101	138	153	57	205	18		
50	758	102	159	154	45	206	31		
51	787	103	154	155	45	207	23		

From this the total intensity of a z-stack ($I_{I,0}$) was calculated as:

$$I_{I,0} = \int_0^z f_{cum,z} \quad (3-2)$$

A numerical (cubic spline) integration routine was used for calculation (Schwarz et al., 1986).

For convenience all values were scaled by the factor 10^{-6} so that all reported values I_I are defined as:

$$I_I = I_{I,0} \cdot 10^{-6} \quad (3-3)$$

3.2.3 Emission wavelength distribution

An additional facility on the LSM 510meta is the so called meta-mode. This allows the fluorescence to be examined in a maximum of 32 channels each receiving a discrete waveband of the emission spectrum and providing an associated image. The maximum fluorescence is available through inspection of the emission spectrum or the images. Composite overlays of images and examination of selected regions allow examination of features of the local spectrum of potential use in characterizing the specimen.

The laser used to excite the sample was the diode (DAPI) laser at 405 nm and at 21 % output intensity with a pinhole opening width of 896 μm . Two different sets of filters were used: HFT406/514 and NT80/20. The HFT406/514 has the disadvantage of cutting out the waveband of 514 nm, but its colour coding seemed to better reflect the actual wavelength distribution of the sample; therefore, both settings were investigated.

Particles from untreated and processed samples (acid washing, IPA/ NH_3 extraction, base washing or oxidising) were imaged using meta-mode.

3.2.4 Fluorescence coverage

The area of a soil particle that emits fluorescence was estimated as follows: the images comprising a z-stack were exported from the proprietary software in bitmap format. These were examined off-line. A region of the image, outside of the particle perimeter was selected to provide a reference of the minimum pixel brightness. All pixels in the range of brightness 0-30 % were then counted to provide the population considered to be background (n_b), represented as red area in Figure 3-6b. Pixels with a brightness in the range of 31-100 % were considered to reflect the presence of fluorophores with a total population n_F .

As the total pixel population in the image (n_T) and the physical area (A) of the specimen represented by the image were known, the fluorescent area of the image A_F was:

$$A_F = (n_T - n_b) \frac{A}{n_T} \quad (3-4)$$

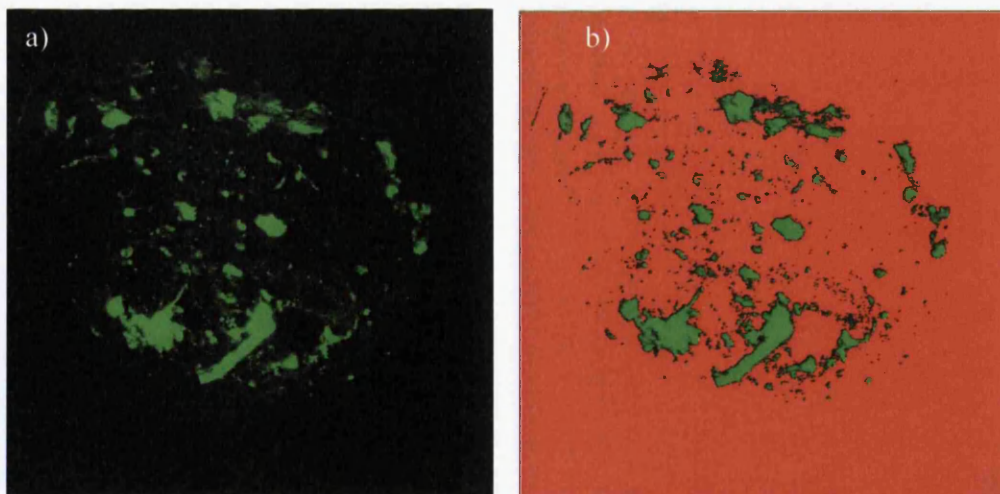


Figure 3-6: a) z-stack projection of soil particle b) selected background (automatically detected after choosing a background pixel) in red for coverage determination.

The projected area of the particle (A_p) was determined directly from an image of the particle in reflected light (the ChD image) obtained with the LSCM. This provided

an estimate of the proportion of projected particle area covered in fluorophores (C_F) as follows:

$$C_F = \frac{A_F}{A_p} \cdot 100 \quad (3-5)$$

The determination of C_F involves the subjective selection of the threshold brightness. The approach used here tends to minimise the consequent variation associated with the various images inspected to guide selection. There is at least some internal consistency at this level, due to the use of standardised parameters.

3.2.5 Number of fluorescent areas

The distribution of (fluorescent) heterogeneous organic material on a soil particle surface is unlikely to be uniform and may be distributed in various ways (e.g. Doerr et al., 2000a) in both large and small patches. The number of fluorescent areas N_F detected on particles may be a measure for this. Areas of pixels above a certain threshold were defined as a pixel group and counted. The intensity threshold used was set to a value of 30. The software then highlights these areas in the image. Figure 3-7a and b also show a comparison between pixel counting methods and the identification of area of fluorescence. The outcomes are, in essence, identical.

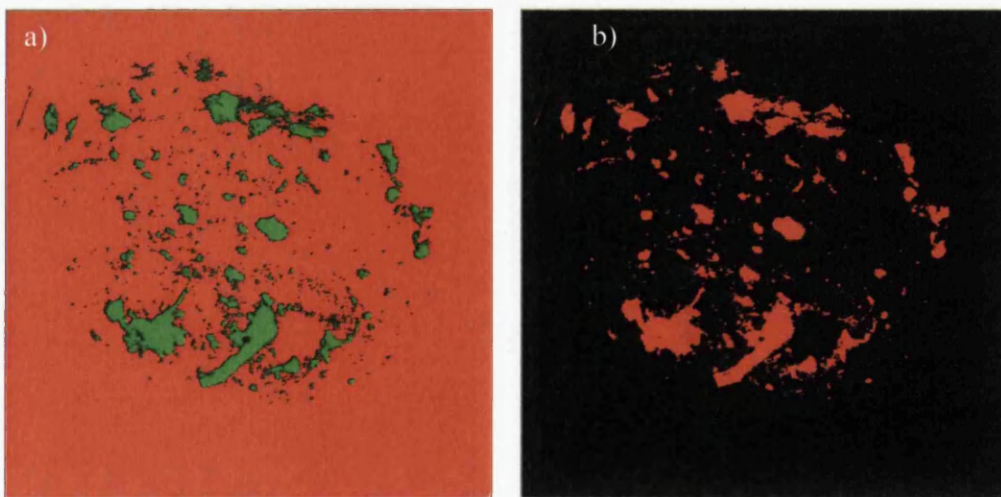


Figure 3-7: a) Selected image background b) fluorescent regions highlighted for N_F determination.

3.2.6 Size of fluorescent areas

An additional subjective measure for the size of individual fluorescent areas (a_F) was introduced in order to estimate the manner in which fluorescent material is distributed on the particle surface. It was decided, by optical inspection of the images, whether the majority of fluorescent regions were small, medium or large in size. In many cases a mixture of two size categories was found so the classes were subdivided to small/medium or medium/large. In some cases a mixture between small and large sized regions was found. Each size class was assigned a numerical rank:

1 – small

2 – medium

3 – large

and for mixtures of size classes : 1.5 – small/medium

2.5 – medium/large

For the few cases where a mixture of large and small areas occurred, a value of 2 (medium) was used. However, this was only necessary for five particles out of 120 examined (1 from AUC, 3 from PT2 and 1 from PTC).

3.2.7 Fluorophore application to soil particles

LSCM can also be used for imaging fluorescence emitted from artificially introduced fluorophores or fluorescent dyes. These are molecules, with known excitation and emission wavelengths, which ideally do not fluoresce in an unbound state and only emit light after excitation when bound to a target functional group. Many such fluorophores exist for cell biological investigations. Most are designed to target binding sites in DNA, RNA or proteins within cells and have the ability to penetrate rough membranes or other cell barriers (Haughland, 2005).

In this study five different fluorophores were tested and their maximum emission and absorption wavelengths are shown in Figure 3-8: Nile red; carboxyfluorescein; pyrene-1-carboxylic acid; rhodamine B and fluorescein isothiocyanate (FITC). All of

them, except Nile red, require intensive sample preparation (details given below) in order for the molecule to bind to the sample. All dyes interact in a different way with parts of the organic matter, e.g. FITC attaches to protein groups via the amino group and carboxy fluorescein acts as H donor in reactions. Detailed binding mechanisms of these dyes are discussed in Haughland (2005).

The intensive sample preparation may present the limiting step for the application in soil science as prolonged contact of dye solutions with soil particles may mobilise and remove organic coatings from particle surfaces, especially as methanol is used as a solvent. (Alcohol solutions are often used for soil extraction procedures, e.g. Roberts et al., 1972 or McGhie et al., 1980.)

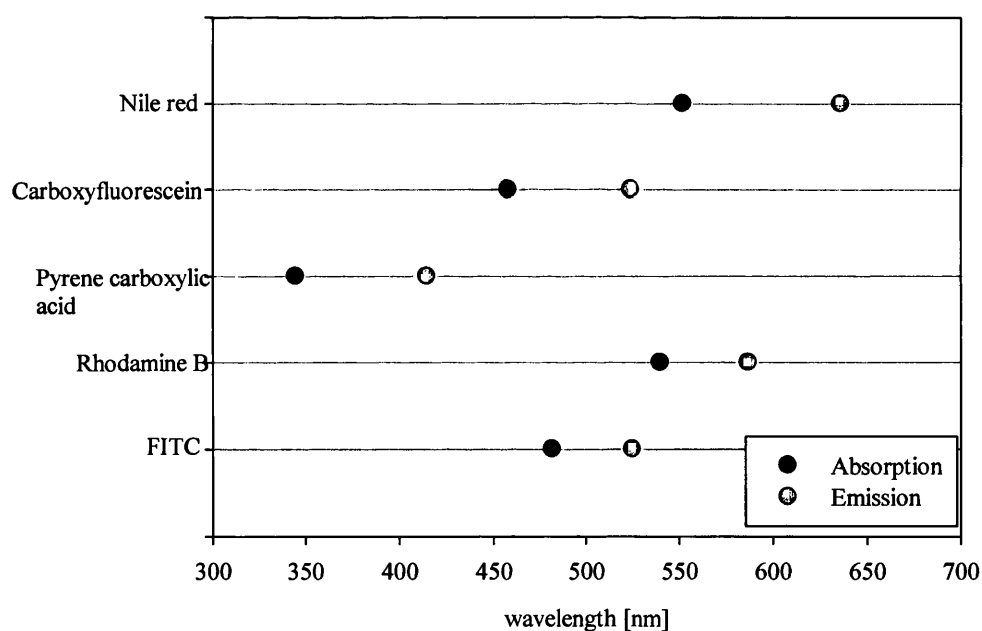


Figure 3-8: Maximum emission and absorption wavelengths. Based on Haughland (2005).

All artificial fluorophores were used at a solution concentration of 1-5 μM , which was subsequently diluted further up to 10^3 times. Nile red was dissolved in water, all

others in methanol. The following preparation steps were carried out for all dye solutions apart from Nile red.

1 g soil sample NL2 was mixed with 100 ml dye solution and shaken for 24 h in a methanol solution at $\text{pH} > 7$. The solution was then decanted and the soil sample washed with methanol and water to remove remaining non-bound dye. Samples were left to air-dry for 24 h at $\sim 20^\circ\text{C}$.

The application of Nile red was easier as it does not fluoresce when dissolved in polar solvents like water, but only when bound to lipids. Thus no removal of excess dye was necessary. The solution was dripped directly from a pipette on to the soil particles and left to dry.

Table 3-2 summarizes the LSCM imaging parameters used for samples enriched with fluorescent dyes.

Table 3-2: Excitation wavelength λ_E , output intensity, pinhole size, filters and beam splitter settings for different fluorescent dyes.

Dye	λ_E [nm]	Output intensity [%]	Pinhole [μm]	Filter ⁱ	Beam splitter ⁱⁱ
carboxyfluorescein	458	53	86	HFT 488	LP 505
pyrene carboxylic acid	405	20	55	HFT 405/514	LP 420
Rhodamine B	543	50	72	HFT 488/543 NFT 545	LP 560
FITC	488	2	66	HFT 488	LP 505
Nile red	543	51	167	HFT 488/543	LP 560

i) HFT: Main dichroic beam splitter; NFT: Secondary dichroic beam splitter.

ii) LPx: long pass filter, wavelengths longer than x are passed through

3.3 Results from testing LSCM for soil particle investigations

All available lasers were tested for auto-fluorescence imaging of soil particles. Initial tests showed that the He/Ne-laser with an emission wavelength of 633 nm did not induce or only very weakly induced auto-fluorescence in soil particles so that image quality was too poor for evaluation. The DAPI-laser, commonly used at 8 % output intensity for an emission wavelength of 405 nm, did induce fluorescence, but image contrast and resolution are also too low for data evaluation (see Figure 3-9c).

Both the He/Ne-laser, with emission wavelength of 543 nm, and the Ar-laser, with emission wavelength of 488 nm, induced high levels of auto-fluorescence in the samples and so images of high contrast and quality were obtained (see Figure 3-10). However, generally some differences existed for fluorescence intensity and fluorescence distribution on particles imaged by the different lasers (Figure 3-9 and Figure 3-10). The images obtained using the He/Ne-laser show a stronger fluorescence emission and often a more network-like distribution on the particle surface. This led to the decision to use both the Ar-laser and He/Ne-laser for all further imaging.

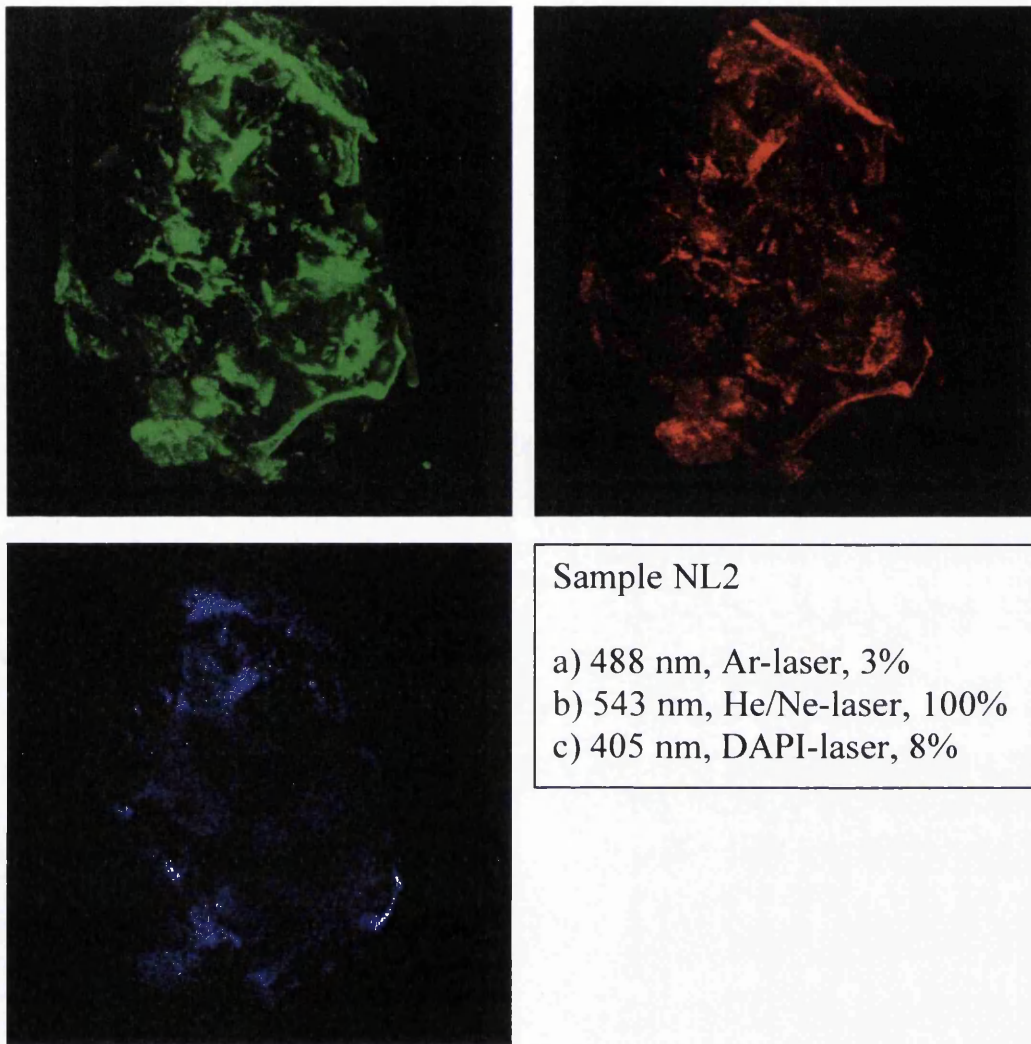


Figure 3-9: Images of a particle from soil sample NL2 obtained using illumination at various excitation wavelengths.

All NL and AU samples had mean diameters between 0.22 and 0.29 mm, so most of their particles were captured within the frame of the image (see Figure 3-9a and b and Figure 3-10c and d). However, particles from GK, PT and UK samples were generally larger than the optical field so that only sections of the particles were imaged (see Figure 3-10a and b).

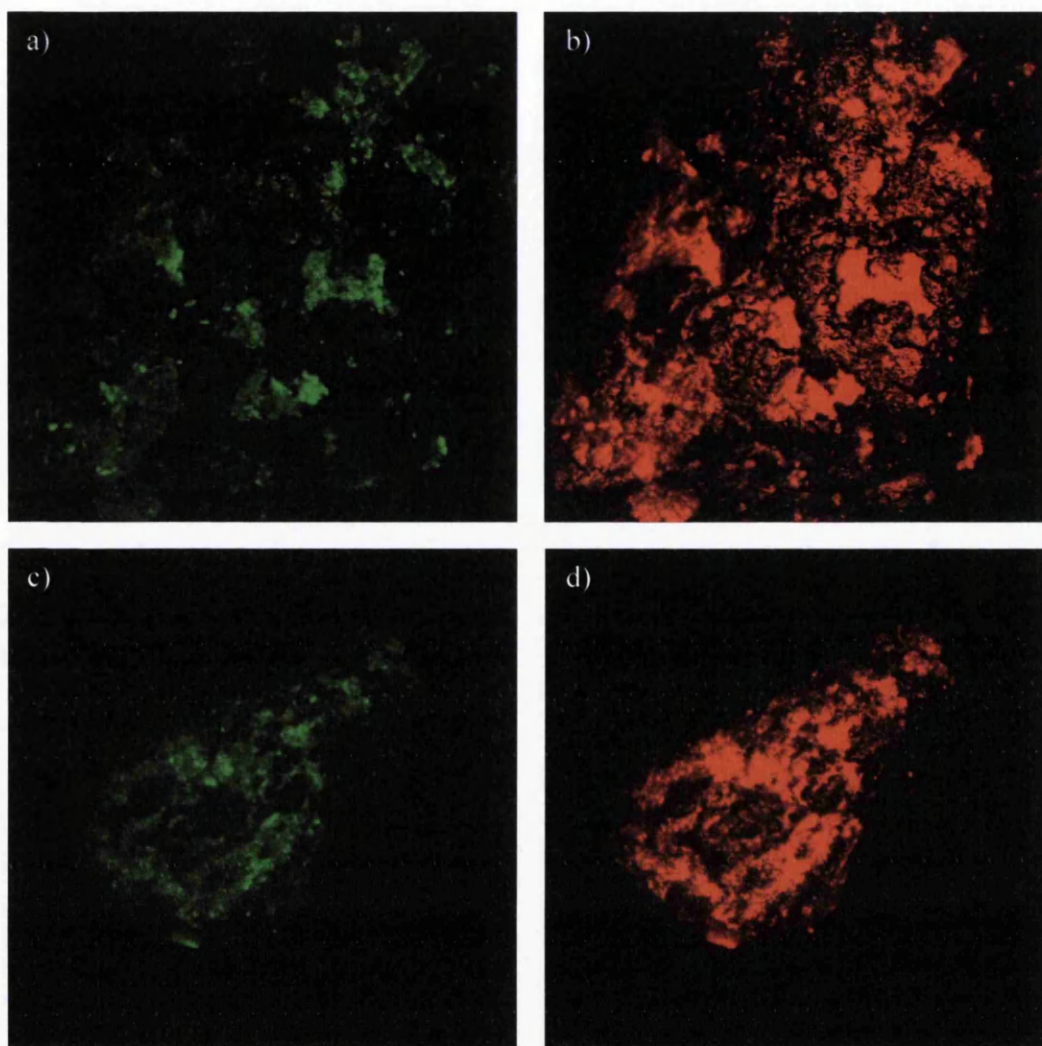


Figure 3-10: Images of particles from samples UK1 (a and b) and AU2 (c and d) excited with an Ar-laser at 3 % output intensity (a and c) and a He/Ne-laser with output intensity of 100 % (b and d).

3.3.1 Removal of organic matter

In order to determine whether the cause and nature of the auto-fluorescence arises from the presence of organic material on the particle or perhaps the mineral itself, soil particles and particles following removal of organics by oxidation (cf. section 2.4.2 for experimental details) were examined (Figure 3-11).

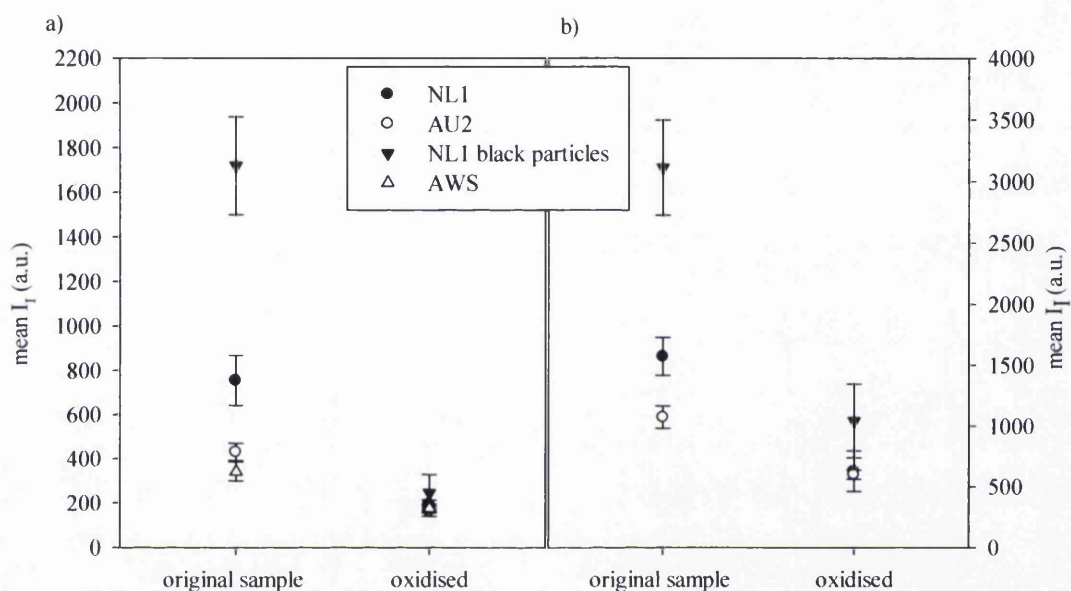


Figure 3-11: Background auto-fluorescence of natural and oxidised particles with a) Ar laser, 3 %, and b) He/Ne-laser, 100 %.

Mean values of I_f , obtained from a minimum of 10 particles per sample, irradiated with the Ar-laser fell in the range 300 – 1700, whereas those of oxidised particles fell in a narrow range ~200 (see Figure 3-11a). Similar data for irradiation with the He/Ne-laser fell within the range 1000 – 3000 for original sample material and 500 – 1400 for the oxidised form (see Figure 3-11b).

The black particles drawn from NL1 were assumed to be composed mainly of organic material, due to their extremely strong fluorescence and the fact that oxidising the sample removed all black particles.

The relative reduction of fluorescence for the He/Ne-laser is smaller than for the Ar-laser for all samples (NL1: 75 vs 60 %, NL1 black particles: 86 vs 66 %, AU2: 63 vs 44 %, with the percentage indicating the reduction of fluorescence when imaging with the Ar- and He/Ne-laser, respectively).

3.3.2 Laser and fluorescence stability

The stability of the fluorescent signal was investigated by repeatedly imaging one focal plane of a sample over a time period of 10 minutes, which is twice as long as the time needed to image a z-stack of a soil particle as described above.

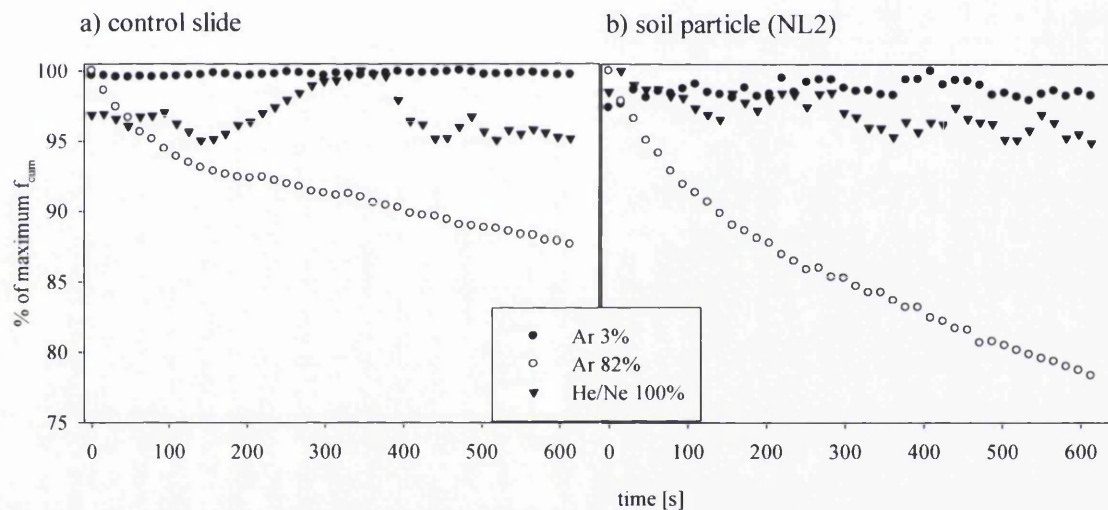


Figure 3-12: The proportion (%) of the maximum fluorescence of one focal plane over 10 minutes for a) standard control slide and, b) soil particle (NL2).

The fluorescence of a standard test slide of a mouse kidney section (Sigma, UK) when irradiated with the Ar-laser at 3 % intensity fluctuated less than 2 %, but using the same laser at 82 % intensity resulted in a decrease in fluorescence over the imaging period of about 12 %. The fluorescence, when using the He/Ne-laser, showed fluctuations of about 5 % but a maximum of fluorescence after 350 s (see Figure 3-12a).

The fluorescence fluctuations from a soil particle over the time period of 10 minutes were similar for both the Ar-laser irradiation at 3 % intensity and irradiation with the He/Ne-laser at ~2.5 % and ~5 % intensity, respectively. Irradiation with the Ar-laser at 82 % reduced fluorescence by 20 % of the original value over the 10 minute interval (see Figure 3-12b), which is rather more pronounced than for the standard test slide.

Reduction in the fluorescence of lecithin coated acid washed sand (AWS) particles was found to be more affected by the imaging procedure than natural soil particles:

- i) the total fluorescence fluctuations during imaging of a time series were twice as high as for natural soil particles;
- ii) the total decrease of fluorescence when imaged with the Ar-laser at 82 % output intensity was also higher than for the natural soil particle (around 35 % of the maximum value compared with 25 % for the soil sample) (see appendix A).

Particles from AU and NL samples were generally small enough to fit within the optical field of the 40x objective. Objective lenses of lower magnification (10x and 20x) which do not need to be immersed in oil provide a larger field of view suitable to accommodate larger particles. Prolonged irradiation of particles from soil sample NL2 with the Ar-laser at 3 % via the 20x objective showed larger fluctuations (~4 %) than particles irradiated via the 40x objective. Use of the 10x objective resulted in an overall decrease of fluorescence of ~9 %, but with a pronounced periodicity of ~150 s (Figure 3-13). When the 10x objective was used in combination with the He/Ne-laser, fluctuations were even stronger, being up to 55 %. The fluctuation observed when using the 20x objective with the He/Ne-laser were also stronger than when used with the Ar-laser (see appendix A).

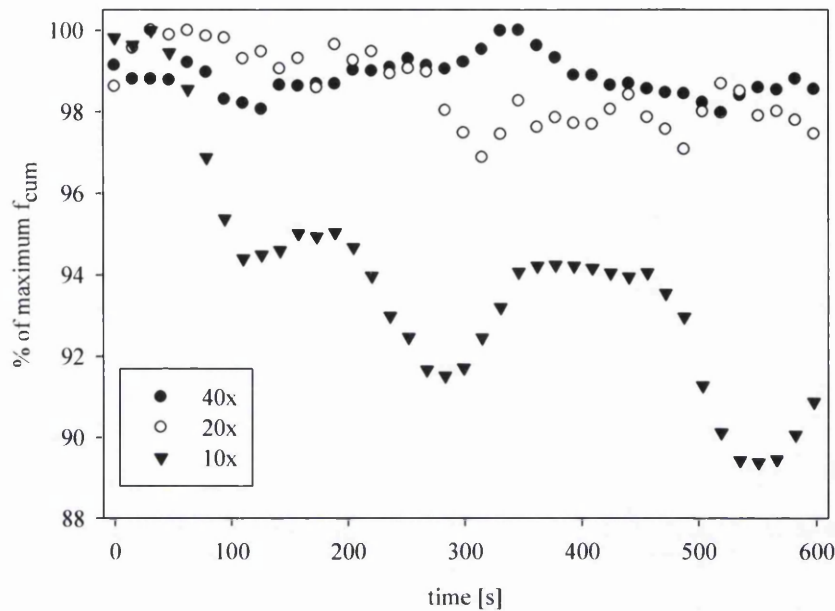


Figure 3-13: Proportion (%) of f_{cum} as a function of time for a particle from soil sample NL2, for irradiation with Ar-laser at 3 %, using various objective lenses.

3.3.3 Image repeatability and reproducibility

When a z-stack of images was obtained repeatedly from an individual particle, with an interval of 10 minutes between successive data capture, the fluorescent intensity ($f_{cum,z}$) at each focal plane in the z-stack was found to decrease with each cycle of data capture (Figure 3-14a). Over a period of 60 minutes, required for the operation, the largest variation occurred at the arbitrary zero focal plane ($f_{cum,z} = 9 \pm 2$ arbitrary units) and the smallest at $\sim 60 \mu\text{m}$ ($f_{cum,z} = 13 \pm 1$ arbitrary units). The comparison of the integral fluorescence over each z-stack showed a steady decline of $\sim 5\%$ over the five cycles of measurement (Figure 3-14b).

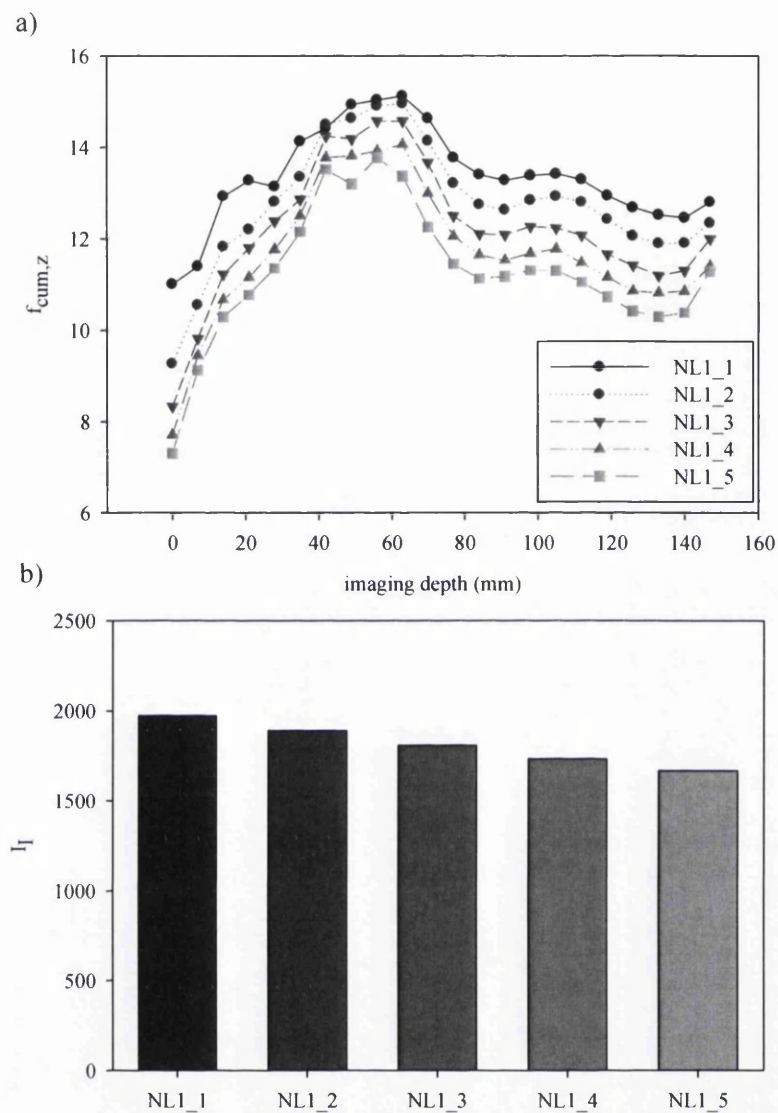


Figure 3-14: a) Fluorescent intensity $f_{cum,z}$ as a function of depth (μm) and, b) integral fluorescence I_f for 5 imaging cycles, using irradiation with the Ar laser at 3 %.

In order to investigate the influence of environmental storage conditions, the fluorescence of various particles before and after storage for 8 days in covered Petri dishes at $\sim 20^\circ\text{C}$ and $\sim 50\%$ RH as measured. These indicate a wide range of reproducibility (Figure 3-15). Acid washed sand particles showed generally similar levels of fluorescence to particles from NL2. In some cases fluorescence increased after 8 days and in others it did not. Lecithin coated AWS particles (label L) also showed this behaviour but generally from 3 to 4 times the levels of fluorescence and

stronger variation after 8 days (~40 % reduction for L1) in comparison with AWS (~30 % for AWS4) and NL2 (~20 % for NL2_3).

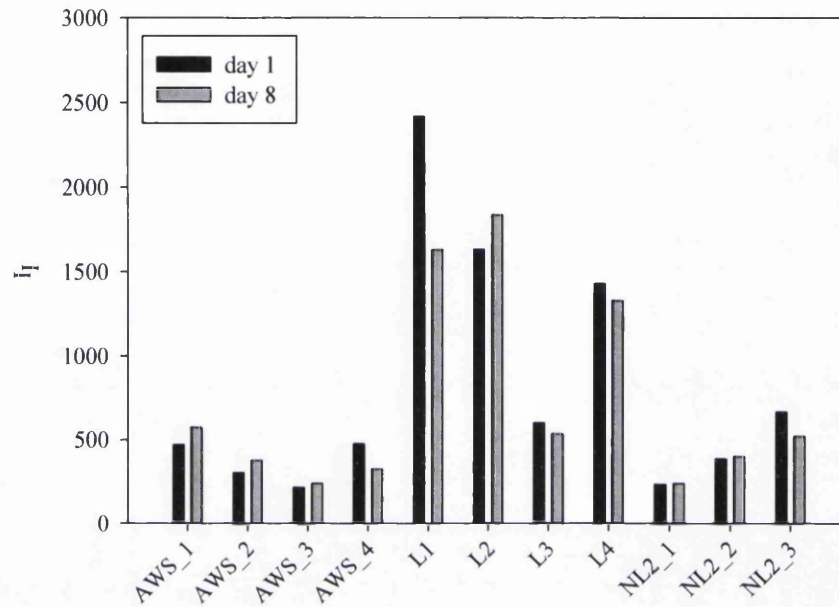


Figure 3-15: Fluorescence intensity I_f of individual particles imaged with Ar-laser at 3 % on day 1 and one week later on day 8.

3.3.4 Emission wavelength distribution

No significant differences were found between the emission wavelengths (λ_F) distribution of particles drawn from various soil samples. Some examples are shown in Figure 3-16.

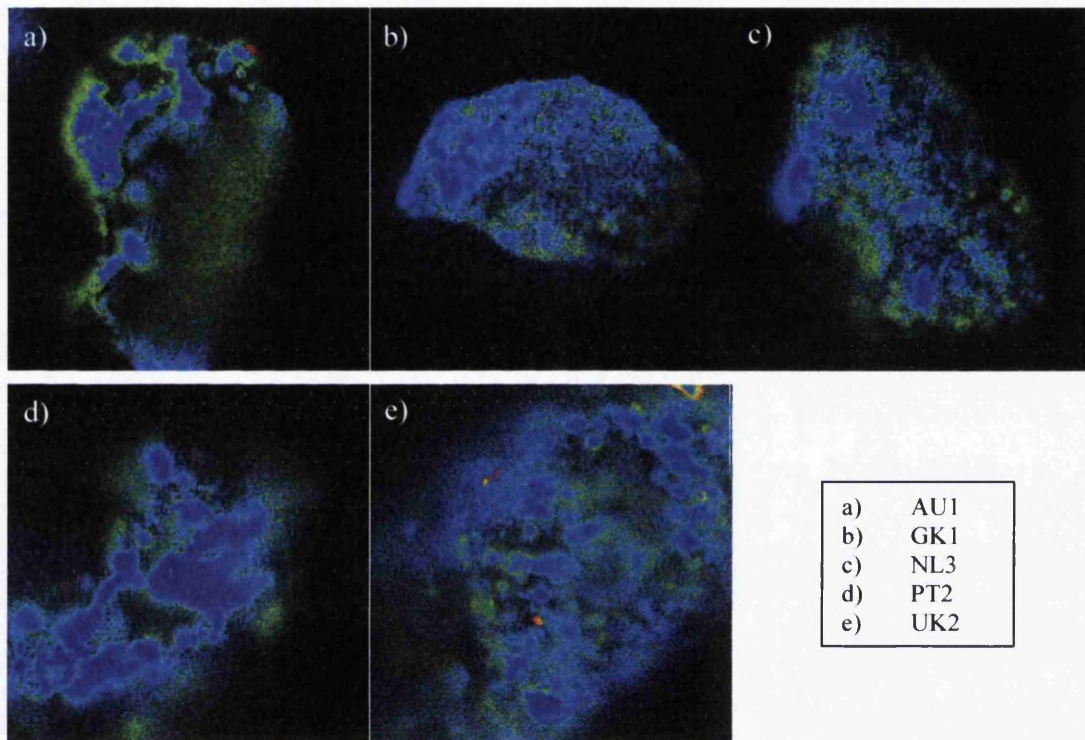


Figure 3-16: Overlay images of fluorescence from various emission wavebands (meta-channels) shown in (false) colour code (emission wavelengths are associated with colour of that wavelength), with main filter HFT 406/514.

Colours represent wave bands. Most particles have a high blue component, at $\lambda_F = 440 - 500$ nm (region of blue marker in Figure 3-17). However, when selecting regions, a strong component at $\lambda_F = 550$ to 630 nm (green to orange) was observed for all particles (as shown in the region of red markers in Figure 3-17), although this does not appear in the colour coded overlays. Information about wavelengths was taken from the emission waveband distribution directly in order to overcome the shortcomings of false colour images.

It is important to note that the reduced intensity at $\lambda_F \sim 514$ nm is probably due to the filter used (refer to section 3.2.3).

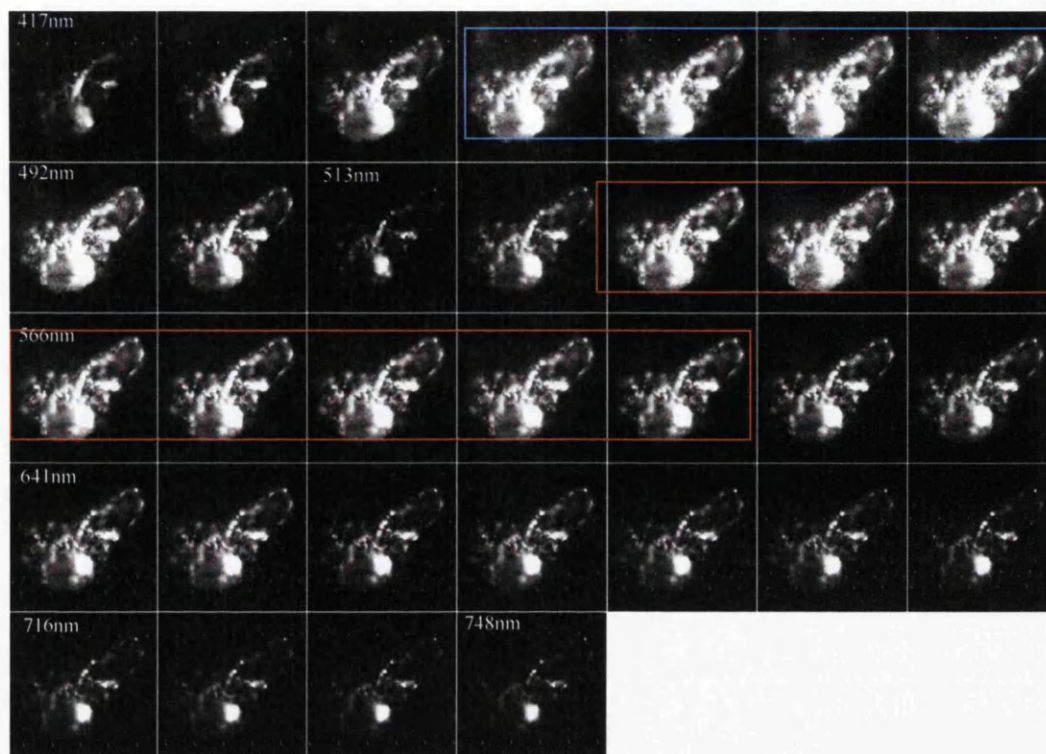


Figure 3-17: Series of images of increasing emission wavebands λ_E (top left to bottom right) with $\lambda_E = (417, 427, 438, \dots, 748)$ of particle from sample AU1. The filter HFT 405/514 was used.

Using a different filter (NT80/20) for meta imaging (which does not exclude $\lambda_F = 514$ nm) led to a similar λ_F distribution. The only difference was the wavelength 514 nm, which was present in these distributions (yellow square in Figure 3-18A). Therefore, the orange colour, dominating the colour coded images, is probably an artefact of the colour coding procedure (Figure 3-18B).

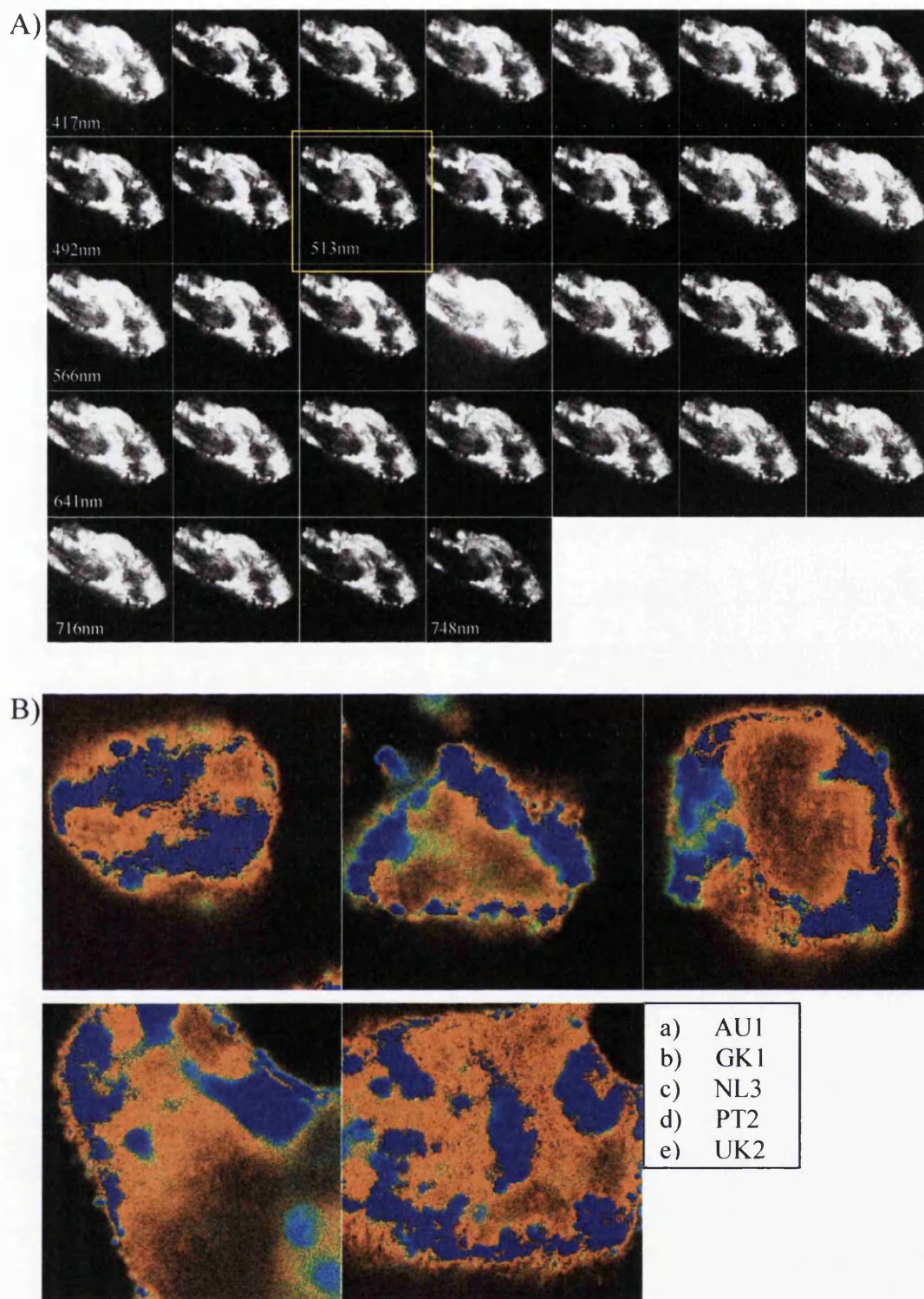


Figure 3-18: A) Series of images of increasing emission wavebands λ_E (top left to bottom right) with $\lambda_E = (417, 427, 438, \dots, 748)$ of a particle from sample AU1, filter NT 80/20. B) Overlay images of fluorescence from various emission wavebands shown in (false) colour code, using the filter NT80/20.

Most of the particles examined from most samples displayed similar fluorescent emission spectra and no significant distinction between samples could be made using this method. However, particles were encountered that showed significant differences with emission maxima at either shorter or longer wavelengths than most samples. Further examination of these particles showed that the associated emission was localized in distinct regions of the particle. Figure 3-19 shows examples of particles with average wavelength distribution (b and d from samples GK2 and PT2, respectively) and of those with distinctly different regions (a and c from samples GK2 and PT2, respectively).

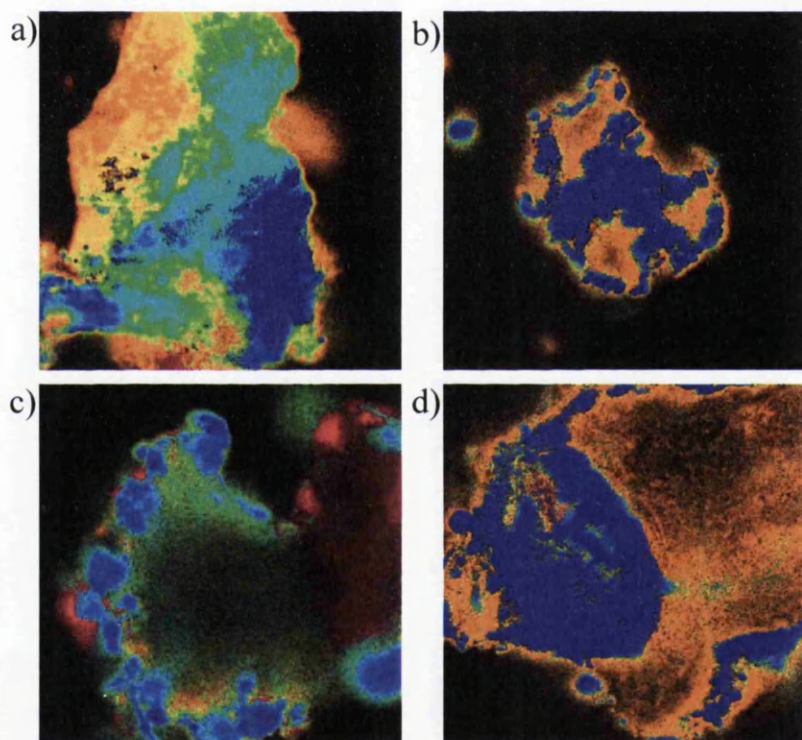


Figure 3-19: Colour coded overlays of wavelength distributions of a) and b) particles from GK2 and c) and d) of particles from PT2.

Acid washing of particles was found to remove the fluorescence maximum $440 < \lambda_F < 500$ nm (Figure 3-20a). Thermal oxidation reduced the particle fluorescence intensity to such an extent that in most cases it was impossible to obtain images using the meta mode. Particles still capable of providing fluorescent images

showed little or no maximum in the range of $550 < \lambda_F < 630$ nm (Figure 3-20d). The situation for particles treated with base was similar (Figure 3-20c), whereas particles extracted with IPA/ NH_3 , generally showed no change in comparison with the λ_F distributions of the original particles (Figure 3-20b).

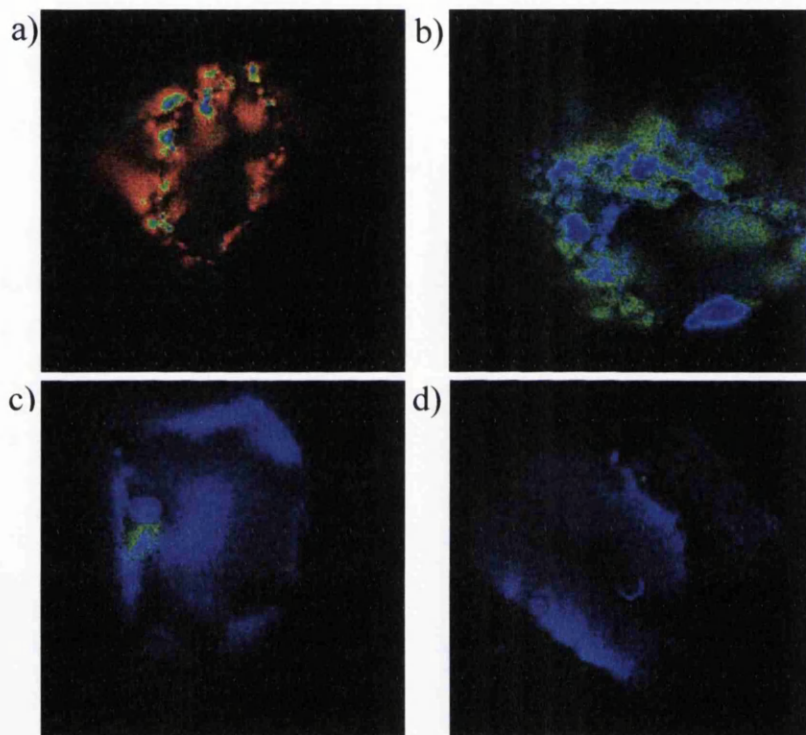


Figure 3-20: Colour coded overlays of wavelength distributions of particles from sample NL1 after a) acid washing, b) IPA/ NH_3 extraction, c) base washing and, d) thermal oxidation.

3.3.5 Fluorophore application

No increase or change in fluorescence intensity was measured for any sample enriched with the fluorophores carboxyfluorescein, pyrene carboxylic acid or FITC (see Table 3-3:). Probably too few binding sites were available within SOM for the dyes or prolonged shaking of the sample in the dye solution led to a removal of organic material from particle surfaces. The latter seems to be more probable due to the relatively insensitive binding mechanisms of the dyes: FITC not only binds to proteins via the amino groups, but also is used as agent for Fe(II) quantification (Zhu

et al., 2002); carboxyfluorescein acts as a H donor in reactions and pyrene carboxylic acid just acts like any carboxylic acid.

Although rhodamine B increased the fluorescence, it was not used for any further investigations due to the very strong increase in fluorescence. The images were very bright after application of rhodamine B, so that no details of the particle surface could be distinguished, even after diluting the dye solution 1:10. Due to the washing step during preparation, it was assumed that no free rhodamine B was available and only dye molecules attached/bound to the particle surface contributed to the strong fluorescence signal. The non-selective binding of rhodamine B was probably one of the main problems in the applications to soils. SOM offers many binding sites to the dye, leading to a relatively even distribution on the particle surface. Rhodamine B not only binds to a variety of functional groups within SOM (Onishi, 1957; Van Aman et al., 1959). Furthermore, the LSCM had to be used with settings similar to those used for imaging natural fluorescence arising from the use of the He/Ne-laser, so that an overlapping of the two fluorescence signal probably occurred.

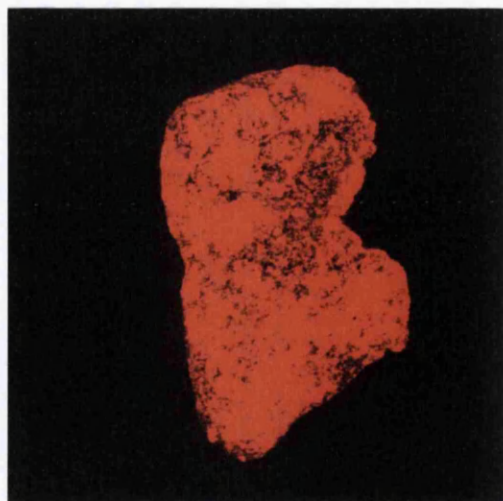


Table 3-3: Mean I_f of sample NL2 imaged with different settings according to dye (see methods section), without dye application and after dye application.

dye	mean I_f without dye	mean I_f with dye
Rhodamine B	616	1531
Carboxyfluorescein	370	330
Pyrene carboxylic acid	1110	1500
FITC	3940	4810

Figure 3-21: NL2 particle after labelling with Rhodamine B, imaged with He/Ne-laser, and settings for Rhodamine B.

The advantage of Nile red is its easy handling compared to other dyes (see methods section). This dye binds to proteins and can be applied directly to the sample without

any preparation as it does not fluoresce in polar solvents like water. This allows investigation of particles already fixed to glass slides, as part of the general specimen preparation procedure, before and after dye application. Two examples of particles imaged after Nile red application are shown in Figure 3-22.

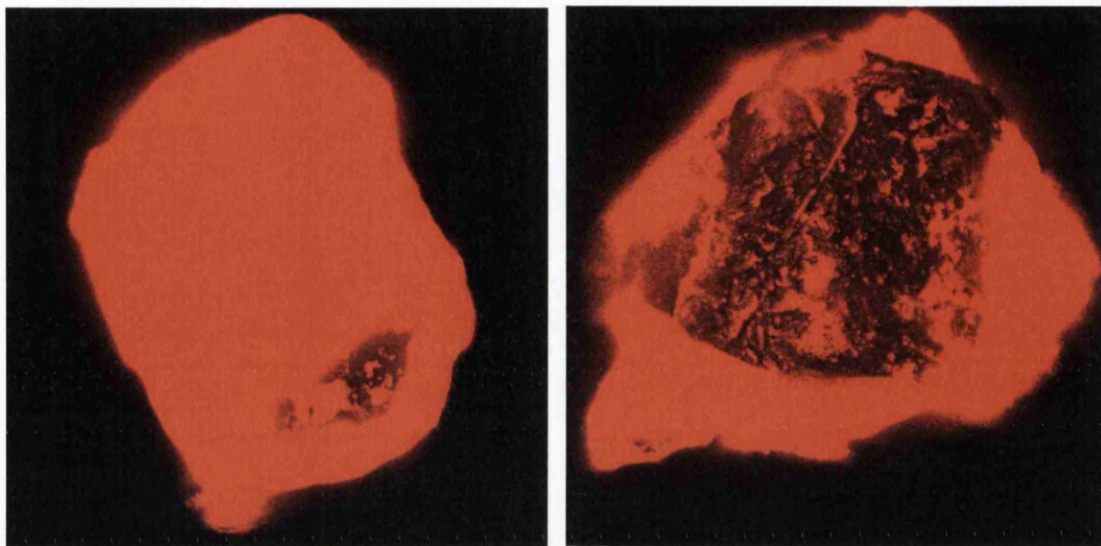


Figure 3-22: Particles from soil sample NL1 dyed with Nile red.

These emitted strong fluorescence and not much detail of the particle surface can be distinguished (Figure 3-22). I_f increased between three to ten times from that of the original particles ($I_f \sim 1200$) after dye application ($I_f \sim 7600$).

Due to the extremely high intensity and ubiquitous dispersion of fluorescence over the particles following Nile red application, no further investigations were carried out. The main problem with the use of such fluorophores, especially with uncharacterised specimens, appears to be the ubiquitous distribution of target binding sites. In the case of Nile red, these are available at any protein structures, which are common in soil organic matter (Scheffer et al., 2002).

3.4 Discussion of method testing

It is evident that examination of soil or other particles using LSCM provides information about particle size, shape and distribution of sites that auto-fluoresce. The natural organic coatings on soil particles consist of humic materials and large biomolecules possessing large conjugated electron and double bond systems. These are considered to be responsible for auto-fluorescence (Slavik, 1998). Lecithin, a relatively small bio-molecule containing double bonds has been shown here to auto-fluoresce on irradiation with laser light.

The data obtained here suggest that there are random variations of ~5 % in the quantitative fluorescence data held within a series of images obtained by repeated scanning of exactly the same specimen. This suggests that there is either

- i) instability in the intensity of the irradiating laser and/or
- ii) instability within the specimen.

The 20-30 % reduction in fluorescence, arising from use of the Ar-laser at 82 % output intensity, suggests that it induces instability in the specimen. The common use of this high output is to quench the fluorescence in biological specimens (to which fluorescent dyes have been added) in a process called photo-bleaching. This can be used for studying diffusion of dye molecules back to their binding sites. The intense radiation disrupts the bonds formed between target functional groups in the specimen and the dye and may even destroy bonds within the dye molecule itself (Slavik, 1998; Hibbs, 2004). The pronounced reduction in the auto-fluorescence of soil particles, observed following high intensities of laser irradiation, may arise from a similar mechanism of quenching. The more commonly used low irradiation intensities (1 mW with the He/Ne- and 3 % of 30 mW with the Ar-laser), for periods ~600 s seem to produce only random fluctuations (5-10 %) in fluorescence, rather than decline associated with photo-bleaching. The random fluctuations (~2 %), observed in data from the standard test slide, may be limited due to its uniform thickness. Biological specimens of non-uniform thickness may produce less precise data. Potential instability in laser output or non-uniform specimens do not seem to pose substantial difficulties in acquiring quantitative measurements of fluorescence.

The strong reduction in fluorescence for lecithin coated AWS particles may be due to the weak bonds between lecithin molecules and the mineral surface after only 24 h equilibration time. Organic substances are known to age, which means that they undergo structural changes and cross-linking enhancing their stability and rigidity (Schaumann et al., 2008). The weaker the bonds the easier they might be modified, dislocated, or broken when irradiated with highly energetic laser light (Slavik, 1998; Hibbs, 2004). The lecithin coated AWS particles as used here may, therefore, not be such good model particles for mimicking soil particles.

The indirect local heating effect that laser irradiation has on the specimen also needs to be considered. Although the photon energy may be insufficient to disrupt weak bonds, interactions that either do or do not lead to fluorescent emission may involve energy dissipation within the specimen. If volatile materials, such as water, are present these may evaporate. Although this would reduce heating of the specimen, any fluorophores dependent on the presence of such materials will be affected.

As specimen particles experience changes in temperature and relative humidity (e.g. passing from conditions of inspection to those of storage), they might respond to these changes. If the extent of hydration of the particle surface is altered, then the condition and precise nature of the organic material, its orientation and the extent of coverage of mineral surfaces, may change (e.g. Piccolo, 2002; Schaumann et al., 2008). These changes may influence specimen fluorescence. Although the laboratory was air-conditioned, it is not clear as to how well this stabilised the environment, especially in relation to relative humidity, in the local environment of the particle. The laser irradiation may increase the local temperature at the particle surface and with that change RH directly at the surface.

The decrease in fluorescence following treatments to remove surface organic material suggests that a significant proportion of the original fluorescence is associated with the organic material. The source of remaining fluorescence in the range of $440 < \lambda_F < 550$ nm appears to be associated with the underlying mineral. This poses some difficulty in the quantitative interpretation of the signals due to the possibility that light emanating from the mineral phase may suffer absorption in an overlaying organic phase. This would reduce the contribution from the mineral, but

not necessarily affect the behaviour of the organic material (Slavik, 1998). This quenching of the mineral fluorescence may be dependent on the type and amount of organic matter present on the particle surface as well as the mineral composition and, therefore, on the sample origin. Despite this complication the levels of fluorescence from various cleaned particles were similar (per unit projected particle area). Although this introduces both systematic and random sources of error, this contribution to the total fluorescence of the sample is small ($I_f \sim 200$ for the Ar-laser) and, therefore, not considered in subsequent sections and chapters.

In contrast to heating, acid treatment of soil particles removed the fluorescent emission maximum at 440 to 500 nm from the λ_F distribution, but did not reduce total fluorescence as much. As HA are insoluble at low pH, acid washing may only remove selected components from the organic matter (Tschapek, 1984; Babejova, 2001; Scheffer et al., 2002) and may not be an adequate procedure for providing a clean mineral surface. The influence of acid and base on the mineral surface also needs to be considered as it is likely to alter it (Jozefaciuk et al., 2002b). This could lead to exposure of mineral components, which themselves may be fluorescent, or metal components, which can either enhance fluorescence (e.g. Mn at $\lambda_F > 300$ nm and Cr at $\lambda_F > 300$) or quench fluorescence (e.g. Fe) in minerals (Rösler, 1991).

Similarly, it can be assumed that the extraction with IPA/NH₃ does not remove all organics, as organic material was still found in the extracted samples (by TOC measurements) (e.g. Ma'shum et al., 1988; Roy et al., 1999). In contrast to acid or base washing, however, a broader spectrum of substances may be removed as IPA/NH₃ extraction is used for a relatively broad extraction of organic material at base pH (Lewandowski et al., 1997; Roy et al., 1999). Therefore, probably only a change in fluorescence intensity, but no change in λ_F distribution occurs. Furthermore it can be assumed that the mineral surface is not damaged by this kind of extraction procedure as is probably the case for highly concentrated acid or base treatments.

3.5 Conclusions of method testing

The following conclusions were drawn from testing LSCM for application in soil particle investigations:

- i) Levels of auto-fluorescence emitted by particles drawn from various samples vary widely.
- ii) Removal of organic matter from their surfaces significantly reduces the fluorescence.
- iii) The total intensity of fluorescence is related to the amount of organic material on the particle surfaces.
- iv) The relationship is likely to be complex due to variability in the density of fluorophores in the organic material.
- v) The mineral may have an influence on the expression of fluorescence in soil particles.
- vi) The application of fluorescent dyes leads to a strong increase in fluorescence of soil particle surfaces, but no additional information could be gained. This was probably due to the unspecific binding mechanisms of the dyes used here.

Each type of molecule has a fluorescent emission independent of the wavelength of the (higher energy) excitation radiation (Rösler, 1991) so that the pattern of fluorescence of a pure compound should be a characteristic property (Slavik, 1998). In contrast, SOM contains numerous different molecules/fluorophores and, therefore, shows a pattern dependent upon the wavelength of the irradiating photons. The heterogeneity of SOM and the variety of chemistries of the associated particles suggest that it is desirable to employ both Ar- and He/Ne-lasers to provide complementary information about particles and the distribution of fluorophores.

The standard procedure for the examination of soil particles was, therefore, to use both lasers to obtain data concerning fluorescence and, additionally, an image of transmitted light (ChD) to obtain information about particle shape and size.

3.6 Application of LSCM to investigations of soil particles: results and discussion

3.6.1 Comparison of lasers

Comparison of mean I_f values obtained using both He/Ne- and Ar-lasers shows that there are systematic differences for all specimens. The relationship between I_f values shows considerable scatter with a linear correlation coefficient of $r = 0.8$ (Figure 3-23). The He/Ne-laser always resulted in higher I_f values and also resulted in much higher background fluorescence (section 3.3.1) when imaging oxidised particles. This was most likely due to the higher intensity at which it was used rather than actual differences in quantum efficiencies at the different wavelengths. However, the steeper gradient of the regression line compared to the 1:1 line indicates either a systematic difference between the features excited by the two lasers and/or a systematic error due to the high levels of fluorescence induced by the He/Ne-laser.

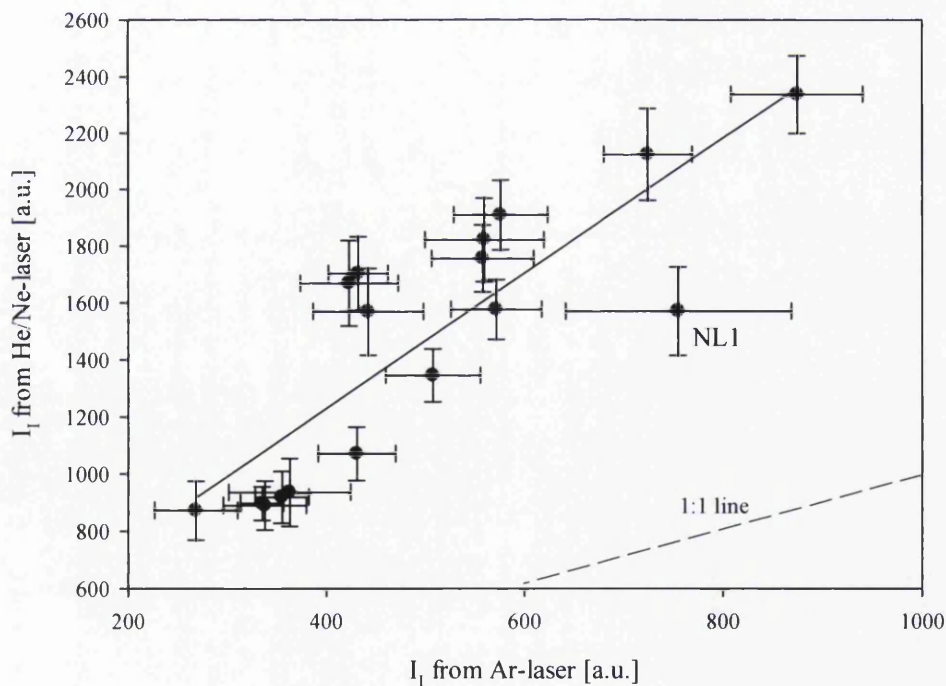


Figure 3-23: Mean I_f of all soil samples (individual particles) measured by He/Ne-laser vs Ar-laser.

Mean I_f values of sample NL1 (identified in Figure 3-23) had much larger standard errors when the Ar-laser was used. The random errors in I_f for other samples were similar and independent of the laser used. Excluding NL1 from the dataset increased the r value to 0.9. For multi-particle specimens, the linear correlation between mean I_f of the two lasers is even stronger with $r = 0.95$ (data are presented in appendix A).

The use of the He/Ne-laser may also lead to a general underestimation of I_f . When a significant proportion of bright pixels in the image saturate (i.e. reach the maximum brightness of 255 in an 8-bit grey scale) then no further detail is available (personal communication: Bryant, 2006). However, this did not appear to be the case for any of the samples used in this study.

The background fluorescence obtained after oxidising particles (compare section 3.3.1) was found to be much higher when the He/Ne-laser rather than the Ar-laser was used. This may be due to a stronger mineral fluorescence of the clean soil particle surface induced by the former. As these effects are difficult to quantify, the Ar-laser was used predominantly for image acquisition, with additional images of most samples obtained using the He/Ne-laser.

3.6.2 Total fluorescence intensity

3.6.2.1 Untreated natural soils

Results from method testing suggest that the intensity of fluorescence was dependent on the amount of organic material present in the bulk sample, which was likely to be present as particle coatings. Therefore, the relationship between TOC and mean total fluorescence I_f of bulk (multi-particle) specimens and of individual particles was investigated.

Correlations between I_f of individual particles and the TOC of the bulk samples from which they were obtained returned $r \sim 0.6$ for the Ar-laser and $r \sim 0.3$ for the He/Ne-laser (Figure 3-24a). These values suggest that only a small proportion of the variation in fluorescence is related to this bulk sample property.

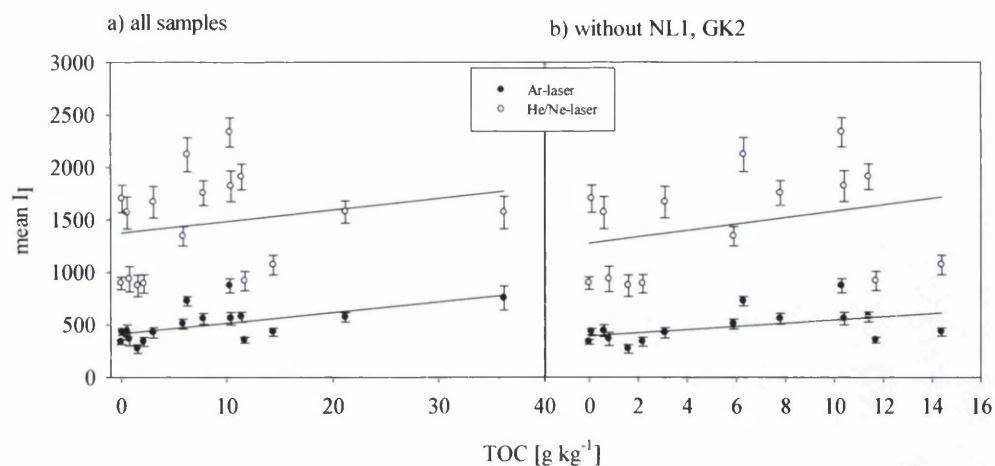


Figure 3-24: Mean I_f of individual particles vs TOC of bulk samples for a) all samples and b) excluding NL1 and GK2.

Samples GK2 and NL1 both have exceptionally high TOC in comparison with all other samples. Such outliers can strongly influence the quality of the correlations. Indeed, a correlation without these two samples (Figure 3-24b) produced lower correlation coefficients of $r = 0.5$ for the Ar-laser (no change in r for the He/Ne-laser).

The relative standard error of mean I_f for individual particles is generally high with $\sim 10\%$ error independent of the laser used and even higher for samples NL1 and GK3 ($\pm 15\%$).

One source of variation could arise from the effect of particle size. The particle area (A) was determined from the ChD-image using the LSM software, which provides a two dimensional view of the particle outline. This was used to provide the area weighted values of fluorescence per unit projected area (I_f/A).

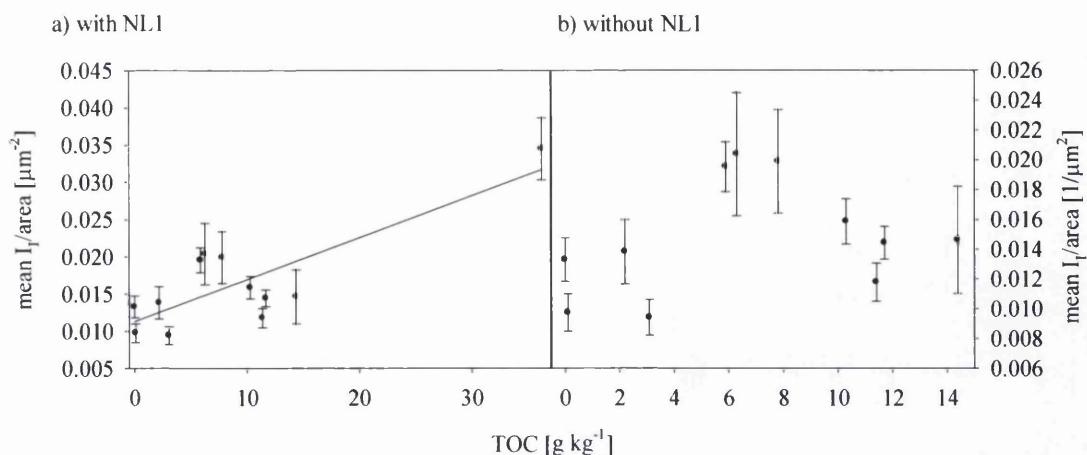


Figure 3-25: Mean I_f/A of individual particles (I_f/A calculated for each particle) vs TOC of bulk samples for a) several samples and b) NL1 excluded.

A linear relationship between bulk sample TOC and mean I_f/A seems to exist with $r = 0.8$ for 12 different soils with three samples per location (AU, NL, PT, UK) (Figure 3-25a). However, r falls to 0.4 when NL1 is excluded from the dataset. Thus it can be assumed that NL1 with its very high TOC dominates the dataset.

Soil particle surfaces are of course not two dimensional so that estimating the surface area from a planar projection of a particle underestimates the real surface area. The actual surface area will depend on roughness. Particle surface roughness (R_{25}) was therefore determined by AFM (chapter 2, section 2.4.4) and using these estimates, a hypothetical surface volume was determined ($V_S = A * R_{25}$). This was done in order to include the factor surface roughness so that the rougher the surface, the bigger the volume.

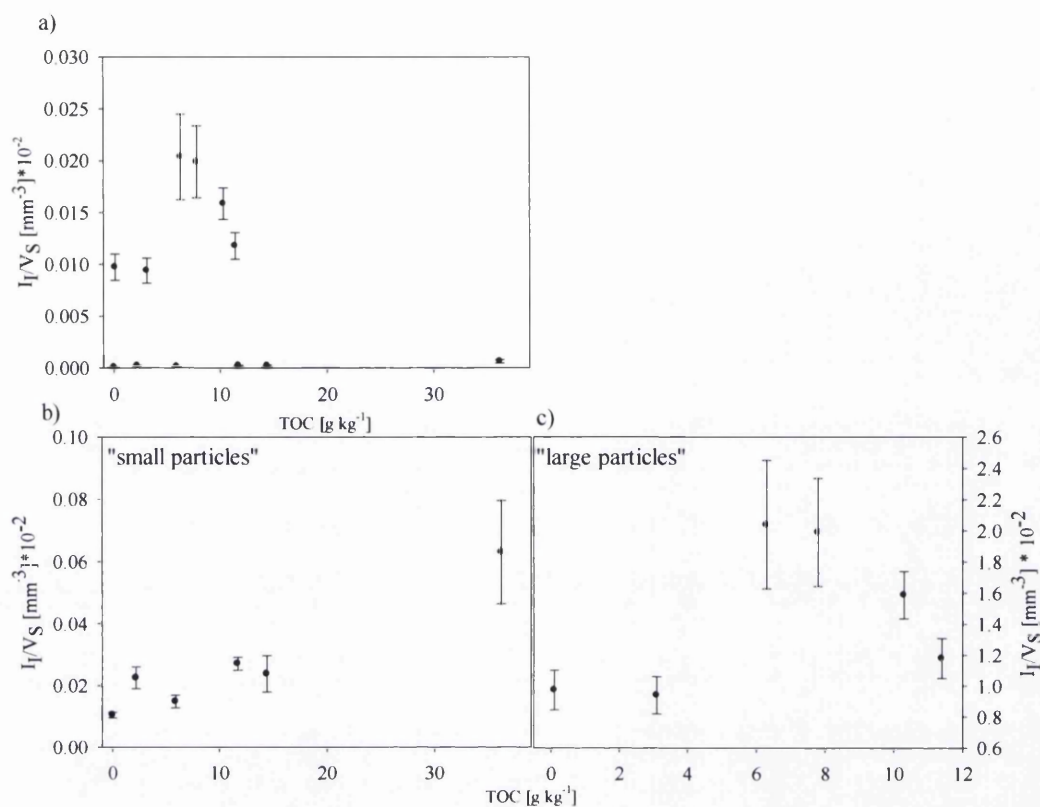


Figure 3-26: Mean I_f/V_s vs TOC. I_f imaged with Ar-laser a) for samples AU, NL, PT and UK b) for samples AU and NL, and c) for samples PT and UK.

The introduction of surface volume as a normalizing factor provides no overall improvement in the relationship I_f/V_s vs TOC for the four soils (Figure 3-26a). Distinguishing between samples with a generally smaller (AU: 0.24 – 0.29 mm and NL: 0.22 – 0.27 mm) and larger (PT: 0.46 – 0.57 and UK: 0.30 – 0.39 mm) particle size distribution (chapter 2, table 2.2) leads to a linear relationship with increasing I_f/V_s for increasing TOC for the small particles (Figure 3-26b) with correlation coefficients $r \sim 1$ including sample NL1 and $r = 0.7$ excluding sample NL1. This relationship was not found for I_f/V_s of larger particles (Figure 3-26c) and neither for the original I_f data of these samples. One reason for the increase of volume weighted fluorescence intensity of small particles with increasing sample TOC may be due to their increased coverage with fluorescent material. On the other hand the coverage on large particles may not increase that much with increasing TOC as they also seem to be rougher (chapter 2, table 2-8) which may lead to thicker but patchier distribution

of the organic matter. Determining the surface area or volume of the particles in the manner described is time consuming and does not appear to improve these correlations significantly. Therefore, the additional work for data analysis seems unjustified and particles from the other five samples were not subjected to this analysis.

Although most samples supposedly have low particulate organic matter content (by optical inspection) and the major component is adsorbed on particle surfaces, bulk sample fluorescence was considered in order to include particulate organic matter fluorescence as this component is included in TOC measurements. However, correlations between mean I_f of multiple particle specimens and TOC were also poor, with correlation coefficients similar to those of single particles ($r = 0.5$ for the Ar-laser and $r = 0.4$ for the He/Ne-laser). Excluding samples NL1 and GK2 from the data set (with much higher TOC than any other sample with 36.2 and 21.2 g kg⁻¹, respectively), improved the correlation significantly to $r = 0.8$ independent of the laser used.

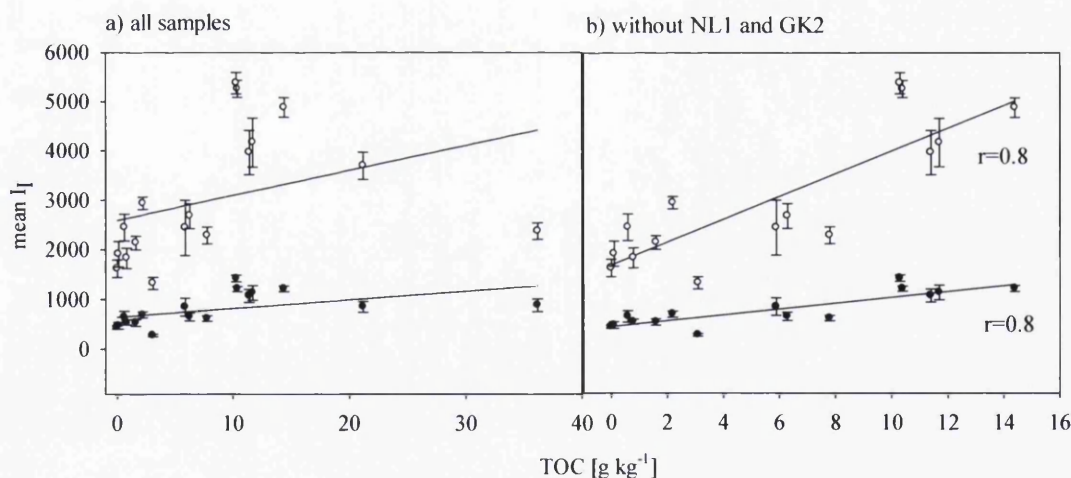


Figure 3-27: Mean I_f of bulk samples vs TOC for a) all samples, and b) without NL1 and GK2.

As an estimate, 3-6 particles (or fractions thereof) were imaged per multi-particle specimen. The total number of particles imaged in this manner was similar to that individually imaged ($N = 20$). It therefore, seems likely that it is not the number of

imaged particles responsible for the improved correlation of total fluorescence and TOC, but other factors like the contribution that particulate organic matter (which enters the specimen tray along with the mineral particles) makes to the total fluorescence.

Optical inspection of samples studied here appeared to indicate the presence of only small quantities of particulate organic matter. Comparisons of bulk properties, like TOC, and individual (mineral) particle properties, like I_f , therefore, may require more detailed information of the distribution of bulk properties within samples to improve their utility.

Distinguishing between sample origins

Although it was assumed that background fluorescence might be similar for all samples, subtle differences in mineral composition or the nature of adsorbed organic material on particle surfaces may arise associated with the sample origin. This may affect the background signal and/or possibly its nature. Therefore, sample origins were taken into consideration separately. Linear correlations are considered, but have to be treated as qualitative guides, as only three or four data points were available for each sample origin.

The correlation of mean I_f of individual particles with TOC for sample origins PT, NL and UK return an r value of ~ 1 . The r value for NL increases slightly when NL1 particles are excluded but this is hardly significant (Figure 3-28a, b and c).

No linear relationship was found for GK and AU samples. Although only three samples per origin were available, it seems GK has a maximum value for I_f at around TOC of 10 g kg^{-1} and increased TOC above this level has no influence on I_f which varies at or below the maximum (Figure 3-28c). Fluorescence from AU samples did not show a linear relationship with the TOC and variations of fluorescence intensity were so large for this sample that no statistically significant difference (t-test, $\alpha = 0.05$) between I_f at TOC 0 g kg^{-1} and 12 g kg^{-1} was found.



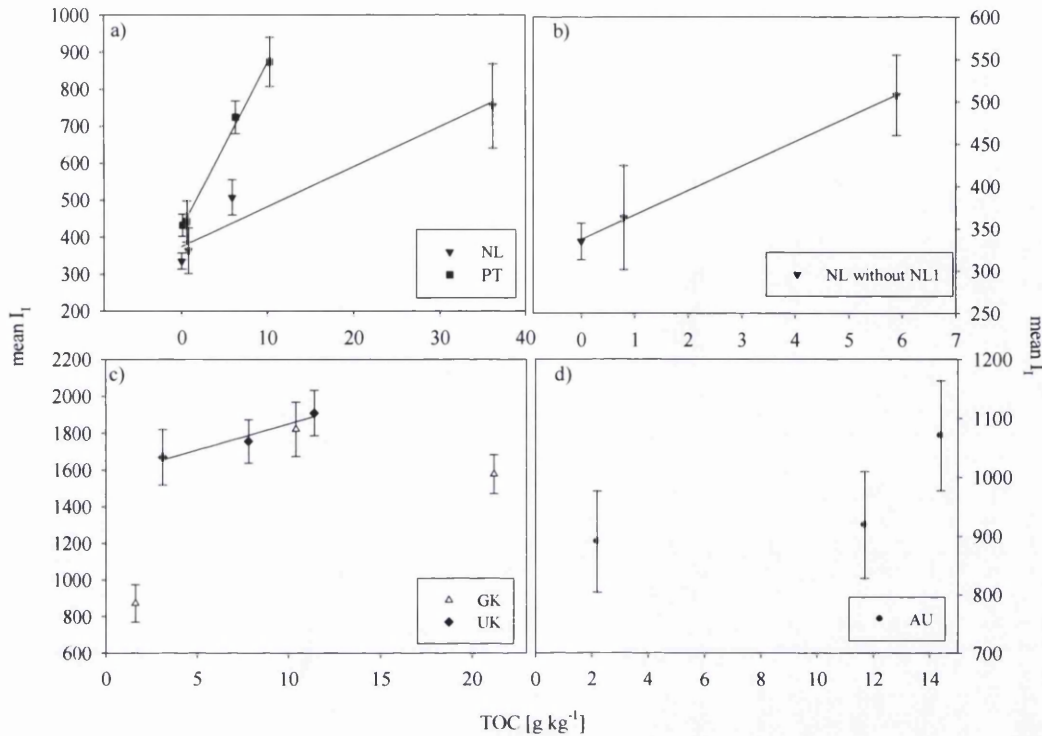


Figure 3-28: Mean I_f of individual particles vs TOC by sample origins and imaged with the Ar-laser for a) samples NL and PT, b) NL samples excluding NL1, c) UK and GK samples, and d) AU samples.

Linear correlations of mean I_f , obtained from imaging of multi-particle specimens, against TOC were not found to be particularly good for NL and PT samples (Figure 3-29a). The r value for NL samples excluding data for NL1 indicated a substantial improvement in r from 0.7 to ~ 1 (Figure 3-29b). The value of r for UK samples was ~ 1 and the correlation for AU samples was also reasonably good with r value of ~ 1 (Figure 3-29c and d respectively). However, the error for sample AU1 (TOC ~ 12 g kg⁻¹) was sufficiently large to render it indistinguishable from the other AU samples. The correlation coefficient, therefore, probably overestimates the quality of the data. GK multi-particle specimens did not show a linear relationship between mean I_f and TOC. The trend towards decreased fluorescence at high TOC was a little more enhanced for multi-particle specimens than for individual particle specimens (cf. Figure 3-28 and Figure 3-29).

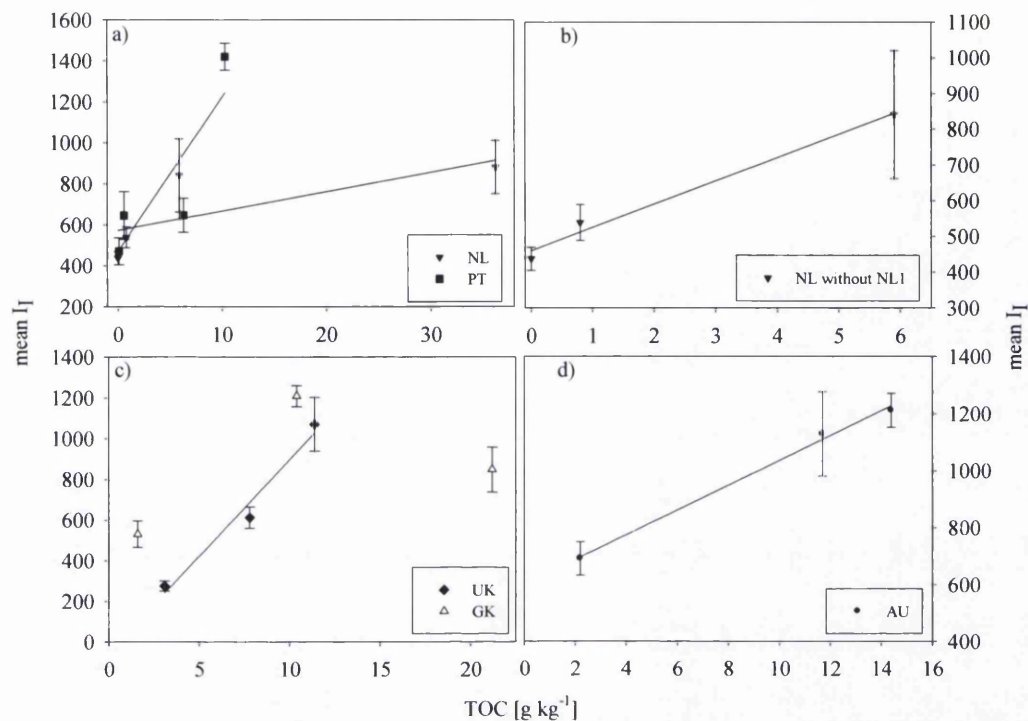


Figure 3-29: Mean I_f of multi-particle specimens vs TOC by sample origins and imaged with the Ar-laser for a) NL and PT samples, b) NL samples excluding NL1, c) UK and GK samples, and d) AU samples.

Fluorescence values obtained with the He/Ne-laser gave very similar results for both single particles and multi-particle specimens. Although mean I_f values were different, correlations were similar to those presented here with similar correlation coefficients (appendix A, table A_1).

The slopes of mean I_f are different for all sample origins for both multi-particle specimens and single particles. Also, a difference in slopes between multi-particle and single particle fluorescence was found. The regression line of individual particles from PT samples was much steeper than those of the others, and the regression lines of multi-particle specimens of both PT and UK have a similarly strong increase in I_f with TOC, whichever laser was used for excitation.

One may speculate that variation in the rate of mean I_f increase is connected to the amount of fluorescent material present in the sample depending on the sample origin. PT and UK samples may contain relatively more material prone to fluorescence than NL samples and relative amounts may be higher with higher TOC for these samples. Mainwaring (2004) showed that PT samples in fact do have very similar distribution and relative amounts of identified organic compounds (such as alkanes, fatty acids, aromatic hydrocarbons).

It is notable that AU samples show a linear relationship between TOC and mean I_f for multi-particle specimens, but not for individual particles. GK samples do not seem to exhibit this correlation in I_f neither for individual particles nor multi-particle specimens. The amount of fluorescent material in GK samples may be independent of the TOC and thus no correlation between mean I_f and TOC was found. AU samples seem to have a relatively high amount of particulate organic material (observed as fine, dark powdered material present in the sample) which may account for the correlation between mean I_f and TOC in multi-particle specimens, but were excluded from measurements made on individual particles.

3.6.2.2 Extracted and cleaned soil samples

Selected soil samples were subjected to various extraction and cleaning procedures (see chapter 2). The chosen samples were NL1, AU2 and UK1 as these were available in sufficient quantities.

Mean I_f of sample NL imaged with the Ar-laser decreased with increasing extraction strength (assessed as decrease in TOC): IPA/NH₃, acid washing, base washing (Figure 3-30a; cf. chapter 2, table 2-9).

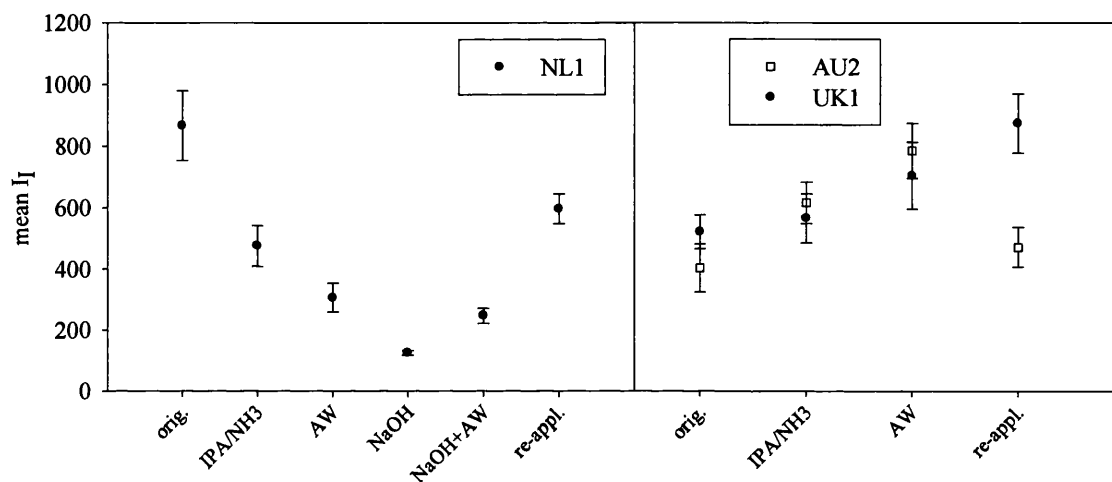


Figure 3-30: Mean of original particles, single extractions with IPA/NH₃, acid washing and NaOH washing and reapplication of extracted material to the extracted particles. All I_f were imaged with the Ar-laser.

Reapplication of the IPA/NH₃ extracts to the extracted particles (in the same proportion in which the extraction was made) by rotary evaporation of the solvent mixture, produced an increase in their fluorescence. The TOC was not returned to the initial value (e.g. as evident by some deposition of extracted organic material on the surface of the evaporator flask) and neither was I_f . However, changes in fluorescence could also partly be caused by fluctuations in the laser (section 3.3.2).

Base washing of soil NL1 followed by washing with acid (NaOH+AW) provided particles whose I_f values were above those produced by base washing (BW) alone.


However, this was not evident in the respective TOC values, as following any of these procedures, no organic matter was detected on the particles as TOC.

Mean values of I_f obtained from particles of UK1 and AU2 soils, subjected to various extraction procedures and irradiated with the Ar-laser, showed a different pattern to those from NL1 (Figure 3-30a and b). In both cases (UK1 and AU2) extracted particles (AW and IPA/NH₃) exhibited an increased I_f , which was above that of the original material. This was also the case when the IPA/NH₃ extract was quantitatively re-applied to the extracted UK1 samples. This material seemed to fluoresce significantly more intensely than the original (t-test, $\alpha = 0.05$). In the case of AU2 re-application seemed, within experimental error, to restore fluorescence to its original level.

Mean values of I_f for particles recovered from various extractions and imaged using the He/Ne-laser for irradiation were very similar in pattern to those obtained using the Ar-laser (see Table 3-4). However, I_f of particles from sample NL1 were restored to their original value after re-application of IPA/NH₃ extract and those of particles of acid washed UK1 were returned to substantially higher values than those of the original particles.

Table 3-4: Mean I_f imaged with He/Ne-laser of original, extracted, acid washed and re-applied particles.

treatment	mean I_f		
	NL1	AU2	UK1
orig.	1700 ± 160	1080 ± 100	1950 ± 150
IPA/NH ₃	1400 ± 120	2230 ± 230	1800 ± 230
AW	900 ± 130	2350 ± 270	2440 ± 390
re-applied to AW	1640 ± 140	1440 ± 170	2440 ± 280


 decreasing TOC,
 increasing,
 extraction strength
 increased TOC but
 less than original

The mean I_f values of particles recovered, at each step, from a sequence of extractions applied to NL1 (Table 3-5) showed that the IPA/NH₃ procedure (first step) produced similar values to those reported in Figure 3-30 and Table 3-4 for a replicate extraction of this soil. A subsequent extraction with water significantly

reduced the fluorescence and TOC of the extracted material. A final extraction with aqueous NaOH resulted in no significant reduction of mean I_f , but a reduction in TOC to the detection limit was observed.

The largest standard error of mean I_f values (Ar-laser) was associated with the IPA/NH₃ extraction at $\pm 18\%$, whereas those associated with water and aqueous NaOH extractions were relatively small at $\pm 8\%$. No such difference was found when the He/Ne-laser was used.

Table 3-5: Sequential extraction of sample NL1 with water, IPA/NH₃, NaOH; mean I_f .

	TOC [g kg ⁻¹]	mean I_f	
		Ar-laser	He/Ne-laser
IPA/NH ₃	1.32	440 \pm 80	1320 \pm 220
water	0.74	250 \pm 20	750 \pm 80
NaOH	n.d.	230 \pm 20	750 \pm 110

It appears that changes in mean I_f of material subjected to these various extractions are dependent on the nature of the sample. No consistent pattern of behaviour emerged suggesting that the detailed nature of organic material in particular soils may have a dominating effect. Whether the material is excited using a Ar- or He/Ne-laser appears to make little difference.

The increase of fluorescence with removal of organic matter seen in some samples could be connected to the increase in bare mineral surface. Although silica itself does not fluoresce, inclusions of e.g. manganese, chromium, titanium or fluorides containing calcium, magnesium or aluminium (e.g. CaF₂, MgF₂, Na₃AlF₆) would lead to mineral fluorescence (Rösler, 1991). The use of strong acids and bases (in this case NaOH and HNO₃) may have an additional influence on the mineral surface and could even attack the upper mineral layers, laying bare underlying layers (Jozefaciuk et al., 2002a), exposing inclusion of the mineral that enhances fluorescence. Oxidising the samples (and thus removing the organic matter), on the contrary, led to a strong reduction of fluorescence in comparison to the original

samples or the acid/base washing. Oxidising the sample at 1050 °C is probably less damaging for the surface (melting point of SiO₂ is ~1700 °C) than an attack with acid/base and, therefore, oxidation may leave the mineral surface in a less disrupted state than chemical etching that arises from acid and/or base washing.

The reduction of water repellency after IPA/NH₃ extraction or acid/base washing without reduction in fluorescence intensity may be due to several factors:

- i) The material extracted itself is not primarily responsible for the fluorescence of the sample. This would be the case if mainly structures like alkanes and other long chain hydrocarbons were extracted with IPA/NH₃. However, this is not the case as shown in previous studies (Mainwaring, 2004; Mainwaring et al., 2004; Morley et al., 2005).
- ii) The organic material is bound in layers to the surface, altering between hydrophilic and hydrophobic layers (e.g. McGhie et al., 1980; Ellerbrock et al., 2005). Extraction does not lead to a complete removal of the organic matter, but only removes the outermost layers, leaving a hydrophilic, tightly bound organic layer on the mineral surface. This layer would probably still exhibit fluorescence, but leave the sample wettable.
- iii) The conformation of the remaining organic material on the surface is altered in such a way that fluorescence is increased, i.e. the remaining fluorescent molecules are more evenly distributed on the sample surface and fluorescence, thus, is increased.
- iv) The mineral surface is altered e.g. by exposing fluorescent inclusions inside the mineral and, therefore, fluoresces.

3.6.3 Distribution of fluorescence

The extent to which particle surfaces were covered with fluorescing material (C_F) was found to be essentially independent of total fluorescence I_T (Figure 3-31) for both Ar- and He/Ne-lasers. Although a general trend of increasing C_F with increasing I_T can be identified, no significant correlation between the two parameters was found.

Total fluorescence, determined from images captured from several optical slices, through the depth of a particle, contains contributions from each slice and some may

include mineral fluorescence. The slices might have been too large ($\sim 5\text{-}8\ \mu\text{m}$) to discriminate between layers of organics on the surface. C_F considers only the fluorescing material on the surface, as it was determined from a three dimensional projection image of the particle, and does not differentiate between different focal planes. Therefore, any trend of increasing C_F with increasing I_f indicates that fluorescence from the surface layer is the primary contribution to I_f .

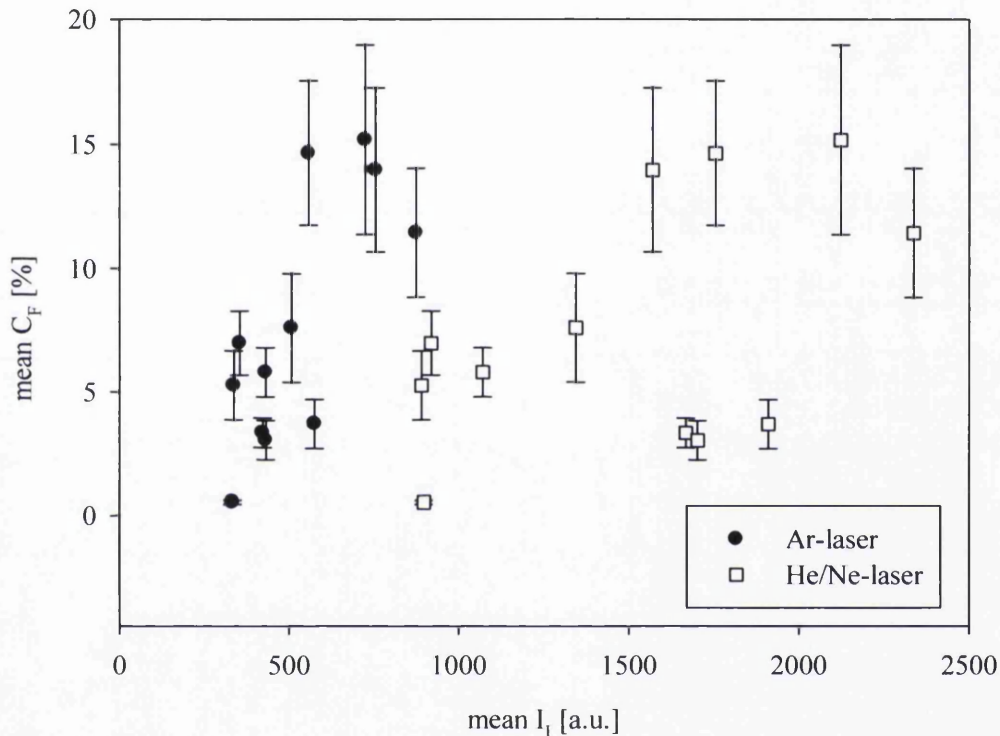


Figure 3-31: Mean C_F vs mean I_f of single particles drawn from natural soil samples AU, NL, UK and PT.

As the standard deviation of mean I_f indicates, the variations between particle fluorescence within one sample can be substantial. Individual particle data for C_F and I_f (Figure 3-32) showed no correlation between the two parameters, but most samples displayed a slight trend of increasing C_F with increasing I_f . However, AU samples seem to be an exception and no increase in C_F with I_f was observed. This was also the case for NL2 and, in the case of NLC the extremely low values of C_F ($< 2\%$)

contain little information. These outcomes are similar to those when mean sample values were considered.

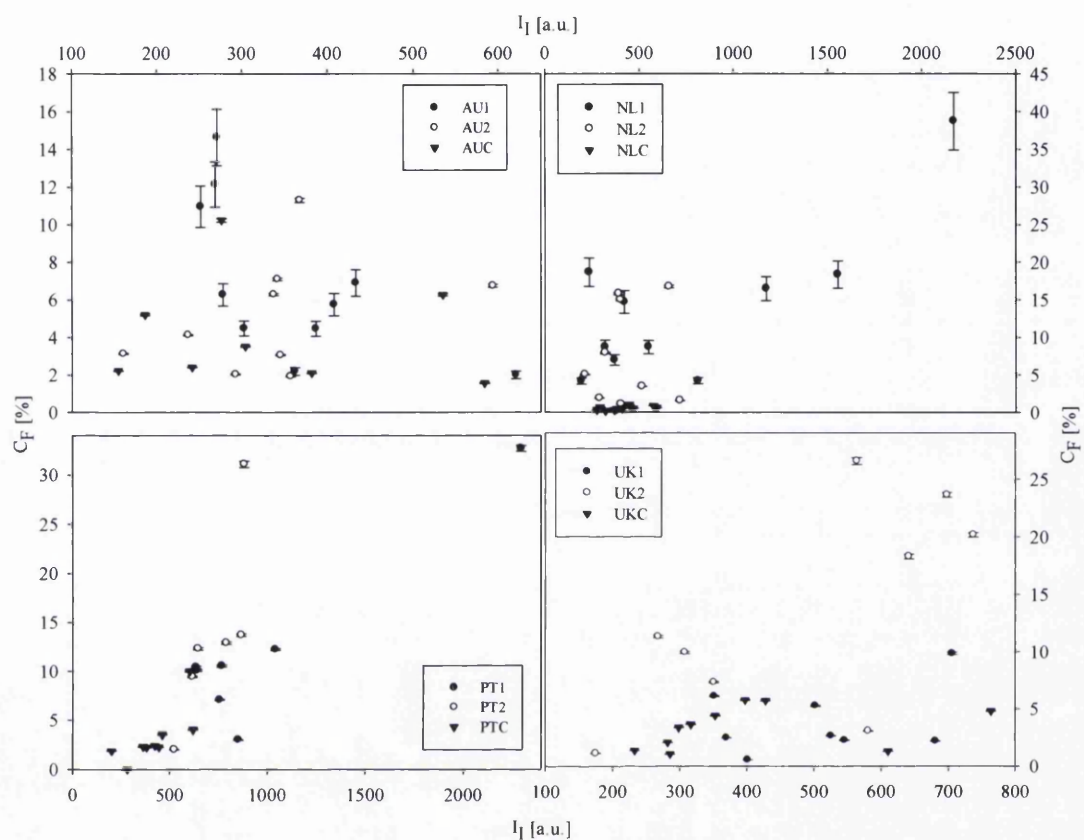


Figure 3-32: C_F vs I_I of individual particles imaged with Ar-laser. Errors were assumed to be no more than 10% of the value as a rough estimate.

As shown in section 3.6.2.2, fluorescence was not completely removed but only reduced following extraction of samples with IPA/ NH_3 . Also I_I was not recovered after re-application of the extract to the extracted particles and the development of I_I upon treatment was dependent on the sample. Coverage (C_F) of the particles with fluorophores did, however, increase from original to extracted and to re-applied, for all samples investigated (Figure 3-33).

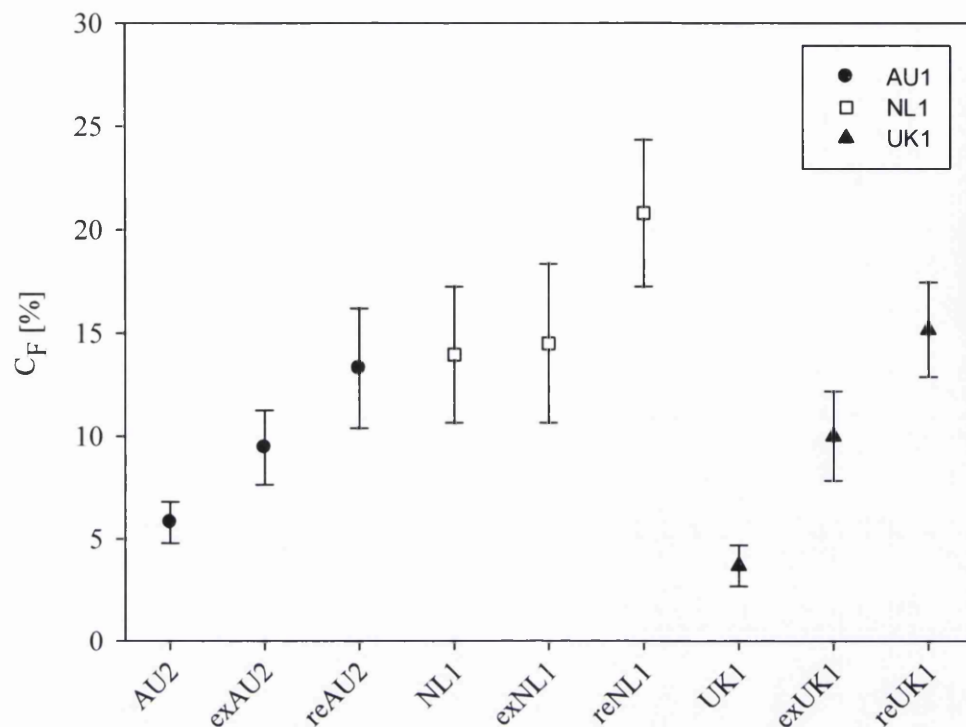


Figure 3-33: C_F of original, extracted and re-applied samples AU2, NL1 and UK1.

The data suggest that organic material is more uniformly distributed on particle surfaces following re-application of extracted material. Several processes may play an important role here:

- i) After extraction some organic material is still present on the particle surface and seemingly more evenly distributed than before, leading to an even distribution of potential binding sites to accommodate the extract when it is re-applied, which in turn promotes an even distribution of organic material.
- ii) Fluorescent material only constitutes a fraction of the particle coatings. In a natural state soils are constantly changing and particle coatings are subjected to biogeochemical degradation processes. Microorganisms may be attached to particle surfaces, but are probably not evenly distributed and preferentially attach to sites with readily available nutrient material. Fluorescing organic material, however, may be mainly composed of large ring structures (von

Wandruszka, 1998) representing less biodegradable material, so that ‘islands’ of fluorescent materials are built (Kalbitz et al., 2003; Kalbitz et al., 2005).

- iii) During extraction procedures, some material re-attaches randomly to the mineral surface in a very thin but even layer, leading to a more homogeneous coverage and when re-applying material, a more homogeneous layer is added to the particle surface, which is expressed in the higher fluorescent coverage.
- iv) The surface roughness of the mineral particle surface may be of importance for the distribution of organic material in a natural state, leading to separate ‘islands’ of organics. Forcing particles into contact with the extract and virtually condensing material on their surface, however, may lead to a very smooth distribution, and, therefore, increase coverage.

Further evaluation of the parameters of fluorescence with respect to properties of the bulk sample, like bulk wettability or TOC, is presented in sections 3.6.4 and 3.6.6.

3.6.4 Number of fluorescent areas

A scatter diagram of mean N_F of various samples plotted against I_I reveals no relation between the two parameters, and no dependency on the laser used for imaging (Figure 3-34).

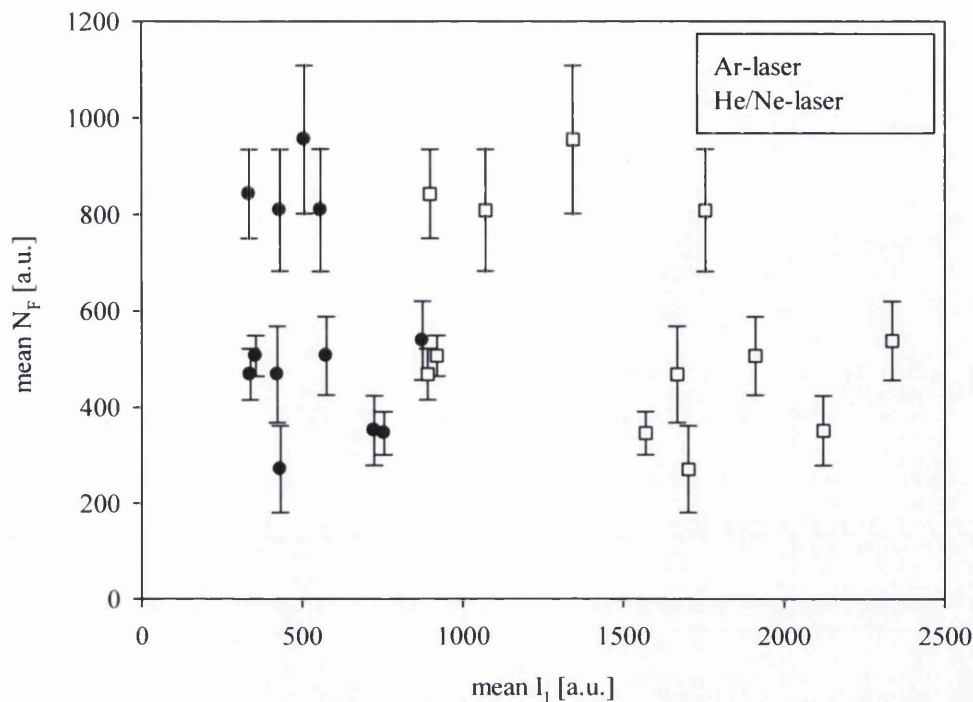


Figure 3-34: Mean N_F vs mean I_f . Error bars represent the standard error, imaged with both Ar- and He/Ne-lasers.

Similar to the scatter of C_F with I_f , N_F and I_f are not necessarily connected. The thickness of the organic layer, which may contribute (wholly or partly) to I_f , is not related to N_F . However, some relationship between the two parameters may arise. The scatter diagrams of individual particle N_F against I_f showed trends towards increased N_F with increasing I_f for some samples (AU, NL, PT, Figure 3-35a-c), but for UK samples no relationship could be established (Figure 3-35d). Individual samples from PT and AU all show similar trends, and those from AU a relatively broad data scattering. NL samples, however, show significant variations between samples. NL2 and NLC both have strongly increased values of N_F with only slightly increasing fluorescence intensity, but NL1 displayed a maximum and constant N_F at ~ 500 for $I_f \geq 500$.

Due to the high variation in N_F within a sample (see Figure 3-35), the mean value is probably an imprecise measure (as indicated by the large error bars in Figure 3-34).

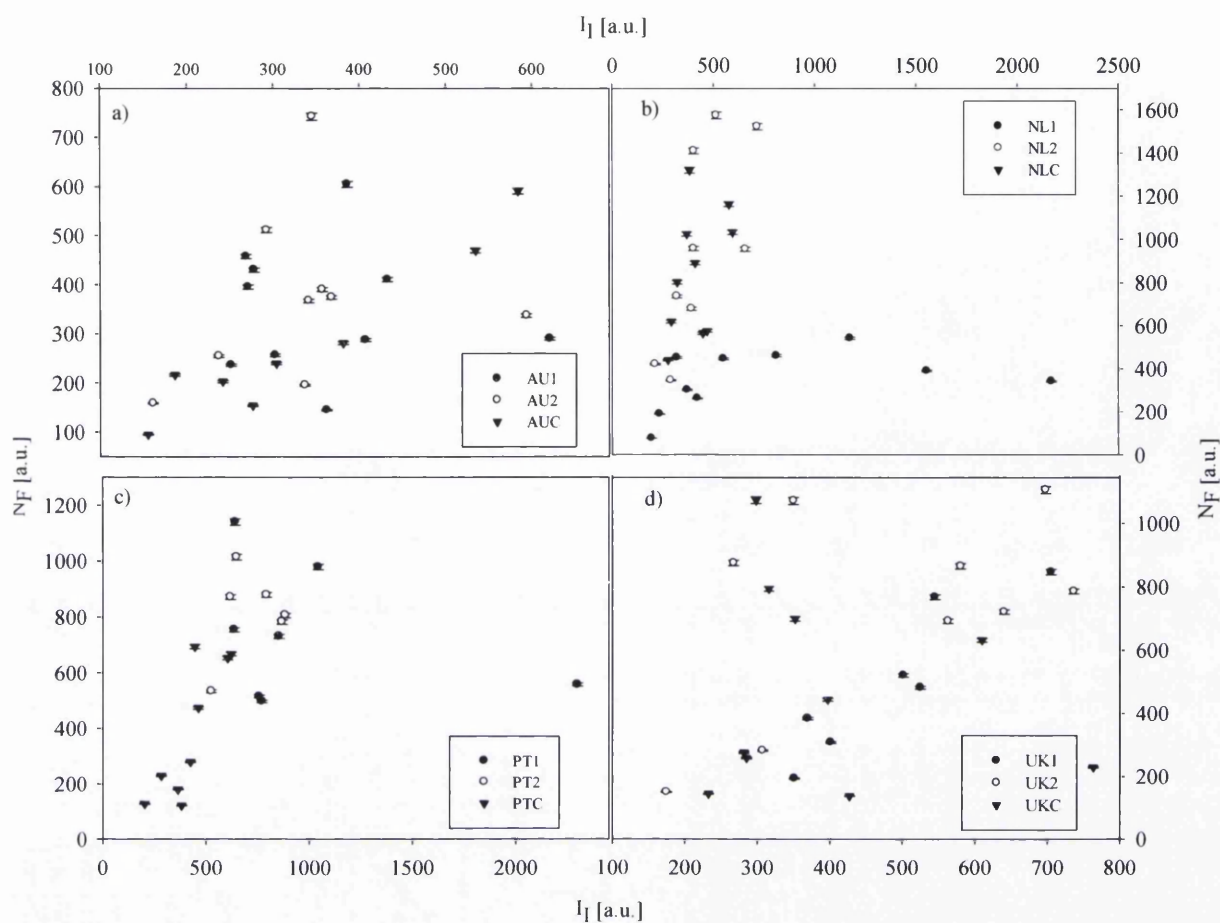


Figure 3-35: N_F vs I_I of individual particles from a) AU, b) NL, c) PT and d) UK samples. Error bars (partly within the limits of the symbols) represent maximum assumed error of 10 % per particle.

In contrast to C_F , no unique relationship between N_F and I_I of the extracted and re-applied samples was found. Both NL1 and UK1 samples showed an increase of N_F from original to extracted and re-applied samples (within the experimental error), similar to C_F . Sample AU2, however, displayed a significant decrease of N_F with extraction and re-application (Figure 3-36).

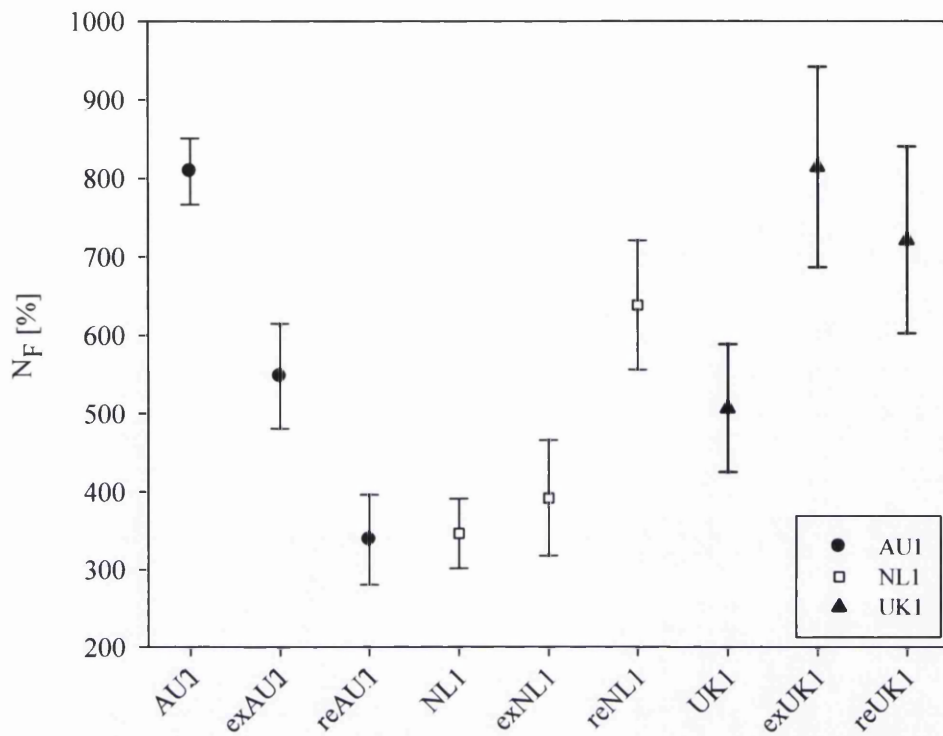


Figure 3-36: N_F of original, extracted and re-applied samples AU2, NL1 and UK1. Error bars represent standard errors.

The mechanism behind the distribution of organic material on the surface, therefore, may be different for this sample than for the others. The reduction of N_F after extraction implies that some fluorescing areas were removed during extraction while others stayed somewhat intact, which may be connected to the roughness of the underlying material. The rougher the mineral, the more patchy the distribution of the organic coating may be ($N_F(\text{AU1}) > N_F(\text{UK1}) > N_F(\text{NL1})$). Extraction would then perhaps only remove organic material from the more exposed sites of the particle, and hence reduce N_F . The re-attachment of organic material probably occurs primarily at sites where organic matter is already attached to the mineral surface. The further reduction of N_F with re-application of the extract may then arise from growth and merging of these coated areas on the mineral surface. For the other two samples (UK1 and NL1) the organic matter present on particles following extraction could be distributed in very small areas on their surfaces, leading to a very high number of

preferential binding sites for organic material. On contact with the extract the sites may grow in size without merging and so preserving N_F . Both, i.e. many small fluorescing areas and few large fluorescing areas, could lead to an increase in the coverage of the mineral surface due to the reduction in organic layer thickness and wider distribution of the material, and therefore N_F and C_F need not to be related. This concept is presented in the drawing below (Figure 3-37).

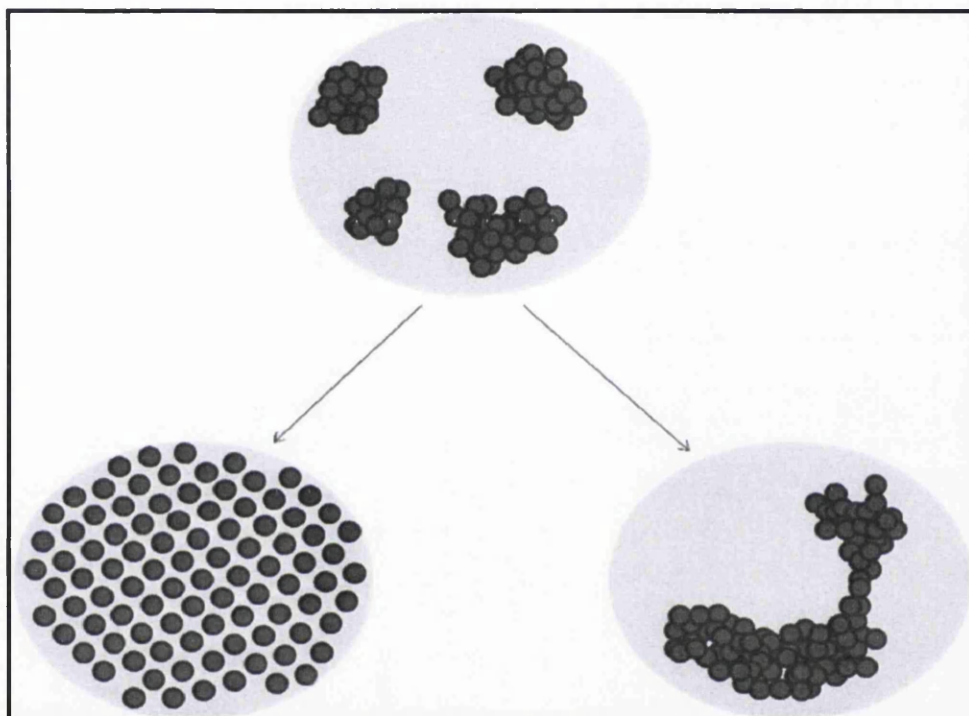


Figure 3-37: Possibilities of redistribution of fluorescing organic matter after re-application of the extracted material, with light grey circles representing particles and small dark circles organic matter molecules/aggregates

Roughness of the original, extracted and re-applied samples, measured by AFM over areas of $5 \times 5 \mu\text{m}^2$, was essentially the same for all samples and subject to large standard deviations within and between particles drawn from the same soil (Table 3-6). This may be due to the small scale measurement. However, the R_{25} values given are always total roughness values. It was not possible to distinguish between the underlying mineral roughness and the total roughness that includes the organic coating. Therefore, the R_{25} values may provide only limited information.

Table 3-6: Mean roughness R_{25} of original, extracted and re-applied samples NL1, AU1 and UK1, measured with AFM on $5 \times 5 \mu\text{m}^2$ areas. Errors are given as standard deviation.

R_{25}	original	IPA/NH3	re-applied
NL1	46.5 ± 19.2	49.4 ± 25.5	54.9 ± 20.6
AU1	53.3 ± 34.2	58.6 ± 33.8	63.0 ± 29.4
UK1	98.4 ± 52.0	74.5 ± 31.8	81.9 ± 35.9

Comparison of C_F and N_F

Both C_F and N_F parameters showed a positive correlation with I_f of extracted soil particles and those to which the extracts were re-applied. This does not mean that both parameters also have to be positively correlated to each other, but some relationship was thought likely and is displayed in Figure 3-38 as a scatter diagram for original, extracted, re-applied AU, NL and UK samples. Several types of behaviour were observed.

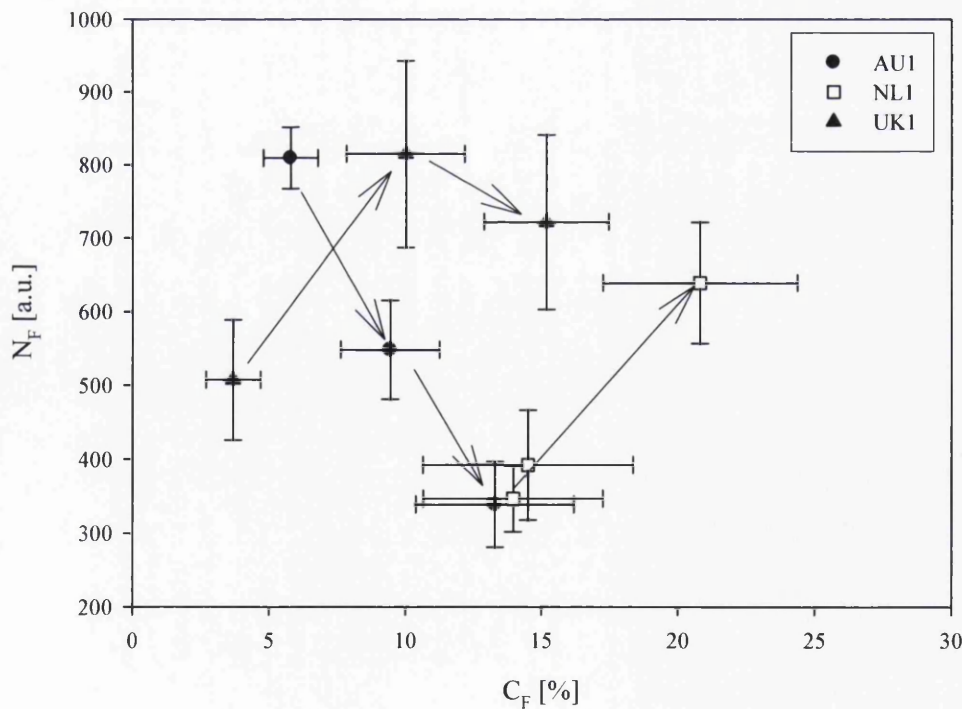


Figure 3-38: Mean N_F vs C_F values of original, extracted and re-applied samples from AU, NL and UK. Arrows represent the sequence of extraction and re-application.

Both NL1 and UK1 samples showed a trend to increased N_F with increasing C_F (which increased for all samples from original to extracted to re-applied) upon extraction and re-application within the experimental error. AU1 samples showed the reverse relationship (arrows from left to right). Generally, C_F values of AU1 and UK1 samples were within a similar range, but those of NL1 samples were found to be higher. N_F values of all samples were similar.

The positive correlation of N_F and C_F (as is the case for UK1 and NL1 samples) indicates an even distribution of fluorescent organic matter on the particle surface in the form of many small separate islands from original to extracted to re-applied samples. The negative correlation of the two parameters (as found for AU1) could hint at fewer larger aggregates on the particle surface, with increasing sizes but reduced number from original to extracted to re-applied particles, supporting the model introduced above (Figure 3-37).

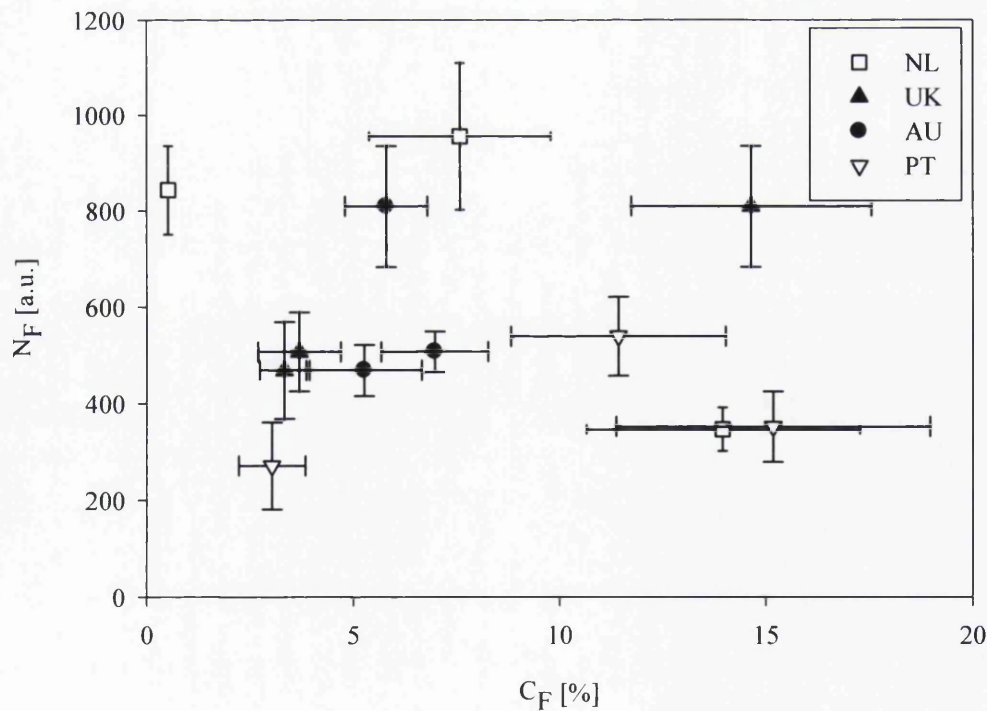


Figure 3-39: Mean N_F vs mean C_F for AU, NL, UK, PT samples. Error bars represent standard errors.

No general trend was found in the correlations between mean C_F and mean N_F of particles from all original samples (AU, NL, PT and UK). No particular dependency on the origin of the samples was found (Figure 3-39). This indicates that other surface properties such as particle roughness may play a role in the distribution of organic material on the particle surface under natural conditions. The aging process of the organic coatings is probably different from sample to sample. Even samples from a similar origin can suffer very different degradation processes that may be dependent on biological factors like the microbial community or physical factors such as pH and water content (Schaumann et al., 2008).

3.6.5 Size of fluorescent areas

The size of the fluorescent areas present on a particle surface was determined solely by optical inspection of the fluorescence images and is a very subjective measure. A standardised automated evaluation was not available (see section 3.2.6). Estimates of both N_F and C_F also involve some subjectivity as they are dependent on the instrument settings chosen for these. As these settings were used throughout, the results, however, are internally consistent and, therefore, comparable. Uncertainties in the estimates of a_F arise from some additional subjective judgements.

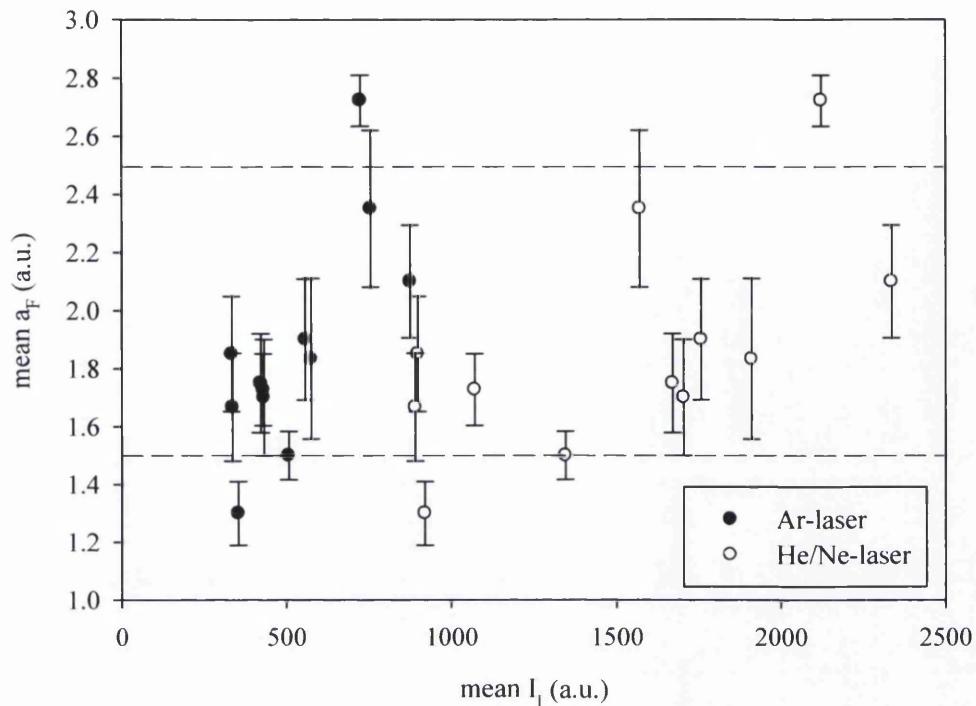


Figure 3-40: a_F vs mean I_1 . Dashed lines represent category limits (small/medium at 1.5, medium/large at 2.5) and error bars represent the standard error.

The correlation between mean a_F of samples and mean I_1 scattered very broadly for data obtained using both Ar- and He/Ne-lasers. No clear trend was apparent (Figure 3-40) and errors were relatively large, so that it was not possible to distinguish between the various samples. The sample with the smallest size ($a_F = 1.3 \pm 0.1$), AU1 also had relatively low I_1 , and that with the largest ($a_F = 2.7 \pm 0.1$), PT1, exhibited a large I_1 . All other samples fall between $1.5 < a_F < 2.5$, which is the mid-size range (between the dotted lines in Figure 3-40).

None of the samples whether original, extracted or re-applied showed a difference in a_F (appendix A).

Due to the subjective manner in which a_F was determined, it is probably imprecise and, therefore, an unsuitable measure for assessing other surface properties of soil particles. No further evaluation was therefore made.

3.6.6 Fluorescence and bulk soil parameters

It is of interest to interrelate the different fluorescent parameters C_F , N_F and I_I in order to understand if any relationships exist between them. No overall correlations between single parameters were found, but TOC and I_I were weakly correlated. It, therefore, seems appropriate to include TOC in a suite of single and multiple linear correlations. These, at least partly, acknowledge the fact that mineral soil particle surface interactions with organic matter are complex with manifold mechanisms operating. Multiple linear regressions revealed some relationships between the parameters C_F , N_F , TOC and mean roughness of the particle surface (R_{25}) with the fluorescence intensity:

- i) A weak multiple linear correlation was found for N_F and C_F with I_I ($r \sim 0.8$). This indicates that both surface coverage and number of fluorescence areas, and with that possibly the layer thickness, influence the measured fluorescence intensity.
- ii) Another weak correlation ($r \sim 0.7$) was found between I_I and C_F , R_{25} and TOC, which indicates that the distribution and surface roughness of the particle sample as well as the total amount of material present are dependent on each other.

However, these correlations are too weak for use as reliable relationships for quantitative prediction. They just illustrate that connections between the various fluorescence parameters and TOC, as well as R_{25} exist, but that their relationships are complicated.

A comparison between parameters of particle fluorescence and bulk soil properties is useful to see whether the former reflect the latter. Figure 3-41a-d shows scatter diagrams of various fluorescence parameters (C_F , N_F , I_I and a_F) and CA as a measure of bulk soil wettability. Apart from data for multi-particle specimen I_I , which showed a slight trend of increasing I_I with increasing CA, no correlations between contact angle and fluorescence parameters were found when the Ar-laser was used. Separating the data for individual samples showed that all UK and NL bulk samples reflect the general tendency to exhibit increased I_I with increasing CA (Table A_1, appendix A). PT bulk samples exhibited a similar, but smaller tendency. Data from AU and GK samples did not follow any such trend. The increase in multi-specimen

fluorescence intensity with the contact angle could be an artefact of the parallel increase in TOC of the samples. However, no correlations were found between either TOC and CA (cf. chapter 7) or multi-particle specimen I_I and CA.

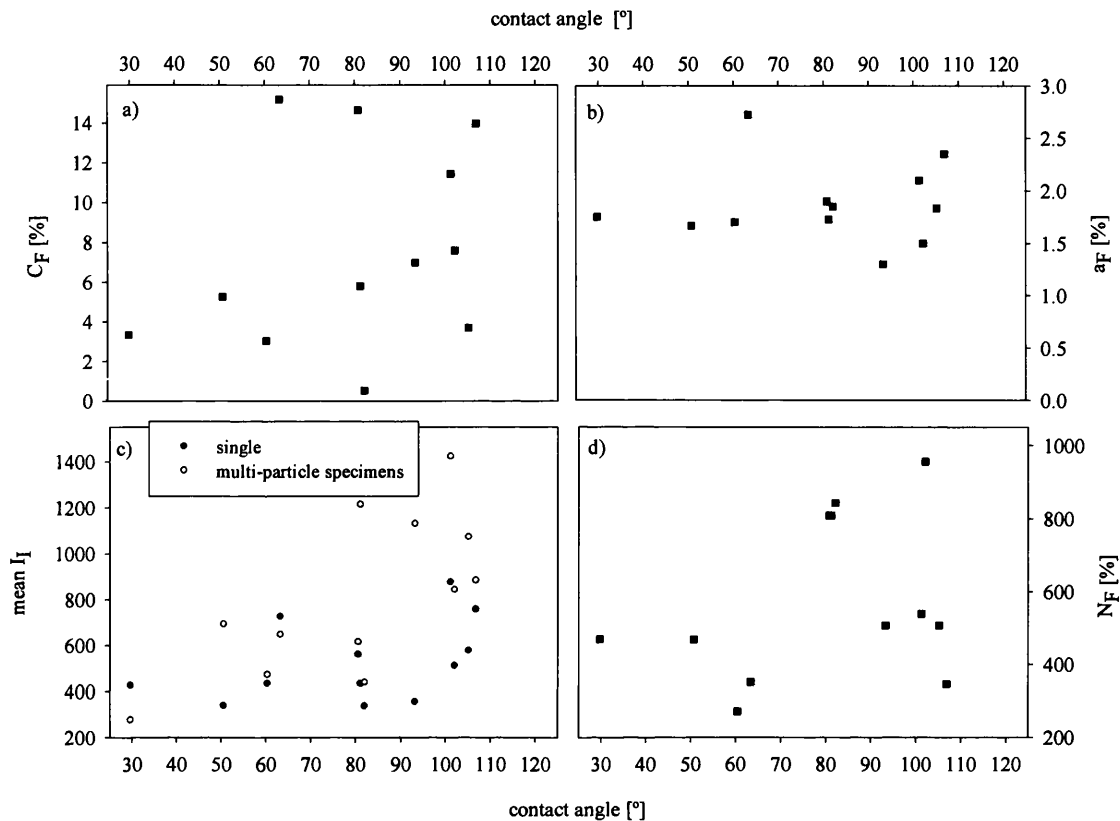


Figure 3-41: a) Mean C_F , b) mean a_F , c) mean I_I and d) mean N_F of single particle images vs CA for various samples using an Ar-laser.

No correlation was found between I_I (the only parameter obtained using the He/Ne-laser) and CA (table A_1, appendix A). Similarly, no correlations were found between WDPT and any of the fluorescence parameters (table A_1, appendix A).

Multi-linear regression of the parameters TOC, C_F , N_F , I_I with CA also showed a weak correlation ($r = 0.8$), but this was too weak to use for quantitative predictive purposes. The correlation between TOC and C_F (as strongest influence) only illustrates that a probably complicated relationship exists between bulk soil wettability and the distribution and amount of fluorescent organic material on soil

mineral particle surfaces. However, other factors like the type of organic matter and the molecular conformation may be of similar or even greater importance in influencing the wettability of a soil sample.

No single correlations or multi-linear regressions were found between WDPT and any of the other parameters. The contact angle of a sample, fluorescence parameters and TOC present the state of the sample at the moment of measurement, whereas WDPT measures the breakdown of water repellency over time, and, therefore, measures the stability of the system. A correlation between WDPT and any of the other parameters, therefore, seems unlikely as they focus on different physical aspects of a sample.

For both CA and WDPT no correlations were found with mean I_f of the original/extracted/re-applied samples. This is probably due to the dissimilar development of I_f with extraction and re-application, which is strongly dependent on the sample (compare section 3.6.2.2), whereas CA and WDPT development with extraction/re-application seems to be similar for all samples.

Table 3-7: Water repellency (measured as WDPT and CA) and mean I_f of samples AU2, NL1 and UK1 after different treatments.

	WDPT [s]	CA _i [°]	mean I_f (Ar-laser)	mean I_f (He/Ne-laser)
AU2				
orig.	0	93	402 ± 79	1074 ± 99
IPA/NH ₃	0	72	616 ± 68	2232 ± 231
AW	0	64	785 ± 89	2350 ± 269
re-applied	7	85	471 ± 65	1439 ± 174
NL1				
orig.	4800	107	866 ± 113	1695 ± 156
IPA/NH ₃	0	89	475 ± 66	1406 ± 123
AW	0	64	306 ± 47	898 ± 129
re-applied	47	128	596 ± 49	1634 ± 140
UK1				
orig.	18000	105	520 ± 55	1949 ± 151
IPA/NH ₃	0	82	566 ± 80	1799 ± 225
AW	0	59	704 ± 109	2437 ± 368
re-applied	37	107	874 ± 96	2435 ± 280

Further considerations about individual particle water repellency, as determined in chapter 4 and fluorescence of individual particles, can be found in chapter 7.

3.6.7 Fluorescence spectra

Use of the confocal microscope in meta mode provides for division of the specimen fluorescence into several wavebands (~ 10 nm resolution) providing an, albeit crude, spectrum. The fluorescence intensity within each waveband was calculated from an image of the specimen associated with the corresponding waveband. An average spectrum was obtained from combination of the various waveband intensities obtained from a selection of particles ($n = 5$) from a soil sample to provide an average waveband intensity I_a for various λ_F . The lowest value of I_a was then subtracted from the others in order to simplify comparison of spectra.

The procedure was applied to one focal plane within the specimen particles (rather than integrated over a z-stack) due to the time-consuming imaging procedure and is appropriate only for qualitative analysis.

The spectra of the soil particles did not show any prominent differences between samples (see Figure 3-42 and appendix A). All spectra have main peaks at the same emission wavelengths: a double peak at $\lambda_F \sim 450 - 460$ nm and $475 - 485$ nm, and other strong peaks at $540 - 560$ nm, $630 - 655$ nm and $706 - 725$ nm with a shoulder at ~ 690 nm. All samples had the main fluorescence emission peak at $\sim 630 - 650$ nm. Apart from these prominent peaks some smaller peaks were found in all samples. One difference seems to be that all NL samples do not have a peak at ~ 525 nm whereas all other samples show this peak.

The similarity of the spectra suggest that little further information would be obtained by imaging emission from various wavebands at different focal planes instead of one focal plane as done here. These were essentially randomly sampled from unique focal planes within each specimen particle contributing to the average spectra presented (Figure 3-42). They would therefore only indicate intra-sample variability.

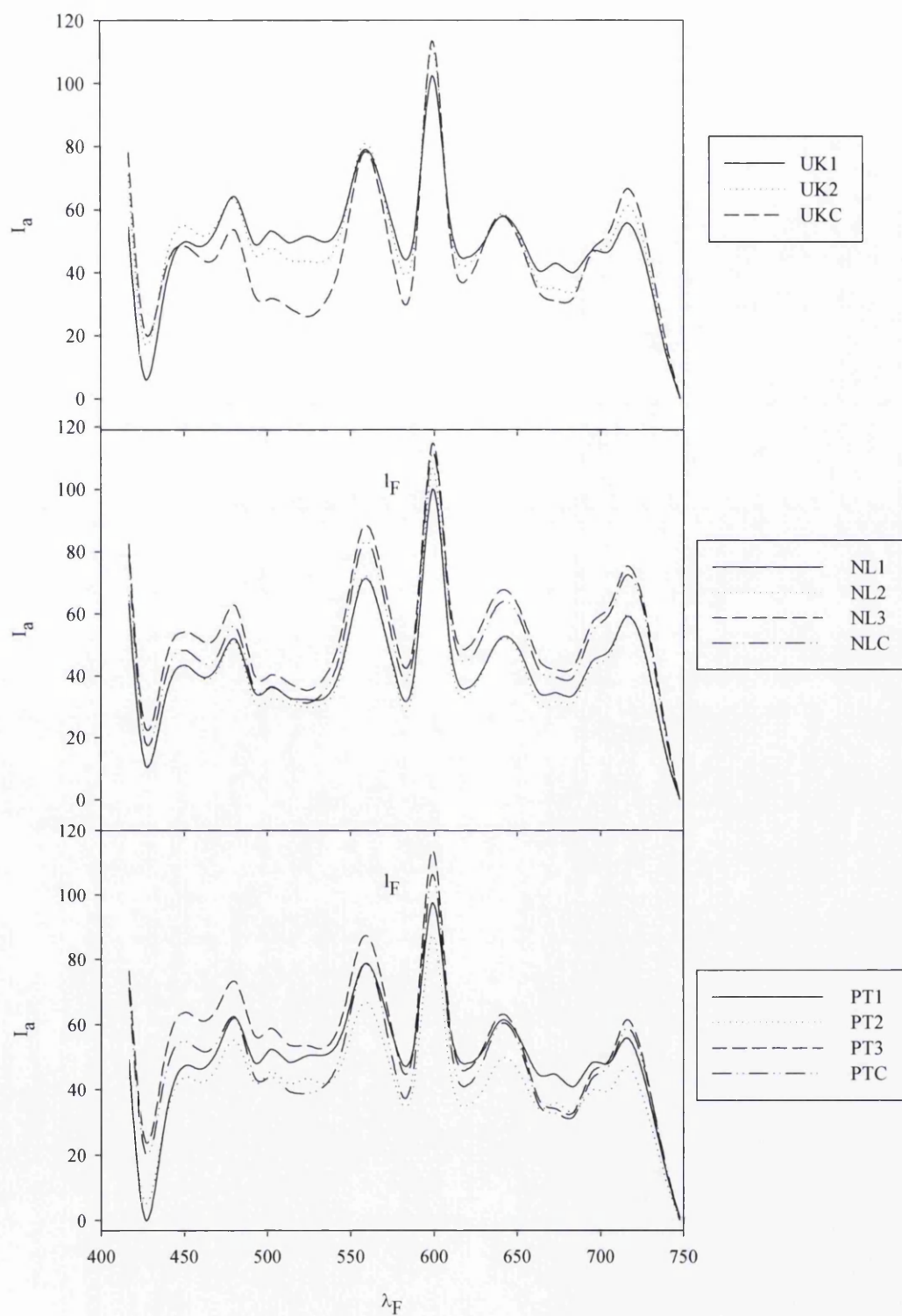


Figure 3-42: Average baseline normalized emission spectra of five particles from UK, NL and PT samples imaged with LSM meta-mode.

Examples of some colour coded images (one particle per sample) are shown in appendix A.

Additional to the investigation of mean λ_F distributions of a whole particle, it was possible to select a specific region and get the local λ_F distribution. This showed that the variation on some particles, especially from samples UK1, PT1 and PT2, was very high, but this had no consequence for the mean spectra of the sample. Figure 3-43a shows example spectra of selected regions of particles from samples PT1, PT2, UK1, GK2 and AU2, that differed from the mean. The respective colour coded overlay images of the particles are shown in Figure 3-43b.

Detailed investigations of extracted particles already showed that no overall distinct difference in organic matter composition was found for bulk samples (Mainwaring, 2004; Mainwaring et al., 2004; Morley et al., 2005). Fluorescence emission imaging confirmed this on the individual soil particle scale. Some individual particles from the samples showed differences in their spectra, but only in certain small regions. This, however, had no influence on the overall emission spectra and more information on these individual particles would be necessary. However, no method available for this study was able to identify the organic material directly on the soil particle surface, which would then allow interpretation on a molecular basis.

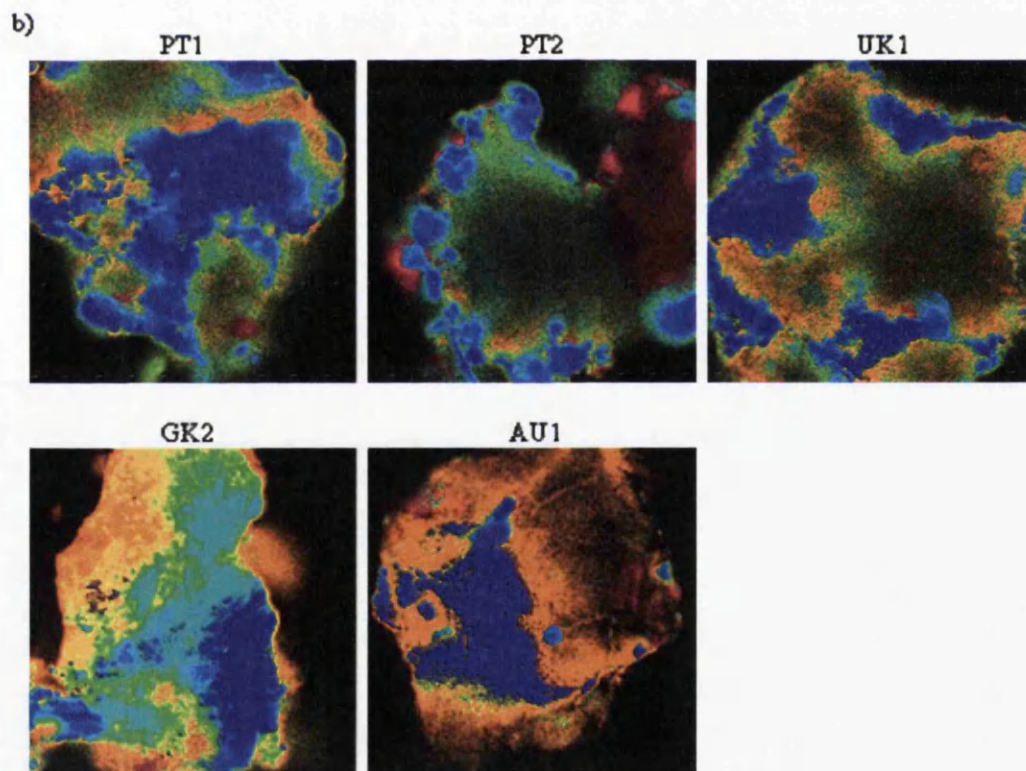
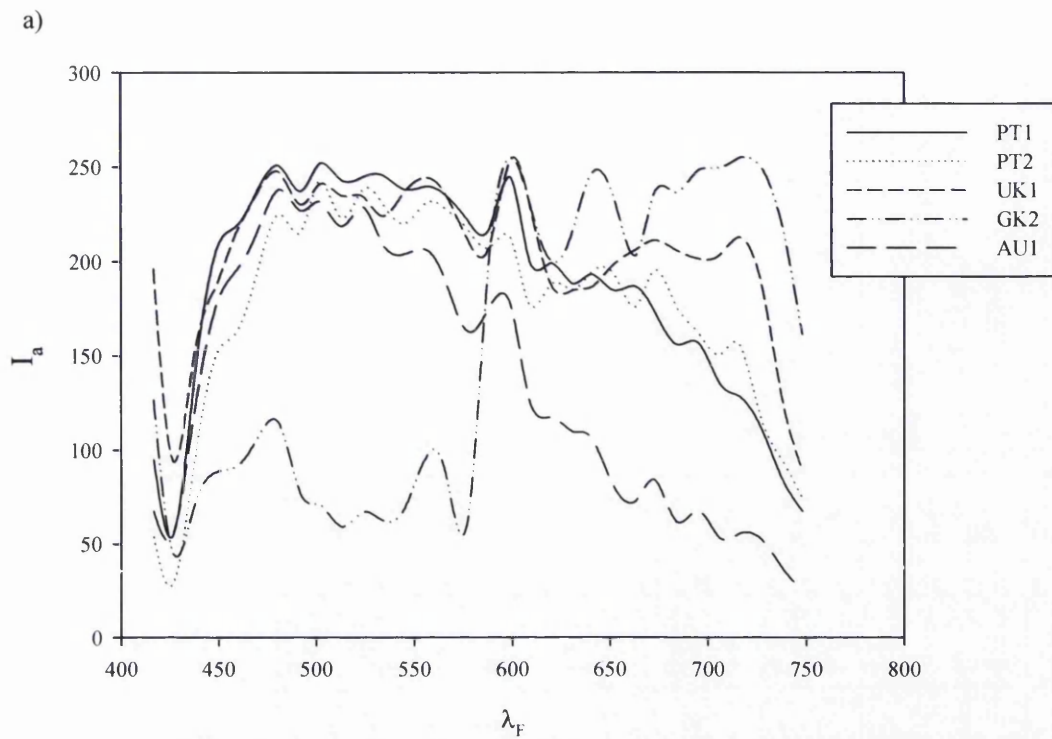


Figure 3-43: a) Spectra of individual regions on selected particles from samples PT1, PT2, UK1, GK2, AU1 and, b) colour coded images of these particles.

3.7 Synthesis

The relationship between fluorescence of single particles, multi-particle specimens and bulk soil properties seems to be very complex. One may speculate that interplay of fluorescence intensity (which determines the amount of fluorescing material), particle coverage, number of fluorescent areas and possibly size of the fluorescent areas is responsible for the expression of bulk soil characteristics. However, this only applies if the fluorescent material can be regarded as representative of the total amount of organic material present in the sample.

This said, the fluorescent matter represents only a part of the total organic matter within the sample and the relative amount of fluorescing organic material may vary from sample to sample. It also may be especially influenced by the nature of the organic material, which would vary with sample origin. However, a weak correlation between TOC and fluorescence was observed for samples with low to mid-range TOC content. Thus, it can be assumed that the amount of fluorescing organic material may provide a rough estimate of the total organic material in these samples and that the relative amount of fluorescing material in each sample is similar.

Although most samples did not contain large amounts of particulate organic matter, the presence of such material seemed to be important for the fluorescence measurement. The correlation between fluorescence intensity and TOC was mainly observed for multi-particle specimen investigations (which include particulate organic matter) and not for individual particles. Multi-particle specimen images may also be more representative than images of individual particles as they account for particle aggregates and large particles. However, different organic compounds can be responsible for the fluorescence at each origin, and different degrees of humification of the organic matter may be especially important regarding the soil profile NL (Kuntze et al., 1988; Scheffer et al., 2002).

As for the origin and nature of the organic material, it is known from previous investigations of the same samples that most contain five main component groups in similar amounts: long chain fatty acids (C_{16} - C_{24}), amides (C_{14} - C_{24}), alkanes (C_{25} - C_{33}), aldehydes or ketones (C_{23} - C_{31}) and complex sterol compounds (Mainwaring,

2004; Doerr et al., 2005b; Morley et al., 2005). Within these groups (except the alkanes) various aromatic compounds were found, which could be responsible for the fluorescence detected. As alkanes were found in all samples (including the wettable ones) it was assumed that they are not primarily responsible for the development of water repellency in the samples reported here. They were, therefore, considered to make a negligible contribution to the fluorescence. All averaged fluorescence spectra were found to be similar and independent of the sample, confirming the findings from previous studies that overall no significant differences in organic matter were detectable in the samples.

UK1, UK2, NL1 and NL2 are known to have large amounts of high molecular mass polar compounds such as fatty acids and sterols, which are probably a main part of the fluorescing compounds, whereas their wettable control samples UKC and NLC have less of these materials (Mainwaring, 2004; Doerr et al., 2005b; Morley et al., 2005). This coincides, in general, with a lower TOC in these wettable samples, so that a correlation between their TOC and fluorescence intensities could be mainly due to such components, which are likely to have large conjugated π -systems that are able to fluoresce.

The mineral material may also play a role for total fluorescence. Although silica itself does not fluoresce, inclusion of manganese or chromium may lead to mineral fluorescence (Rösler, 1991). The nature of the mineral, therefore, may also be of importance and depend on the sample source. As samples have diverse origins their mineral components may reflect these.

Additionally, changes in the moisture content of the samples cannot be excluded and eventually swelling or shrinking of organic matter may occur during measurement (e.g. Todoruk et al., 2003; Schaumann et al., 2004). Although it might not change the amount of fluorescing groups within a sample, the distribution of organics on the surface, its coverage and with that the fluorescence intensity could be affected. Water may also be needed for hydration to produce fluorophores. However, all samples were air-dried prior to analysis and fluorescence measurements were conducted in an air-conditioned laboratory at 20 °C, so that changes in moisture were reduced as much as possible. Investigations of soil particles under natural conditions and

comparison with air-dried particles or investigations under changing moisture conditions could clarify the influence of water content on fluorescence. The change in moisture content would best be investigated using a water immersion objective in order to image the kinetics of water uptake, otherwise drying could occur during the imaging procedure.

The variability in fluorescence of particles drawn from a sample was found to be high for all samples. This suggests that individual differences exist between particles and agrees with the suggestion that e.g. for the expression of water repellency only a few particles in a hundred are necessary in order to render a whole sample water repellent (Bisdom et al., 1993; Bauters et al., 1998; Bachmann et al., 2000a). The conformation and distribution of organic matter on individual particles may, therefore, be important for the expression of bulk soil properties. Thus, conformation and distribution should be investigated in direct relation to the particle properties, like the wettability of the individual particles. A method for the determination of such particle wettabilities was developed in this study and is presented in chapter 4. The results from fluorescence investigations in comparison with measurements of individual particle wettability are presented in chapter 7.

The extraction of soil samples with IPA/NH₃ did not remove all organic material (as shown in previous investigations, Mainwaring, 2004; Doerr et al., 2005b; Morley et al., 2005). The development of fluorescence intensity after extraction with IPA/NH₃, acid/base washing and a quantitative re-application of the extracted material suggested that several, possibly partly antagonistic and sample dependent mechanisms were occurring. For samples where fluorescence decreased with extraction, two main processes were suggested:

- i) non-fluorescent and fluorescent material was removed in equal parts or
- ii) extractions preferentially removed fluorescent material.

For samples without reduction or even increase of fluorescence after extractions the following mechanisms were discussed:

- i) organic matter was removed “layer-wise” during the extraction which may have led to an increase in fluorescence depending on the composition of the underlying layers;

- ii) non-fluorescing material was extracted which previously may have acted as quenching agent, and
- iii) the underlying mineral showed increased fluorescence emission due to its availability after extraction or its properties were changed due to acid/base attack exposing fluorescent areas within the mineral matrix. Inclusions of certain minerals such as manganese or chromium compounds may induce fluorescence in minerals (Jozefaciuk et al., 2002a).

The alteration of fluorescence, from its original level, when organic extracts were re-applied to the extracted soil material, may have many causes associated with modes and mechanisms of re-attachment to particle surfaces:

- i) The molecules were extracted without destruction and re-attach in a similar manner as before.
- ii) Extraction destroyed macromolecules and fluorophores are created/destroyed.
- iii) The bonding and structure arising from solvent evaporation is dissimilar to the natural processes of soil genesis.
- iv) Re-adsorption of the organic extract obscures existing fluorophores.

These mechanisms also encompass changes in the area of mineral surface covered by organic material and the population of sites suitable for adsorption of material. The distribution of the organic material with re-application may be connected to the roughness of the particle surface. This in turn could influence the distribution of remaining organic material by shielding material from extraction if layers are very thick, e.g. on surfaces with high roughness. Whether that is the bare mineral surface or organics remaining on the mineral surface after extraction is probably of less importance than the availability of attractive binding sites for the extracts. Therefore, the nature of the mineral and the distribution of remaining organic matter may be crucial. Many available binding sites (like organic matter distributed somewhat evenly on the surface) may lead to a highly spotty coverage of the particle surface in contrast to aggregations of organic material into large areas of newly deposited organic material. As time elapses in a natural soil the action of microbes and water on the organic material may return such artificially modified soil particles to their original state.

3.8 Conclusions

The various parameters associated with fluorescence defined here, such as total intensity, intensity normalized per particle surface area, percent of particle surface coverage with fluorescent material, and number of fluorescent areas or mean size of fluorescent areas, did not provide consistent or conclusive information in relation to bulk soil properties. The inter- and intra-sample variation was high. The expression of bulk soil properties may be governed by properties of individual particles. If this is the case, surface properties, like particle wettability, need to be investigated separately and compared with parameters of fluorescence in order to gain precise information.

The following chapters (mainly chapters 4 and 6) employ and test various methods for the description of soil particle surface properties in order to elucidate possible mechanisms affecting bulk soil wettability.

Chapter 4
Measuring particle water repellency:
development of a
“micro Wilhelmy plate method”

4.1 Introduction

The common method for investigating the wetting behavior of powdered materials is the capillary rise method (Preuss et al., 1998) or a modified Wilhelmy plate method (WPM). For the latter, the powder is fixed on a plate and then brought into contact with water (Woche et al., 2005) (see chapter 1.4.11). Both methods provide data for powdered material averaged over many particles rather than for individual particles. This is useful if the materials under investigation are pure and have a very narrow size distribution (as is the case in pharmaceutical applications).

Soil, however, is polydisperse and soil particles may exhibit a range of wettabilities within any particular sample, which somehow determine the overall wettability of bulk soil. The ability to estimate individual particle wettability is important in facilitating comparisons with data obtained from other (microscopic) particle investigations. It cannot be assumed that macroscopic soil properties, such as soil water repellency, can be directly correlated with individual particle characteristics, because it is not possible to assume that every particle within a bulk soil sample has similar wetting characteristics (Bisdom et al., 1993).

Bisdom et al. (1993) investigated sieve fractions from sandy soil samples and suggested that only some particles in each sample were responsible for the occurrence of its macroscopic water repellency. Similar to these observations, Bauters et al. (1998) found that the addition of only 3 wt% of extremely hydrophobic grains to a clean and wettable sand altered the wetting behaviour of the sample to an extent that fingered flow was reported. At around 5-6 % of hydrophobic grain content, the spontaneous infiltration of water into the sand was impeded and, thus, the material became water repellent. The proportion of hydrophobic material necessary to render a wettable sandy sample water repellent was much higher in experiments conducted by Bachmann et al. (Bachmann et al., 2000a). About 20 % hydrophobic grains were needed to obtain a CA of 20 °, 50 % for a CA ~ 70 ° and 80 % for a CA > 90 °. Shirtcliffe et al. (2006) found that the transition of water repellent to wettable conditions in soils occurred at a contact angle of ~50 °. The different proportions of hydrophobic material may be attributed to the different methods used for assessment

of water repellency and, probably, to the different materials used to render particles hydrophobic. Bachmann et al. (2000a) used the sessile drop method for contact angle measurement and treated particles with dimethyldichlorosilane, whereas Bauters et al. (1998) measured WDPTs and treated particles with octadecyltrichlorosilane. Bisdom et al. (1993) estimated the proportion of hydrophobic particles from examining and quantifying water repellency in sieve fractions of natural sandy soil samples.

Although these studies have added to the understanding of bulk soil water repellency, no information was provided about the range of wetting properties of the individual particles. Identifying such soil particle characteristics (e.g. individual particle wettability) therefore seems necessary. A method used in materials science for the determination of both interfacial tension of a liquid-liquid or liquid-gas system and the contact angle of a solid material with the interface is the so called sphere tensiometer based on the same physical principle as the WPM (Scheludko et al., 1975; Huh et al., 1976). WPM is a common method for powder or liquid investigations. It measures the force required to detach a solid sample from the liquid surface, which is proportional to the surface tension of the liquid. The technique is mostly used to determine the surface tension of liquids, but can also be used to determine contact angles between a solid and a liquid whose surface tension is known (see Figure 1-2 in chapter 1.4.1.1) (e.g. Chawla, 1994; Gilboa et al., 2006; Richter et al., 2006). The contact angle is calculated directly from the force measurement providing that the geometry of the sample is known (equation 1-7). It can also be determined optically from an image by measuring the angle formed between the solid and the tangent to the liquid lamella at the point of contact.

In contrast to the WPM which measures the detachment force between liquid and solid, sphere tensiometry records force curves while pulling a spherical sample through the interface between the two phases. Using very clean materials and precise instrumentation the latter is a highly sophisticated, but very complex method for exact determination of interfacial tensions and contact angles (Huh et al., 1976). Diameters of spheres used normally range between 1.6 mm and 6 mm (Gunde et al., 1995; Zhang et al., 1996; Zhang et al., 1997).

Although sphere tensiometry has not been used for measuring the wettability of solids, it could, theoretically, be used for this purpose as it is based on the physical principle of surface tension. This in turn is closely connected with the contact angle (Fieber et al., 1979; sections 1.3 and 1.4).

The adaptation and combination of these two techniques - WPM and sphere tensiometry - for determining the wettability of individual particles is explored and described in this chapter. The aim of this work was to develop a method for estimating the wettability of individual particles. As the development of the method is primarily based on the WPM it is referred to as the “micro Wilhelmy plate method” (“mWPM”). Two different approaches were chosen in order to obtain data: i) optical measurements (“o-mWPM”) and ii) gravimetric measurements (“g-mWPM”). In the following, these two methods are evaluated separately and then compared. The o-mWPM was also applied to soil particles from both water repellent and wettable samples, in order to estimate the range of particle wettability in soil samples, and its applicability for natural material is discussed.

4.2 Materials and methods

4.2.1 Samples

A range of glass and plastic ballotini of various sizes and displaying different degrees of wettability were used as standard particles. Two sizes of glass ballotini with average diameters of 120 μm and 270 μm were chosen. Some of these were mixed with FabsilTM (Grangers, UK), a silicon based water repellent liquid formulation designed for the treatment of textiles, and left to dry. This rendered the ballotini strongly water repellent. Polymethylmethacrylate ballotini (PMMA, brand name Diakon) with an average diameter of 270 μm were used as wettable to slightly hydrophobic material.

Additionally, soil particles from the water repellent samples NL2 and UK1 and from the wettable samples NLC and UKC were used in order to test the applicability of the technique to soil particles (cf. chapter 2).

4.2.2 Bulk contact angle measurement

Contact angles of single layer bulk materials, including those treated with Fabsil™ (as described above), were measured as described in chapter 2.2.2. Results and abbreviations used for various specimens are shown in Table 4-1. Measurements on smooth surfaces were carried out on glass and Fabsil coated glass slides. The contact angle of Diakon measured on a smooth surface is taken from Gottenbos et al. (2000).

Table 4-1: Contact angle of bulk materials (measured on single layers) and smooth surfaces of glass and Fabsil™ coated glass.

material / sample	abbreviation	contact angle on single layer [°]
glass ballotini, 120 µm	SG	53.0 ± 2.6
glass ballotini, 270 µm	GL	53.1 ± 1.3
Diakon, 270 µm	DIA	100.3 ± 1.3
hydrophobized glass ballotini, 120 µm	SGwr	128.0 ± 2.2
hydrophobized glass ballotini, 270 µm	GLwr	125.6 ± 0.7
smooth glass surface	-	29.9 ± 1.2
smooth water repellent glass surface	-	103 ± 0.6
NL2	-	102 ± 1
NLC	-	82 ± 1
UK1	-	105 ± 0.5
UKC	-	30 ± 1
hydrophobized NL2	NL2wr	126 ± 1
hydrophobized NLC	NLCwr	125 ± 1

¹ from Gottenbos et al. (2000)

4.2.3 Estimation of the proportion of water repellent particles per sample

To provide an estimate of the proportion of water repellent particles per soil sample a sample of material (0.5 g) was sprinkled slowly onto a water surface (~3 cm²). Particles left floating after one minute were then collected and their size and fluorescence were measured (compare Chapter 3). The experiment was repeated with longer time intervals of 1 h, 5 h, 8 h, 24 h and up to 48 h. Additionally, the experiment was repeated with acid washed and base washed particles which are considered to be fully wettable (see chapter 3 for method).

4.3 Particle wettability determination using the optical micro Wilhelmy plate method (o-mWPM)

4.3.1 Method

Several particles were sprinkled on a glass slide and then individual particles were selected randomly using the tip of a needle. These were glued individually to the middle of a microscope cover slip (one particle per cover slip) using waterproof cyanoacrylate adhesive (Anglin' glueTM, Fisherman's choice, UK). A total of at least 15 particles per sample were used. The cover slips were then fixed to a special device, which was designed to fit the syringe holder of the goniometer. The device consisted of a stainless steel tube enveloping a longer steel rod that was fitted with disks on both ends. The upper disk was clamped into the syringe holder of the goniometer and the lower was used as a platform to hold a glass cover slip using double sided adhesive tape. The particle was thus suspended from the lower face of the horizontal cover slip (see Figure 4-1). A clean glass microscope slide with a large water droplet (> 1 ml) was placed underneath the particle. The large surface area of water in comparison with the particle ensured a planar water surface in the contact region between them. The particle was then lowered towards the water (Figure 4-1a) at a speed of 0.011 mm s⁻¹ using the instrument's stepper motor. When in contact with the water surface it was stopped and retracted (Figure 4-1b) until the attached

water lamella broke. The events were controlled using the associated PC and were recorded using the instrument's video camera.

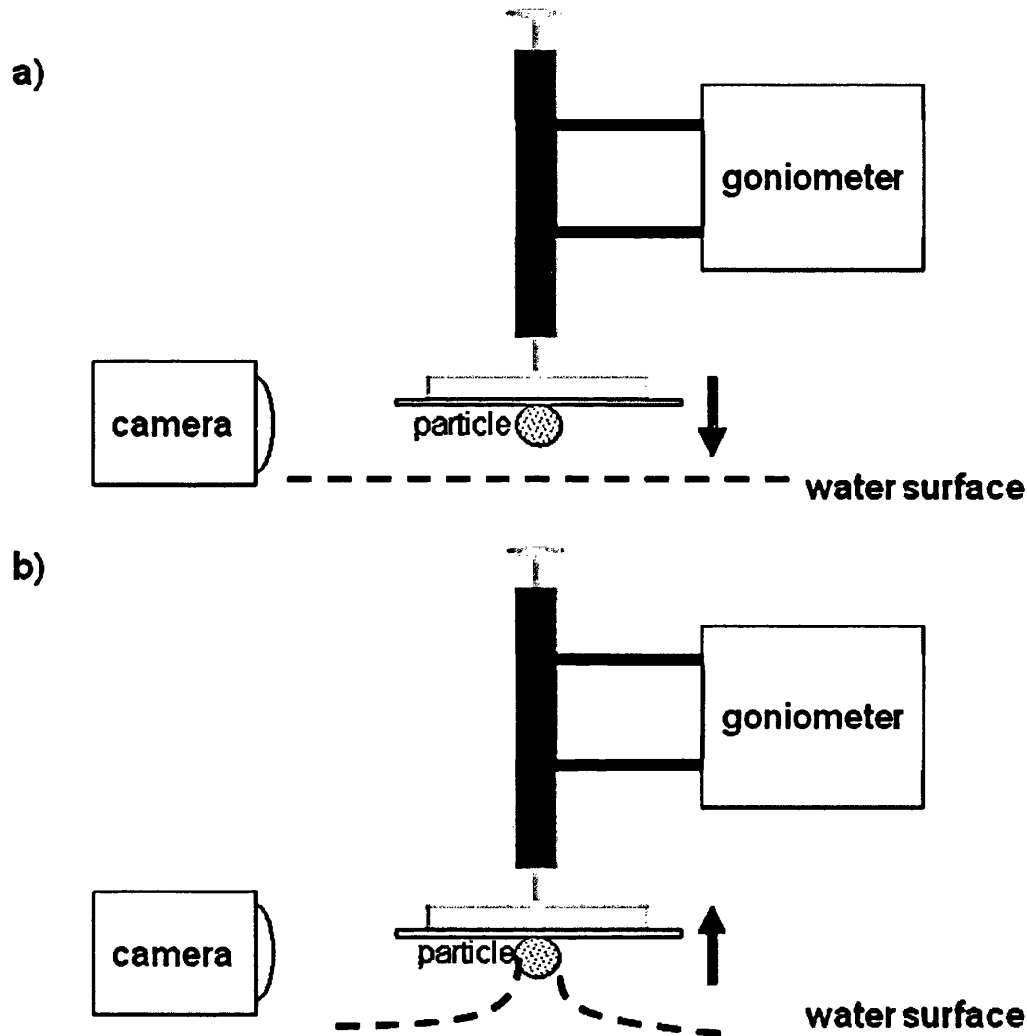


Figure 4-1: Diagram of a) approach of particle to water surface and, b) retraction of particle with water lamella attached.

Data were obtained by choosing two frames from the video: the first showing the water surface without contacting the particle to determine the baseline (i.e. the reference height of the free water surface); the second being the last frame before the lamella broke (see Figure 4-2). The images were then evaluated using SigmaScan Pro 5[®] software (SYSTAT Software Inc.). Data markers were set for the diameter of the particle, for several data points along the water line (pink crosses in

Figure 4-2), for the wetted perimeter (blue crosses in Figure 4-2) and at the midpoint of the particle. Additional data markers were set at cross points of a horizontal line through the lowest point of the particle and the water line (red crosses in Figure 4-2). From these data the intersection of baseline and water lamella was calculated.

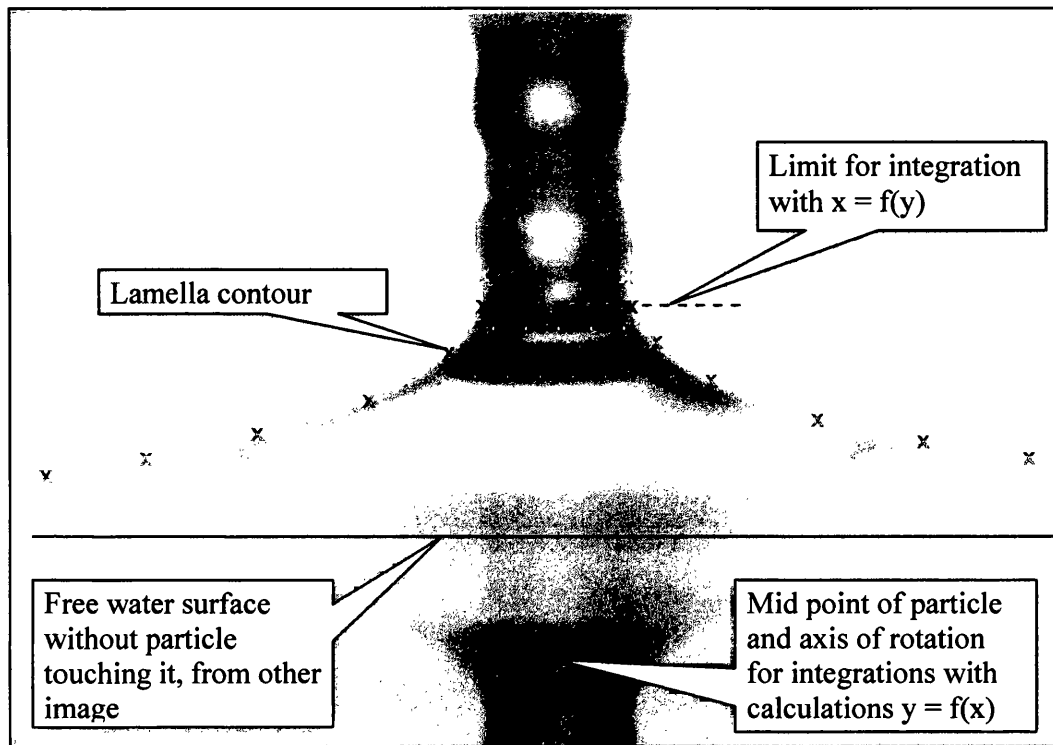


Figure 4-2: Determination of co-ordinates of the liquid surface just before the lamella breaks.

The data were saved as text files and then transferred to a program, which converted frame pixel co-ordinates to metric units (using a factor of 0.514 mm / 278 pixels, at the prescribed magnification which was fixed for all experiments). The program then calculated:

- i) the distance (h) between the free liquid surface (baseline) and the base of the particle,
- ii) the particle diameter (d),
- iii) the wetted diameter of the particle (d_w),
- iv) the volume (V) of water drawn between the free surface and the particle (assuming circular symmetry),

- v) the increase in potential energy of that water (E_{pot}), relative to the free surface and,
- vi) the wetted perimeter L (the contact line of liquid on the solid), from the wetted diameter (assuming a spherical particle shape).

The volume of water and the potential energy were calculated by numerical integration and rotation about the axis. It was possible to consider the volume as a stack of cylinders or set of cylindrical annuli, whose elements are rotated around the axes, allowing both approaches to be used and their outcomes to be compared. As the chosen elements could lie on either side of the particle and, in some cases, lateral asymmetry occurred, integrations were performed independently using data associated with the individual sides. In doing so, several estimates of V and E_{pot} were available for comparison.

Two numerical integration procedures were carried out: (i) trapezium integration employing the rule where an element under the curve is described as a trapezium (Merziger et al., 1996) and (ii) a cubic spline integration, which uses cubic polynomials for piecewise integration over subintervals (Schwarz et al., 1986). Four integrations were carried out for each side of each particle comprising cubic spline integration and trapezium integration with rotation along the x-axis (following, for convenience, rotation of the image) and along the y-axis, respectively.

4.3.2 Results from o-mWPM

4.3.2.1 Lamella height measurements

The lamella height of water pulled up by an individual particle was considered to represent the wettability of that particle. A linear correlation (with $r \sim 1$) between lamella height (h) and contact angle (θ) of the bulk material on a flat surface was found for the materials GL, DIA and GLwr (Figure 4-3 a). Mean h values of SG and SGwr ballotini were about 0.05 mm smaller than those of GL and GLwr ballotini, respectively. Glass beads GL and GLwr, as well as DIA ballotini, had a similar mean diameter, whereas the glass beads SG and SGwr were about half that size. The differences between h of the samples GL, GLwr and DIA were significant ($p = 0.01$).

The influence of particle size was reduced by utilization of the dimensionless ratio h/d with d being the individual particle diameter (Figure 4-3b). This reduces the difference between the mean h of wettable glass ballotini SG and GL, and has a similar effect on water repellent glass ballotini GLwr and SGwr. The wettable SG and GL group was found to be significantly different from the water repellent GLwr and SGwr group ($p = 0.01$). h/d reduced the difference between GL, SG and DIA samples. Both GL and SG materials were wettable and can be clearly differentiated from water repellent glass beads (GLwr and SGwr).

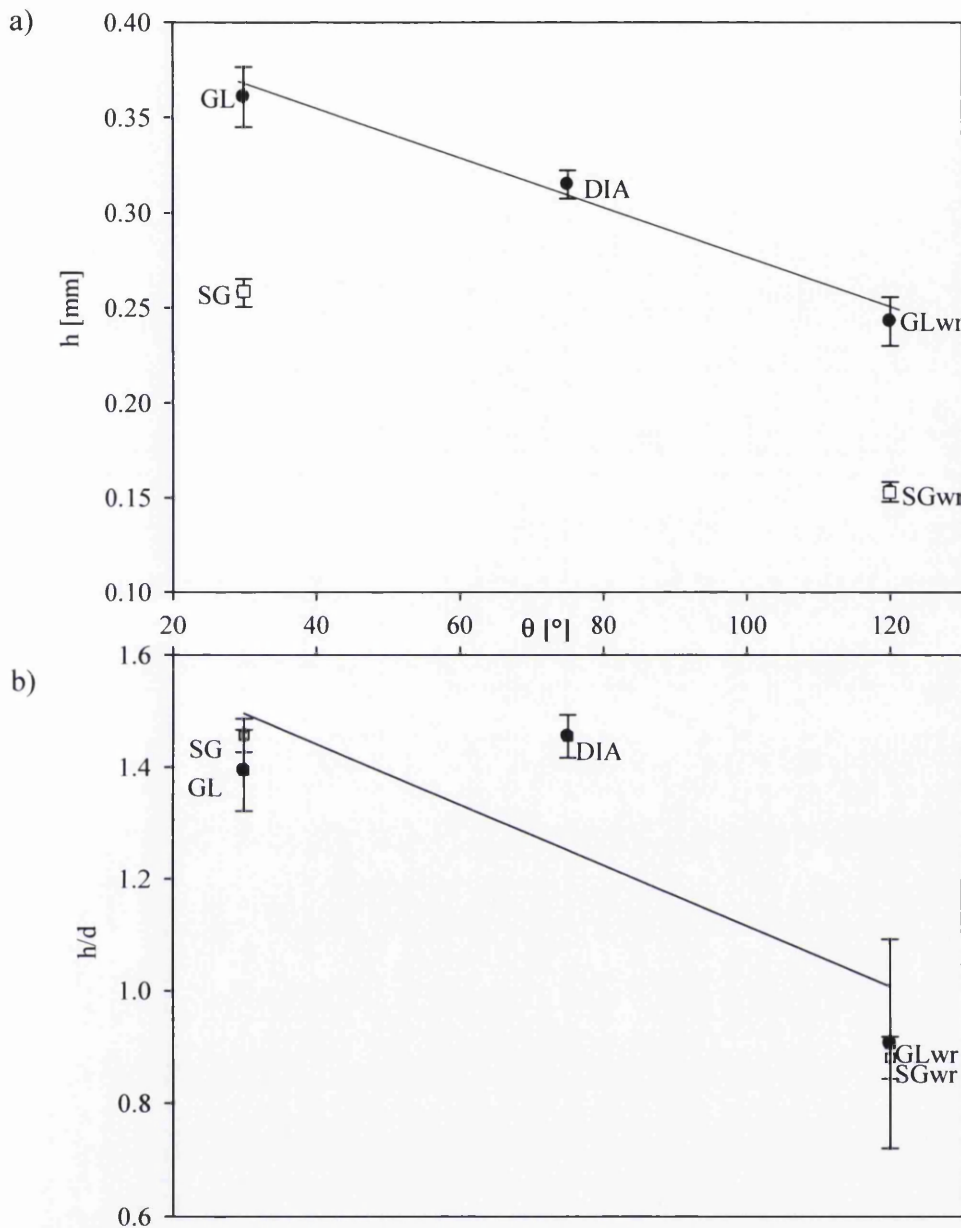


Figure 4-3: a) θ of bulk material vs height of water lamella and, b) θ of bulk material vs lamella height normalized by particle diameter.

Box plots (a form of frequency distribution describing the distribution of data in a simple way) of all samples are shown in Figure 4-4. The box represents 50 % of the data with the solid line inside as the median of the distribution and the dashed line as their mean. The upper whisker represents 90 % of the data (90th percentile) and the

lower 10 % (10th percentile). The “xs” are defined as outliers of the data distribution and, thus, represent maximum and minimum values.

GL and GLwr have a very narrow h/d distributions for 50 % of the values (box), but a wide distribution is found for 90 % of their values and the outlying points are much higher / lower than the 90th / 10th percentile, respectively. SG, DIA and SGwr show a much broader distribution for 50 % of the values, but 90 % and outlying points are very close to the 25th and 75th percentile (see Figure 4-4).

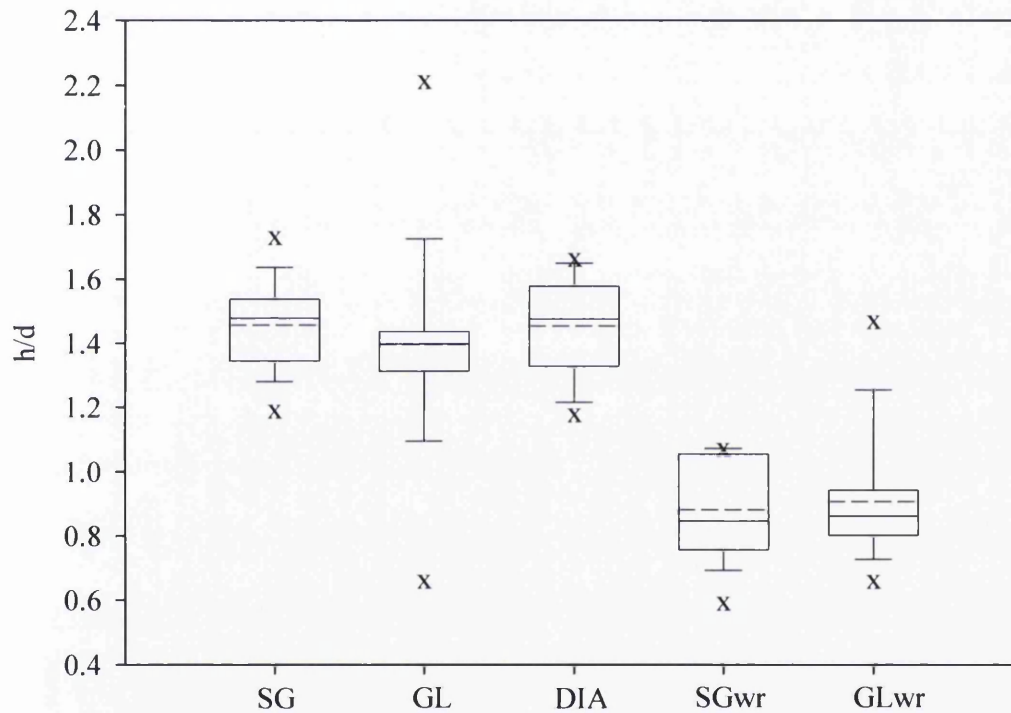


Figure 4-4: Distribution width for each sample given as box plots.

4.3.2.2 Calculation of potential energies

It was considered that E_{pot} could serve as another measure of individual particle wettability. Although the particles were spherical, E_{pot} values calculated from the left and right hand sides of the video frames were often found to be different, but set apart from very far outlying values the data group around the 1:1 line (Figure 4-5). It

can thus be assumed that the two sides are similar. In a few cases, and depending on the sample, differences of up to 30 % were found between the two sides. The average difference between sides, however, was 15 % and, for further considerations, mean values of the left and right hand side were used.

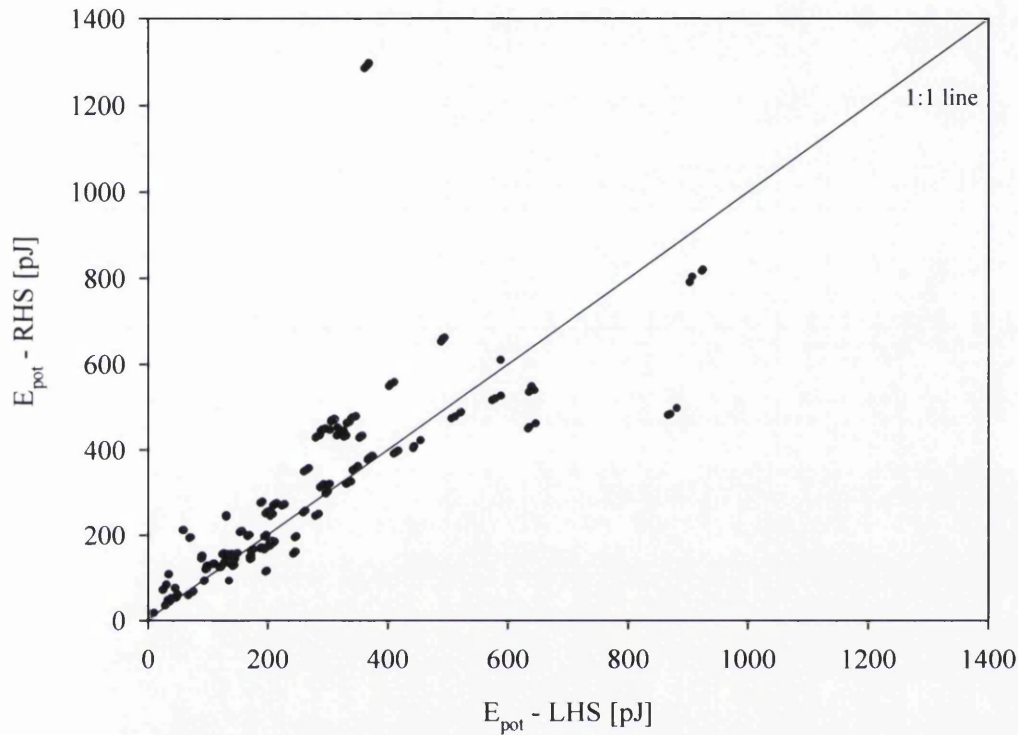


Figure 4-5: Integrals of right hand side data vs left hand side data for all samples based on the integration procedures and geometric elements used for integration.

Cubic spline and trapezium rule integration procedures applied to squat cylinders and annuli resulted in similar values for E_{pot} (see Figure 4-6 and appendix B). The trapezium integration seemed stable with respect to random variability in the source data. However, variation in raw data caused some spectacular failures in the cubic spline integration procedure for both squat cylinders and annuli elements. Where it performed satisfactorily, it indicated that the trapezium procedure was of adequate precision and the estimates arising from this latter procedure were used here.

Figure 4-6 shows the relationship between height and potential energy for particles from the GL sample (particles from all other materials are presented in appendix B). It is obvious that with increasing height of the water lamella the potential energy also increases in a linear relationship as expected ($E_{pot} = m \cdot g \cdot h$). However, data are scattered relatively broadly.

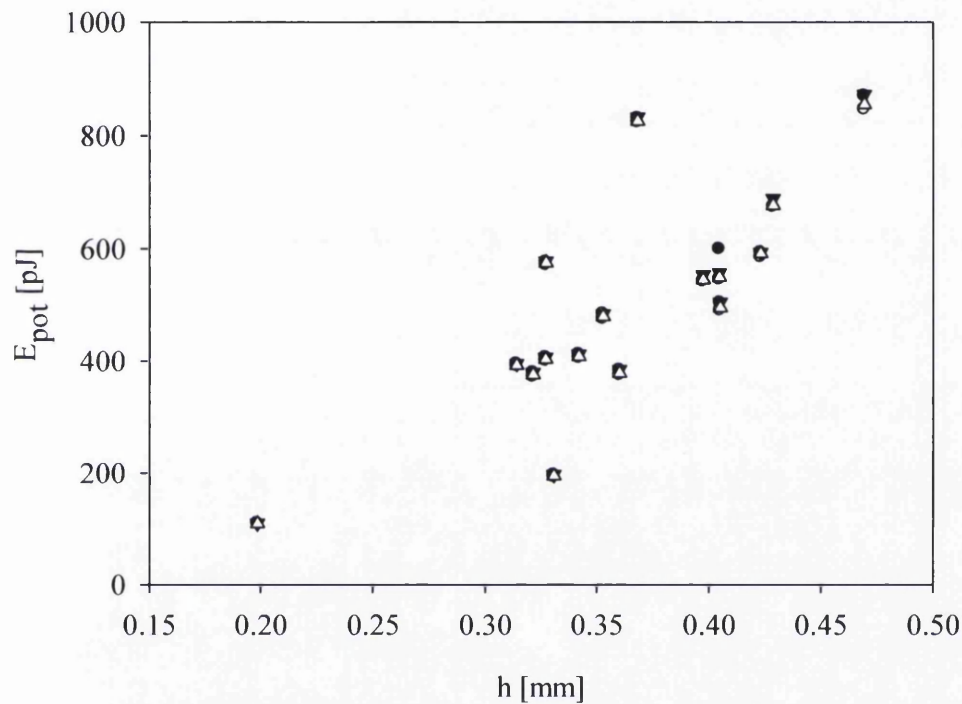
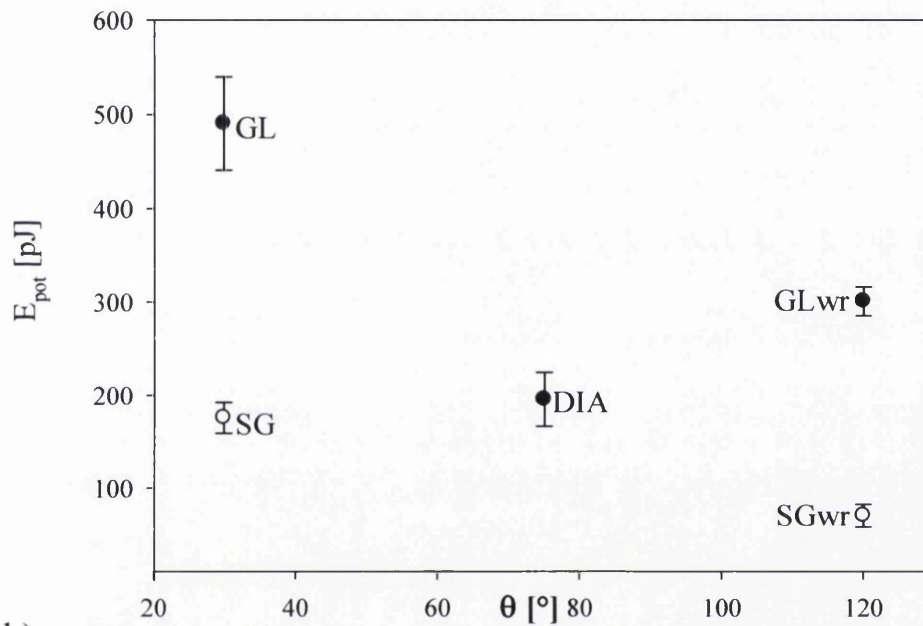


Figure 4-6: Mean E_{pot} vs h of sample GL.

No clear correlation was found for mean E_{pot} of individual particles and contact angles of a flat surface of the corresponding material measured by the sessile drop technique (Figure 4-7a). Although the wettable GL particles have a higher mean E_{pot} than water repellent GLwr particles, the wettable DIA particles have the lowest mean E_{pot} within this size category. Both mean E_{pot} of SG and SGwr are lower than those for all other particles examined, probably due to the size of the particles resulting in a smaller water lamella and, therefore, lower potential energy. However, if the potential energy is normalised by the respective particle diameter, the measure

E_{pot}/d shows a good correlation with the contact angle within the large particle size range (samples GL, DIA and GLwr, Figure 4-7b, $r \sim 1$). However, SG and SGwr have much lower E_{pot}/d than GL and GLwr, respectively, thus indicating the size alone may not be the only factor influencing the measurement.

a)



b)

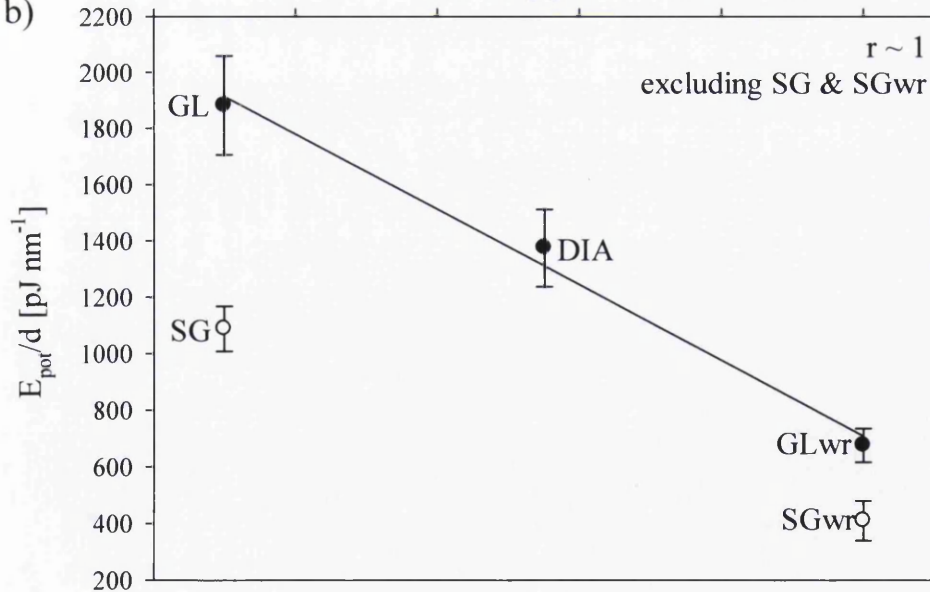


Figure 4-7: a) Mean E_{pot} and b) mean E_{pot}/d of individual particles vs contact angle of the material on a flat surface.

Other measures, such as height normalised by the wetted perimeter (h/L), showed distributions similar to the actual height distribution (appendix B). However, SG had a higher h/L ratio than GL.

4.3.2.3 Reproducibility of measurements

Lamella heights were found to vary somewhat when measurements were made repeatedly on the same particle without intermediate drying, but no directional behaviour was observed. However, differences between repetitions were small with a maximum standard deviation of around 6% of the measured lamella height (appendix B).

Repeated measurements of lamella height of individual particles (model materials and soil particles) were carried out after rotating the particle in the imaging field by $\sim 90^\circ$. No significant differences in the lamella height were observed with changes in position of the particle, but the apparent particle diameter varied strongly depending on the individual particle. Model particles had very similar apparent diameters independent of their position in the image due to their regular shape. Some soil particles, however, were of cylindrical shape and if orientated horizontally on the holder, the apparent diameter was strongly dependent on the direction of observation.

Therefore, the consideration of the ratio h/d may be error-prone for soil samples.

4.4 Particle wettability determination using the gravimetric micro Wilhelmy plate method (g-mWPM)

4.4.1 Method

An individual particle was randomly chosen and glued to the shorter side of a microscopic glass slide using double sided adhesive tape. The microscopic slide was then inserted into the holder of a tensiometer (DCAT 21, DataPhysics Instruments GmbH, Filderstadt, Germany), which was connected to a electronic balance (Figure 4-8).

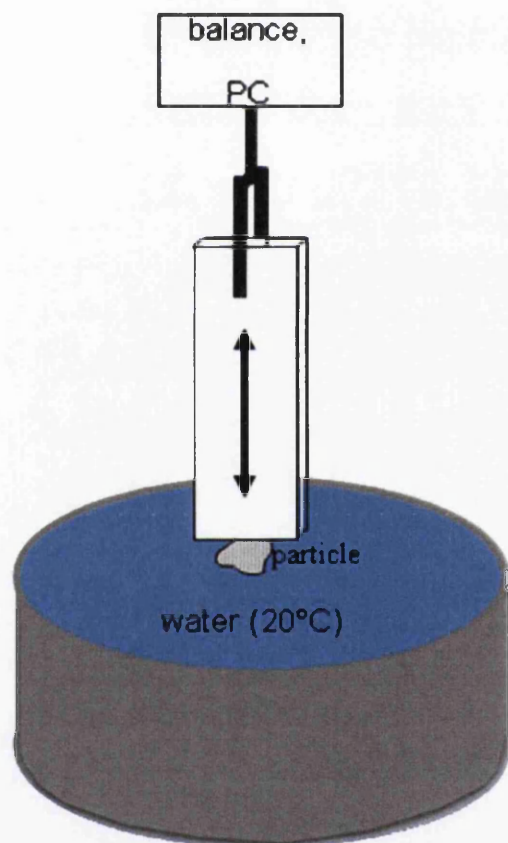


Figure 4-8: Set-up for SCAT21 tensiometer (DataPhysics) with a single particle glued to a microscopy glass slide.

The measurement is automated and controlled by the SCAT11 software (DataPhysics Instruments GmbH). With the specimen in place, the balance was tared and the sample was slowly lowered, at a speed of 0.01 mm s^{-1} , into a container of water at $20 \text{ }^\circ\text{C}$. The weight change necessary to trigger a measurement was set to 0.08 mg and immersion depth of the sample was set to 0.06 mm and 0.1 mm . This was measured from the point the balance registered the required weight change. After some initial trials involving the use of both depths it was found that the precision and value of the lamella breakpoint was similar in both cases (Table 4-2). So the immersion depth of 0.1 mm was selected for further work.

Table 4-2: Lamella breakpoint (p) calculated from different immersion depths for materials GL, DIA and GLwr for five particles per material using three repetitions for each immersion depth.

		p [mm] for immersion depth	
		0.06 mm	0.1 mm
GL	1	0.52 ± 0.01	0.51 ± 0.01
	2	0.55 ± 0.01	0.53 ± 0.01
	3	0.45 ± 0.01	0.42 ± 0.01
	4	0.55 ± 0.01	0.54 ± 0.01
	5	0.47 ± 0.01	0.42 ± 0.01
DIA	1	0.44 ± 0.01	0.39 ± 0.01
	2	0.44 ± 0.07	0.46 ± 0.02
	3	0.39 ± 0.01	0.42 ± 0.01
	4	0.45 ± 0.01	0.42 ± 0.03
	5	0.47 ± 0.01	0.41 ± 0.05
GLwr	1	0.28 ± 0.01	0.25 ± 0.01
	2	0.31 ± 0.01	0.28 ± 0.02
	3	0.39 ± 0.02	0.37 ± 0.01
	4	0.27 ± 0.01	0.21 ± 0.02
	5	0.25 ± 0.01	0.25 ± 0.04

The system recorded the weight of the water pulling on the sample (in g) in relation to the position of the sample (in mm), with the point of origin set at the maximum

immersion depth. This allowed construction of a weight vs distance curve (Figure 4-9).

As the specimen was withdrawn, a water lamella was pulled up and the weight registered on the balance increased (region A in Figure 4-9). Close to the breakpoint of the lamella, the weight of the water lifted by the particle reached a maximum and the contact angle between water lamella and particle became zero (point B in Figure 4-9). The lamella then thinned as water drained from it under the influence of gravity. This process happened quickly (in the range of ms) and within a short distance (~0.05 mm, point C in Figure 4-9) of the water lamella breakpoint. A tangent was drawn on the curve between points B and C and a horizontal line drawn at maximum mass. The intersection between these was defined as the lamella breakpoint (see inset in Figure 4-9).

This point may not represent the real height of the water lamella pulled up by the particle as the height measurement only starts at the moment of the defined weight change. The lamella break point, therefore, is not referred to as lamella height but as sample position (p). All values were also corrected by the immersion depth of 0.1 mm and the starting value $C_s \sim 0.4$ for all samples, so that:

$$p = B - 0.1mm - C_s \quad (4-1)$$

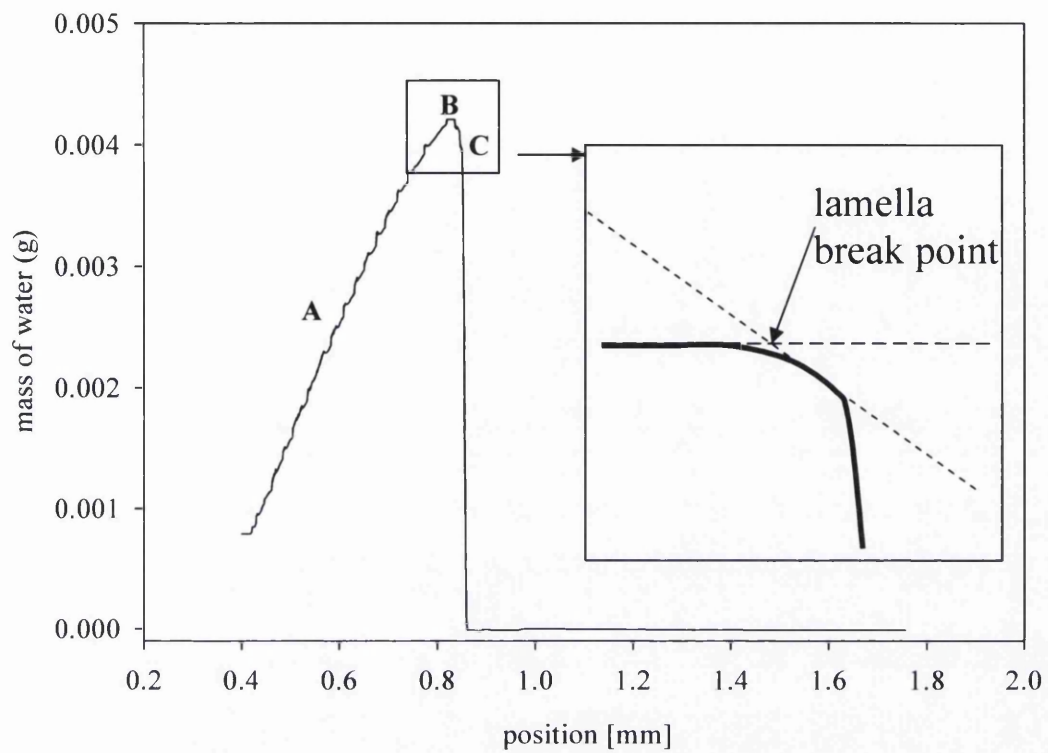


Figure 4-9: Typical weight vs distance curve for a spherical particle: A) at increasing distance from liquid surface, B) at maximum force/ maximum weight of water pulled up by sample, and C) thinning liquid lamella reduces the force pulling on the particle.

4.4.2 Results of the g-mWPM

Samples GL, DIA and GLwr of similar size were investigated with this method. GL and GLwr particles were significantly different in terms of sample position (p). DIA particles had a similar mean height water lamella to that of the wettable glass particles, although their contact angles differed significantly (Figure 4-10a).

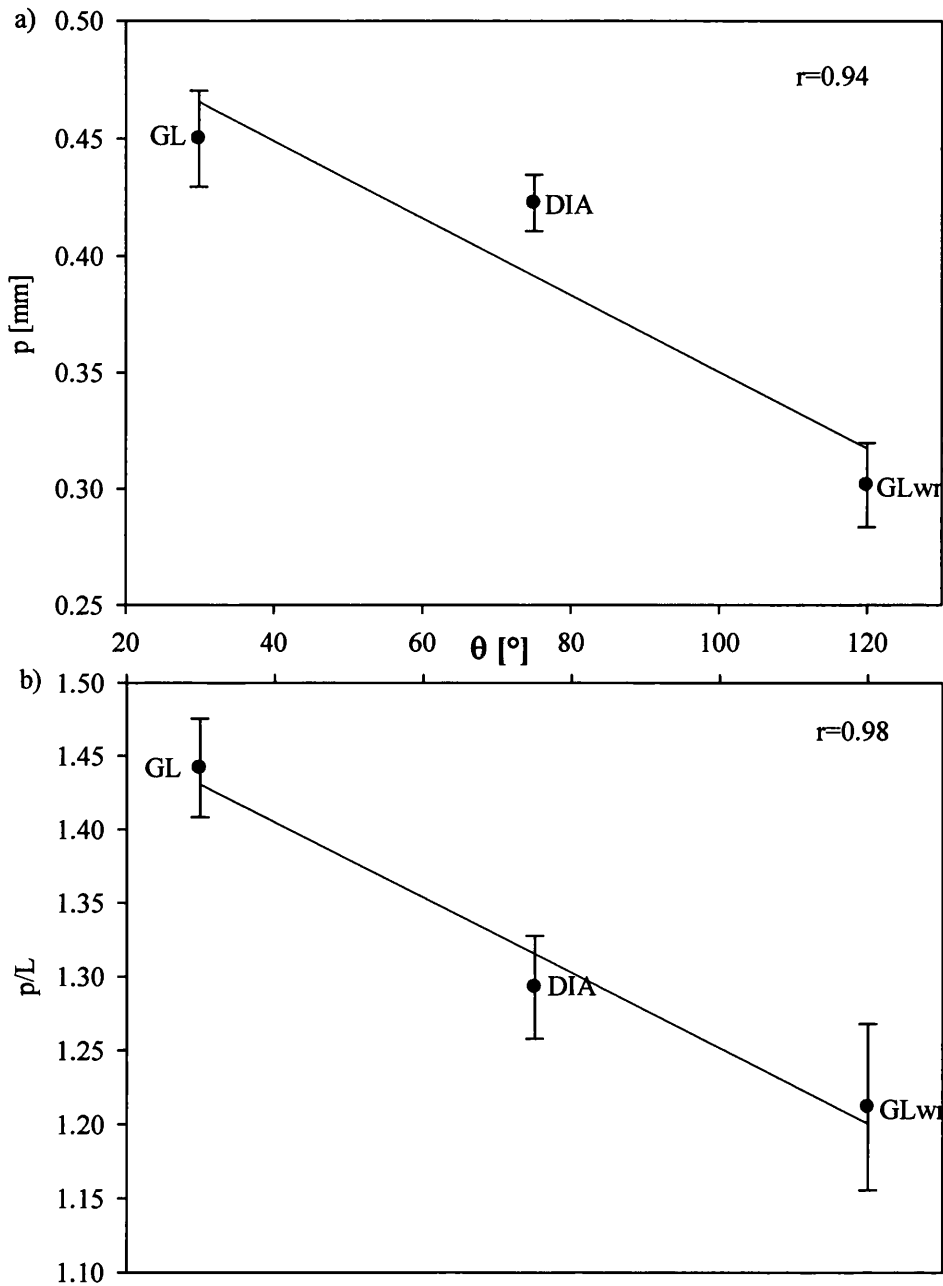


Figure 4-10: a) position of sample (p) relative to liquid surface vs contact angle θ on a smooth surface and b) p normalized by wetted length (L) vs θ . Error bars equal standard error.

In order to compensate for the variation in particle size, the wetted particle perimeter (L) was estimated from the maximum force (F_{\max}) and surface tension of water (γ_L). This was necessary as the method does not offer a direct facility for determination of particle size by optical means.

$$F_{\max} = m_{\text{water}} g = L \gamma_{\text{water}} \cos \theta \quad (4-2)$$

The contact angle θ was assumed to be zero at maximum force (see Figure 4-9b); thus, L was calculated as:

$$L = \frac{m_{\text{water}} g}{\gamma_{\text{water}}} \quad (4-3)$$

The correlation of p/L with contact angle (Figure 4-10b) is an improvement over that of p itself. Unfortunately, it was not possible to verify the behaviour for particles substantially different in size from these due to a lack of availability of a range of materials within an alternative and narrow size class.

4.5 Discussion and comparison of o-mWPM and g-mWPM

Two similar methods for measuring individual particle wettability have been evaluated: o-mWPM and g-mWPM. Both involved bringing particles into contact with a free water surface and raising it to form a water capillary or lamella which eventually ruptures. Absolute values of h calculated from images obtained by o-mWPM and the position p recorded by g-mWPM for particles with similar size and properties were found to differ. Nevertheless, a good linear correlation between the two methods was found ($r \sim 1$, Figure 4-11). As only three points were available for correlation, the data need to be considered carefully. The data deviate from the 1:1 line, indicating a systematic difference between the two methods, which is probably due to the different principles underlying these measurements. The determination of p from the g-mWPM is an approximation of the lamella height. This in turn is

dependent on the precision and accuracy of the balance in relation to detecting the weight change that triggers measurements. The o-mWPM also approximates the measurement of the lamella height, which, in principle, could be very accurate with suitable equipment. However, the method as used here was restricted by the capturing speed of the camera. Use of a high speed camera would allow observation of lamella thinning and precise location of its breakpoint, albeit at the expense of some resolution in the images. Using a high speed camera could improve data quality and would even allow imaging the thinning of the water lamella.

The standard error of the mean h and p of all samples is similar for o-mWPM and g-mWPM, suggesting a comparable level of precision for both methods.

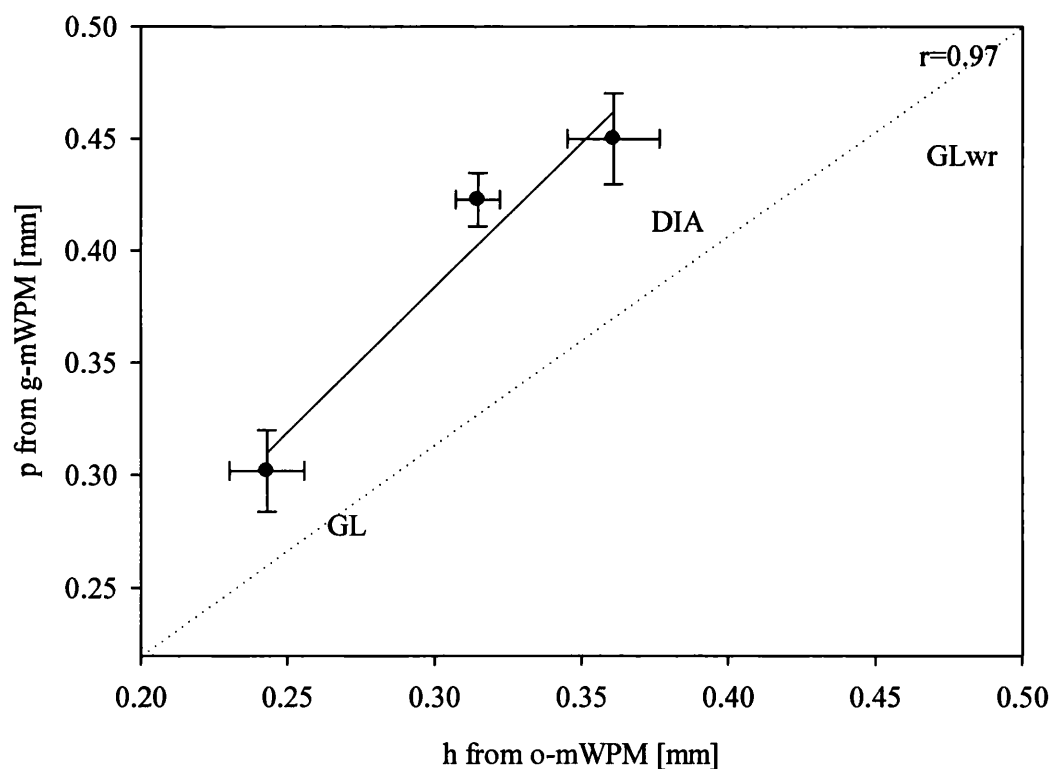


Figure 4-11: Mean lamella heights determined by tensiometer (g-mWPM) vs goniometer (o-mWPM).

Compensation for variation in particle size by considering h/d or P/L appears to be useful as it reduces the differences associated with material of the same surface properties (such as glass beads).

The similarity in the strength of correlations involving E_{pot}/d and h/d suggest that the latter might just as well be used for comparison with other data as it is readily amenable to manual evaluation directly from the appropriate video frames. The more detailed, but also more time consuming, evaluation of E_{pot} appears to be unwarranted.

Both o-mWPM and g-mWPM appear to be able to detect differences between model particles of different wettabilities. The o-mWPM provides additional information about particle diameter and wetted perimeter. The handling of o-mWPM is straightforward, but the evaluation by g-mWPM is easier and less time-consuming. Sample preparation is similar for both samples and not very time-consuming. Particles need to be selected individually and glued to a glass slide. The sample measurement time is also similar for both methods.

Data quality would be improved if more detailed information about draining of water from the lamella and its rupture in combination with information about particle size and shape were available. Therefore a combination of both methods whereby images of the particle and water lamella are obtained together with the force measurement of the DCAT tensiometer may be useful. Using a substantially higher frame rate than is employed by the 'easydrop' instrument may deliver additional information about the exact time of lamella rupture and lamella thinning just before rupture.

4.6 Application of the o-mWPM to soil particles

The key aim of the investigation was enable determination of the range of wettabilities occurring amongst natural soil particles. The soil samples used in this study are described in detail in chapter 2 and experimental details are as presented in 4.3.1 above.

4.6.1 Results

4.6.1.1 Lamella height measurement of natural soil particles

The distributions of lamella height obtained from the analysis of individual particles selected from wettable and water repellent soils showed significant overlap (Figure 4-12a). Data from o-mWPM showed that the range of h for the wettable soil UKC practically falls within that for the water repellent soil UK1, but the latter shows a significant proportion of data below that of UKC. The distribution width of UK1 is larger than that of UKC. Distributions for both wettable soil NLC and water repellent soil NL2 were found to be quite similar. However, a significant difference exists between the UK and NL sample pairs in terms of size distribution. Particles from UK samples are larger than those from NL samples (see chapter 2), so that a comparison of h between these samples is difficult.

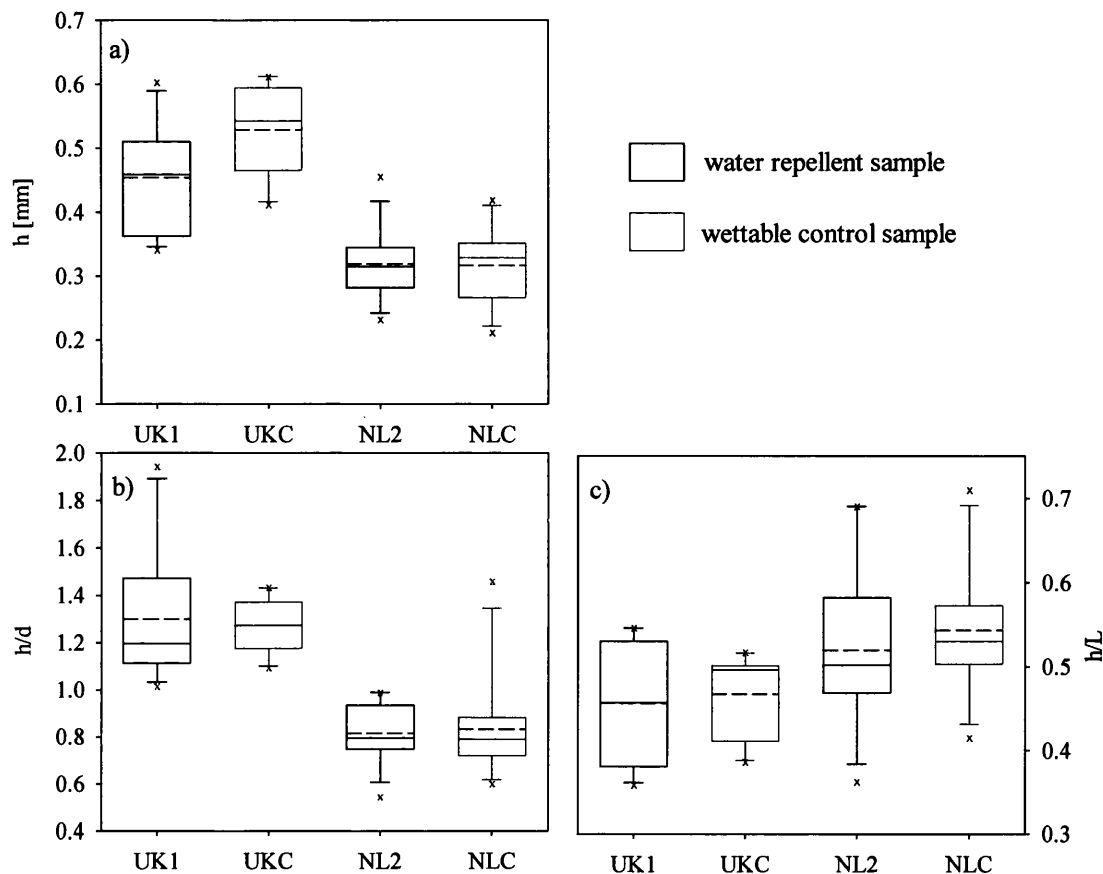


Figure 4-12: Box plots of the distribution of h , h/d and h/L of various soil samples. The dashed line represents the arithmetic mean, the solid horizontal line the median and x outliers.

Again, the UK pair had significantly different normalised height distributions h/d from those of the NL pair that fell well below those of the UK pair (Figure 4-12b). The h/d distribution for UKC was found to fall well within that of UK1 and, as for h , no difference between NL2 and NLC was found. The distribution width of h/d for UK1 was again larger than that for UKC.

Lamella height h normalised by the wetted perimeter L also showed that the UKC distribution falls well within the limits of UK1 and the two are essentially indistinguishable from each other. The distributions of the NL pair are also similar,

but with means, medians and limits above those of the UK samples. Both water repellent samples show a broader h/L distribution than the wettable ones.

The mean lamella heights of UK1 and UKC samples were higher than those of any model particulate material, whereas NL2 and NLC both have a mean h similar to that of DIA. Mean h/d values of both UK samples are between those of GL and GLwr. Both NL samples have mean values in the region of that of SGwr (Figure 4-3).

4.6.1.2 Comparison of particles before and after coating with a hydrophobic agent

Measurements of lamella heights before and after exposing individual particles to water repellent material showed consistent differences with reduction of h following exposure. This was found to be the case for model (glass and Diakon) particles and for those taken from both wettable NLC and water repellent NL2 soil samples (Figure 4-13). The values of h seem to be reduced by a consistent amount for most of the particles of each type. This was especially evident for glass ballotini (GL) and particles of NLC. The reduction in h values of GL and DIA particles, and those of particles from NL2 and NLC, following (water repellency) treatment with Fabsil, were significant. The soil particles showed more absolute variation than GL or DIA particles (Table 4-3). The highest absolute reduction occurred for NL2 particles. Absolute and relative reductions of h for all investigated particles are shown in Table 4-3.

Table 4-3: Absolute and relative mean reductions of h after coating with Fabsil™.

	h reduction in mm	h reduction in %
GL	0.16 ± 0.01	52.6 ± 1.4
DIA	0.15 ± 0.01	52.6 ± 1.8
NL2	0.24 ± 0.04	38.7 ± 2.8
NLC	0.22 ± 0.01	45.6 ± 1.0

The h values of all particles rendered hydrophobic with Fabsil returned h values within a narrow absolute range ($0.07 \text{ mm} < h < 0.12 \text{ mm}$) well below that of the original particles (Figure 4-13).

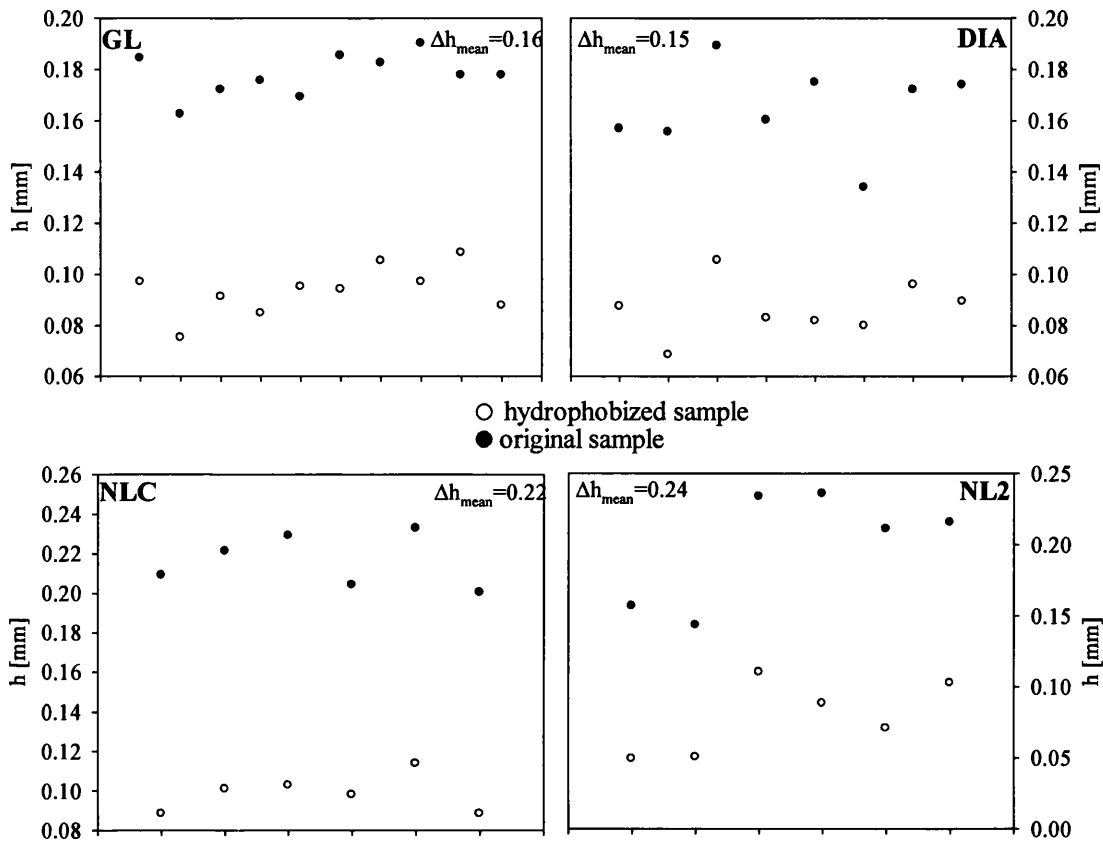


Figure 4-13: Lamella height h of original and hydrophobized samples.

The addition of a hydrophobic reagent to the samples may have changed the surface energy of all particles to the same value as their surface was rendered similar after coating. Therefore, normalization of h (by dividing h by the values obtained after particles had been rendered hydrophobic) should have eliminated some influence of other surface characteristics, such as shape. However, this was not the case, as the relative reduction of h was similar for each particle from one sample. (Figure 4-13).

4.7 Relative amount of hydrophobic and hydrophilic particles per bulk sample

Following sprinkling of soil particles on to a water surface and observing the proportion remaining afloat or sinking after 1 minute, little or no difference was found between the behaviour of wettable and water repellent soil samples. Observations after 48 h suggested that no change in proportions had occurred. This behaviour was also observed with acid or base washed particles, such that similar proportions floated or sank. This suggests that mechanisms other than water repellency influence the division or separation.

The difference found between the particles floating and those that sank was the mean particle size (Table 4-4). Those that sank were found to be significantly larger than those that floated. This suggests that particle weight was the main factor perhaps with smaller influences from particle density, shape and roughness, especially if air may be trapped between rough surface features limiting the area of contact with water.

Table 4-4: Fluorescence, mean size and mean surface area of floating and non-floating particles.

	I_f		mean d [μm]	mean A [μm^2]
	(Ar-laser)	(He/Ne-laser)		
AW floating	268 \pm 60	935 \pm 183	188 \pm 12	30813 \pm 4374
AW non-floating	326 \pm 56	1191 \pm 199	238 \pm 11	48117 \pm 5269
NaOH floating	178 \pm 20	622 \pm 68	181 \pm 7	2565 \pm 2042
NaOH non-floating	197 \pm 51	892 \pm 160	204 \pm 7	35515 \pm 2627

In industrial processing, other methods for the determination of the hydrophobic/hydrophilic ratio are used. For example, in the coal industry floatation is used to separate hydrophobic from hydrophilic coal particles (e.g. Marmur et al., 1985). However, this method does not seem directly applicable to soil particles as they become wettable some time after being forced into contact with water.

4.8 Discussion

If h or h/d is considered as an indirect measurement of particle wettability, then the wide range of values obtained for particles drawn from the same soil sample strongly suggests that wettability is a distributed property. This means water repellency is probably not caused by particles with uniform properties, but particles with a wide range of properties within one sample. This is in agreement with work suggesting that behaviour of the bulk material may be influenced by the presence of a small proportion of hydrophobic particles (Bisdom et al., 1993; Bauters et al., 1998; Bachmann et al., 2000a). Difference in wettability of particles of similar size suggests that the property may be non-uniformly distributed around individual particles.

The wide distributions of h/d and h/L for particles from UK1 and NL2 suggest that there is a considerable range of individual particle wettability associated with soils exhibiting water repellency in comparison with those that are readily wettable. Nearly all particles within wettable soil samples can be considered to be wettable. Only a small proportion of hydrophobic particles appear to be necessary for a soil to exhibit water repellency (where many particles are involved in the assessment, Bisdom et al., 1993; Bauters et al., 1998; Bachmann et al., 2000a). However, simple flotation was found to have insufficient sensitivity to distinguish between soils exhibiting bulk wettable and water repellent behaviour. This may be due to surface properties like roughness, which may lead to air inclusions between particle pores and water surface, and the fact that soil particles may be rendered wettable once forced into contact with water. Aggregates composed of hydrophobic and hydrophilic particles may exhibit either wettable or water repellent behaviour when tested by flotation, depending on their orientation on the water surface.

From the application of these methods to the assumed isometric particles drawn from sandy soils the use of h/d or h/L ratios appears to be useful in compensating for effects of particle size. The orientation of particles of more irregular shape may need to be considered and a more appropriate estimate of an equivalent circular diameter

or wetted perimeter obtained from a more detailed examination of the particle as it is rotated about the axis normal to the water surface. Previous work on soil aggregates suggested various possibilities for equivalent diameter calculation, such as use of a mean diameter of a particle aggregate (Dexter et al., 1985).

The data obtained here support the assumption that particles from the water repellent sample NL2 may have different wettabilities, given that the variation in reduction is highest for this sample. It is known from previous studies using the same particles (Mainwaring et al., 2004) that NL2 and UK1 contain large portions of large polar compounds. If the distribution of water repellency is much broader in NL2 than UK1 this may indicate a possibly more irregular distribution of such compounds on the particles in NL2 than UK1. The difference between UKC and NLC, although both are completely wettable and contain only very small amounts of TOC, may indicate that other influences apart from the surface chemistry may be of importance. These could be roughness and particle size. However, particle size effects were excluded using h/d and h/L , but differences between the samples were still existent.

It is well established that the surface roughness of bulk samples influences their wettability (de Gennes et al., 2004). The surface roughness of individual particles may also influence particle wettability and adsorbed material may contribute to this roughness either reducing or increasing roughness. The wettable sample NLC shows a broader distribution of h than NL2 and also has a higher average surface roughness (see chapter 2.3.4). Even h/d values for NLC particles are still more broadly scattered than those of NL2. The mean roughness of UKC particles is smaller than that of UK1 particles and all UKC distributions are smaller than UK1 distributions. Therefore, it seems that the higher the mean particle roughness, the higher the variability in the particle wettability. Factors unrelated to the intrinsic surface wettability of the sample could be responsible for this variability such as entrapped air in surface irregularities and uneven water drainage when raising the particle from the water surface (*ibid*). In combination with different chemical properties of the surface this effect may even be amplified.

The more widely scattered h values obtained from particles of UKC in comparison with the narrower ranges of h/d and h/L seem to reflect the relatively broad particle size range of this soil sample. On the other hand, the similarity of the particle size distributions of NL2 and NLC suggests that the size is not significant in accounting for the differences in individual particle or bulk soil wettability of these samples.

However, as far as absolute values for comparison of different samples from different origins are concerned, the mWPM needs some further investigation. Between the two different sample pairs a general difference exists. This could be due to any number of reasons, like different mineralogy, roughness, nature of organic coatings. In order to use the mWPM for determination of absolute particle wettability, a thorough calibration using standard materials of different known wettabilities would need to be carried out. This should ideally involve particles of various different wettabilities but similar roughness and shape factors to the samples in question.

The almost consistent reduction in lamella height following addition of the hydrophobic agent to individual particles suggests that some intrinsic properties of the original particle surface remains influential to the measurement. This could for example be due to preferential binding of the hydrophobic agent to hydrophobic areas on the particle surface.

In principle, if more agent were added to provide a more even coating, a more consistent value of h or h/d may result. However, the detailed nature of the distribution of the added hydrophobic agent on these individual particles was not known. The data suggest that the method of application of the agent has some degree of consistency. However, it is also possible that the surface roughness of the particles was changed by the addition of the hydrophobic agent.

The addition of a hydrophobic agent, which decreased h of an individual particle, indicates a relative increase of water repellency and leads to the suggestion that removal of existing hydrophobic material may increase wettability and, therefore, h . This may be possible by exposing the particle, and its supporting cover slip, to a low

pressure, low temperature radio frequency oxygen plasma to facilitate a gentle but complete oxidation of surface organic material. However, this may also modify the effective surface roughness of the particle in a manner depending on the distribution of organic mineral and could even influence the mineral surface itself by oxidation of inorganic material.

4.9 Conclusions

Both micro-scale adaptations of the Wilhelmy plate method (mWPM) are able to detect differences between the wettabilities of model spherical particles from different types of samples and of particles before and after treatments applied to modify their wettability. Examination of particles drawn from soils with known bulk wettabilities produced a wide range of data whose precise interpretation was difficult. This may be due to irregularities in particle shape and roughness, surface chemical heterogeneity and representative sampling of particles. The ability to predict bulk soil wettability from the means or median values of such individual particle measurements was found to be poor. However, data suggest that the position and width of the distributions of individual particle measurements represent the differences between wettable and water repellent bulk samples: h/d and h/L . Distributions of water repellent samples are broader and include smaller values than those of wettable samples. The data indicate that the distribution of large polar compounds, responsible for the water repellency in UK1 and NL2, may be different for these samples.

Examination of individual particles by mWPM is a simple and non-destructive way to investigate relative differences in particle wettability. If the geometry of the particle is known and reference material with known wettability is available absolute wettabilities can be determined. Particles are available for further examination and modification using other microscopy techniques.

The mWPM offers a relatively fast possibility for the investigation of particle wettability within powdered material. The o-mWPM is a very simple method and

does not require specialised equipment. A camera and stepper-motor driven sample holder are sufficient. Additionally, it offers the possibility to investigate the particle shape. The data analysis, however, is somewhat time-consuming. A minimum of two images per sample are necessary and ~15 minutes are needed for image evaluation. The data evaluation of the g-mWPM is much faster and mostly automated. The measurement is also automated and, therefore, less dependent on subjective judgements made by the operator. However, the disadvantage here is that no optical component is included and sample shape evaluation is not possible. It would, therefore, be desirable to combine the g-mWPM with a camera in order to gain the advantages offered by the other method.

The technique is potentially very valuable for particle investigations if particle surface properties are under investigation and can complement other methods (e.g. scanning electron microscopy (SEM), atomic force microscopy (AFM), fluorescence imaging, microscopy).

Chapter 5

Effects of artificially induced changes in pH on soil water repellency

5.1 Introduction

A general introduction to the influence of pH on soil water repellency was presented in chapter 1. Soils of high pH are generally found to be more readily wettable than those of lower pH and the latter seem to be more prone to development of water repellency. This has been explained as being due to the deprotonation of functional groups on organic molecules at higher pH (e.g. Bayer et al., 2007). This increases the availability of negatively charged groups and the organic matter can be readily hydrolyzed and consequently wetted. However, some soils with neutral pH have been shown to develop water repellency (e.g. Graber et al., 2009). In general no clear relationship between soil pH and water repellency was found so far (e.g. Wallis et al., 1992; Hurraß et al., 2006). The influence of soil pH on water repellency is not fully understood, but several mechanisms have been proposed to explain it:

- i) changes in the surface charge of organic material (Jozefaciuk et al., 2002b; Bayer et al., 2007),
- ii) conformational changes in the organic matter due to repulsive or attractive forces of charged organic molecules, or parts thereof (Deo et al., 2005; Bayer et al., 2007),
- iii) changes of the underlying mineral surface charge (Jozefaciuk et al., 2002b) and
- iv) changes in the bacterial and fungi community, which, for example, stimulate production of hydrophobic material, degradation of hydrophobic material or result in cell destruction at extremes of pH and release cell material (e.g. Roper, 2005; Lin et al., 2006; Bayer et al., 2007).

Few studies have systematically investigated the influence of pH changes on soil sample wettability. Bayer and Schaumann (2007) investigated the change of pH and its influence on soil wettability upon addition of liquid aqueous HCl and aqueous NaOH to soil samples. In this approach the addition of the liquid itself may provide opportunities for the re-arrangement of large organic molecules or flexible side-chains and it is thus difficult to distinguish between such effects and the influence of a pH change on wettability.

A different method of investigation was chosen by Graber et al. (2009). Instead of changing the soil pH directly, salt solutions of different pH were used to measure drop penetration times. (This is effectively a modified form of the WDPT test.) Although, this may have an influence on the local pH of the area in contact with the droplet, only very short-term influences of pH were investigated. The time frame for infiltration of the droplet in this study was a maximum of one hour, so that possible conformational changes in the organic matter are restricted to these short activation times and are confined to the soil surface.

At the field scale, pH changes are normally achieved through addition of powdered lime whose effect is only noticeable when water is introduced and/or microbial activity reacts to its presence. The lime provides a readily wettable surface which may dominate the available surface area exposed to incoming water (Roper, 2006). These factors are difficult to control and separate from others in the soil system.

In the current study, a new method of changing soil pH was developed. Instead of liquid addition, samples were treated with gaseous NH_3 to increase their pH and HCl to decrease it. This eliminates possible changes in the arrangement of soil organic matter caused by the addition of a liquid (and any associated wetting and drying processes) and is perhaps the most direct approach to isolating pH effects currently available.

5.2 Methods

In order to change the pH of soil samples, they were exposed to varying amounts of gaseous HCl and NH_3 . Details of both methods are described below. Details of pH measurement and wettability determinations were given in chapter 2, section 2.4.1. Samples with sufficient material available for investigation were NL, UK and AU. For sample AU7 only a pH increase was investigated due to a lack of sample material available for a more comprehensive investigation.

In a collaborative study with the University of Koblenz-Landau in Germany independent, but similar experiments were conducted with two sets of samples. Each set comprised one water repellent and one wettable sample taken directly adjacent to each other (within centimetres). One sample set was derived from a former sewage field in Berlin Buch (samples BW, BR) and another from an inner city park in Berlin (samples TW, TR). The experiments were carried out in a similar way as described below (Diehl, personal communication; Diehl et al., submitted). Some experimental details varied, such as the absolute amounts of acid or base used, but the general experimental procedure was similar. A draft manuscript resulting from this collaboration has been submitted to the journal *Geoderma* and is included here (appendix C). This manuscript focuses on the differences between the two German sample sites and aims mainly to explain the different response of those samples to the pH treatment. The current study focuses on the similarities and differences between the samples used throughout this thesis, in order to gain knowledge of the general processes involved in the response of soil wettability to pH. In the following, some of the results obtained in the German study are also shown as they provide a valuable comparison with the experimental data obtained here. All methodological details for the German samples are given in appendix C.

5.2.1 pH increase

A bottle of aqueous NH_3 (35 %) was fitted with a silicone stopper. A hollow glass tube was inserted through this stopper. The exposed end was connected to silicone tubing fitted with a quick release clamp. This tubing served as a septum. A syringe with a hypodermic needle was inserted into the tube to access the headspace of the bottle and withdraw gaseous ammonia from it. The system was airtight and the clamp was used for reducing the pressure inside the bottle as necessary. This pressure was sufficient to fill the syringe without the need to withdraw its plunger. After filling the syringe with a prescribed volume of gaseous ammonia (between 1 and 40 ml for 40 g of sample) it was transferred quickly into an amber screw cap bottle (240 ml) with PTFE / silicone septum containing the soil sample (Figure 5-1).

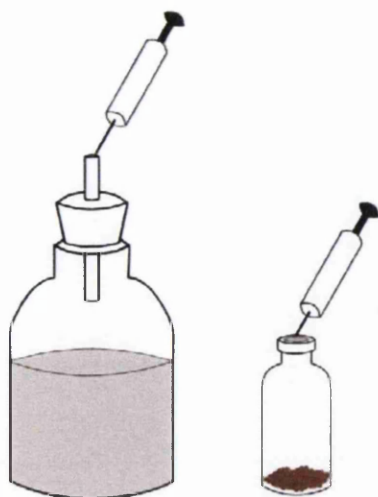


Figure 5-1: Experimental setup for gaseous NH_3 addition.

Depending on the availability of sample material, 10 or 40 g of soil were used and the volume of ammonia was adjusted accordingly. The bottles containing sample material and ammonia gas were left to equilibrate for 24 h at 20 °C. They were then left open to the atmosphere for one hour in order to allow excess ammonia to escape prior to measurement of pH and WDPT.

The WDPTs and pH of some samples (NL2, NLC, UK1 and UKC) previously treated with gaseous NH_3 were re-measured after 3 months in order to study the stability of pH and associated wettability changes. For sample AU, the material available was insufficient to allow this. Therefore another sample (AU7) of similar origin was used instead (chapter 2, table 2-2).

5.2.2 pH decrease

The method used for increasing the pH was not feasible for addition of gaseous HCl. While it was possible to obtain a syringe full of HCl gas, the delivery of the gas into the sample bottles resulted in an immediate increase in pressure so that only a small volume could be introduced. An open system was chosen instead (see Figure 5-2). A needle was attached to a silicone tube ensuring an airtight connection. The tube was then connected to a wash bottle filled with aqueous HCl. A second bottle containing

10 g of soil sample, and a third one with aqueous NaOH, were connected in series using silicone tubing. Each connection was fitted with a clamp so that the bottle in the middle containing the soil sample could be removed when clamps were shut and thus the bottle closed. The outlet of the third bottle was also fitted with a clamp so that it too could be sealed and isolated. This clamp was opened briefly to relieve the build up of pressure during use.

Air (several amounts between 40 and 180 ml) was introduced into the system using a syringe. This was discharged through the needle. As air passed through the first wash bottle, it was enriched with HCl and transported to the second bottle where it was brought into contact with the sample. As this had an open connection to the third bottle not all the HCl transported with the air was necessarily retained with the soil, but some may have passed directly to the third bottle. The need for several steps made a quantitative estimate of the actual amount of HCl interacting with the soil effectively impossible. The NaOH contained in the third bottle served to neutralize any HCl passing through it, so that it was prevented from leaving the system when pressure was relieved by opening the clamp on the outlet.

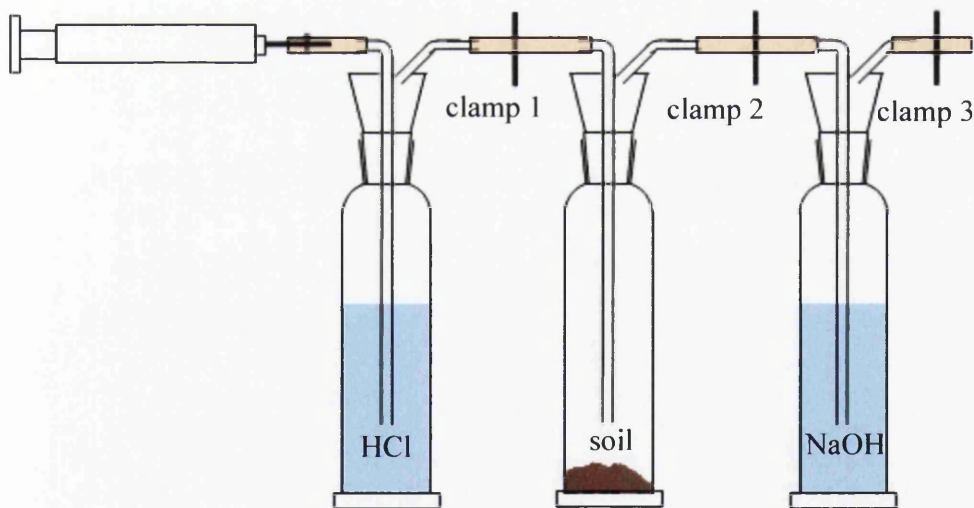


Figure 5-2: Experimental set-up for gaseous HCl addition.

After the gas was added to the system, clamps 1 and 2 (Figure 5-2) were closed and the bottle containing the soil sample removed from the system and left to equilibrate for 24 h at room temperature (20 °C). It was then opened and left for another hour to allow excess gaseous HCl to escape prior to pH and WDPT determinations.

5.3 Results

5.3.1 pH reaction to acid and base

The amount of NH_3 available for reaction with the soil is directly proportional to the amount of gas added to the sample as all gas taken from the headspace of the NH_3 bottle was transferred into the soil bottle. However, the amount of HCl available to react with the soil was not directly related to the amount of air passed into the system due to the necessity to relieve pressure whilst preventing loss of HCl to the atmosphere (see Figure 5-2). The vapour pressure of ammonia is considerably greater than that of aqueous HCl (e.g. vapour pressure for aqueous HCl [36 %] at 20 °C is 14.1 Pa and aqueous ammonia [21.4 %] 32 kPa at 19.9 °C) so a higher throughput of gas is required to acidify soil than to increase alkalinity. No pressure relief was necessary following addition of ammonia gas to soil indicating that little additional air was introduced. This indicates a fast reaction between ammonia and sample material occurred which quickly reduced the pressure in the head space of the bottle. This was not the case following the addition of gaseous HCl so that apparently slower reactions between soil and HCl seem to occur and/or less recipient sites in the soil may be available for reactions.

The range of soil pH resulting from the treatments was between pH 2 and 9 (Figure 5-3). Few samples reached these extremes. Most samples show an approximately sigmoidal relationship of pH as function of introduced gas volume, but have more than one inflection point. Some samples did not approach maximum (e.g. UK2, AU1, NL1) or minimum pH values (UK2, NL2, AU2) within this experimental range.

Samples UK1 and UK2 reacted similarly to the addition of NH_3 or HCl and reached similar end values, but UK1 shows a more pronounced plateau around the original

pH (Figure 5-3a). The pH of sample UKC reached the maximum pH of ~9 after the addition of only 10 ml NH_3 and generally showed the least variation in pH of all samples.

The pH of sample NL1 reacted to the addition of HCl, but only at volumes >60 ml was a change in pH found. The slope of pH increase upon NH_3 addition is shallowest for this sample and it reached the lowest end value of pH ~7 in comparison with the other NL samples, which all behaved similarly (Figure 5-3b).

The pH of AU1, AU2 and AU7 changed similarly upon the addition of NH_3 and HCl more upon the addition of NH_3 and reached a higher final pH. The addition of HCl changed the pH of AUC less than that of other samples. Only after the addition of 180 ml of HCl was a significant reduction was found (Figure 5-3c).

On addition of small volumes of gas (< 40 ml HCl, < 5 ml NH_3), most samples show little or no change in pH (Figure 5-3). This is readily evident (as a wide plateau in pH) with samples AU1, AUC and NL1. Other samples show this plateau on addition of HCl, but not with NH_3 (UK1 and AU2).

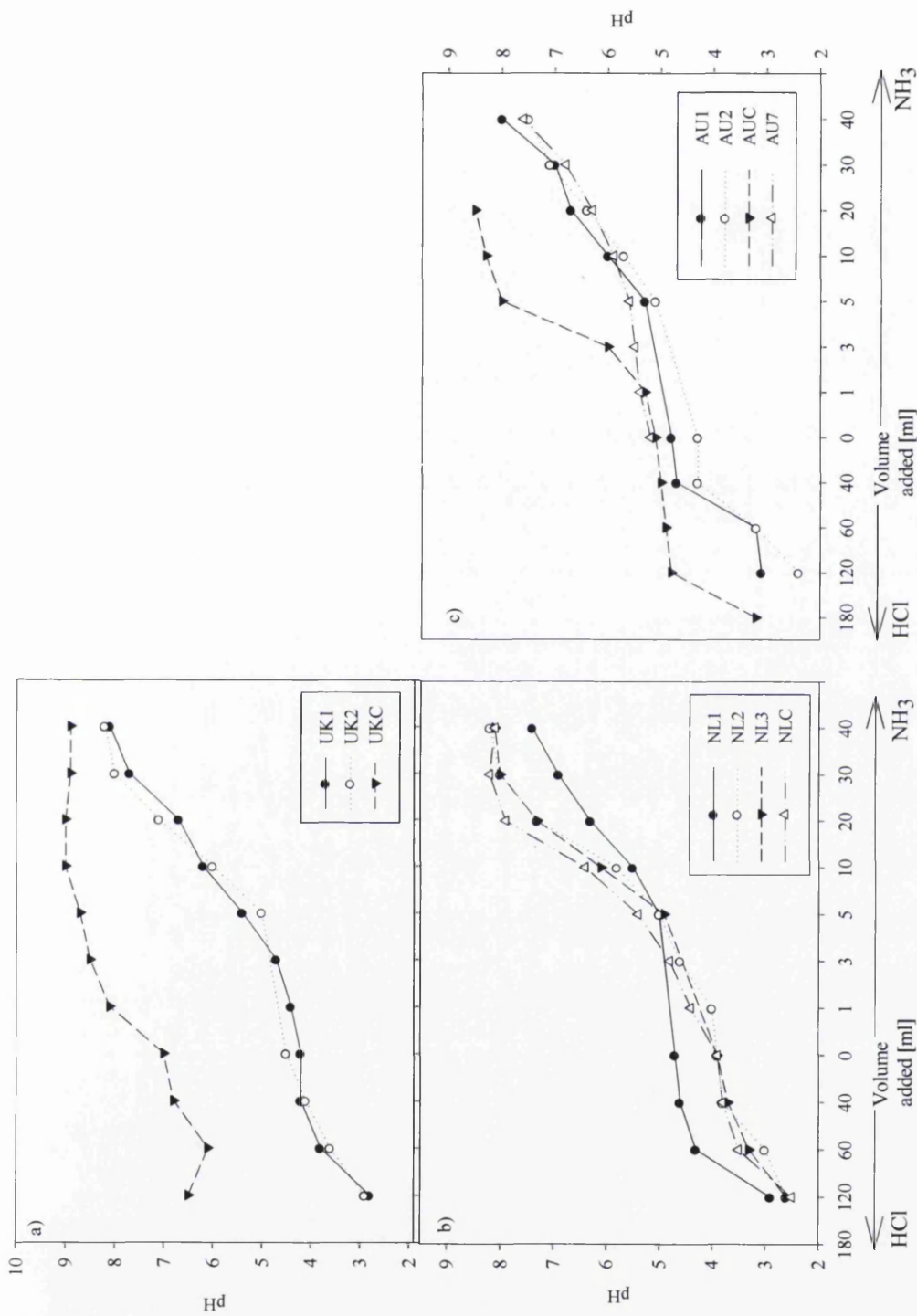


Figure 5-3: pH vs amount of gaseous HCl or NH₃ added to soil samples a) UK samples, b) NL samples, and c) AU samples.

5.3.2 Changes in wettability

The WDPT of all the water repellent samples was found to decrease strongly with increase in pH (Figure 5-4). This observation is in agreement with some previous findings (Karnok et al., 1993; Steenhuis et al., 2005; Hurraß et al., 2006; Bayer et al., 2007). All originally wettable samples remained wettable over the pH range investigated.

Samples NL3 and UK2 became completely wettable (WDPT < 5 s) at the highest pH reached (around pH 8 - 9). The WDPT class of all other samples also decreased significantly from originally extremely water repellent (NL1, NL2 and UK1), severely water repellent (AUC) or strongly water repellent (AU1) to only slightly water repellent.

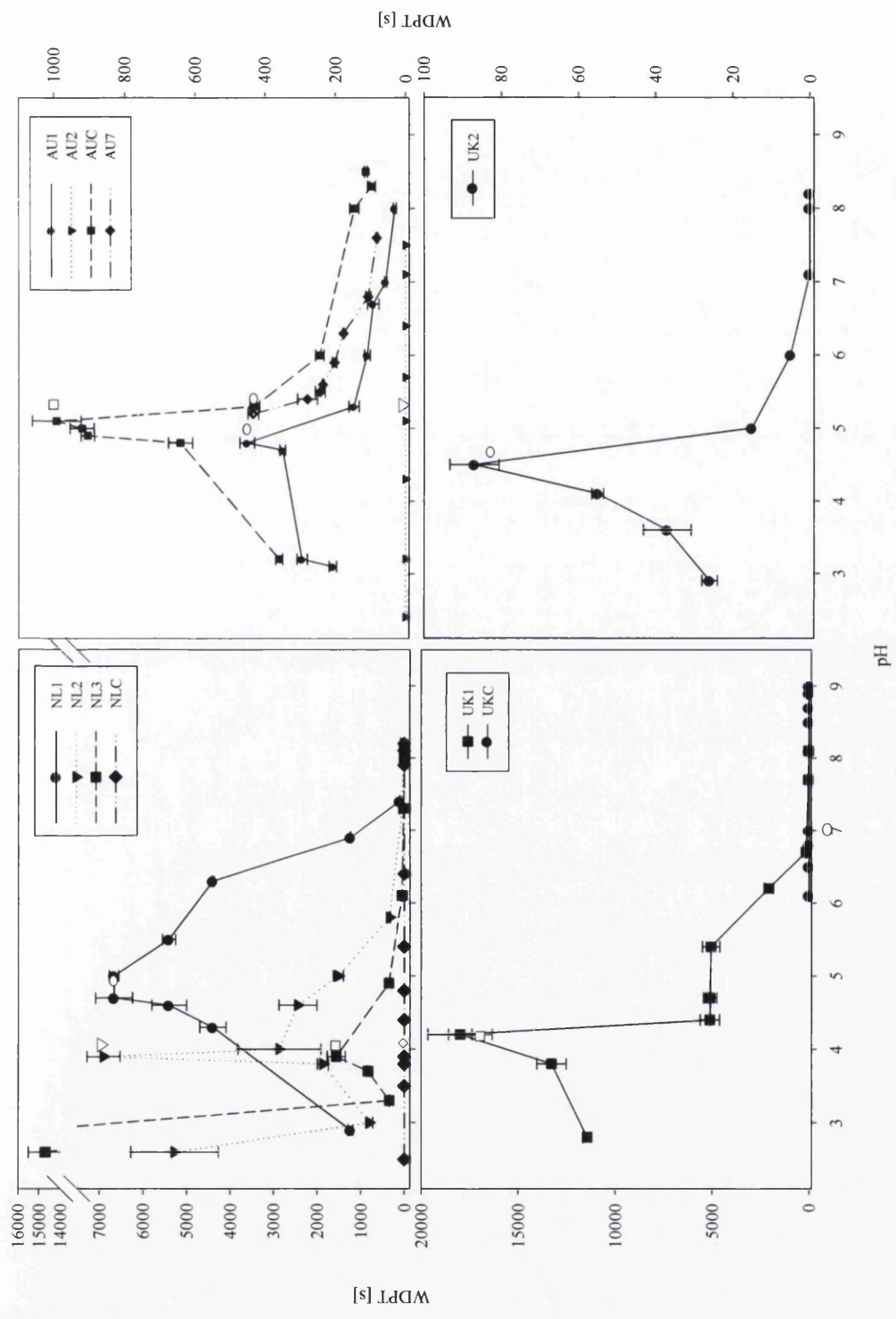


Figure 5-4: WDPPT vs pH after treatment with gaseous HCl and NH₃ of all samples. Open symbols represent original values. UK samples are shown in two graphs for better resolution (different scales of WDPPT).

The German samples show a similar behaviour of WDPT upon changes of pH (Figure 5-5) to the AU, NL and UK samples. This was in contrast to an earlier study (Bayer et al., 2007) where samples from Tiergarten showed an increase of WDPT after addition of liquid aqueous NaOH, whereas samples from Buch were completely wettable over the whole pH range. The addition of liquid increases soil moisture content, which could also induce changes similar to those observed following cycles of wetting and drying, hence augmenting those associated with the reagents adjusting the pH (*ibid*). It is noticeable that a difference in behaviour exists between samples from these two origins below their original pH values. Both Tiergarten samples show a reduction of WDPT, but both samples from Buch at some point express water repellency similar to the original and even higher. A thorough discussion of the differences between these two sample origins and the proposed mechanisms is given in appendix C.

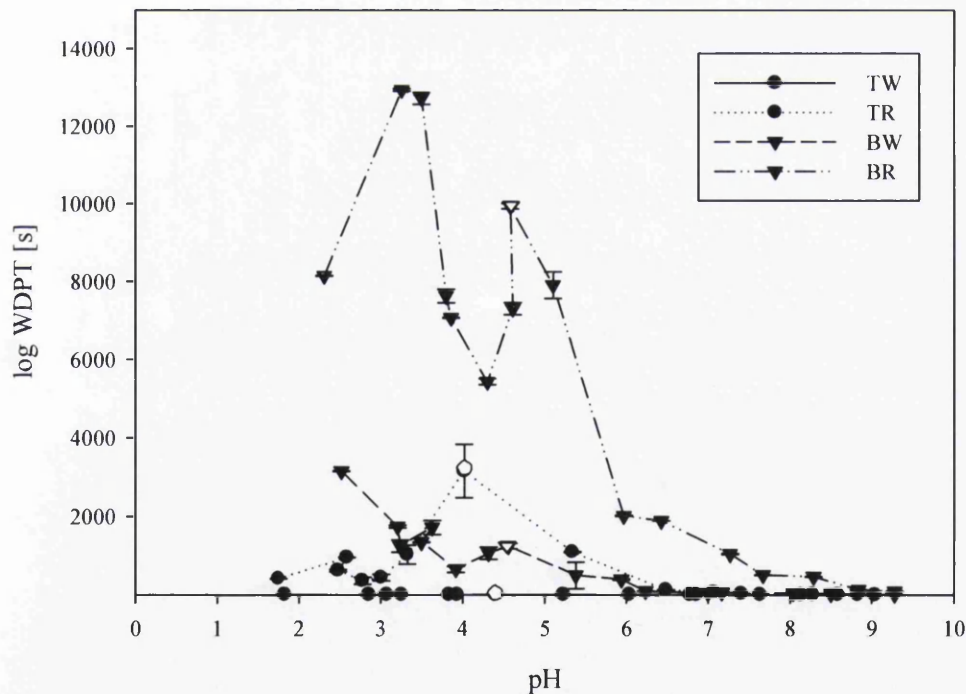


Figure 5-5: WDPT vs pH after treatment with gaseous HCl and NH₃ of the German samples (TW, TR, BW, BR). Open symbols represent original values.

5.3.3 Re-evaluation after three months

Measurements of sample pH, made three months after the treatment with ammonia, were consistently found to be below those made after 24 h for, with the largest decreases corresponding with samples treated with the largest volumes of gas. The pH of sub-samples AU7 suffered the smallest changes and the pH of most sub-samples of UKC returned to their original value of pH ~ 7 (within the experimental error; Figure 5-6).

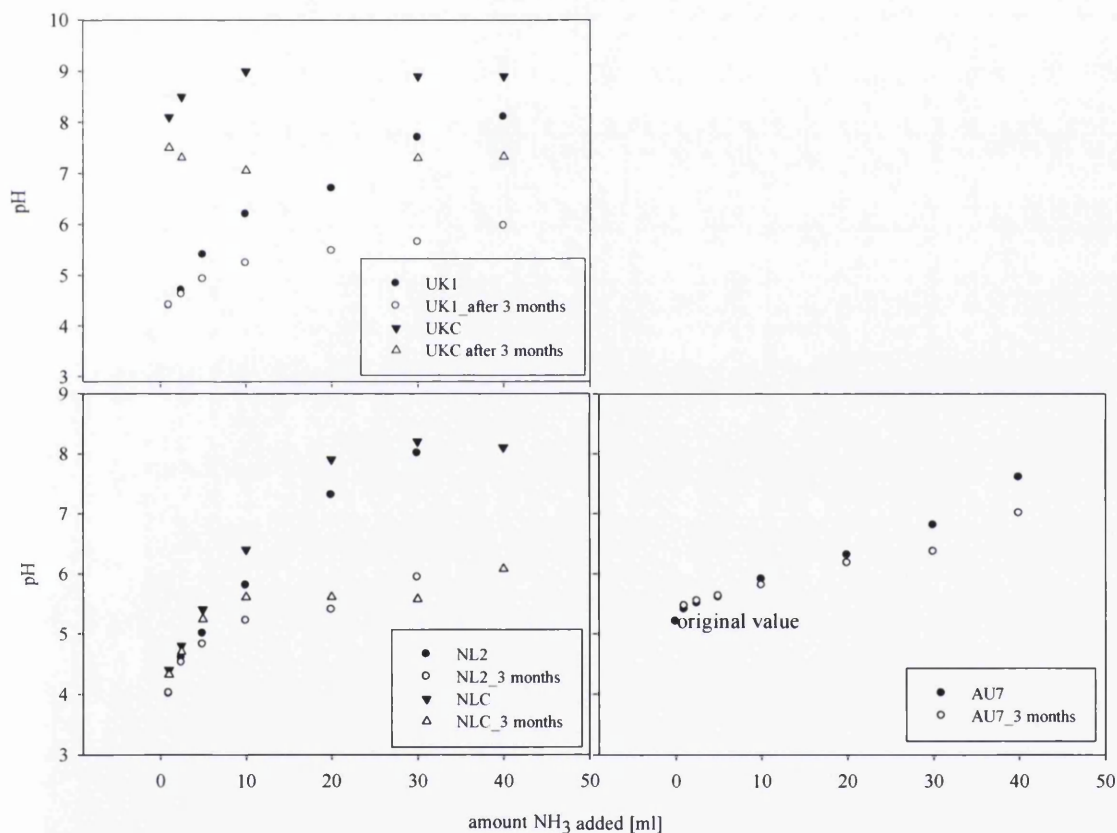


Figure 5-6: pH vs amount of NH_3 added to the sample directly after the treatment (black symbols) and 3 months later (open symbols). Errors bars for pH are within the symbol limits.

Figure 5-7 shows the changes in WDPT at three months after the initial addition of ammonia. All wettable samples (UKC and NLC) remained completely wettable after three months. The WDPTs of all UK1 samples were longer after three months than directly after addition of ammonia. This was also the case for all NL2 sub-samples to

which more than 10 ml of ammonia gas had been added. Sub-samples treated with less than this amount exhibited slightly reduced WDPT after three months. The WDPTs of all AU7 ammonia treated sub-samples were significantly reduced to below 30 s after three months (see Figure 5-7).

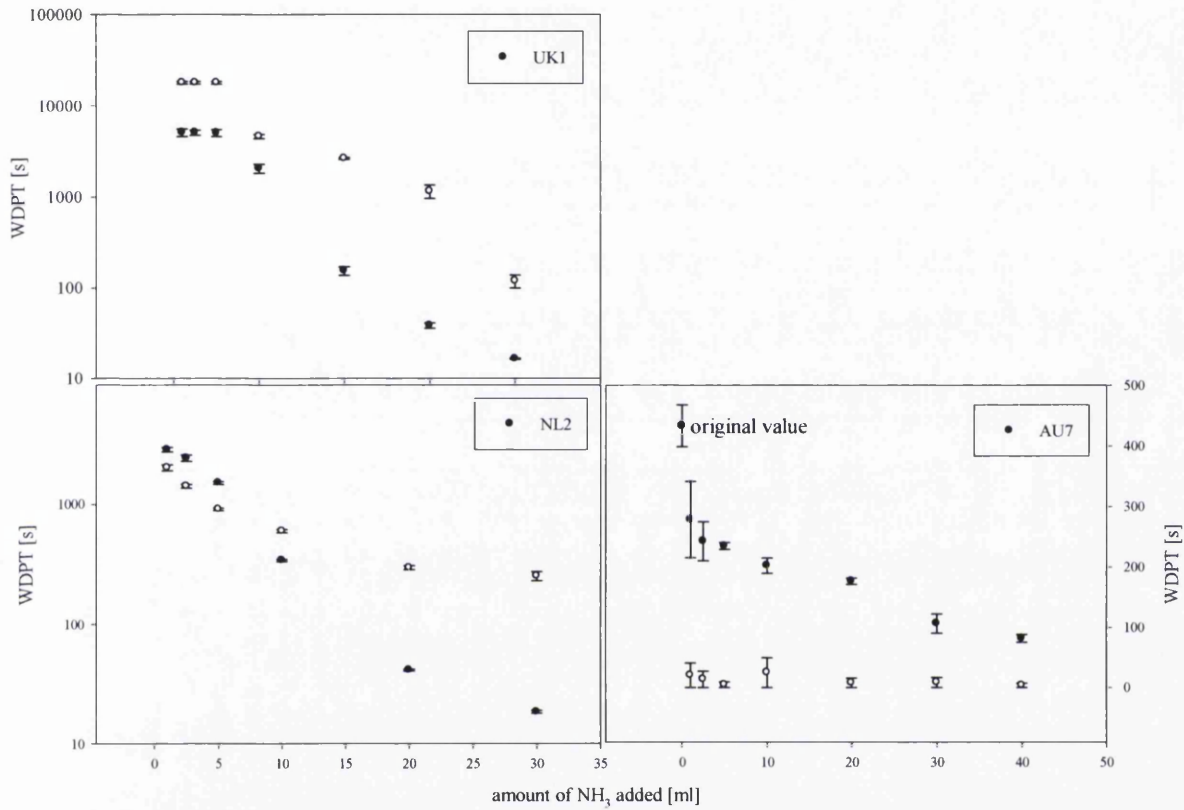


Figure 5-7: WDPT vs amount of NH_3 added to the sample directly after the treatment (black symbols) and 3 months later (open symbols).

5.4 Discussion

The newly developed method for pH change via the gas phase was successful in changing soil pH. This provides the opportunity to directly change soil pH, avoiding influences from liquid addition that alone may alter soil wettability.

The addition of gaseous ammonia led to increased soil pH in all samples. Larger amounts of gaseous HCl were necessary in order to acidify the soil samples, but a distinct decrease of soil pH could be achieved. Although all samples showed pH changes after acid/base addition, the strength of reaction was different depending on the samples.

The re-investigation of samples after three months showed that pH changes were partly reversible, including the re-establishment of soil water repellency in some samples. However, not all samples were affected in a similar manner and neither were original pH nor original WDPT values reached.

The general decrease of water repellency upon the increase in pH, achieved by addition of ammonia, may be due to a deprotonation of functional groups at the surface and with that an increase in surface charge within the organic matter (e.g. Jozefaciuk et al., 2002b; Deo et al., 2005).

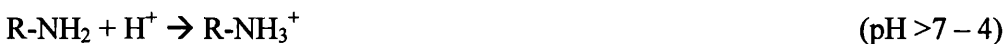
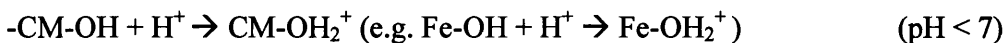
The WDPT of all samples also decreased with a reduction in pH, achieved by addition of gaseous HCl. In contrast, several publications report an increase in repellency with reduction in soil pH, which is interpreted as being due to protonation reducing negative surface charge towards electroneutrality (Hurraß et al., 2006; Bayer et al., 2007). The reduction in water repellency may be explained in terms of disturbance of the conformational equilibrium of the organic matter. When HCl is added to the sample, a disruption of the organic matter on the particle surface may occur, causing a re-orientation and temporarily leading to better wettability. Increased wettability may also be a consequence of oxidation reactions and acid catalyzed condensation reactions destroying parts of the organic matrix (Bayer et al., 2007) or a destruction of the mineral material (Jozefaciuk et al., 2002a). Even though the samples were dry, some areas will still contain minimal amounts of water and the

addition of gaseous HCl may reduce the pH in these regions very strongly, possibly leading to local changes in the organic matter via the mechanisms mentioned above. However, as such a low pH is normally not reached under natural conditions, this phenomenon is considered here as being of limited relevance for the wettability of soils.

A comparison between the WDPT changes and the respective buffer curves (Figure 5-3) indicates that some samples did not reach their maximum pH. It can be speculated that a more complete deprotonation of their organic matter may have rendered them rapidly wettable if the volumes of gas (HCl or NH₃) had been further increased. On the other hand, it may be possible that the capacity for ammonia uptake was reached, i.e. no reactive sites were available for binding, and further addition would not have had an influence.

The plateau in the pH trend found upon addition of small quantities of acid or base indicates some buffering capacity in the soils at original soil pH. Buffering is considered to occur mainly in the solid mineral or organic matter phases. Several buffer systems are considered to be involved in the process in this pH region (Süsser et al., 1991; Scheffer et al., 2002).

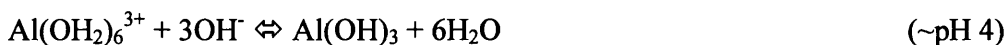
- i) Clay minerals (CM) and oxides or humic substances: functional groups on these sites may be protonated and/or H⁺ exchanged with metals (M) from complexes leading to loss of exchangeable cations.



- ii) Silicates: leaching of exchangeable Al into soil solution, loss of exchangeable cations and destruction of minerals.



iii) Oxides/ hydroxides/ hydroxysulfates: Al, Fe leaching into soil solution



Some samples (e.g. NL1, Figure 5-3) show considerable buffering upon addition of ammonia. Although some buffer systems tend to operate in either acidic or basic pH ranges, others like carboxylic groups in humic substances can operate both by responding to base by deprotonation and to acid by protonation. The reaction times of these buffer systems vary widely, depending on the ease of access to sites, so that some buffer curves may reflect only these most reactive and accessible sites in a system. The batch-wise method of an effective solid state potentiometric titration reported here, coupled with the mobility of gases, suggests that ample opportunities were created for contact with active sites.

Both NLC and UKC samples are the samples with lowest TOC content per sample origin (NL: 0.8 g kg⁻¹ and UK: 0 g kg⁻¹, although investigations by fluorescence microscopy suggested that trace amounts of organics are present). Therefore, the differences between UKC and NLC from the other UK or NL samples, respectively, may be connected to the amount of organic matter content of the samples. If the strength of reaction of the soil to the addition of HCl or NH₃ is connected to the organic matter content, this indicates that the organic matter is mainly responsible for any buffering reactions occurring in these samples. It is known that soils rich in humic substances generally have high buffering capacities (Ceppi et al., 1999).

The buffering in AU samples may possibly be attributed more to the mineral matrix or inorganic components (mainly clay minerals) than to humic substances as no dependence on the amount of SOM was observed for these samples. If the mineral sites are protonated and associated with ammonium ions, they may then also attract water vapour, which hydrates the surface, and chemically assist wettability, holding both ammonium ions and water at the surface.

Additionally, factors such as clay and particulate organic matter content have to be taken into account as especially clay minerals are strongly involved in buffering reactions.

Differences in the distribution of organic matter in terms of coverage and layer composition may be another contributing factor. A film of non-polar material in the outermost layer may prevent access of acid or base to the reactive sites (AU samples) or a uniform distribution of organic matter on the mineral particle surface may prevent access to reactive sites of the mineral matrix. Thus, the ratio of mineral surface to organic cover may have to be considered.

Apart from reacting directly with the organic matter or mineral surface both ammonia and hydrogen chloride could (at least partly) dissolve in the remaining water contained in the sample. Although the samples are air-dried some water is still present. This water possibly exists as distinct and very small droplets inside the sample as, at such low water contents, not enough water is present to form a continuous water film on particle surfaces (e.g. Israelachvili, 1992). If such regions of water droplets exist, the ammonia/ hydrogen chloride could change the pH of these droplets and, therefore, the sample pH at strongly localised spots at the sample surface. If this is the case, changes would occur mainly in these localised areas. The changes occurring within the sample could then be slower than changes due to direct interaction of acidic/basic gas with the organic/mineral surface.

If, as discussed above, the ammonia reacts with the water remaining in the sample, diffusion and equilibration processes may lead to a loss of ammonia over the time period of three months, again reducing the pH during the process. These changes may also indicate that the samples did not reach an equilibrium state before and that changes are still going on either back to their original state or as a result of a new equilibrium due to the changed chemistry of the organic matter or mineral surface. Changes in the conformation of organic matter or at the mineral surface probably occur on various time scales up to months (e.g. Ma'shum et al., 1985; Roy et al., 2000; Diehl et al., 2007). Several conformational and structural changes may occur during that time such as cross-linking of side chains of the organic matter or

reorientation of those chains into a more favourable energetic state (e.g. Schaumann, 2006a; Bayer et al., 2007).

The changes in pH between 24 h and three months after the addition of ammonia were smallest for AU7. This suggests the surface that was available for retaining ammonia was more stable over that time frame compared to all the other samples examined. Additionally, one may speculate that conformational changes of the organic material in this sample are of a slower nature than those of all other samples examined. This could be due to an association with the mineral surface that was possibly altered by the base addition (Jozefaciuk et al., 2002a). Alterations to the interactions of the changed mineral surface and the organic matter may occur over a longer time and lead to complete re-arrangement of the organic matter as binding mechanisms would be changed (e.g. Ceppi et al., 1999; Jozefaciuk et al., 2002a).

Distinguishing between the influence of the mineral matrix and organic material on the buffering capacity of the soil is difficult, as other influences such as the surface area of soil particles accessible to base/acid interaction may be of importance when considering differences between samples. Rougher mineral surfaces may lead to a more patchy distribution of organic material on the particle surface and, thus, increased layer thickness of organic material at comparable total amount, which again may lead to decreased accessibility of base/acid reactive sites. Also, the type of organic matter present in the sample is likely to influence the reaction to base/acid interaction. However, previous studies on these samples have shown that at least similar groups of organic material in similar percentage are present in most samples used here (Mainwaring, 2004; Morley et al., 2005).

Micro-organisms may also be involved in the changes of wettability and even pH both short and long term. The drying and storage of samples in a relatively dry atmosphere (RH ~ 50 %) prior to pH determinations provided soil water contents < 1 % dry weight. Bacteria are able to survive in such environments, but sudden and significant increase in their population density seems very unlikely (Schlegel, 1992). However, the addition of small amounts of ammonia may e.g. increase microbial activity as it adds an additional source of nitrogen and, for some specialised microorganisms, of energy, associated with the metabolising of organic matter

(Schlegel, 1992; Kowalchuk et al., 2001) and may change pH over the course of three months. On the other hand, higher concentrations of ammonia may be toxic (Schlegel, 1992; Fidanza et al., 2007) and, thus, decrease microbial activity. Fungal growth and growths of fungal networks were not observed. The evaluation of microbial activity, therefore, would be a valuable addition to this experiment as the influence of the microbial community on changes in wettability on short- and long-term bases could not be examined here.

5.5 Conclusions

The method of gas addition to soil samples was successful in changing the sample pH without affecting their water content and so introducing the additional changes that arise from the wetting associated with the addition of aqueous acids or bases.

It appears that there are various buffer systems present in soils treated with gases. These may depend on the concentration and distribution of organic material in the samples. In other soils, minerals and inorganic compounds may provide the dominant role unless they are covered with a thin dense film of organic material that confers only a small TOC.

Independent of the buffer system of the sample and the mechanisms behind the change in pH all samples show a similar development of wettability upon pH change. They became more wettable with increasing pH and also with decreasing pH (apart from sample BR, that showed increased wettability at pH 3). Some samples showed a re-increase of water repellency at very low pH (< 2), but this may be less relevant under natural conditions.

Examining samples directly after the change in pH investigates only rapidly occurring responses to the changed conditions. Additionally, slow conformational rearrangements in the organic matter may occur as indicated by the observed changes in pH and WDPT of samples three months after sample treatments. Again two out of three sample origins showed a reversal of previously induced changes towards the

original values, indicating some sort of equilibrium state of the organic matter prior to the induced change. Although the reversal of wettability is not necessarily connected with only one state of organic matter it is possible that several conformations lead to a similar bulk soil wettability.

In order to gain more information about the nano-scale properties of soil particles with changed pH, AFM investigations were carried on selected samples. These are presented in the following chapter.

Chapter 6
Atomic force microscopy (AFM) investigations
of pH adjusted soil particles

6.1 Introduction

Atomic force microscopy (AFM) was invented by Binnig et al. (1986) and can be applied to practically every surface as the samples do not require any special preparation. It is not a traditional microscopy technique as it does not use direct optical examination of the specimen, but instead visualizes a surface by scanning a sharp tip over it. AFM is an essentially non-destructive technique for imaging and characterization with up to atomic resolution, and commonly used in measurements of interaction between solid surfaces and probes (Paredes et al., 2003). For a schematic overview of the method see Figure 6-1a. An SEM image of an AFM cantilever with tip is shown in Figure 6-1b.

A laser beam is focused on the back of a cantilever and the position of the reflected beam is recorded by a position-sensitive-photo-diode (PSPD) detector. The PSPD can measure changes in the position of the laser beam as small as 1 nm, thus giving extremely high resolution of the cantilever deflection. A topographic map of the surface can be generated by scanning (dragging) the tip over the surface. Additional parameters, such as mean roughness (R_a), can be obtained from such maps using proprietary software.

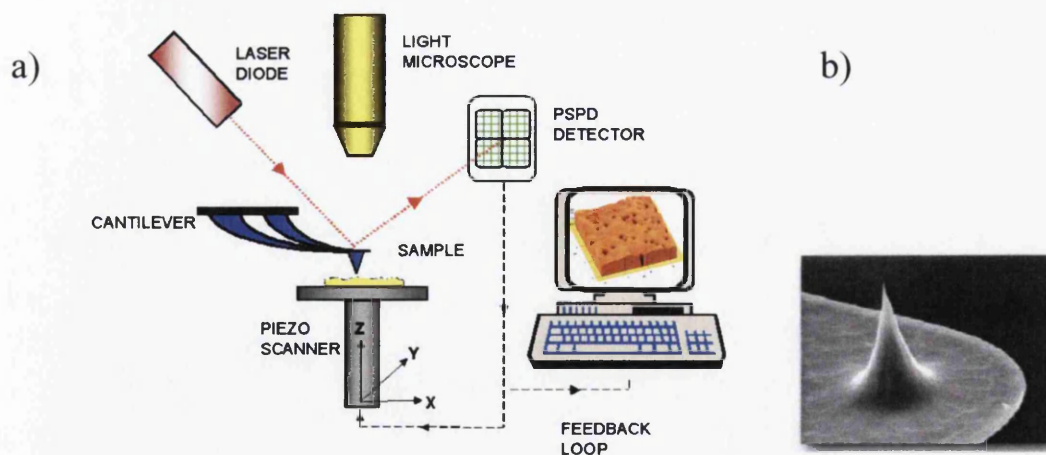


Figure 6-1: a) Schematic overview of AFM operation (from Bowen et al., 1997), and b) SEM image of an AFM tip.

AFM may also be operated in tapping mode (where a small amplitude vibration is imposed on the scanning cantilever) to avoid surface damage by dragging the tip. As the tip interacts with the surface, the frequency of vibration changes. This provides information about the material properties of the surface. Data for both phase shift and tip position are captured simultaneously to provide phase and topographic images of exactly the same region of the specimen. Comparison of phase images with corresponding topography assists identification of different components in composite materials and can differentiate between hard and soft regions and their relative heights (Jiang et al., 2002).

In addition to topographic images, force – distance curves may be obtained at one or more contact points on the surface. The cantilever is used to bring the tip down into contact with the surface and then to withdraw it. During this process any deflection of the tip from its intended position arising from interactions with the specimen surface is recorded. This provides data for a tip-sample deflection-distance curve as depicted in Figure 6-2. Region A represents a moment when the cantilever is far from the surface and has no interaction with it so that the cantilever deflection is zero. When the cantilever approaches the surface, the tip interacts with it and a ‘jump-in’ contact usually occurs (see region B in Figure 6-2). Similarly, as the cantilever is retracted a ‘jump-off’ usually occurs (region F). When the tip is in contact with the surface (region C for approach and D for withdrawal) the cantilever deflection is equal to the displacement of the sample surface/piezo scanner (Noel et al., 2004). Measurements may be made in both liquids and gases. However, when measured in air, there is significant capillary force between tip and specimen. In order to convert the recorded data into force vs sample-tip separation curves, zero force, zero distance, cantilever spring constant and cantilever deflection sensitivity must be known or determined.

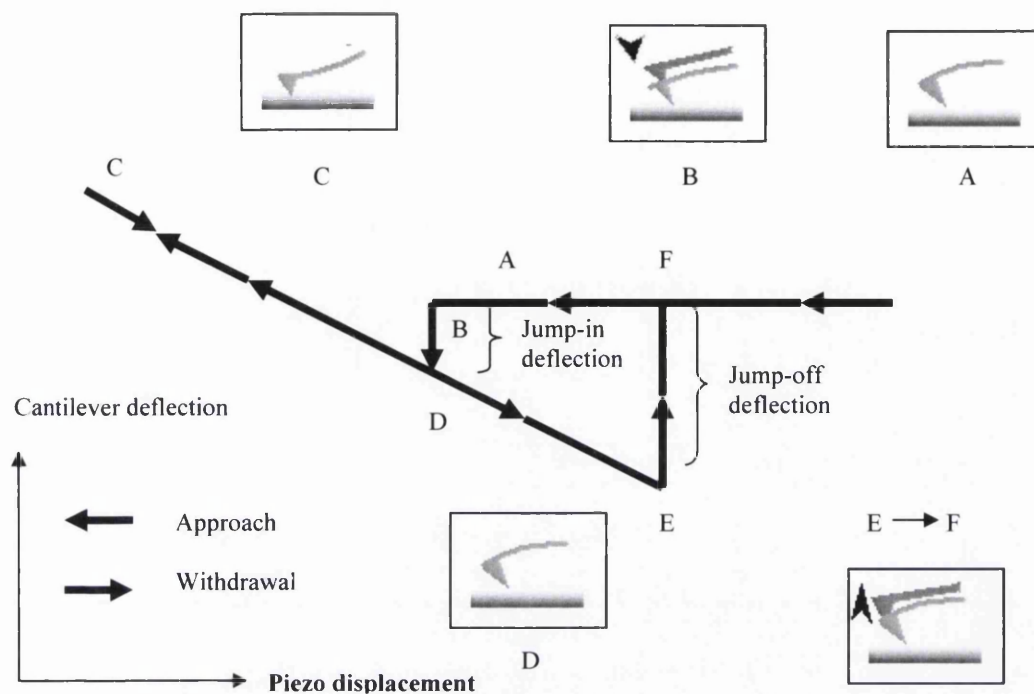


Figure 6-2: Schematic representation of the deflection-distance curve (from Noel et al., 2004).

If the spring constant of the cantilever and vertical deflection at the moment when jump-off occurs ($\Delta z_{\text{jump-off}}$) are known, then the adhesion force (F_{adh}) between the tip and specimen can be calculated using Hooke's law (assuming an elastic regime):

$$F_{\text{adh}} = k_{\text{tip}} \cdot \Delta z_{\text{jump-off}} \quad (6-1)$$

where k_{tip} is the force/tip constant.

AFM has been applied successfully in materials characterisation (e.g. Albrecht et al., 1988; Bowen et al., 1997; Paredes et al., 2003; Boussu et al., 2005) and other surface characterisation processes down to the atomic level. It has also been applied to the study of aggregate size and shape of humic, fulvic acids and other natural organic matter (NOM) from aquatic systems adsorbed on smooth surfaces (e.g. Namjesnik-Dejanovic et al., 1997; Balnois et al., 1999; Lead et al., 1999; Wilkinson et al., 1999). The size of adsorbed aggregates of HA, of relatively hydrophobic nature, extracted from peat seems to be dependent on the solution pH (Balnois et al., 1999).

At low pH (pH ~ 3) large aggregates were dominant and co-existed with individual molecules, but at higher pH (pH ~ 7) no aggregates were found. This was explained by the electrostatic repulsion of the de-protonated groups in HA leading to an extended conformation of individual macro-molecules, whereas at low pH neutralisation and shielding of charge on those groups favoured coiling of molecules and inter-molecular bonding (*ibid*).

The first study of humic substances under natural conditions, i.e. on soil particle surfaces under dried and field moist conditions, was conducted by Gerin and Dufrene (2003). Although this study shows that AFM may be a useful tool in soil particle surface investigations it also points out the shortcomings of using contact mode AFM, which may displace or distort soft organic matter. Cheng et al. (2008) used topographical images and phase images in tapping mode as well as force-distance measurements of soil and model particle surfaces to describe their nano-properties and relate them to bulk soil properties such as TOC and water repellency. Sub-samples of some of the soils investigated (*ibid*) were also used in the present work. The samples taken from the soil profile (NL samples) show an increase in roughness (calculated from 10 topographical images) with increasing soil depth and decreasing TOC, but for model particles coated with HA the trend was reversed. This increase of roughness with depth was explained by the ageing of organic material for the natural soil particles where the organic matter closer to the surface is exposed to highest micro- and meso-organism activity and water percolation causing hydrodynamic shear and smoothing of the surface (Cheng et al., 2008). In contrast, the highest amount of material covering the surface of clean model particles resulted in the roughest surface, which, under natural conditions, would undergo changes over time, such as microbial or chemical degradation.

Phase images reflect surface mechanical, elastic and chemical properties as well as local topography. They can thus provide information about (soft) organic matter distribution (coverage and thickness) on (hard) soil particle surfaces. The bright areas in images (higher phase angles) usually represent soft organic matter and dark areas (lower phase angles) hard mineral surface, as shown for glass and HA covered glass (Cheng et al., 2008). On natural soil particles the roughness and non-uniform coverage have to be considered and lead to broad phase angle distributions (*ibid*).

The force between a clean glass surface and the AFM tip was calculated to be much larger (with a smaller standard deviation) than that between HA coated glass and the tip (*ibid*). This can be explained by the significant contribution made by the capillary force to the adhesion force in humid air. Water vapour can condense on the tip and sample and forms a water capillary between them. Hydrophilic surfaces attract more water and, therefore, have higher capillary force contributions than hydrophobic surfaces. The humic acid used was found to have a higher contact angle than clean glass and contains hydrocarbon moieties that could inhibit water condensation. This relationship was found for natural soil particles, where NL1, with the strongest bulk water repellency, also had the smallest AFM adhesion force and NL3 with low bulk water repellency had the highest adhesion force. Again, the influence of the surface roughness had to be considered and the rougher surfaces exhibited broader force distributions (Cheng et al., 2008).

In chapter 5 the effect of pH change on bulk soil water repellency was examined. The alterations in pH and associated changes in water repellency did not involve contact with aqueous media and subsequent drying, which are processes known to affect the persistence of water repellency. Here the outcomes of the application of AFM techniques for examination of the surfaces of individual particles are presented. Adhesion force measurements made at these surfaces provide evidence of the scale of local surface hydrophobicity and its distribution. This provides complementary information allowing a comparison between individual particle and bulk soil properties in relation to changes in the bulk soil pH. The aim of this specific study was to find supporting evidence for assumed changes taking place in the organic material of natural soil samples after artificially induced changes in soil pH. If this change in wettability is also expressed at the particle level, as discussed above, the force measured on the particle surface should increase in samples with higher pH. The surface roughness of similarly sized soil particles, selected for examination, was assumed to be similar and unaffected by the procedure to effect the pH change.

6.2 Method

Adhesion forces between an AFM tip and soil particles were measured using a Dimension 3100 scanning probe microscope (Digital Instruments, Santa Barbara, CA) in contact mode. A cantilever with a v-shape end and a spring constant of 0.26 N m^{-1} (Veeco, Cambridge, UK) was used for force measurements. The ramp size was set to 1000 nm and a maximum loading of 15 nN was applied. Five particles were selected randomly from each sample and glued onto a microscope glass slide (for detailed method see chapter 4).

A topographic image ($1 \times 1 \mu\text{m}$ with 512×512 pixels) of an area of particle surface was captured and an array of 15×15 points selected for force measurements within it. A total of 8 areas, selected from the five particles (per sample), were examined and the force data pooled together to provide 1800 point force measurements. The force distribution was calculated from the pooled data.

As the force was measured in contact mode, the topographic images were obtained using a point and shoot module. This provides little information about the distribution of organic matter on the particle surface and images were not very clear due to possible distortion of the organic matter and the high roughness of the samples (Gerin et al., 2003). Surface topographical (height) and phase images of specimens obtained previously (with the same AFM instrument, but using tapping mode) were kindly made available by Dr. Shuying Cheng. These two images were captured simultaneously with tapping mode cantilevers (Olympus, Tokyo, Japan) with a spring constant of 42 N m^{-1} and a nominal tip radius of 5 nm at a scan rate of 1 Hz. All imaging parameters were kept constant (Cheng et al., 2008). From these images the mean roughness (R_a) was determined for $1 \times 1 \mu\text{m}^2$ and $5 \times 5 \mu\text{m}^2$ areas (see chapter 2).

Soil samples examined were NL1 and UK1 and their corresponding sub-samples, which after processing resulted in the highest soil pH (see Chapter 5 and Table 6-1). Additionally, the UK1 sub-sample adjusted to the lowest soil pH was investigated. Adjustments of soil pH were achieved through addition of gaseous HCl or NH_3 (see chapter 5).

Table 6-1: pH, WDPT and TOC of NL1 before and after treatment with gaseous NH₃ and HCl.

	original pH	pH after NH ₃ treatment	original WDPT [s]	WDPT after NH ₃ treatment [s]	pH after HCl treatment	WDPT after HCl treatment [s]	TOC [g kg ⁻¹]
NL1	4.7	7.4	4800	106	n.d.	n.d.	36.2 ± 2.9
UK1	4	8.1	18000	17	2.8	11400	11.4 ± 2.7

Only sample UK1 was investigated by AFM after HCl treatment, due to the limited amount of material of sample NL1 available.

6.3 Results and discussion

Topographical images and phase images show typical areas representative of the surface of particles drawn from soils UK1 and NL1 (Figure 6-3). Light areas represent surfaces of high elevation and dark ones surfaces of lower height. The overall height differences in topographical images indicate the roughness of the surface and mean particle roughness (R_a) calculated from image data. The height difference for the UK1 specimen is bigger than that for NL1 (see Figure 6-3a and c). This is reflected in the mean R_a values for these and all the other areas examined: UK1: $R_a = 13.9 (\pm 2.8)$ nm and $98.4 (\pm 22.3)$ nm, NL1: $R_a = 8.5 (\pm 0.3)$ nm and $46.5 (\pm 6.8)$ nm, for $1 \times 1 \mu\text{m}^2$ or $5 \times 5 \mu\text{m}^2$, respectively.

Although the soil profile NL showed a relationship between increasing TOC and decreasing roughness, this was not found for all samples (Cheng et al., 2008). UK1 has a much lower TOC and appears to be rougher than NL1 (see Table 6-1). Other factors such as the particle size distribution may influence surface roughness, i.e. UK1 particles have a larger mean size (0.33 mm) than those of NL1 (0.27 mm).

The range of phase angles is higher for NL1 than for UK1 (see Figure 6-3b and d as examples). The phase angle indicates different textures of materials, with lower phase angles representing harder surfaces and *vice versa* (Cheng et al., 2008). This appears to reflect the relatively high TOC content ($36.3 \pm 2.9 \text{ g kg}^{-1}$) of the bulk NL1

sample in comparison with that of UK1 ($11.4 \pm 2.7 \text{ g kg}^{-1}$). NL1 probably has a more complete coverage of mineral surfaces, with a more variable thickness of soft organic matter, than UK1 whose mineral surfaces may be more sparsely covered by a (generally) thinner layer of organic materials, which barely cushion them. However, this interpretation assumes that the mechanical nature of the organic material is independent of its origin and history.

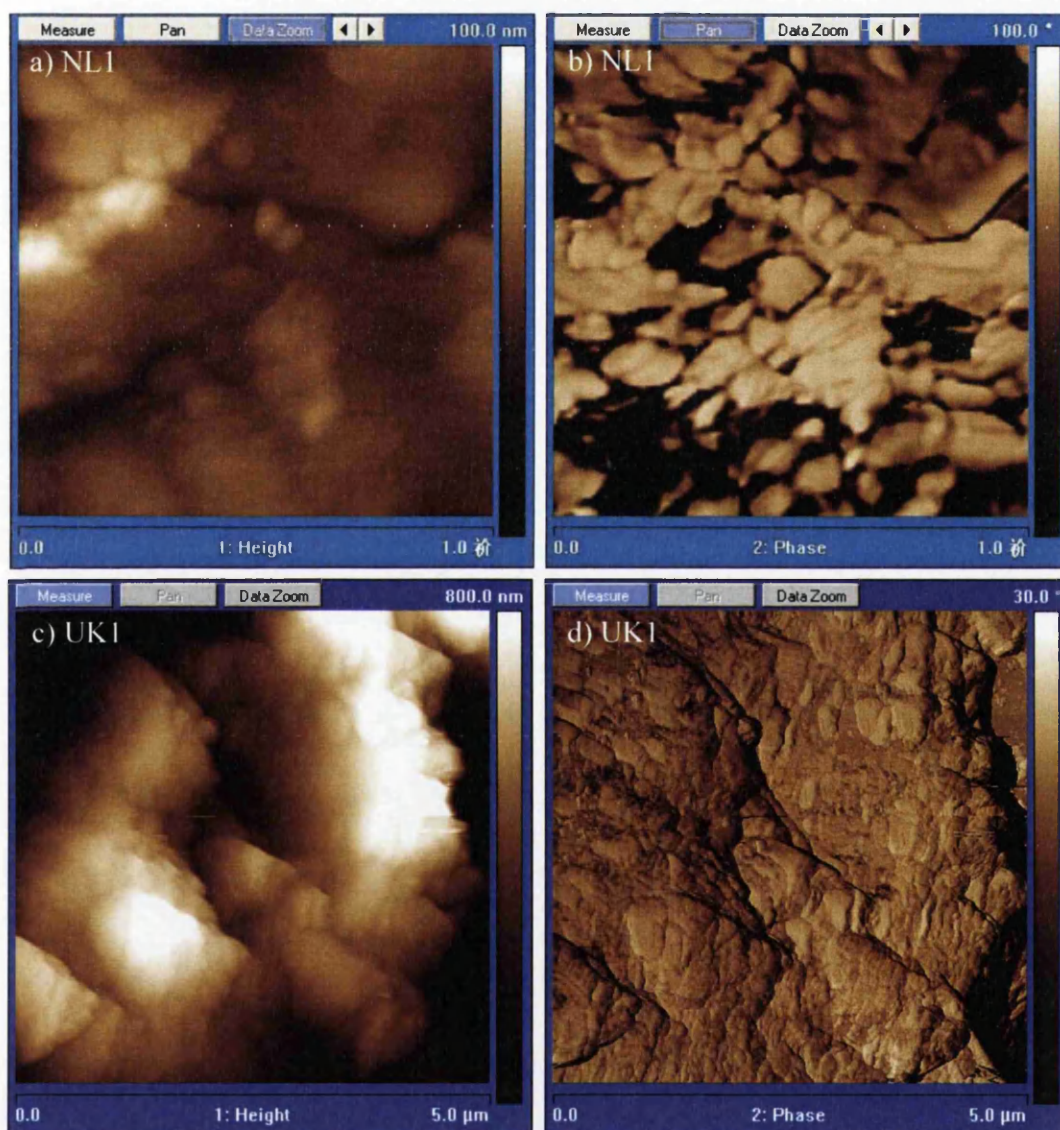


Figure 6-3: a) and c) AFM topography images and b) and d) phase angle images of sample NL1 and UK1 particle surfaces (provided by Dr. Shuying Cheng).

The mean adhesion force of sample UK1 is 20 ± 13 nN (\pm standard deviation) and the distribution lies between 0 and 60 nN with a dominant mode between 10 and 15 nN (see Figure 6-4a). After an increase of pH to 8.1 the force distribution became evenly spread, with no dominant mode, but appears to comprise three overlapping symmetrical distributions of similar amplitude (see Figure 6-4b). The mean force increased significantly to 37 ± 16 nN.

A decrease in pH from the original value (4) to pH 2.9 resulted in a mean force of 24 ± 16 nN and a dominant mode at ~ 10 nN with a second lower mode between 25 and 35 nN (see Figure 6-4c). In comparison with the force distribution at pH 8.1 (Figure 6-4b) it might appear that data have been shifted down towards lower force values and form the same overlapping trio of distributions, but now with reduced modal amplitudes as the force increases (Figure 6-4c).

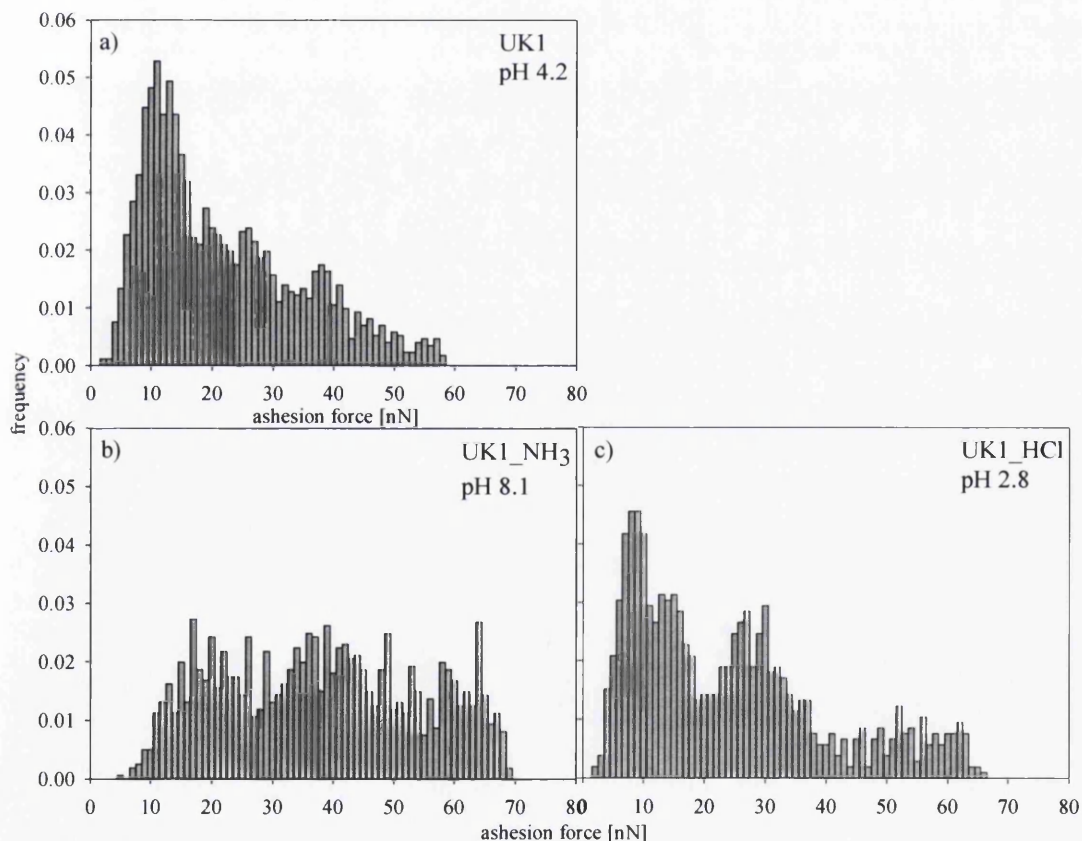


Figure 6-4: Adhesion force distribution on particles from sample a) UK1, b) UK1 with increased pH after treatment with gaseous NH₃, and c) UK1 after treatment with gaseous HCl.

The force distribution obtained from particles of NL1 (at the original pH 4.7) shows a predominant mode between 5 and 15 nN and a mean of 9 ± 4 nN (Figure 6-5a). The distribution following an increase to pH 7.4 is similar in shape, but the amplitude of the mode is reduced, and the mean force increased to 12 ± 9 nN. There is a spread of force data to high values (Figure 6-5b), although at low frequency, suggesting behaviour of a similar type to that of UK1, but which does not occur to the same extent.

The force distributions of NL1 are narrower than those of UK1. After increasing the pH a distinct mode was retained for NL1 but not for UK1 (cf. Figure 6-4 and Figure 6-5).

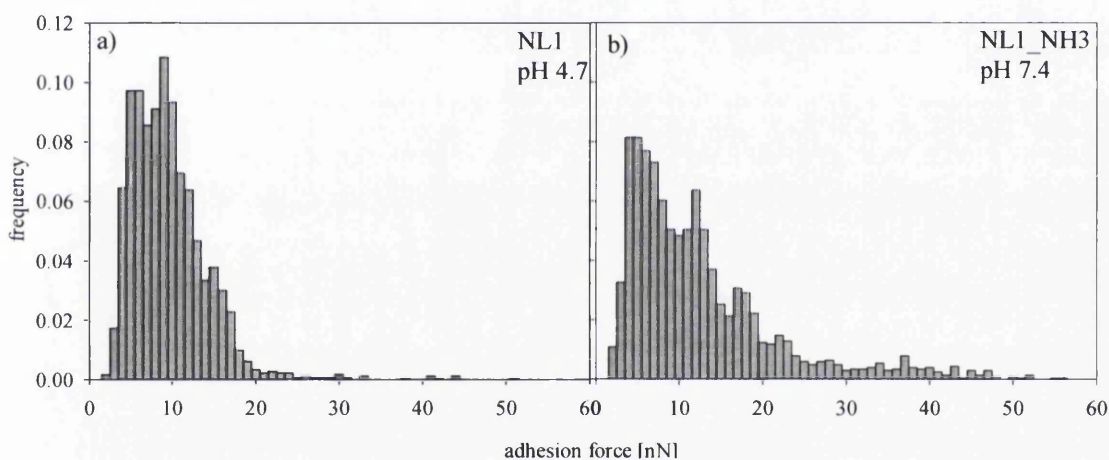


Figure 6-5: Adhesion force distribution on particles from sample a) NL1 and b) NL1 with increased pH after treatment with gaseous NH₃.

An increase in pH increases deprotonation of undissociated weakly acidic groups in the organic matter and, therefore, increases its bulk and local hydrophilicity. The more hydrophilic particle surface may lead to development of a thicker water film on the organic surface, which increases the capillary force between tip and specimen.

Although the soil particles are essentially dry, the enhanced intrinsic pH facilitates deprotonation as water capillaries form during tip-specimen contact in the AFM. This enhances the hydration of the local surface and encourages the development of a

strong adhesion force through the attraction of water for the surface. Although the particles are dry and bulk water content is low, some water is bound to the particle surface (Israelachvili, 1992; Findenegg et al., 2008). This water has been described as gel-like or non-freezing water and may have different properties from free water (Findenegg et al., 2008), but may still act as a facilitating agent for deprotonation.

The increased frequency of force data at high values, for distributions obtained from soil particles at elevated pH, also suggests an increase in the availability of hydrophilic sites, although the modest increase in the mean force may not be a useful statistical parameter to represent the surface.

A more detailed discussion (in relation to a broader range of samples) of changes occurring on soil particle surfaces arising from pH adjustment and its influence on wettability is presented in chapter 5.

Some differences between the force distributions for these samples may arise from their different surface roughness and TOC contents (Cheng et al., 2008) as the roughness affects the area of contact between the AFM tip and specimen. This in turn affects the force exerted on similar interactions at the same pressure, thus broadening the force distribution. The breadth of UK1 distributions is probably partly due to its higher surface roughness in comparison with that of NL1. It is also likely that the high organic content of NL1 may mask the intrinsic mineral surface roughness by occupying the hollows and crevices and presenting a more chemically uniform surface. The manner and conditions under which organic matter is integrated into soil may also affect the mode of adsorption to mineral surfaces so that the effect on surface roughness could be quite variable. It was unfortunately not possible to measure the force at exactly the same position before and after pH change with the equipment available at the time of this study. Hence, no information about detailed changes in a specific location could be gained. A new AFM system (made by Veeco) promises the possibility to measure force during imaging with tapping mode using a specialised cantilever. In combination with a sample holder that enables precise determination of location, this offers new possibilities for investigations of particles after subjecting them to e.g. pH changes.

The humidity of ambient air provides the source of water vapour, which forms the capillary at the AFM tip–specimen contact point. The relative humidity (RH) was not well controlled during measurements, but usually was in the range 37–43 %. This may have introduced some independent variation to the adhesion force. There is also some variation (which can be up to 40 % in extreme cases depending on the manufacturer) in the spring constants of the cantilevers (Jing et al., 2007). It was necessary to use a new cantilever with each sample. However, these cantilevers were all taken from the same batch.

Such factors render a reliable comparison of absolute values between samples difficult and so, as yet, the precise influence of TOC on surface roughness cannot be quantified. It is also possible that the relative frequencies of hydrophilic and hydrophobic sites on a particle surface may prove to be better indicators of wettability than the estimate of the mean adhesion force.

6.4 Conclusions

AFM force measurements can be used to investigate surface hydrophobicity. The adhesion force measurements using AFM confirmed a change to a more hydrophilic surface following adjustment of pH as suggested by bulk wettability measurements made on corresponding samples drawn from bulk material. However, no detailed information about changes in surface properties could be gained as it is currently not possible to measure the force at exactly the same position before and after the pH treatment. Further advances in sample preparation and AFM technology may allow this obstacle to be overcome.

Both roughness and organic matter distribution affect the force measurements so that high surface roughness and uneven organic distribution on soil particle surfaces have to be considered for interpretation of force measurements made on soil particle surfaces. Therefore, the systematic investigation of pH change on organic material (e.g. humic acids) on a smooth surface may prove useful to eliminate such influences and provide reference data for the interpretation of the data gained on complex soil

particle surfaces. It has, for example, been possible to investigate the conformation of dissolved organic matter (DOM) and natural organic matter (NOM) (e.g. Lead et al., 1999; Maurice et al., 1999; Namjesnik-Dejanovic et al., 2001) and to differentiate between hydrophobic and hydrophilic areas in humic acids attached to flat surfaces (Maurice et al., 1999). New AFM systems (e.g. the Icon from Veeco) allow additional measurements of surface properties parallel to topographical images, such as force measurements and measurements of surface rigidity. This allows a mapping of the properties and would help investigations of highly heterogeneous systems like soil particles.

Another promising approach may be the use of electrostatic force microscopy (EFM), which could provide more information about the charge and charge distribution of the organic material. This, however, cannot be easily applied to soil particles because the specimen or an underlying connected layer needs to be conductive. The roughness of samples also influences the quality of such measurements, so that investigations on flat surfaces are more promising. Therefore, the application seems to be restricted to organic material adsorbed on flat and conductive surfaces (e.g. Das et al., 2006).

Chapter 7
Synthesis and Conclusions

7.1 Introduction

This chapter provides (i) a summary of the key results of this work; (ii) an evaluation of the methods used and developed; (iii) assessments of the application and transferability of methods between various scales ranging from sub-particle, individual particle, multi-particle (single layer arrays) to bulk soil; (iv) conclusions drawn from this study and (v) recommendations for further work. A variety of correlations between various particle properties, described in previous chapters, are examined to assist with these assessments. The various estimates of soil water repellency used in this study are compared and discussed, and the limitations of the study and recommendations for future research are identified and discussed.

More specifically, the following questions are addressed:

- What are the main findings of this work?
- In how far were the central research questions answered in this study?
- How may the information provided by the various methods be inter-related and related to the phenomenon of bulk soil water repellency?
- What techniques may be used to further probe the soil system in order to examine surface properties of soil particles, such as the particular arrangement of organic molecules on a surface?

Key findings of this study were:

- Individual soil particles irradiated, at wavelengths $\lambda = 488$ nm and $\lambda = 543$ nm, in a laser scanning confocal microscope auto-fluoresce due to the presence of an organic coating. (Chapter 3)
- Although not all organic material present in a soil sample can be assumed to fluoresce, a relationship between fluorescence and total organic carbon content was found. Therefore, it can be assumed that the fluorescing material represents an approximately consistent proportion of the total material in all samples. It can thus also be assumed that fluorescence measurements can be used to describe the organic matter coating on the surface of soil particles in terms of coverage, distribution and amount present. (Chapter 3)

- All parameters of fluorescence show large standard deviations. This indicates an uneven distribution of organic material within samples. (Chapter 3)
- The two methods developed for particle water repellency measurement (g-mWPM, o-mWPM) detect differences in water repellency between particles of known wettability (clean glass ballotini, hydrophobic coated glass ballotini, Diakon ballotini). (Chapter 4)
- Differences between the wettabilities of individual soil particles were detected by o-mWPM. The particle wettability varied strongly within a soil sample, indicating that the bulk soil wettability is a widely distributed property at the individual particle scale. (Chapter 4)
- The parameters on the particle scale showed mostly only weak correlation with bulk wettability, but a multi-factor correlation, including several fluorescence parameters, was found, suggesting that mechanisms inducing bulk soil water repellency are complex. (Chapters 3 and 4)
- Changing the sample pH artificially without changing the moisture content led to a change in wettability. (Chapter 5)
- The changed wettability following the adjustment of pH was also observed at the micro-scale. AFM measurements showed an increase in the hydrophilicity of particle surfaces after the adjustment. (Chapter 6)

7.2 Bulk soil water repellency measurements

Both methods for determining bulk soil water repellency, WDPT and contact angle (introduced in chapter 2), are appropriate measurements for describing this soil property. The relationship between the two measurements has been investigated previously, but no universal relationship was found as they are relating to somewhat different soil properties (e.g. King, 1981; Doerr, 1998; Diehl et al., submitted). WDPT measures the time a droplet needs to penetrate into a soil and, therefore, can be interpreted as a measure of the persistence of water repellency. The contact angle on the other hand, is obtained within the first minute after water droplet application measuring the state at that moment and, thus, represents the initial strength of water repellency. Differences in relationships between WDPT and contact angle found in

various studies could also be due to variation in water drop volumes, sample preparation (like compaction) and environmental conditions during measurements. WDPT is, in general, a relatively subjective measure as the researcher needs to decide when droplet penetration is complete. This can be difficult, especially for samples containing fine material, as this tends to be pulled upwards by the surface tension of the water obscuring the surface of the water droplet underneath. This limits the comparability of absolute values between studies.

In this study an increase in WDPT with contact angle was found for $\theta > 85^\circ$ and $\text{WDPT} > 20$ s (Figure 7-1). However, a correlation was poor due to data scatter. WDPT appeared to be insensitive as it did not vary between soil samples whose contact angles fell within the range of $30^\circ < \theta < 80^\circ$. This is in agreement with a recent study (Diehl et al., submitted) which found that WDPT is not sensitive to contact angle changes at values < 10 s, but measurements of contact angles of sessile drops were found to be sensitive over the whole range of measured values (10 – 110°).

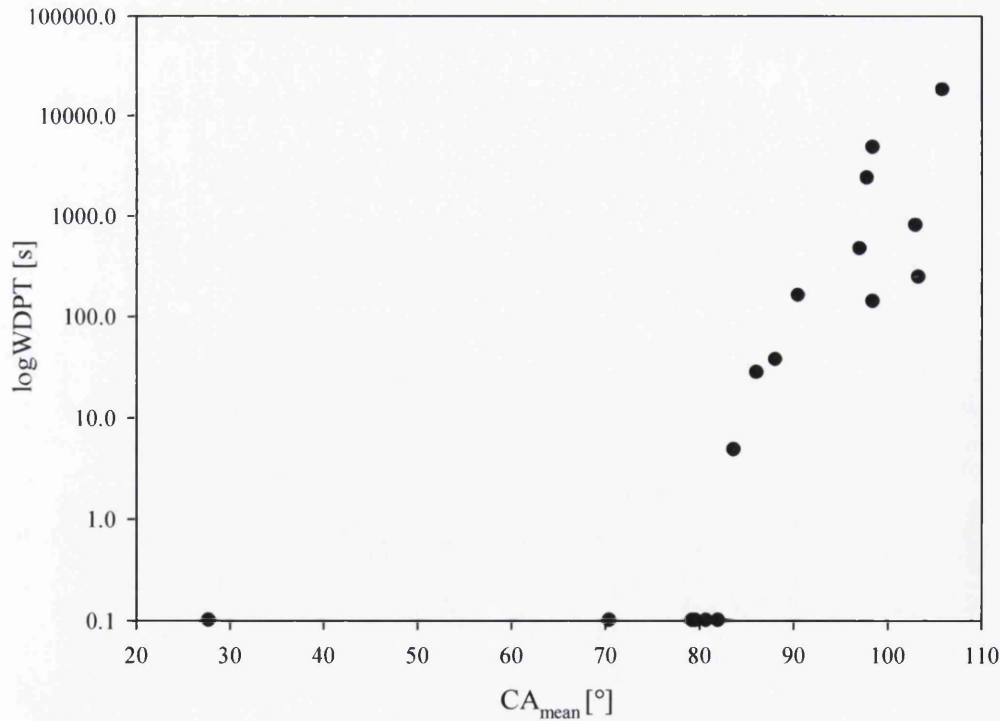


Figure 7-1: log WDPT vs contact angle of all samples. Minimum logWDPT values were taken as being 0.1 s.

The commonly used, but arbitrary WDPT boundary value of < 5 s between wettable and slightly water repellent samples (as described in chapter 2, section 2.3.1) may not be of practical use in the light of these findings. If the WDPT is insensitive to contact angle changes at penetration times < 10 s no useful information is gained from a boundary of < 5 s. Therefore, it may be better to adopt a wettable – water repellent transition boundary at 10 s as used by Adams et al. (1970). Additionally, the determination of the contact angles of samples below this boundary may be useful in order to better define their wettabilities as demonstrated by Shirtcliffe et al. (2006). Here, contact angles $< 50^\circ$ on rough uneven surfaces, as found on soil samples, were considered wettable, whereas contact angles $> 50^\circ$ were considered to indicate slight water repellency or sub-critical water repellency.

A question remains as to how far WDPTs < 10 s are environmentally relevant. On a level surface, under vegetation cover, such short WDPTs will not present a problem, but on steep unvegetated slopes and after fires, even such a short delay in infiltration may promote erosion, by run-off, during heavy rainfall. The relevance of short WDPT, so called sub-critical water repellency, therefore, depends on the environment. Sub-critical water repellency also influences the water distribution within soils and, thus, may influence promotion of preferential flow. The additional effort of determining contact angles of samples with short WDPTs may be worthwhile for locations with critical environmental conditions. The decision as to whether complementary assessments of water repellency are chosen for investigations depends on the research aim. Samples with sub-critical water repellency should preferably be investigated by contact angle as it is the more sensitive measurement. In less critical environments WDPT may be more appropriate and adequate. Another method especially developed for cases of sub-critical water repellency is the measurement of sorptivity of water against that of ethanol (which is not affected by water repellency, Tillman et al., 1989; Hallett et al., 1999). This method defines a water repellency index proportional to the infiltration rate of water. However, sample preparation in the laboratory removed the water repellent behaviour of the samples and it therefore may be primarily used for field investigations (Tillman et al., 1989).

In this study, the contact angle was chosen to represent soil wettability for correlation with most other soil sample and particle properties as it reflects the initial wettability of the material. Nevertheless, WDPT data were obtained for all samples as they were considered relevant for environmental implications of water repellency and facilitate comparison with previous measurements made on the same samples in earlier studies (e.g. Doerr et al., 2004; Mainwaring et al., 2004; Morley et al., 2005). The original WDPTs measured directly after sampling and then after subsequent drying in 2001 (*ibid*) differ significantly from those measured in this study (Figure 7-2). Under the same conditions of storage, most samples (apart from samples AUC, NL1 and UK1) became less water repellent during storage. In contrast, the WDPTs of AUC, NL1 and UK1 increased from 0 s to 800 s, 180 s to 4800 s and 900 s to 18000 s, respectively. Several mechanisms could produce these diverse changes. The so-called ageing of SOM (e.g. Schaumann, 2006b), which is described as conformational changes in soil organic matter structure due to chemical or physical changes or microbial activity (e.g. Hallett et al., 1999; Roper, 2005; Schaumann, 2006b; Diehl et al., in press). Conformational changes in the organic matter may include formation of hydrogen or cation bridges and, therefore, extended networks of organic molecules may form. Within these networks some regions may be more hydrophilic others more hydrophobic (Maurice et al., 1999; Pan et al., 2008). The formation of micro-pores may also be favoured (e.g. Jaeger et al., 2006; Jaeger et al., 2007) and this may lead to inclusion of the remaining water, leaving hydrophobic groups oriented towards the air interface, rendering a soil more hydrophobic. The ionic strength of the soil solution may increase locally when soils are dried, and, therefore, increase the density of ions available for binding organic molecules and forming such extended networks. Alternatively other mechanisms must be available to render soils more wettable, such as microbial activity (which needs at least low amounts of water) or other slow re-arrangement processes with time that may lead to destruction of the organic matter network. This may leave more hydrophilic moieties and/or mineral sites exposed at the surface, thus, rendering the surface more hydrophilic. In case of soils with high ionic strength of the soil solution, drying may lead to precipitation of salts if the solubility product is exceeded. These salts could lead to an improvement in wettability. However, all the speculations made above need to be tested in order to determine which processes produce these long-term

changes following the initial drying and storage of samples under relatively stable environmental conditions.

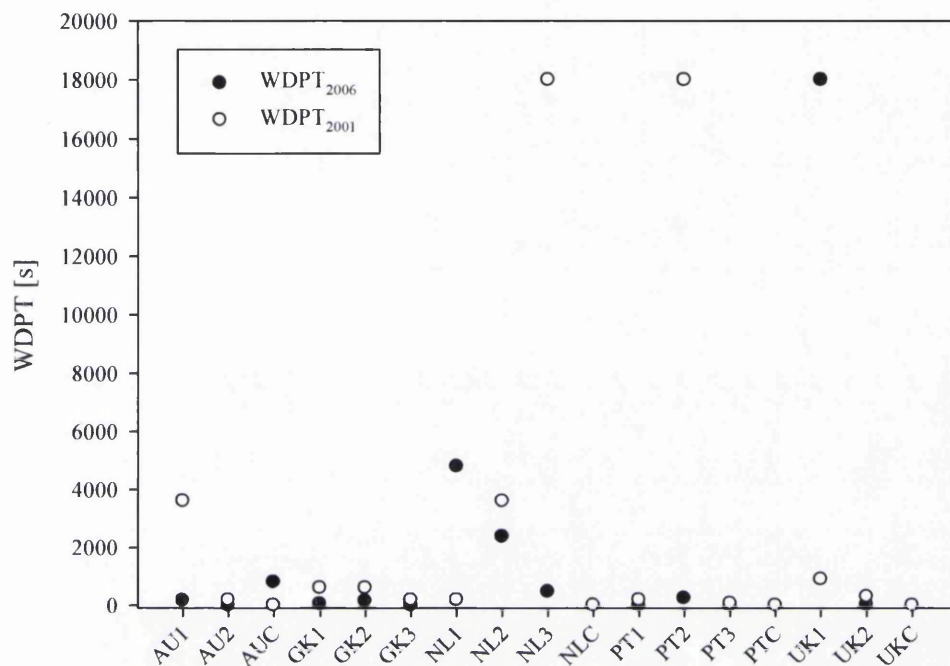


Figure 7-2: WDPT as measured in 2001 and 2006. Values from 2001 are given as the upper limit of the corresponding WDPT category (cf. chapter 2).

A comparison of the wettability of samples that have been stored under dissimilar conditions may be even more difficult as the development of water repellency, with time, seems to depend on drying and storage temperatures, relative humidity and other factors (e.g. de Jonge et al., 1999; Doerr et al., 2002; Bayer et al., 2007). As shown above, not even samples stored under similar conditions show similar water repellency development with time. Therefore, in order to compare samples, a similar treatment should be chosen and a measurement protocol followed. That means the sample preparation and storage conditions should be stated in detail. If other temporally variable soil properties, such as water content, pH, microbial activity etc, are correlated with sample wettability the evaluation of all parameters should be carried out at the same time in order to gain a snap-shot of the state of the sample at that point in time.

Generally, the correlation of different bulk soil measurements may be difficult as they do not sample the same soil properties. The wettability of soils is variable while TOC can be assumed to be comparatively constant during sample storage in a laboratory and changes only slowly under field conditions, e.g. during the course of the year. Attempts to predict the prevailing level of soil water repellency by means of correlations with TOC content, clay content and other more or less static soil properties, therefore, seem to be of limited value.

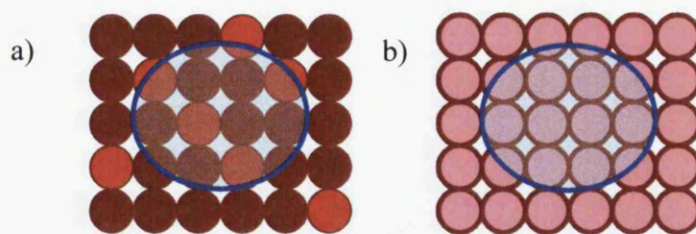
The experiments conducted in chapter 4 demonstrate that not all particles within a water repellent soil exhibit water repellency or possess similar wettabilities. Measurements of WDPT and contact angle always sample the properties of arrays of particles, providing average values of the pertinent properties exposed at the surface. In order to determine the mechanisms underlying water repellency, and possibly develop a model which allows confident prediction of its occurrence, it is necessary to understand the characteristics of the various surfaces present and their contribution to the expression of water repellency. This is also important when considering temporal changes in water repellency. If only a few grains within a sample are hydrophobic, for modest changes in the properties of these surfaces it may be sufficient to render the array wettable, whereas an array containing many hydrophobic grains may remain under their influence.

The number of particles typically included in measurements of bulk sample wettability such as WDPT and contact angle is of interest if bulk wettability measurements are compared to individual particle measurements. For a rough calculation it may be assumed that with a water soil contact angle of 90° and a droplet forming a perfect hemisphere with a diameter of 3 mm (this equals a volume of $\sim 14 \mu\text{l}$), the droplet has a contact area of $\sim 7 \text{ mm}^2$. Assuming one sandy soil particle has a diameter of $200 \mu\text{m}$ and is also a perfectly shaped sphere, it has a maximum circular area of $\sim 0.03 \text{ mm}^2$. This provides contact between ~ 200 particles and the water droplet. This will clearly depend on the droplet volume, the contact angle and the particle size distribution. The volume of water used in this study for contact angle measurements was $15 \mu\text{l}$ (cf. chapter 2).

7.3 Comparison of particle properties and bulk soil measures

In this study, different methods for describing soil particle properties have been developed, tested and applied to particles drawn from various sandy samples of different origins. In the previous chapters it was shown that mean values of these particle properties such as fluorescence and particle wettability correlate only weakly with bulk soil properties (TOC, bulk soil wettability). Possible reasons for this were discussed and are summarised below for particle auto-fluorescence and particle wettability:

- i) The expression of bulk soil water repellency (measured by WDPT or contact angle) may be described as an average of wettabilities of the particles in contact with the water droplet (i.e. ~200 particles per water droplet). However, the bulk wettability is not necessarily determined by an arithmetic mean of the particle properties involved (cf. chapter 4). Slight water repellency could be caused by a mixture of some very hydrophobic grains and wettable grains (Figure 7-3a). The measurement of bulk wettability in this case would not deliver any information about the individual surface properties of the soil particles as it is a mean of very different surface properties. In contrast, if slight water repellency is caused by a homogeneous system of slightly hydrophobic grains (Figure 7-3b), bulk wettability measurements contain information about these surfaces, e.g. the surface free energy that is similar for all surfaces.



water repellent soils

Figure 7-3: Particle arrays containing a) wettable (brown) and some strongly hydrophobic grains (red) and b) only grains with a uniform, slightly hydrophobic surface (pink).

- ii) The linear correlation between TOC and particle fluorescence intensity (I_f) suggests that one partly reflects the other ($r \sim 0.6$). Although not all organic material fluoresces, it suggests that fluorescence can be used as a surrogate measure of this material too. (Chapter 3)
- iii) The improved correlation between the fluorescence from multi-particle specimens ($r \sim 0.8$), which may contain fine organic fluorescent particulates, and TOC suggests that such fine organic particulates are present in soil. These are not associated with the individual mineral particles. Apart from their contribution to fluorescence such fine organic particles may influence soil wettability. (Chapter 3)
- iv) The measurement of particle auto-fluorescence, performed by integration of the fluorescence obtained from several optical slices of the particle, is affected by some uncertainty for thick specimens. This arises when the optical slices are not directly adjacent to each other and gaps exist between them whilst continuity of fluorescence is assumed within the gap. There is usually also some subjective judgement involved in the selection of the optical plane from which to start the analysis. (Chapter 3)
- v) The poor correlation between fluorescence measurements and those of bulk soil wettability may reflect a poor and variable representation of particle properties in the latter (as described in (i) above). Although the thickness of the layer over which fluorescence is measured is relatively small in relation to the particle sizes examined, a minimum requirement for a reasonable correlation would perhaps be contact with water over this layer during the wettability measurement. The variable distribution of fluorescent material over the particle surface and with depth suggests a potential roughness to this material in addition to any contribution from the mineral substrate. This approach, reported in chapter 3, provides a multi-parameter linear correlation between contact angle and the fluorescence parameters I_f , C_F and N_F , as well as the TOC of the sample. This returned a correlation coefficient $r = 0.8$. The relationship between measured and predicted contact angle (on this purely heuristic basis) is shown in Figure 7-4. Apart from the experimental value of contact angle of $\sim 30^\circ$ for sample UKC, the predicted and experimental values were in reasonable agreement. Excluding data for sample UKC from the set led to an improvement of the correlation with r increasing to ~ 0.9 .

However, the use of the associated regression equations for the prediction of soil water repellency is not deterministic, although the procedure may assist in the development of a more general predictive capability. Nevertheless, the data support the fact that the quantity, distribution and thickness of organic matter present in a sample interact with other factors to influence the wettability of the soil samples investigated here. (Chapter 3)

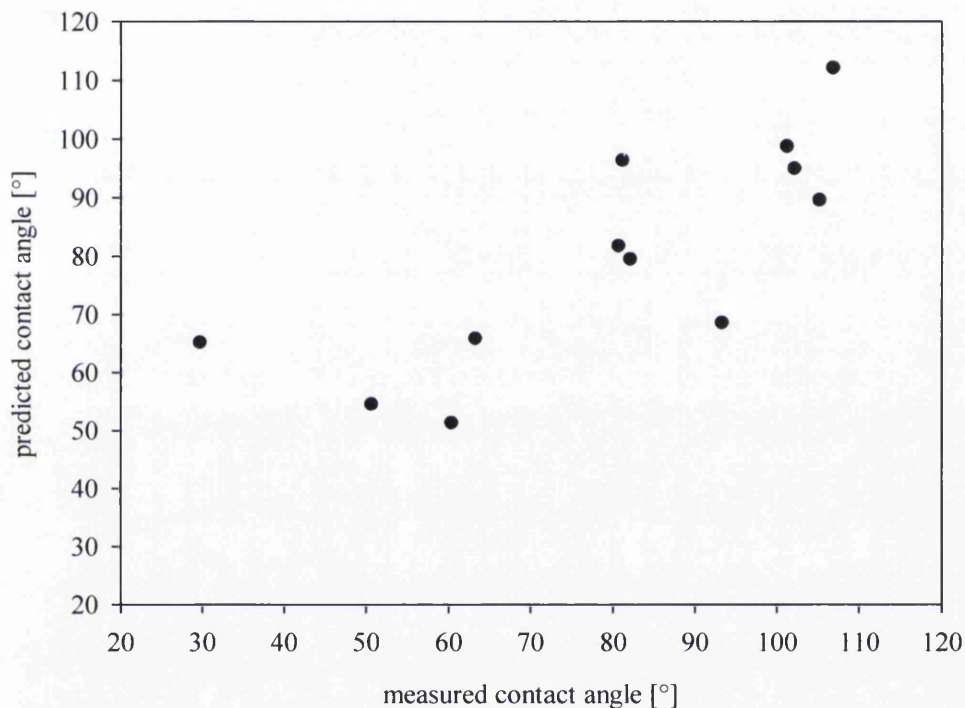


Figure 7-4: Predicted vs measured contact angle.

vi) Measurements by AFM showed that mean surface roughness (mean of 5 regions on 5 particles) varied significantly between samples, but standard deviation of the mean was high for all samples and no correlations of other parameters and roughness were found. The micro-structure of a particle may have an impact on the wettability of the bulk sample by influencing the water distribution at that scale, i.e. within inter-particle pores. Correlation of the bulk soil wettability, measured as contact angle, and the micro-roughness measured by AFM, however, did not reveal a general relationship between

the two measurements (Figure 7-5). However, particles with roughness > 80 nm were only found for three samples with high contact angle ($> 80^\circ$). On porous surfaces that are, as such, only slightly hydrophobic a high surface roughness may lead to an additional hydrophobic effect, by trapping air between liquid and solid surface in the nanopores. This could enhance apparent water repellency in samples with very rough particle surfaces, similar to macroscopic rough samples that display hydrophobicity (e.g. Shirtcliffe et al., 2004; McHale et al., 2005; Shirtcliffe et al., 2006). The roughness determined by AFM includes the contributions from any organic material on the surface. Phase data from the AFM also indicate regions where the surface is soft, suggesting the potential for conformational rearrangement of material associated with these regions. This would provide opportunities for the expression of hydrophobicity. (Chapter 6)

Two fundamentally different effects may play a role in the development of soil water repellency: surface roughness effects, which are purely physical in nature, and the chemical nature of the surfaces. These two effects may be apparent in the scatter of contact angle with micro-roughness (Figure 7-5). In the region between the two dashed lines, samples show increasing contact angle with increasing micro-roughness (this includes particles from samples UK1, PT2, NLC, PT3, GK3 and GK1), and suggests a dominance of the physical surface roughness effect. No dependency of contact angle and micro-roughness was found for samples between the dotted lines (this includes particles drawn from samples NL1, GK2, AU1, AUC and NL2), suggesting that the physical effect was less important and that the chemical nature of the surface may be the dominant influence on wettability. The samples falling in both regions (AU2, UK2, PT1, PTC and UKC) may be influenced equally by both physical and chemical properties. The regions of influence suggested here reflect to some extent the amount of organic matter present in the samples. Those with very high TOC (NL1, GK2) are found in the group where the chemical influence dominates and those with lower TOC (GK3, PT2) in the range where physical influence dominates. As samples from both regions exhibit extreme water repellency, both factors seem equally potent in inducing water repellency in soils. However, some slightly hydrophobic surfaces are probably present in all samples, as roughness on its own cannot induce water repellency.

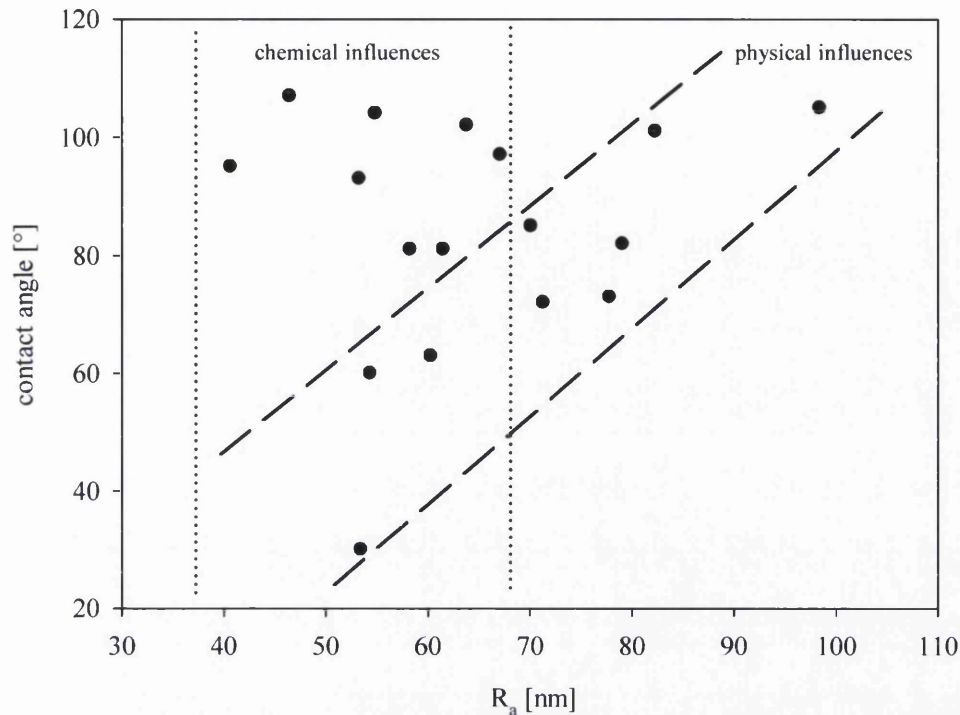


Figure 7-5: Contact angle vs micro roughness (as measured by AFM on $5 \times 5 \mu\text{m}^2$), dotted and dashed lines indicating different influence factors on the bulk wettability.

7.4 Comparison of different particle properties

Measurements of several individual particle properties were introduced in this study (chapters 3 and 4). These show that the distribution of such properties in soil may be broad. Mean values of, for example, fluorescence, individual particle water repellency or roughness may be associated with considerable variations. No simple and significant two-way correlations of means of any of these individual particle properties were found. Correlations between the fluorescence parameters of individual particles (a: I_f , b: C_F , c: N_F ; Figure 7-6) and their corresponding lamella height, measured by o-mWPM, as an indicator of particle wettability, reveal little of particular interest. A slight trend of increasing values of both N_F and I_f with increasing lamella height was found. However, data scatter is significant and in order to test this further a considerable number of additional data points would be required.

Given the time-consuming procedure of data acquisition and analysis it is questionable whether the additional effort would be justified.

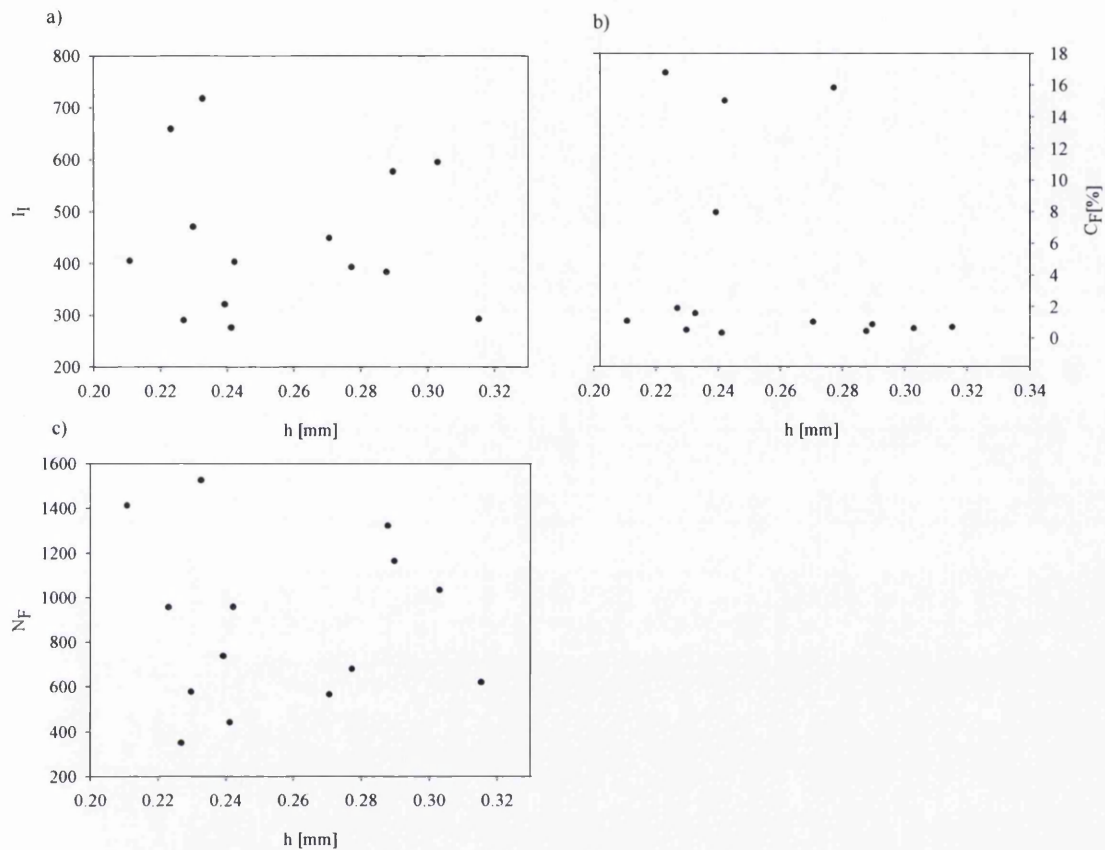


Figure 7-6: a) I_f , b) C_F and c) N_F of single individual particles vs h determined by mWPM.

No multi-parameter correlations were found between fluorescence measurements and the lamella heights. One reason for this may be the influence of particle surface roughness. This probably influences wettability in a similar manner to the roughness of a particle array, where air is trapped between liquid and solid at depressions in the surface when the particle comes into contact with water affecting the local contact angle (see chapters 1 and 4; e.g. Shirtcliffe et al., 2004; Shirtcliffe et al., 2006; McHale et al., 2007).

The mean values of micro-roughness R_a measured by AFM (chapters 2 and 6) are representative of selected regions of selected particles. Detailed analysis of the surface roughness of an individual particle is both time-consuming and difficult. Features at the scale of the length of the AFM probe are difficult or impossible to scan. Data are confined to regions where the features are below this length. Even in the case where, for example, a 200 μm particle presents a relatively large and featureless planar region, an individual $5 \times 5 \mu\text{m}^2$ scan will merely sample $\sim 0.1\%$ of the surface. The LSCM offers an additional facility to estimate the surface roughness of a specimen, in this case one soil particle or a large fraction thereof, without additional analysis time. However, this requires additional software that was not available at the time of this study.

Additionally, the orientation of a particle needs to be considered when its water repellency is measured by mWPM (cf. chapter 4). It is unlikely that the particle surface will be regular or chemically homogeneous. During the process of attachment of the particle to the support, there is little chance to select its orientation. It is possible that it may present alternative types of surface to the support on a purely random basis. It is not clear as to how representative the exposed surface of the particle is in relation to the surface as a whole. This source of variation may be superimposed on effects arising from the general orientation of the particles, which can vary strongly depending on their shape. The mWPM method is likely to provide data representative of symmetrical particles with homogeneous surface chemistry. In the field, natural sand particles form components of aggregates and of a large porous and permeable medium. They possess points and areas of contact with other particles and contribute other regions of surface to pore walls. When they are removed from the field and subjected to processing, drying and storage, aggregates are disrupted and contact areas separated. It seems reasonable to assume that, in the field, areas of particle/particle contact will experience a different history of exposure to percolating fluid than regions of inter-particle pore walls and are, therefore, likely to possess different surface chemistries as a consequence. As soil particles are irregular in shape and size they may form contacts significantly larger in area than those occurring in a bed of for example uniformly sized spherical particles. It has been suggested that these areas of inter-particle contacts (within aggregates) are likely to be of less

significance in relation to soil wettability in the field (Urbanek et al., 2007), although they contribute to many measurements and assessments made in the laboratory.

7.5 Summary

Two methods for the investigation of individual soil particle surfaces have been developed and tested in this work. The mWPM was used to test individual particle wettability and LSCM was used to probe the distribution of organic material over particle surfaces. Fluorescence may provide some insight into reorganisation and rearrangement of this material arising from changes in environmental conditions. Long-term investigations of the same particle are possible providing that the instrumental parameters and operating conditions are faithfully reproduced. The technique is still limited by the resolution available with the wavelength of the radiation involved. Thus, changes at the scale of $< 1\text{-}2\ \mu\text{m}$ are unlikely to be detected. Changes at the level of individual molecules will require other methods that can operate at such small scales (e.g. scanning electron microscopy (SEM) or environmental scanning electron microscopy (ESEM)). The mWPM gives insight into the distribution of soil wettability at the individual particle scale. This may allow estimation of the proportion of water repellent surfaces. In combination with an estimate of the specific surface area of the soil this may provide a bulk parameter useful for comparison with model predictions of water distribution in water repellent soils.

Investigation of soil particle surfaces poses various challenges arising from the high heterogeneity of soil sample material. This is reflected in the large variations in measurements for particles of essentially similar size and mineralogy drawn from individual soil samples. These are probably not well represented by mean values within broad distributions, which suggest many and various contributions to the variance.

The changes between water repellent and wettable soil conditions are commonly attributed (mainly on the basis of circumstantial evidence and speculation) to the

conformation of the organic matter on soil particle surfaces and the changes in conformation in response (over a range of timescales) to local conditions.

Soil water repellency is probably caused by an interaction of particles with a variety of different surface properties distributed across their surfaces at a variety of scales. If speculations concerning molecular conformations are correct then the properties affecting water repellency may also vary in both space and time. Two quite different situations may arise, above the individual particle scale, where a soil with properties uniformly distributed on each particle may express the same (strong) water repellency as a soil containing a mixture of two populations of particles with wettable and non-wettable properties. In the former case a significant and uniform adjustment of properties is needed to confer wettability, but in the latter, perhaps, conversion of only a small proportion of particles to a wettable state may influence the bulk behaviour. The mWPM method may be able to differentiate these two cases as it is possible to distinguish between wettable and strongly repellent particles, but acquisition of representative data is likely to be time-consuming. It may not be sensitive enough to distinguish slight differences in wettability associated with the effect of surface roughness. The method is non-destructive and may allow individual particle wetting behaviour to be observed over time between repeated contacts with water films.

If the surface roughness (a physical state) of individual particles contributes to the development of bulk soil water repellency (as suggested by Figure 7-5) then the chemistry of raised topographic features is also likely to be of influence. If these consist of mineral material, then it is likely that they will be hydrophilic, whereas if organic material is present, which, in itself, may contribute to topography, then a wider range of behaviour is possible. This may include physical removal of organic material from high peaks by abrasion as well as removal by microbial 'grazing'. This in turn affects particle micro-topography. The heterogeneous and polydisperse nature of soil humic materials and the strong tendency to adsorb on surfaces (at the usual environmental pH in wet soil) probably provides little opportunity for the establishment of an equilibrium distribution of organic material. Little preference may be shown for any particular type of topography on initial contact which may well immobilise a large portion of the molecule. The interplay of both physical and

chemical factors are, therefore, likely to influence the development and modification of soil wettability in all but the most extreme cases.

The effort required to render water repellent soils wettable may depend strongly on the mechanism responsible for water repellency. As shown in chapter 5, not all samples react similarly to the addition of acid and base, suggesting that different mechanisms may be involved in water repellency development and the manner in which it changes with time. In the case of chemically hydrophobic surfaces, the addition of surfactants able to convert a hydrophobic surface to a hydrophilic one or microbial degradation of hydrophobic material may alter wettability. In the case of water repellency influenced primarily by physical aspects such as roughness, these measures may be less successful, as the surfaces themselves may already be mostly wettable. Soil water repellency is likely to be of relevance not only for water uptake into soils, but also for sorption of nutrients and contaminants. If water repellency is caused mainly by a chemically hydrophobic surface other sorption mechanisms may dominate than in the case of a very rough, but mainly hydrophilic surface that may also display macroscopic water repellency.

The prediction and management of soil wettability remains a very complex problem and may not be resolved using the methods commonly available as too many factors influence its development, persistency and intensity. The more detailed knowledge we gain on the biological, chemical and physical processes occurring during the evolution of a soil in relation to the development and change of water repellency, the better we are prepared for this task and for tailoring solutions for individual sites. This may enable us to manage water repellency in a sustainable way, taking advantage of it when beneficial to do so and by amelioration when not, in order to make better use of water resources.

Suggestions for further work

The methods introduced in this study deliver information about organic coatings on individual soil particles and soil particle wettability. However, information on the even smaller scale, at the molecular level, is needed in order to fully understand the development of and mechanisms behind soil water repellency. Therefore, other methods are required to investigate the organisation of material at this scale.

However, only few techniques are able to gain information about elemental compositions and distributions, especially within such a complex heterogeneous system like soil organic matter. In the following some promising methods for such investigations are discussed.

One possibility would be to create fluorescent dyes that bind to specific functional groups within soil organic matter to predict their spatial distribution within the organic surface coverage. Such fluorescent dyes exist for (micro)biological applications and were tested in this study (cf. section 3.3.5) for their applicability to soil particles. Those currently available commercially require elaborate sample preparation, which wets and modifies the surface and they do not bind strongly. The development of specialised fluorescent dyes would, thus, be necessary.

Other possibilities for a total analysis of the composition of the organic matter *in situ* could involve SEM or ESEM in combination with energy dispersive X-ray spectroscopy EDX (also called EDS, Cheng et al., 2004), where the EDX system is able to provide an elemental composition of the sample. These methods often require a relatively complex sample preparation and essentially destructive analysis so that any changes in individual specimen behaviour, which are of particular interest here, are beyond its scope. The advantage of ESEM is a working pressure close to atmospheric, so that artefacts in sample imaging caused by the vacuum in the chamber of a conventional SEM are minimized. However, the resolution of the instrument is commonly poorer than that of SEM, but it is possible to observe the development of water droplets and films at the micro-scale and infer local properties from their formation and behaviour.

XRD (X-ray diffraction) and XRF (X-ray fluorescence) also deliver information about the elemental composition of a sample. XRD has been used, for example, to investigate the structure of proteins (Lösche, 1997), but like other methods (e.g. infrared spectroscopy DRIFT) the spatial resolution is poor, although the depth of beam penetration into the substrate can be varied by changing the beam voltage. However, both systems require arrays of particles as specimens, which ideally should be flat in order to minimise effects from light scattering due to surface roughness.

The methods described above are powerful tools for investigations of elemental compositions, however, the interpretation of data obtained from systems as complex as soil is likely to benefit from comparison with those obtained from model particles and organic materials.

Apart from investigations of the surface chemistry of soil particles, distinguishing the chemical influences on wettability from possible physical effects may be of interest for future research. In the case of mainly chemically influenced water repellency, the treatment of soils may be easier and feasible by the addition of surfactants. In the case of mainly physical effects (as an extreme example) this may not help as the particle surfaces themselves may be only slightly hydrophobic. Distinguishing between these two mechanisms may, therefore, be of interest for water repellency management. However, in natural soils both influences probably contribute to water repellency development. A first approach to learn more about the two states would be to create particle surfaces (similar to soil particles in size and general shape) of different roughness with exactly the same surface chemistry and also surfaces with similar roughness but different and known surface chemistry and conformation. If such surfaces can be produced in particulate form to produce a range of mixtures, then these may serve as a suitable range of model soils.

The role of soil micro-organisms was not investigated in this study, but should be included in further research. The long term changes in soil wettability (over several years) reported for soils examined in this and previous work may result from microbial activity. A small quantity of water is held in the samples during storage and may be recycled within the soil. This water may provide for a low level of continuous microbial activity. In natural systems microbial activity will always be of importance for soil building processes and, thus, probably also for development and changes in water repellency.

One of the most important tasks for future research will be to up-scale findings from the particle level to the macroscopic level, i.e. field scale. This needs models that use information on water repellency gained on the micro-scale to predict water flow and uptake in the field. Such information, however, is currently only obtained via the disruption of the structure of soil as it exists in the field. Therefore, it is necessary to

obtain information about this structure on a smaller scale. This could perhaps be achieved through sampling a suitably large core of soil material so that the structure may be examined by non-destructive techniques such as X-ray tomography and/or magnetic resonance imaging (MRI). These may provide details of the pore structure and distribution and the distribution of air and water within it. It may then be possible to sample individual soil aggregates and examine the influence of inter-particle contacts on the nature and distribution of their surface properties in relation to their position in the pore space.

Summary of main conclusions

- i) Water repellency is a phenomenon that affects soil and is influenced by the physico-chemical properties of regions within individual sandy soil particles and manifest at the scale of such individual particles and within arrays of particles constituting or approximating bulk soil. In order to fully understand this phenomenon, it is likely that the contributions made at all of these scales, and their interactions, need to be considered.
- ii) The changing of bulk soil sample properties (like pH) is displayed on both bulk and particle scale. Therefore, the influence of environmental conditions on the particle scale seems to be of high importance for soil wettability.
- iii) Physical and chemical properties of the soil particle surfaces are to some extent distinguishable. They influence particle wettability to various degrees and, for most samples, it is likely that an interplay occurs between them.
- iv) Soil water repellency appears to be rather unpredictable due to the highly complex interactions at various scales involving approximately constant physical factors and variations in chemical factors and processes.

Recommendations for further research

- i) The *in situ* investigation of particle surface chemistry and elemental composition (by the various methods discussed above) is necessary in order to identify chemical structures on the particle surface and, therefore, possibly identify hydrophobic and hydrophilic regions on the particle surface.
- ii) In order to identify mechanisms behind the changes in water repellency, it is necessary to develop methods that allow investigations of particles at exactly the same position before and after environmental changes. A new AFM

system (by Veeco) promises to offer this possibility not for elemental investigations themselves, but for surface properties like softness and hydrophilicity together with topographic information.

- iii) Investigations of the mineral particle surface (e.g. by XRD) as well as its organic coverage may help to gain information about the association process of mineral and organic phase. Depending on the underlying mineral, different adsorption processes for the organic material may dominate, which may well influence the arrangement of organic material on the surface and, thus, the development of water repellency. Therefore, it would be necessary to first investigate total particle surfaces, then remove the organic coatings and re-investigate the same particle again, as no method is currently available with a high spatial resolution to build up 3D models of a particle surface. The challenge here again is posed by the re-investigation of exactly the same particle surface before and after treatment.
- iv) The role of soil biota should be investigated, as it may influence soil chemistry by degradation processes, through its dependence on soil moisture, and also effective roughness and contributions to aggregate formation.
- v) This study has demonstrated that water repellency is not evenly distributed within soil. Investigations of undisturbed soil followed by careful and highly selective sampling of individual particles from soil aggregates may help to identify the impact and nature of inter-particle contacts and the manner in which the contact areas may differ from regions where particle surfaces constitute the wall of a pore. Water distribution within soil could be investigated by magnetic resonance imaging (MRI) in order to identify wet and dry domains or X-ray tomography for investigating the pore system within soil that then may be selected for more detail by analysis.

Bibliography

- Adams S., Strain B.R. and Adams M.S. (1970) Water-repellent soils, fire, and annual plant cover in a desert scrub community of southeastern California. *Ecology*, 51, 696-700.
- Alberts J.J. and Takacs M. (2004) Comparison of the natural fluorescence distribution among size fractions of terrestrial fulvic and humic acids and aquatic natural organic matter. *Organic Geochemistry*, 35, 1141-1149.
- Albrecht C.F., Joubert J.J. and De Rycke P.H. (2001) Origin of the enigmatic, circular, barren patches ('Fairy Rings') of the pro-Namib. *South African Journal of Science*, 97, 23-27.
- Albrecht T.R. and Quate C.F. (1988) Atomic resolution with the atomic force microscopy on conductors and non-conductors. *J. Vac. Sci. Technol. A*, 6, 271-275.
- Altfelder S., Streck T. and Richter J. (1999) Effect of air-drying on sorption kinetics of the herbicide Chlortoluron in soil. *J. Environ. Qual.*, 28, 1154-1161.
- Atkins P.W. (1998). Physical Chemistry. Oxford, Oxford University Press.
- Babejova N. (2001) An influence of changing the humic acids content on soil water repellency and saturated hydraulic conductivity. *Journal of Hydrology and Hydromechanics*, 49, 291-300.
- Bachmann J., Ellies A. and Hartge K.H. (2000a) Development and application of a new sessile drop contact angle method to assess soil water repellency. *Journal of Hydrology*, 231-232, 66-75.
- Bachmann J., Horton R., van der Ploeg R.R. and Woche S.K. (2000b) Modified sessile drop method for assessing initial soil-water contact angle of sandy soil. *Soil Science Society of America Journal*, 64, 564-567.
- Bachmann J., Woche S.K., Goebel M.O., Kirkham M.B. and Horton R. (2003) Extended methodology for determining wetting properties of porous media. *Water Resources Research*, 39.
- Balnois E., Wilkinson K.J., Lead J.R. and Buffle J. (1999) Atomic force microscopy of humic substances: effects of pH and ionic strength. *Environmental Science & Technology*, 33, 3911-3917.
- Bauters T., DiCarlo D., Steenhuis T. and Parlange J.-Y. (1998) Preferential flow in water-repellent sands. *Soil Science Society of America Journal*, 62, 1185-1190.
- Bayer C., Martin-Neto L., Mielniczuk J. and Saab S. (2002) Tillage and cropping system effects on soil humic acid characteristics as determined by electron spin resonance and fluorescence spectroscopies. *Geoderma*, 105, 81-92.
- Bayer J. and Schaumann G.E. (2007) Development of soil water repellency in the course of isothermal drying and upon pH changes in two urban soils. *Hydrological Processes*, 2266-2275.
- Benda L., Miller D., Bigelow P. and Andras K. (2003) Effects of post-wildfire erosion on channel environments, Boise River, Idaho. *Forest Ecology and Management*, 178, 105-119.
- Benito E., Santiago J.L., de Blas E. and Varela M.E. (2003) Deforestation of water-repellent soils in Galicia (NW Spain): effects on surface runoff and erosion under simulated rainfall. *Earth Surface Processes and Landforms*, 28, 145-155.
- Berens A.R. (1989) Transport of organic vapors and liquids in poly(vinyl chloride). *Makromolekulare Chemie, Macromolecular Symposia*, 29, 95-108.

- Berglund K. and Persson L. (1996) Water repellence of cultivated organic soils. *Acta Agriculturae Scandinavica, Section B, Soil and Plant Science*, 46, 145-152.
- Binnig G., Quate C.F. and Gerber C. (1986) Atomic force microscope. *Physical Review Letters*, 56, 930-933.
- Bisdorn E.B.A., Dekker L.W. and Schoute J.F.T. (1993) Water repellency of sieve fractions from sandy soils and relationships with organic material and soil structure. *Geoderma*, 56, 105-118.
- Blackwell P. (1996) Water repellent soils: managing water repellent soils. *Farmnote*, 109.
- Blackwell P.S. (2000) Management of water repellency in Australia, and risks associated with preferential flow, pesticide concentration and leaching. *Journal of Hydrology*, 231-232, 384-395.
- Bond R.D. (1964) The influence of the microflora on the physical properties of soils. II. Field studies on water repellent sands. *Australian Journal of Soil Research*, 2, 123-131.
- Boussu K., Van der Bruggen B., Volodin A., Saauwaert J., Van Haesendonck C. and Vandecasteele C. (2005) Roughness and hydrophobicity studies of nanofiltration membranes using different modes of AFM. *Journal of Colloid and Interface Science*, 286, 632-638.
- Bowen R.W., Mohammad W.A. and Hilal N. (1997) Characterisation of nanofiltration membranes for predictive purposes - use of salts, uncharged solutes and atomic force microscopy. *Journal of Membrane Science*, 126, 91-105.
- Bozer K.R., Brandt G.H. and Hemwall J.B. (1969). Chemistry of materials that make soils hydrophobic. *Proc. Symp. Water Rep. Soils*. University of California, Riverside.
- Buczko U., Bens O. and Durner W. (2006) Spatial and temporal variability of water repellency in a sandy soil contaminated with tar oil and heavy metals. *Journal of Contaminant Hydrology*, 88, 249-268.
- Buczko U., Bens O. and Huttel R.E. (2007) Changes in soil water repellency in a pine-beech forest transformation chronosequence: influence of antecedent rainfall and air temperatures. *Ecological Engineering*, 31, 154-164.
- Cahn J.W. (1977) Critical point wetting. *Journal of Chemical Physics*, 66, 3667-3672.
- Capriel P., Beck T., Borchert H., Gronholz J. and Zachmann G. (1995) Hydrophobicity of the organic matter in arable soils. *Soil Biology and Biochemistry*, 27, 1453-1458.
- Cassie A.B.D. and Baxter S. (1945) Large contact angles of plant and animal surfaces. *Nature (London, United Kingdom)*, 155, 21-2.
- Ceppi S.B., Velasco M.I. and De Pauli C.P. (1999) Differential scanning potentiometry: surface charge development and apparent dissociation constants of natural humic acids. *Talanta*, 50, 1057-1063.
- Chawla A.B., Buckton G., Taylor, K. M. G.; Newton, J. M.; Johnson, M. C. R. (1994) Wilhelmy plate contact angle data on powder compacts: considerations of plate perimeter. *European Journal of Pharmaceutical Sciences*, 2, 29-39.
- Chen J., Gu B., LeBoeuf E.J., Pan H. and Dai S. (2002) Spectroscopic characterization of the structural and functional properties of natural organic matter fractions. *Chemosphere*, 48, 59-68.
- Chen J., LeBoeuf E.J., Dai S. and Gu B. (2003) Fluorescence spectroscopic studies of natural organic matter fractions. *Chemosphere*, 50, 639-647.

- Cheng S., Bryant R., Doerr S.H., Williams P.R. and Wright C.J. (2008) Application of atomic force microscopy to the study of natural and model soil particles. *Journal of Microscopy-Oxford*, 231, 384-394.
- Cheng X., Janssen H., Barends F.B.J. and denHaan E.J. (2004) A combination of ESEM, EDX and XRD studies on the fabric of Dutch organic clay from Oostvaardersplassen (Netherlands) and its geotechnical implications. *Applied Clay Science*, 25, 179-185.
- Cisar J.L., Williams K.E., Vivas H.E. and Haydu J.J. (2000) The occurrence and alleviation by surfactants of soil-water repellency on sand-based turfgrass systems. *Journal of Hydrology*, 231-232, 352-358.
- Clifford J. (1975). Properties of Water in Capillaries and Thin Films. *In: Water in Disperse Systems*. Franks F. (ed.). New York, Plenum Press. 5: 75-131.
- Clothier B.E., Green S.R. and Deurer M. (2008) Preferential flow and transport in soil: progress and prognosis. *European Journal of Soil Science*, 59, 2-13.
- Clothier B.E., Vogeler I. and Magesan G.N. (2000) The breakdown of water repellency and solute transport through a hydrophobic soil. *Journal of Hydrology*, 231-232, 255-264.
- Contreras S., Canton Y. and Sole-Benet A. (2008) Sieving crusts and macrofaunal activity control soil water repellency in semiarid environments: evidences from SE Spain. *Geoderma*, 145, 252-258.
- Crockford H., Topalidis S. and Richardson P. (1991) Water repellency in a dry sclerophyll eucalypt forest - measurements and processes. *Hydrological Processes*, 5, 405-420.
- Das A., Lei C.H., Thomas H.E., Elliott M., Macdonald J.E., Glarvey P. and Turner M.L. (2006). EFM phase investigation of the metal-organic film interface, Elsevier Science Bv.
- Das D.K. and Das B. (1972) Characterization of water repellency in Indian soils. *Indian Journal of Agricultural Sciences*, 42, 1099-1022.
- de Gennes P.D. (1988). Dynamics of wetting. Liquids at interfaces. Les Houches, North Holland. Elsevier Science Publishers B.V.
- de Gennes P.G., Brochard-Wyart F. and Quéré D. (2004). Capillarity and wetting phenomena: drops, bubbles, pearls, waves. New York. Springer Science & Business Media Inc.
- de Jonge L.W., Jacobsen O.H. and Moldrup P. (1999) Soil water repellency: effects of water content, temperature and particle size. *Soil Science Society of America Journal*, 63, 437-442.
- DeBano L.F. (1969a). Water movement in water-repellent soils. *Proc. Symp. Water Rep. Soils*. University of California, Riverside.
- DeBano L.F. (1969b) Water repellent soils: A worldwide concern in management of soil and vegetation. *Agricultural Science Review*, 7, 11-18.
- DeBano L.F. (1971) The effect of hydrophobic substances on water movement in soil during infiltration. *Soil Science Society of America Proceedings*, 35, 340-343.
- DeBano L.F. (1981). Water repellent soils: a state-of-the-art. Berkeley, California, Pacific Southwest Forest and Range Experiment Station: 20pp.
- DeBano L.F. (2000a) The role of fire and soil heating on water repellency in wildland environments: a review. *Journal of Hydrology*, 231-232, 195-206.
- DeBano L.F. (2000b) Water repellency in soils: a historical overview. *Journal of Hydrology*, 231-232, 4-32.

- DeBano L.F., Mann L.D. and Hamilton D.A. (1970) Translocation of hydrophobic substances into soil by burning organic litter. *Soil Science Society of America Proceedings*, 34, 130-133.
- DeBano L.F., Savage S.M. and Hamilton D.A. (1976) The transfer of heat and hydrophobic substances during burning. *Soil Science Society of America Journal*, 40, 779-782.
- Dekker L.W., Doerr S.H., Oostindie K., Ziogas A.K. and Ritsema C.J. (2001) Water repellency and critical soil water content in a dune sand. *Soil Science Society of America Journal*, 65, 1667-1674.
- Dekker L.W., Oostindie K., Kostka S.J. and Ritsema C.J. (2005) Effects of surfactant treatments on the wettability of a water repellent grass-covered dune sand. *Australian Journal of Soil Research*, 43, 383-395
- Dekker L.W. and Ritsema C.J. (1994) How water moves in a water repellent sandy soil: 1. Potential and actual water repellency. *Water Resources Research*, 30, 2507-2517.
- Dekker L.W. and Ritsema C.J. (1996a) Preferential flow paths in a water repellent clay soil with grass cover. *Water Resources Research*, 32, 1239-1249.
- Dekker L.W. and Ritsema C.J. (1996b) Uneven moisture patterns in water repellent soils. *Geoderma*, 70, 87-99.
- Dekker L.W. and Ritsema C.J. (1996c) Variation in water content and wetting patterns in Dutch water repellent peaty clay and clayey peat soils. *Catena*, 28, 89-105.
- Dekker L.W., Ritsema C.J., Oostindie K. and Boersma O.H. (1998) Effect of drying temperature on the severity of soil water repellency. *Soil Science*, 163, 780-796.
- Deo P., Deo N., Somasundaran P., Jockusch S. and Turro N.J. (2005) Conformational changes of pyrene-labeled polyelectrolytes with pH: effect of hydrophobic modifications. *Journal of Physical Chemistry B*, 109, 20714-20718.
- Derjaguin B.V. and Churaev N.V. (1986). Properties of water layers adjacent to interfaces. Fluid Interfacial Phenomena 'A Wiley-Interscience publication'. C. A. Croxton. New York, John Wiley & Sons Ltd.: 663-738.
- Dexter A.R. and Kroesbergen B. (1985) Methodology for determination of tensile strength of soil aggregates. *Journal of agricultural engineering research / publ. for the British Society for Research in Agricultural Engineering*, 31, 139-147.
- Diaz-Fierros Viqueira F. (1977) Effects of sample storage on the physical and biological properties of organic soils. *Anales de Edafologia y Agrobiologia*, 36, 69-79.
- Diehl D., Bayer J.V., Woche S.K., Bryant R., Doerr S.H. and Schaumann G.E. (submitted) Reaction of soil water repellency on artificially induced changes in soil pH.
- Diehl D., Ellerbrock R.H. and Schaumann G.E. (in press) DRIFT-Spectroscopy of untreated and dried soil samples of different wettability. *European Journal of Soil Science*.
- Diehl D. and Schaumann G.E. (2007) The nature of wetting on urban soil samples: wetting kinetics and evaporation assessed from sessile drop shape. *Hydrological Processes*, 21, 2255-2265.
- Doerr S.H. (1998) On standardising the "Water Drop Penetration Time" and the "Molarity of an Ethanol Droplet" techniques to classify soil hydrophobicity: a case study using medium textured soils. *Earth Surface Processes and Landforms*, 23, 663-668.

- Doerr S.H., Dekker L.W., Ritsema C.J., Shakesby R.A. and Bryant R. (2002) Water repellency of soils: the influence of ambient relative humidity. *Soil Science Society of America Journal*, 66, 401-405.
- Doerr S.H., Douglas P., Evans R.C., Morley C.P., Mullinger N.J., Bryant R. and Shakesby R.A. (2005a) Effects of heating and post-heating equilibration times on soil water repellency. *Australian Journal of Soil Research*, 43, 261-267.
- Doerr S.H., Douglas P., Morley C.P., Llewellyn C.T., Mainwaring K.A., Haskins C., Johnsey L., Ritsema C.J., Stagnitti F., Ferreira A. and Ziogas A. (2004). Organic compounds associated with water repellency in sandy soils. Soil Abiotic and Biotic Interactions and the impact on the Ecosystem and Human Welfare. P. M. Huang, A. Violante and J.-M. Bollag. Enfield, USA, Science Publishers: 444.
- Doerr S.H., Llewellyn C.T., Douglas P., Morley C.P., Mainwaring K.A., Haskins C., Johnsey L., Ritsema C.J., Stagnitti F., Allinson G., Ferreira A.J.D., Keizer J.J., Ziogas A.K. and Diamantis J. (2005b) Extraction of compounds associated with water repellency in sandy soils of different origin. *Australian Journal of Soil Research*, 43, 225-237.
- Doerr S.H., Ritsema C.J., Dekker L.W., Scott D.F. and Carter D. (2007) Water repellence of soils: new insights and emerging research needs. *Hydrological Processes*, 21, 2223-2228.
- Doerr S.H., Shakesby R.A., Dekker L.W. and Ritsema C.J. (2006) Occurrence, prediction and hydrological effects of water repellency amongst major soil and land-use types in a humid temperate climate. *European Journal of Soil Science*, 57, 741-754.
- Doerr S.H., Shakesby R.A. and Walsh R.P.D. (1996) Soil hydrophobicity variations with depth and particle size fraction in burned and unburned Eucalyptus globulus and Pinus pinaster forest terrain in the Águeda basin, Portugal. *Catena*, 27, 25-47.
- Doerr S.H., Shakesby R.A. and Walsh R.P.D. (1998) Spatial variability of soil hydrophobicity in fire-prone eucalyptus and pine forests, Portugal. *Soil Science*, 163, 131-324.
- Doerr S.H., Shakesby R.A. and Walsh R.P.D. (2000a) Soil water repellency: its causes, characteristics and hydro-geomorphological significance. *Earth Science Reviews*, 51, 33-65.
- Doerr S.H. and Thomas A.D. (2000b) The role of soil moisture in controlling water repellency: new evidence from forest soils in Portugal. *Journal of Hydrology*, 231-232, 134-147.
- Douglas P., Mainwaring K.A., Morley C.P. and Doerr S.H. (2007) The kinetics and energetics of transitions between water repellent and wettable soil conditions: a linear free energy analysis of the relationship between WDPT and MED/CST. *Hydrological Processes*, 21, 2248-2254.
- Drummond C. and Israelachvili J. (2004) Fundamental studies of crude oil-surface water interactions and its relationship to reservoir wettability. *Journal of Petroleum Science & Engineering*, 45, 61-81.
- Ellerbrock R.H. and Gerke H.H. (2004) Characterizing organic matter of soil aggregate coatings and biopores by Fourier transform infrared spectroscopy. *European Journal of Soil Science*, 55, 219-228.
- Ellerbrock R.H., Gerke H.H., Bachmann J. and Goebel M.-O. (2005) Composition of organic matter fractions for explaining wettability of three forest soils. *Soil Science Society of America Journal*, 69, 57-66.

- Ewald M., Belin C., Berger P. and Weber J.H. (1983) Corrected fluorescence spectra of fulvic acids isolated from soil and water. *Environmental Science & Technology*, 17, 501-504.
- Feeney D.S., Hallett P.D., Rodger S., Bengough A.G., White N.A. and Young I.M. (2006) Impact of fungal and bacterial biocides on microbial induced water repellency in arable soil. *Geoderma*, 135, 72-80.
- Ferreira A.J.D., Coelho C.O.A., Walsh R.P.D., Shakesby R.A., Ceballos A. and Doerr S.H. (2000) Hydrological implications of soil water-repellency in Eucalyptus globulus forests, north-central Portugal. *Journal of Hydrology*, 231-232, 165-177.
- Fidanza M.A., Cisar J.L., Kostka S.J., Gregos J.S., Schlossberg M.J. and Franklin M. (2007) Preliminary investigation of soil chemical and physical properties associated with type-I fairy ring symptoms in turfgrass. *Hydrological Processes*, 21, 2285-2290.
- Fieber C. and Sonntag H. (1979) Theoretical consideration on the applicability of the sphere method for measuring interfacial-tension and contact-angle. *Colloid and Polymer Science*, 257, 874-881.
- Findenegg G.H., Jahnert S., Akcakayiran D. and Schreiber A. (2008) Freezing and melting of water confined in silica nanopores. *Chemphyschem*, 9, 2651-2659.
- Franco C.M.M., Clarke P.J., Tate M.E. and Oades J.M. (2000a) Hydrophobic properties and chemical characterization of natural water repellent materials in Australian sands. *Journal of Hydrology*, 231-232, 47-58.
- Franco C.M.M., Michelsen P.P. and Oades J.M. (2000b) Amelioration of water repellency: application of slow-release fertilisers to stimulate microbial breakdown of waxes. *Journal of Hydrology*, 231-232, 342-351.
- Franco C.M.M., Tate M.E. and Oades J.M. (1995) Studies on non-wetting sands. I. The role of intrinsic particulate organic matter in the development of water-repellency in non-wetting sands. *Australian Journal of Soil Research*, 33, 253-263.
- Gaillardon P. (1996) Influence of soil moisture on long-term sorption of Diuron and Isoproturon by soil. *Pesticide Science*, 47, 347-354.
- Garbassi F., Morra M. and Occhiello E. (1998). Polymer surfaces: from physics to technology. Chichester, John Wiley & Sons Ltd.
- Garkaklis M.J., Bradley J.S. and Wooller R.D. (2000) Digging by vertebrates as an activity promoting the development of water-repellent patches in sub-surface soil. *Journal of Arid Environments*, 45, 35-42.
- Gerin P.A. and Dufrene Y.F. (2003) Native surface structure of natural soil particles determined by combining atomic force microscopy and X-ray photoelectron spectroscopy. *Colloids and Surfaces B-Biointerfaces*, 28, 295-305.
- Gilboa A., Bachmann J., Woche S.K. and Chen Y. (2006) Applicability of interfacial theories of surface tension to water-repellent soils. *Soil Science Society of America Journal*, 70, 1417-1429.
- Gilmour D.A. (1968) Water repellence of soils related to surface dryness. *Australian Forestry*, 32, 143-148.
- Giovannini G. and Lucchesi S. (1983) Effect of fire on hydrophobic and cementing substances of soil aggregates. *Soil Science*, 136, 231-236.
- Goebel M.O., Bachmann J., Woche S.K., W.R. F. and Horton R. (2004) Water potential and aggregate size effects on contact angle and surface energy. *Soil Science Society of America Journal*, 68, 383-393.

- Gottenbos B., van der Mei H., C. and Busscher H., J. (2000). Initial adhesion and surface growth of *Staphylococcus epidermidis* and *Pseudomonas aeruginosa* on biomedical polymers. 50, 208-214.
- Graber E.R., Ben-Arie O. and Wallach R. (2006) Effect of sample disturbance on soil water repellency determination in sandy soils. *Geoderma*, 136, 11-19.
- Graber E.R., Tagger S. and Wallach R. (2009) Role of divalent fatty acid salts in soil water repellency. *Soil Science Society of America Journal*, 73, 541-549.
- Gunde R., Hartland S. and Mäder S. (1995) Sphere tensiometry: A new approach to simultaneous and independent determination of surface tension and contact angle. *Journal of Colloid and Interface Science*, 176, 17-30.
- Hallett P.D., Douglas J., Ritz K., Wheatley R.E. and Young I.M. (2002) Plant root and microbial derived soil water repellency. *Plant, soils & environment*. 1, 148-151.
- Hallett P.D., Baumgartl T. and Young I.M. (2001) Subcritical water repellency of aggregates from a range of soil management practices. *Soil Science Society of America Journal*, 65, 184-190.
- Hallett P.D., Nunan N., Douglas J.T. and Young I.M. (2004) Millimeter-scale spatial variability in soil water sorptivity: scale, surface elevation, and subcritical repellency effects. *Soil Science Society of America Journal*, 68, 352-358.
- Hallett P.D. and Young I.M. (1999) Changes to water repellence of soil aggregates caused by substrate-induced microbial activity. *European Journal of Soil Science*, 50, 35-40.
- Harper R.J. and Gilkes R.J. (1994) Soil attributes related to water repellency and the utility of soil survey for predicting its occurrence. *Australian Journal of Soil Research*, 32, 1109-1124.
- Harper R.J., McKissock I., Gilkes R.J., Carter D.J. and Blackwell P.S. (2000) A multivariate framework for interpreting the effects of soil properties, soil management and landuse on water repellency. *Journal of Hydrology*, 231-232, 371-383.
- Haughland R.P. (2005). The Handbook - a guide to fluorescent probes and labeling technologies, Invitrogen Corp.
- Hendrickx J.M.H., Dekker L.W. and Boersma O.H. (1993) Unstable wetting fronts in water-repellent field soils. *Journal of Environmental Quality*, 22, 109-118.
- Hendrickx J.M.H., Dekker L.W., Van Zuilen E.J. and Boersma O.H. (1988). Water and solute movement through a water repellent sand soil with grass cover. Proceedings of the International Conference and Workshop on the Validation of Flow and Transport Models for the Unsaturated Zone, Ruidoso, New Mexico, New Mexico State University.
- Hibbs A.R. (2004). Confocal microscopy for biologists. New York, Kluwer Academic / Plenum Publishers.
- Hiemenz P.C. (1977). Principles of colloid and surface chemistry. New York, Marcel Dekker, Inc.
- Horn R. and Baumgartl T. (2000). Dynamic properties of soils. Handbook of soil science. M. E. Sumner. Boca Raton, CRC Press.
- Horne D.J. and McIntosh J.C. (2000). Hydrophobic compounds in sands in New Zealand - extraction, characterisation and proposed mechanisms for repellency expression. *Journal of Hydrology*, 231-232, 35-46.
- Horne D.J. and McIntosh J.C. (2003). Hydrophobic compounds in sands from New Zealand. In: Soil water repellency. Occurrence, consequences, and amelioration. C. J. Ritsema and L. W. Dekker. (Eds.). Wageningen, The Netherlands. Elsevier.

- Hubbell D.H. (1988) Developmental aspects of water-repelleny of sandy soils. *Soil Science Society of America Journal*, 52, 1512-1514.
- Hubbert K.R. and Oriol V. (2005) Temporal fluctuations in soil water repelleny following wildfire in chaparral steplands, southern California. *International Journal of Wildland Fire* 14, 439-447.
- Huh C. and Mason S.G. (1976) Sphere Tensiometry - evaluation and critique. *Canadian Journal of Chemistry-Revue Canadienne De Chimie*, 54, 969-978.
- Hurraß J. and Schaumann G.E. (2006) Properties of soil organic matter and aqueous extracts of actually water repellent and wettable soil samples. *Geoderma*, 132, 222-239.
- Imeson A.C., Verstraten J.M., van Mulligen E.J. and Sevink J. (1992) The effects of fire and water repelleny on infiltration and runoff under Mediterranean type forest. *Catena*, 19, 345-361.
- Ismail S.M. and Ozawa K. (2007) Improvement of crop yield, soil moisture distribution and water use efficiency in sandy soils by clay application. *Applied Clay Science*, 37, 81-89.
- Israelachvili J.N. (1992). Intermolecular and Surface Forces. London, Academic Press.
- Jaeger F., Grohmann E. and Schaumann G.E. (2006) ¹H NMR relaxometry in natural humous soil samples: insights in microbial effects on relaxation time distributions. *Plant and Soil*, 280, 209-222.
- Jaeger F., Grohmann E. and Schaumann G.E. (2007) Microbial and swelling effects on pore size distribution in humous soil samples. *Magnetic Resonance Imaging*, 25, 581.
- Jaramillo D.F., Dekker L.W., Ritsema C.J. and Hendrickx J.M.H. (2000) Occurrence of soil water repelleny in arid and humid climates. *Journal of Hydrology*, 231-232, 105-111.
- Jex G.W., Bleakley B.H., Hubbell D.H. and Munro L.L. (1985) High humidity-induced increase in water repelleny in some sandy soils. *Soil Science Society of America Journal*, 49, 1177-1182.
- Jiang P., Xie S.S., Pang S.J. and Gao H.J. (2002) The combining analysis of height and phase images in tapping-mode atomic force microscopy: a new route for the characterization of thiol-coated gold nanoparticle film on solid substrate. *Appl. Surf. Sci.*, 191, 240-246.
- Jing G.Y., Ma J. and Yu D.P. (2007) Calibration of the spring constant of AFM cantilever. *J. Electron Microsc (Tokyo)*, 56, 21-25.
- Johnson A.C., Bettinson R.J. and Williams R.J. (1999) Differentiating between physical and chemical constraints on pesticide and water movement into and out of soil aggregates. *Pesticide Science*, 55, 524-530.
- Jordan A., Martinez-Zavala L. and Bellinfante N. (2008) Heterogeneity in soil hydrological response from different land cover types in southern Spain. *Catena*, 74, 137-143.
- Jozefaciuk G. and Bowanko G. (2002a) Effect of acid and alkali on surface properties of minerals. *Clays and Clay Minerals*, 50, 771-783.
- Jozefaciuk G., Muranyi A. and Alekseeva T. (2002b) Effect of extreme acid and alkali treatment on soil variable charge. *Geoderma*, 109, 225-243.
- Jungerius P.D. and de Jong J.H. (1989) Variability of water repelleny in the dunes along the Dutch coast. *Catena*, 16, 491-497.

- Kalbitz K., Schmerwitz J., Schwesig D. and Matzner E. (2003) Biodegradation of soil-derived dissolved organic matter as related to its properties. *Geoderma*, 113, 273-291.
- Kalbitz K., Schwesig D., Rethemeyer J. and Matzner E. (2005) Stabilization of dissolved organic matter by sorption to the mineral soil. *Soil Biology and Biochemistry*, 37, 1319-1331.
- Karnok K.A., Rowland E.J. and Tan K.H. (1993) High pH treatments and the alleviation of soil hydrophobicity on golf greens. *Agronomy Journal*, 85, 983-986.
- Keizer J.J., Coelho C.O.A., Shakesby R.A., Domingues C.S.P., Malvar M.C., Perez I.M.B., Matias M.J.S. and Ferreira A.J.D. (2005) The role of soil water repellency in overland flow generation in pine and eucalypt forest stands in coastal Portugal. *Australian Journal of Soil Research*, 43, 337-349.
- Keizer J.J., Doerr S.H., Malvar M.C., Ferreira A.J.D. and Pereira V. (2007) Temporal and spatial variations in topsoil water repellency throughout a crop-rotation cycle on sandy soil in north-central Portugal. *Hydrological Processes*, 21, 2317-2324.
- King P.M. (1981) Comparison of methods for measuring severity of water repellence of sandy soils and assessment of some factors that affect its measurements. *Australian Journal of Soil Research*, 19, 275-285.
- Koc Y., de Mello A.J., McHale G., Newton M.I., Roach P. and Shirtcliffe N.J. (2008) Nano-scale superhydrophobicity: suppression of protein adsorption and promotion of flow-induced detachment. *Lab on a Chip*, 8, 582-586.
- Kögel-Knabner I. (1997) ^{13}C and ^{15}N NMR spectroscopy as a tool in soil organic matter research. *Geoderma*, 80, 243-270.
- Kostka S.J. (2000) Amelioration of water repellency in highly managed soils and the enhancement of turfgrass performance through the systematic application of surfactants. *Journal of Hydrology*, 231-232, 359-368.
- Kowalchuk G.A. and Stephen J.R. (2001) Ammonia-oxidising bacteria: A Model for molecular microbial ecology. *Annu. Rev. Microbiol.*, 55, 485-529.
- Kuntze H., Roeschmann G. and Schwerdtfeger G. (1988). *Bodenkunde*. Stuttgart, Eugen Ulmer GmbH.
- Kvitek L.P., Kovarikova, L.; Hrbac, J. (2002) The study of the wettability of powder inorganic pigments based on dynamic contact angle measurements using Wilhelmy method. *Chemica*, 41, 27-35.
- Lamparter A., Deurer M., Bachmann J., Wilhelmus H. and Duijnsveld M. (2006) Effect of subcritical hydrophobicity in a sandy soil on water infiltration and mobile water content. *Journal of Plant Nutrition and Soil Science*, 169, 38-46.
- Lead J.R., Balnois E., Hosse M., Menghetti R. and Wilkinson K.J. (1999) Characterization of Norwegian natural organic matter: size, diffusion coefficients, and electrophoretic mobilities. *Environment International*, 25, 245-258.
- Leighton-Boyce G., Doerr S.H., Shakesby R.A. and Walsh R.P.D. (2007) Quantifying the impact of soil water repellency on overland flow generation and erosion: a new approach using rainfall simulation and wetting agent on in situ soil. *Hydrological Processes*, 21, 2337-2345.
- Leighton-Boyce G., Doerr S.H., Shakesby R.A., Walsh R.P.D., Ferreira A.J.D., Boulet A. and Coelho C.O.A. (2005) Temporal dynamics of water repellency and soil moisture in eucalypt plantations, Portugal. *Australian Journal of Soil Research*, 43, 269-280.

- Lemmnitz C., Kuhnert M., Bens O., Guntner A., Merz B. and Huttl R.F. (2008) Spatial and temporal variations of actual soil water repellency and their influence on surface runoff. *Hydrological Processes*, 22, 1976-1984.
- Letey J. (1969). Measurement of contact angle, water drop penetration time, and critical surface tension. Water repellent soils. Proceedings of a Symposium on Water Repellent Soils. L. F. DeBano and J. Letey. University of California: Riverside, CA: 43-47.
- Letey J. (2001) Causes and consequences of fire-induced soil water repellency. *Hydrological Processes*, 15, 2867-2875.
- Letey J., Carrillo M.L.K. and Pang X.P. (2000) Approaches to characterize the degree of water repellency. *Journal of Hydrology*, 231-232, 61-65.
- Letey J., Osborn J. and Pelishek R.E. (1962) Measurement of liquid-solid contact angles in soil and sand. *Soil Science*, 93, 149-153.
- Lewandowski J., Leitschuh S. and Koss V. (1997). Schadstoffe im Boden: eine Einfuehrung in Analytik und Bewertung. Heidelberg, Springer Verlag.
- Lin C.Y., Chou W.C., Tsai J.S. and Lin W.T. (2006) Water repellency of Casuarina windbreaks (*Casuarina equisetifolia* Forst.) caused by fungi in central Taiwan. *Ecological Engineering*, 26, 283-292.
- Litvina M., Todoruk T. and Langford C.H. (2003) Composition and structure of agents responsible for development of water repellency in soils following oil contamination. *Environmental Science and Technology*, 37, 2883-2888.
- Llewellyn C.T. (2004). Studies of the molecular basis of soil water repellency. Chemistry Department. Swansea, Univerisity of Wales Swansea. PhD: 205.
- Llewellyn C.T., Doerr S.H., Douglas P., Morley C.P. and Mainwaring K.A. (2004) Soxhlet extraction of organic compounds associated with soil water repellency. *Environmental Chemistry Letters*, 2, 41-44.
- Lösche M. (1997) Protein monolayers at interfaces. *Current Opinion in Solid State and Materials Science*, 2, 546-556.
- Ma'shum M. and Farmer V.C. (1985) Origin and assessment of water repellency of a sandy South Australian soil. *Australian Journal of Soil Research*, 23, 623-626.
- Ma'shum M., Tate M.E., Jones G.P. and Oades J.M. (1988) Extraction and characterisation of water-repellent materials from Australian soils. *Journal of Soil Science*, 39, 99-110.
- Mainwaring K.A. (2004). Chemical characterisation and repellency-inducing effects of organic compounds isolated from sandy soils. Department of Chemistry. Swansea, University of Wales Swansea. Ph.D.: 293.
- Mainwaring K.A., Morley C.P., Doerr S.H., Douglas P., Llewellyn C.T., Llewellyn G., Matthews I. and Stein B.K. (2004) Role of heavy polar organic compounds for water repellency of sandy soils. *Environmental Chemistry Letters*, 2, 35-39.
- Marmur A., Chen W. and Zografis G. (1985) Characterization of particle wettability by the measurement of floatability. *Journal of colloid and interface science*, 113, 114-120.
- Mataix-Solera J., Arcenegui V., Guerrero C., Mayoral A.M., Morales J., Gonzalez J., Garcia-Orenes F. and Gomez I. (2007) Water repellency under different plant species in a calcareous forest soil in a semiarid Mediterranean environment. *Hydrological Processes*, 21, 2300-2309.
- Mataix-Solera J. and Doerr S.H. (2004) Hydrophobicity and aggregate stability in calcareous topsoils from fire-affected pine forests in southeastern Spain. *Geoderma*, 118, 77-88.

- Maurice P.A. and Namjesnik-Dejanovic K. (1999) Aggregates structures of sorbed humic substances observed in aqueous solution. *Environmental Science & Technology*, 33, 1538-1541.
- McGhie D.A. and Posner A.M. (1980) Water repellence of heavy textured Western Australian surface soil. *Australian Journal of Soil Research*, 18, 309-323.
- McGhie D.A. and Posner A.M. (1981) The effect of plant top material on the water repellence of fired sands and water repellent soils. *Australian Journal of Agricultural Research*, 32, 609-620.
- McHale G., Newton M.I. and Shirtcliffe N.J. (2005) Water-repellent soil and its relationship to granularity, surface roughness and hydrophobicity: a materials science view. *European Journal of Soil Science*, 56, 445-452.
- McHale G., Shirtcliffe N.J., Newton M.I. and Pyatt F.B. (2007) Implications of ideas on super-hydrophobicity for water repellent soil. *Hydrological Processes*, 21, 2229-2238.
- McKissock I., Gilkes R.J. and van Bronswijk W. (2003) The relationship of soil water repellency to aliphatic C and kaolin measured using DRIFT. *Australian Journal of Soil Research*, 41, 251-265.
- Merziger G., Mühlbach G., Wille D. and Wirth T. (1996). *Formeln & Hilfen zur höheren Mathematik*. Hannover, Binomi.
- Minsky M. (1988) Memoir on inventing the confocal scanning microscope. *Scanning*, 10, 128-138.
- Miyamoto S. and Bird J.B. (1978) Effects of two wetting agents on germination and shoot growth of some southwestern range plants. *Journal of Range Management*, 31, 74-75.
- Miyata S., Kosugi K., Gomi T., Onda Y. and Mizuyama T. (2007) Surface runoff as affected by soil water repellency in a Japanese cypress forest. *Hydrological Processes*, 21, 2365-2376.
- Morley C.P., Mainwaring K.A., Doerr S.H., Douglas P., Llewellyn C.T. and Dekker L.W. (2005) Organic compounds at different depths in a sandy soil and their role in water repellency. *Australian Journal of Soil Research*, 43, 239-249.
- Namjesnik-Dejanovic K. and Maurice P.A. (1997) Atomic force microscopy of soil and stream fulvic acids. *Colloids and Surfaces a-Physicochemical and Engineering Aspects*, 120, 77-86.
- Namjesnik-Dejanovic K. and Maurice P.A. (2001) Conformations and aggregate structures of sorbed natural organic matter on muscovite and hematite. *Geochimica Et Cosmochimica Acta*, 65, 1047-1057.
- Noel O., Brogly M., Castelein G. and Schultz J. (2004) In situ estimation of the chemical and mechanical contributions in local adhesion force measurement with AFM: the specific case of polymers. *European Polymer Journal*, 40, 965-974.
- Onishi H. (1957) Photometric determination of thallium with rhodamine B. *Bull. Chem. Soc. Japan*, 30, 567-571.
- Pan B., Ghosh S. and Xing B. (2008). Dissolved organic matter conformation and its interaction with pyrene as affected by water chemistry and concentration. *Environ. Sci. Technol.*, 42, 1594-1599.
- Paredes J.I., Martínez-Alonso A. and Tascón J.M.D. (2003) Application of scanning tunneling and atomic force microscopies to the characterization of microporous and mesoporous materials. *Microporous and Mesoporous Materials*, 65, 93-126.
- Piccolo A. (2002) The supramolecular structure of humic substances: A novel understanding of humus chemistry and implications in soil science. *Advances in Agronomy*, 75, 57-134.

- Pierson F.B., Robichaud P.R., Moffet C.A., Spaeth K.E., Williams C.J., Hardegree S.P. and Clark P.E. (2008) Soil water repellency and infiltration in coarse-textured soils of burned and unburned sagebrush ecosystems. *Catena*, 74, 98-108.
- Preuss M. and Butt H.-J. (1998) Measuring the contact angle of individual colloidal particles. 208, 468-477.
- Regalado C.M. and Ritter A. (2009). A bimodal four-parameter lognormal linear model of soil water repellency persistence. *Hydrological Processes*, 23: 881-892.
- Richter L. and Vollhardt D. (2006) Force measuring methods for determination of surface tension of liquids: a comparison. *Physical Chemistry*, 43, 256-261.
- Riedel E. (1999). Allgemeine und anorganische Chemie. Berlin, Walter de Gruyter.
- Ritsema C.J. and Dekker L.W. (2000) Preferential flow in water repellent sandy soils: principles and modeling implications. *Journal of Hydrology*, 231-232, 308-319.
- Roberts F.J. and Carbon B.A. (1971) Water repellence in sandy soils of south-western Australia. I. Some studies related to field occurrence. *Field station record*, 10, 13-20.
- Roberts F.J. and Carbon B.A. (1972) Water repellence in sandy soils of south-western Australia. II. Some chemical characteristics of the hydrophobic skins. *Australian Journal of Soil Research*, 10, 35-42.
- Robichaud P.R. (2000) Fire effects on infiltration rates after prescribed fire in northern Rocky Mountain forests, USA. *Journal of Hydrology*, 231-232, 220-229.
- Robichaud P.R. and Hungerford R.D. (2000) Water repellency by laboratory burning of four northern Rocky Mountain forest soils. *Journal of Hydrology*, 231-232, 207-219.
- Rodriguez-Alleres M., Benito E. and de Blas E. (2007a) Extent and persistence of water repellency in north-western Spanish soils. *Hydrological Processes*, 21, 2291-2299.
- Rodriguez-Alleres M., de Blas E. and Benito E. (2007b) Estimation of soil water repellency of different particle size fractions in relation with carbon content by different methods. *Science of the Total Environment*, 378, 147-150.
- Roper M.M. (2004) The isolation and characterisation of bacteria with the potential to degrade waxes that cause water repellency in sandy soils. *Australian Journal of Soil Research*, 42, 427-434.
- Roper M.M. (2005) Managing soils to enhance the potential for bioremediation of water repellency. *Australian Journal of Soil Research*, 43, 803-810.
- Roper M.M. (2006) Potential for remediation of water repellent soils by inoculation with wax-degrading bacteria in south-western Australia. *Biologia*, 61, S358-S362.
- Rösler H.J. (1991). Lehrbuch der Mineralogie. Leipzig, Deutscher Verlag für Grundstoffindustrie.
- Roy J.L., McGill B. and Rawluk P. (1999) Petroleum residues as water-repellent substances in weathered nonwetable oil-contaminated soils. *Canadian Journal of Soil Science*, 79, 367-380.
- Roy J.L. and McGill W.B. (1998) Characterization of disaggregated nonwetable surface soils found at old crude oil spill sites. *Canadian Journal of soil science*, 80, 143-152.
- Roy J.L. and McGill W.B. (2000) Flexible conformation in organic matter coatings: an hypothesis about soil water repellency. *Canadian Journal of Soil Science*, 80, 143-152.
- Roy J.L. and McGill W.B. (2002) Assessing soil water repellency using the molarity of ethanol droplet (MED) test. *Soil Science*, 167, 83-97.

- Roy J.L., McGill W.B., Lowen H.A. and Johnson R.L. (2003) Relationship between water repellency and native and petroleum-derived organic carbon in soils. *Journal of Environmental Quality*, 32, 583-590.
- Savage S.M., Osborn J., Letey J. and Heaton C. (1972) Substances contributing to fire-induced water repellency in soils. *Soil Science Society of America Proceedings*, 36, 674-678.
- Scanlon B.R., Tyler S.W. and Wierenga P.J. (1997) Hydrologic issues in arid, unsaturated systems and implications for contaminant transport. *Reviews of Geophysics*, 35, 461-490.
- Schaumann G.E. (2006a) Soil organic matter beyond molecular structure. I. Macromolecular and supramolecular characteristics. *Journal of Plant Nutrition and Soil Science*, 169, 145-156.
- Schaumann G.E. (2006b) Soil organic matter beyond molecular structure. II. Amorphous nature and physical aging. *Journal of Plant Nutrition and Soil Science*, 169, 157-167.
- Schaumann G.E. and Bertmer M. (2008) Do water molecules bridge soil organic matter molecule segments? *European Journal of Soil Science*, 59, 423-429.
- Schaumann G.E., Braun B., Kirchner D., Rotard W., Szewzyk U. and Grohmann E. (2007) Influence of biofilms on the water repellency of urban soil samples. *Hydrological Processes*, 21, 2276-2284.
- Schaumann G.E., Hurraß J., Müller M. and Rotard W. (2004). Swelling of organic matter in soil and peat samples: insights from proton relaxation, water absorption and PAH extraction. *Humic Substances: Nature's Most Versatile Materials*. E. A. Ghabbour and G. Davies. New York, Taylor and Francis, Inc.: 101-117.
- Scheffer F. and Schachtschabel P. (2002). *Lehrbuch der Bodenkunde*. Heidelberg Berlin, Spektrum Akademischer Verlag.
- Scheludko A.D. and Nikolov A.D. (1975) Measurement of surface-tension by pulling a sphere from a liquid. *Colloid and Polymer Science*, 253, 396-403.
- Schlegel H.G. (1992). *Allgemeine Mikrobiologie*. Stuttgart, Georg Thieme Verlag.
- Schlichtling E., Blume H.P. and Stahr K. (1995). *Bodenkundliches Praktikum: eine Einführung in pedologisches Arbeiten für Ökologen, insbesondere Land- und Forstwirte und für Geowissenschaftler.*, Blackwell.
- Schwarz H.R. and Köckler N. (1986). *Numerische Mathematik*. Wiesbaden, B.G. Teubner Verlag/GWV Fachverlage GmbH.
- Schwuger M.J. (1996). *Lehrbuch der Grenzflächenchemie*. Stuttgart, Georg Thieme Verlag.
- Scott D.F. (2000) Soil wettability in forested catchments in South Africa; as measured by different methods and as affected by vegetation cover and soil characteristics. *Journal of Hydrology*, 231-232, 87-104.
- Shakesby R.A., Coelho C.O.A., Ferreira A.J.D., Terry J.P. and Walsh R.P.D. (1993) Wildfire impacts on soil erosion and hydrology in wet Mediterranean forest. *International Journal of Wildland Fire*, 9, 95-110.
- Shirtcliffe N.J., McHale G., Newton M.I., Chabrol G. and Perry C.C. (2004) Dual-scale roughness produces unusually water-repellent surfaces. *Advanced Materials*, 16, 1929-1932.
- Shirtcliffe N.J., McHale G., Pyatt F.B., Newton M.I. and Doerr S.H. (2006) Critical conditions for the wetting of soils. *Applied Physics Letters*, 89, article no. 094101.
- Slavik J. (1998). Single and multiple spectral parameter fluorescence microscopy. *Digital image analysis of microbes*. M. H. F. Wilkinson and F. Schut. Chichester, John Wiley & Sons Ltd: 93-114.

- Spaeth K.E., Pierson F.B., Robichaud P.R. and Moffet C.A. (2007) Hydrology, erosion, plant, and soil relationships after rangeland wildfire. *Proceedings: Shrubland Dynamics-Fire and Water*, 62-68.
- Steenhuis T.S., Hunt A.G., Parlange J. and Ewing R.P. (2005) Assessment of the application of percolation theory to a water repellent soil. *Australian Journal of Soil Research*, 43, 357-360
- Steenhuis T.S., Rivera J.C., Hernández C.J.M., Walter M.T., Bryant R.B. and Nektarios P. (2001) Water Repellency in New York State soils. *International Turfgrass Society Research Journal*, 9, 624-628.
- Sunderman H.D. (1983) Soil Wetting Agents. 4pp.
- Süsser P. and Schwertmann U. (1991) Proton buffering in mineral horizons of some acid forest soils. *Geoderma*, 49, 63-76.
- Taumer K., Stoffregen H. and Wessolek G. (2005) Determination of repellency distribution using soil organic matter and water content. *Geoderma*, 125, 107-115.
- Terashima M., Fukushima M. and Tanaka S. (2004) Influence of pH on the surface activity of humic acid: micelle-like aggregate formation and interfacial adsorption. *Colloids and Surfaces A: Physicochem. Eng*, 247, 77-83.
- Tillman R.W., Scotter D.R., Wallis M.G. and Clothier B.E. (1989) Water repellency and its measurement by using intrinsic sorptivity. *Australian Journal of Soil Research*, 27, 637-644.
- Todoruk T., Litvina M., Kantzas A. and Langford C.H. (2003) Low-field NMR relaxometry: a study of interactions of water with water-repellant soils. *Environmental Science and Technology*, 37, 2878-2882.
- Tschapek M. (1984) Criteria for determining the hydrophilicity - hydrophobicity of soils. *Zeitschrift für Pflanzenernährung und Bodenkunde*, 147, 137-149.
- Urbanek E., Hallett P., Feeney D. and Horn R. (2007) Water repellency and distribution of hydrophilic and hydrophobic compounds in soil aggregates from different tillage systems. *Geoderma*, 140, 147-155.
- van't Woudt B.D. (1959) Particle coatings affecting the wettability of soils. *Journal of Geophysical Research*, 64, 263-267.
- Van Aman R.E., Hollibaugh F.D. and Kanzelmeyer J.H. (1959) Spectrophotometric determination of antimony with rhodamine B. *Anal. Chem.*, 31, 1783-1785.
- Van Dam J.C., Hendrickx J.M.H., Van Ommen H.C., Bannink M.H., Van Genuchten M.T. and Dekker L.W. (1990) Water and solute movement in a coarse-textured water-repellent field soil. *Journal of Hydrology*, 120, 359-379.
- Varela M.E., Benito E. and de Blas E. (2005) Impact of wildfires on surface water repellency in soils of northwest Spain. *Hydrological Processes*, 19, 3649-3657.
- Verheijen F.G.A. and Cammeraat L.H. (2007) The association between three dominant shrub species and water repellent soils along a range of soil moisture contents in semi-arid Spain. *Hydrological Processes*, 21, 2310-2316.
- Vogler E.A. (1998) Structure and reactivity of water at biomaterial surfaces. *Advances in Colloid and Interface Science*, 74, 69-117.
- von Wandruszka R. (1998) The micellar model of humic acid: evidence from pyrene fluorescence measurements. *Soil Science*, 163, 921-930.
- Wallach R., Ben-Arie O. and Graber E.R. (2005) Soil water repellency induced by long-term irrigation with treated sewage effluent. *Journal of Environmental Quality*, 34, 1910-1920.
- Wallis M.G. and Horne D.J. (1992) Soil water repellency. *Advances in Soil Science*, 20, 91-146.

- Wallis M.G., Horne D.J. and McAuliffe K.W. (1990) A study of water repellency and its amelioration in a yellow-brown sand. 1. Severity of water repellency and the effects of wetting and abrasion. *New Zealand journal of agricultural research*, 33, 139-144.
- Wang Z., Wu Q.J., Wu L., Ritsema C.J., Dekker L.W. and Feyen J. (2000) Effects of soil water repellency on infiltration rate and flow instability. *Journal of Hydrology*, 231-232, 265-276.
- Ward P.R. and Oades J.M. (1993) Effect of clay mineralogy and exchangeable cations on water-repellency in clay-amended sandy soils. *Australian Journal of Soil Research*, 31, 351-364.
- Wenzel R.N. (1949) Surface roughness and contact angle. *Journal of Physical and Colloid Chemistry*, 53, 1466-7.
- White N.A., Hallett P.D., Feeney D., Palfreyman J.W. and Ritz K. (2000) Changes to water repellence of soil caused by the growth of whit-rot fungi: studies using a novel microcosm system. *FEMS Microbiology Letters*, 184, 73-77.
- Wild A. (1993). Soils and the environment: an introduction. Cambridge, UK, Cambridge University Press.
- Wilkinson K.J., Balnois E., Leppard G.G. and Buffle J. (1999) Characteristic features of the major components of freshwater colloidal organic matter revealed by transmission electron and atomic force microscopy. *Colloids and Surfaces A: Physicochemical and Engineering Aspects*, 155, 287-310.
- Wilkinson M.H.F. (1998). Optical systems for image analysed microscopy. Digital image analysis of microbes. M. H. F. Wilkinson and F. Schut. Chichester, John Wiley & Sons Ltd: 65-91.
- Wilson T. (1993). Image formation in confocal microscopy. Electronic light microscopy. D. Shotton. New York, Wiley-Liss: 231-246.
- Witter J.V., Jungerius P.D. and ten Harkel M.J. (1991) Modelling water erosion and the impact of water repellency. *Catena*, 18, 115-124.
- Woche S.K., Goebel M.O., Kirkham M.B., Horton R., Van der Ploeg R.R. and Bachmann J. (2005) Contact angle of soils as affected by depth, texture, and land management. *European Journal of Soil Science*, 56, 239-251.
- Wolf G. (1997). Neuromorphologie. Methoden der Hirnforschung: Eine Einführung. U. Kischka, C.-W. Wallesch and G. Wolf. Heidelberg Berlin, Spektrum Akademischer Verlag GmbH: 1-19.
- York C.A. and Canaway P.M. (2000) Water repellent soils as they occur on UK golf greens. *Journal of Hydrology*, 231-232, 126-133.
- Young T. (1855). Miscellaneous Works of the Late Thomas Young. London, Murray.
- Zavala L.M., González F.A. and Jordán A. (2009) Intensity and persistence of water repellency in relation to vegetation types and soil parameters in Mediterranean SW Spain. *Geoderma*, 152, 361-374.
- Zettlemoyer A.C., Micale F.J. and Klier K. (1975). Adsorption of Water on Well-Characterized Solid Surfaces. Water in Disperse Systems. F. Franks. New York, Plenum Press. 5: 249-289.
- Zhang L., Ren L. and Hartland S. (1996) More convenient and suitable methods for sphere tensiometry. *Journal of Colloid and Interface Science*, 493-503.
- Zhang L., Ren L. and Hartland S. (1997) Detailed analysis of determination of contact angle using sphere tensiometry. *Journal of Colloid and Interface Science*, 192, 306-318.

- Zhu G., Zhu Z. and Qui L. (2002) A fluorimetric method for the determination of iron(II) with fluorescein isothiocyanate and iodine. *Analytic Sciences*, 18, 1059-1061.
- Ziogas A.K., Dekker L.W., Oostindie K. and Ritsema C.J. (2005) Soil water repellency in north-eastern Greece with adverse effects of drying on the persistence. *Australian Journal of Soil Research*, 43, 281-289
- Zisman W.A. (1964) Relation of equilibrium contact angle to liquid and solid constitution: contact angle, wettability and adhesion. *Advances in Chemistry Series*, 43, 1-51.

A Appendix to chapter 3

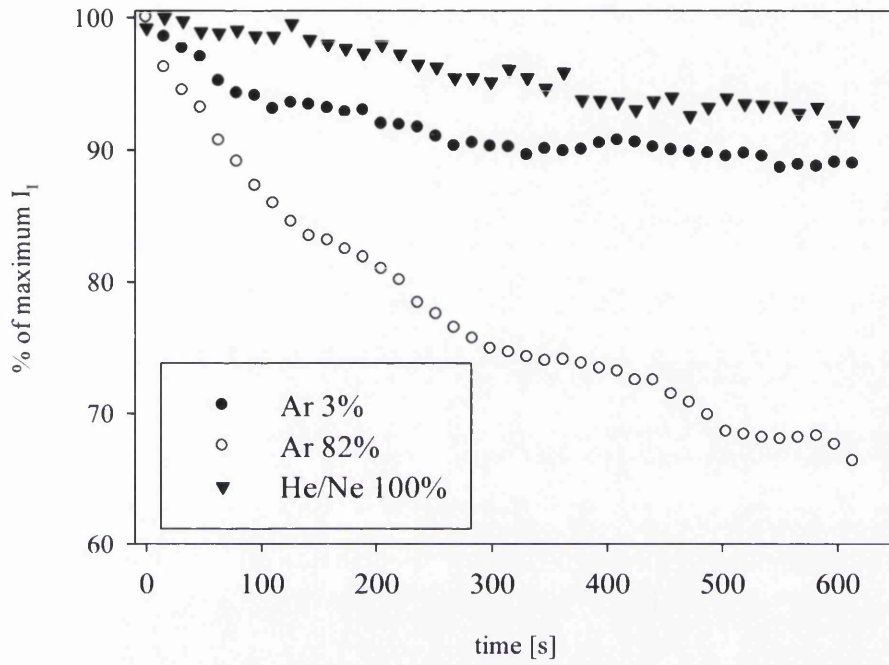


Figure A-1: Proportion [%] of the maximum fluorescence of one focal plane over 10 minutes for a lecithin coated sand particle, imaged with different laser settings.

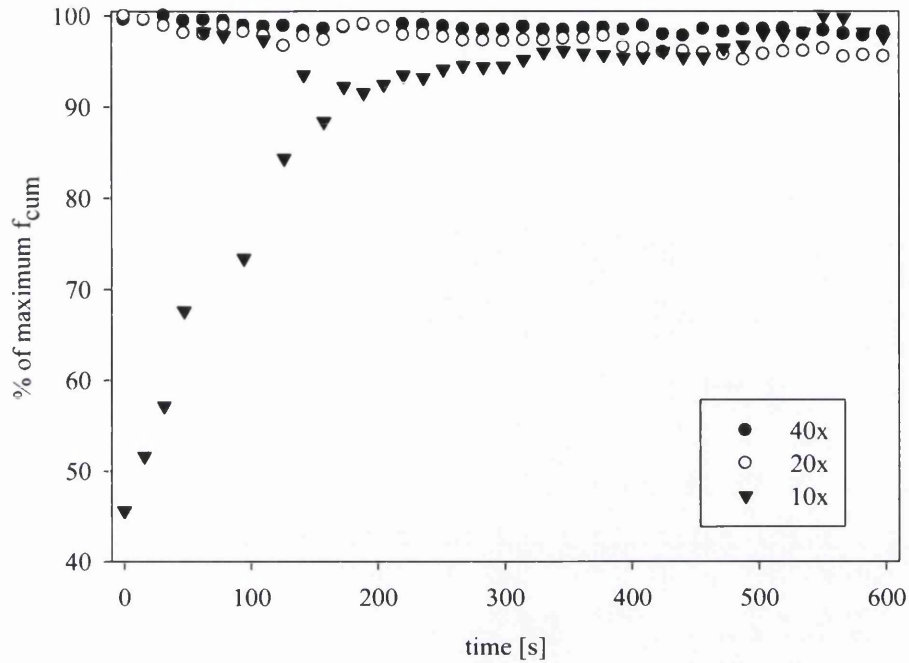


Figure A-2: Proportion [%] of f_{cum} as a function of time for a particle from soil sample NL2, irradiation with He/Ne-laser at 100 %, various objective lenses.

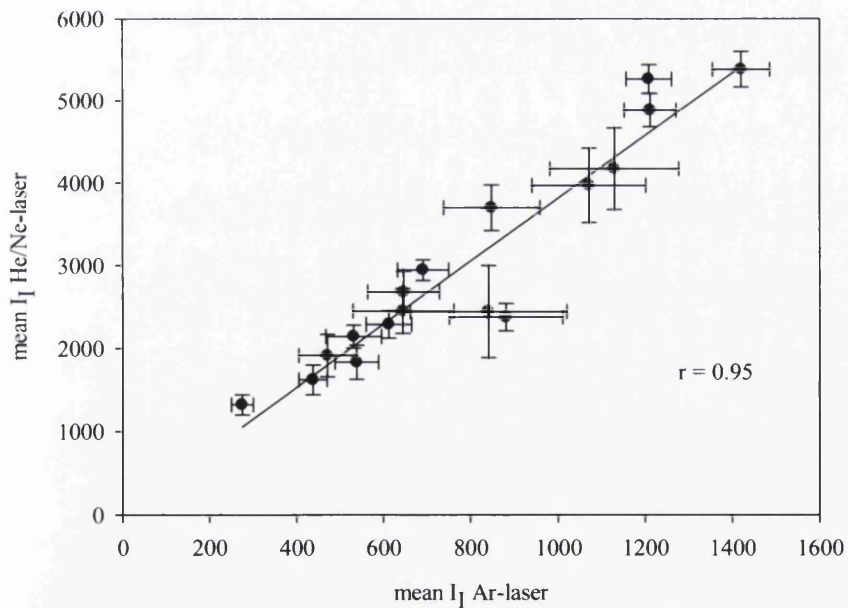


Figure A-3: Mean I_1 of all soil samples (multi-particle specimens) measured by He/Ne-laser vs. Ar-laser.

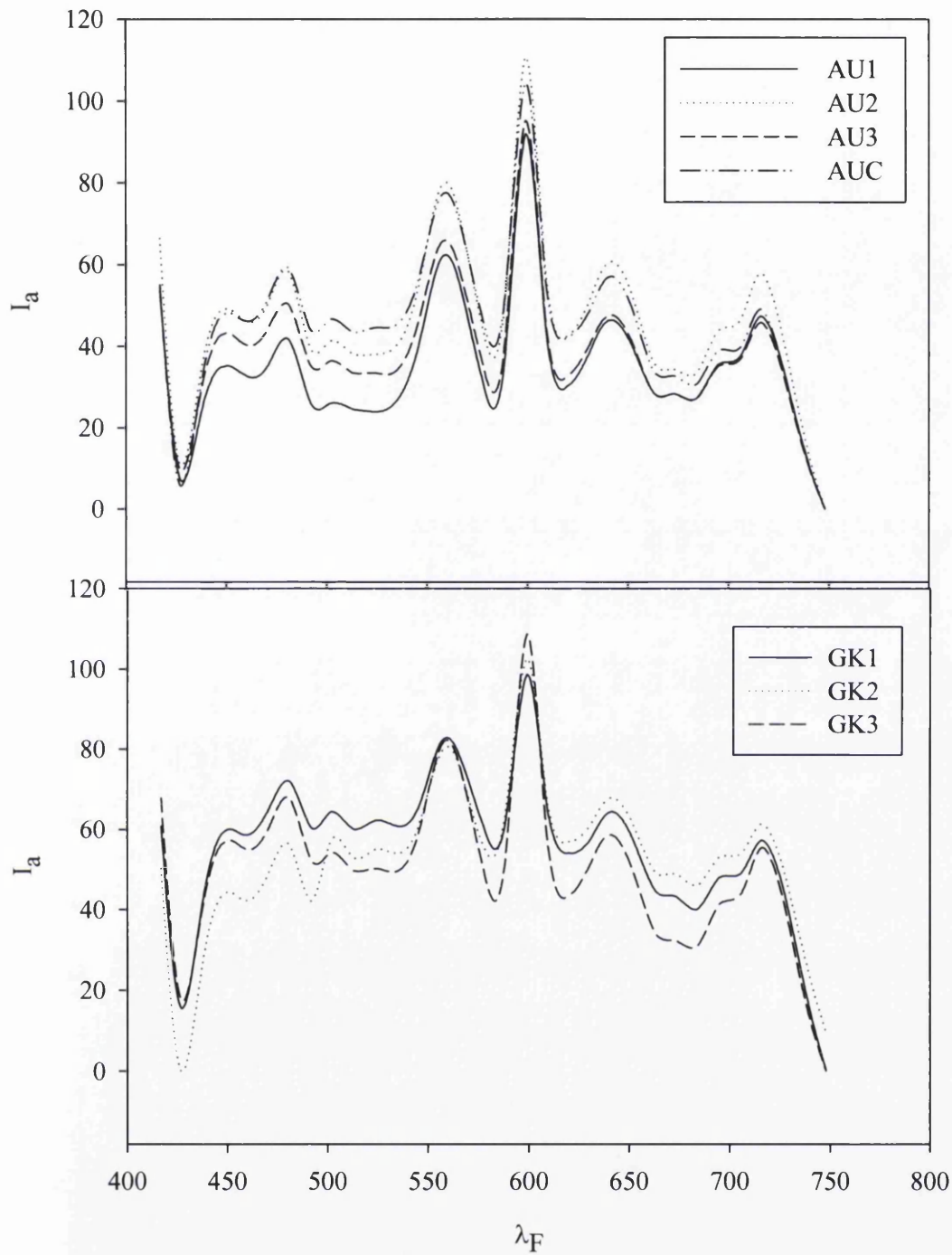


Figure A-4: Baseline normalized emission spectra average of five particles from AU and GL samples imaged with LSM meta-mode.

Table A_1: TOC and wettability measures (CA and WDPT) of bulk soil samples, mean fluorescence measures (I_I , C_F , N_F , a_F) of individual particles and multi-particle specimens.

	TOC [g kg ⁻¹]	CA [°]	WDPT [s]	single mean I_I Ar-laser	single mean He/Ne-laser	C_F [%]	N_F	a_F	Multi- specimen I_I Ar-laser	Multi- specimen I_I He/Ne-laser
AU1	11.7	93	160	355 ± 27	919 ± 90	7.0 ± 1.3	507.1 ± 42.1	1.3 ± 0.1	1129 ± 148	4168 ± 494
AU2	14.4	81	0	430 ± 39	1070 ± 93	5.8 ± 1.0	809.1 ± 126.1	1.7 ± 0.1	1211 ± 59	4880 ± 200
AUC	2.2	107	800	337 ± 42	889 ± 86	5.3 ± 1.4	468.6 ± 53.0	1.7 ± 0.2	690 ± 59	2943 ± 124
GK1	10.4	85	40	559 ± 59	1821 ± 148	n.d.	n.d.	n.d.	1208 ± 52	5260 ± 172
GK2	21.2	95	140	571 ± 45	1576 ± 105	n.d.	n.d.	n.d.	848 ± 110	3696 ± 276
GK3	1.6	72	0	268 ± 41	872 ± 103	n.d.	n.d.	n.d.	531 ± 64	2142 ± 137
NL1	36.2	107	4800	754 ± 113	1570 ± 155	14.0 ± 3.3	346.2 ± 44.8	2.4 ± 0.3	881 ± 129	2374 ± 164
NL2	5.9	102	2400	507 ± 47	1344 ± 92	7.6 ± 2.2	955.6 ± 153.4	1.5 ± 0.1	841 ± 179	2440 ± 555
NL3	0.8	97	470	363 ± 61	935 ± 119	n.d.	n.d.	n.d.	538 ± 50	1831 ± 204
NLC	0	82	< 5	335 ± 21	897 ± 58	0.5 ± 0.08	843.0 ± 92.2	1.9 ± 0.2	437 ± 32	1621 ± 177
PT1	6.3	63	0	724 ± 44	2122 ± 162	15.2 ± 3.8	351.9 ± 72.7	2.7 ± 0.1	646 ± 82	2678 ± 249
PT2	10.3	101	250	874 ± 66	2336 ± 138	11.4 ± 2.6	538.6 ± 81.6	2.1 ± 0.2	1420 ± 65	5378 ± 216
PT3	0.6	73	0	442 ± 55	1568 ± 152	n.d.	n.d.	n.d.	645 ± 116	2450 ± 269
PTC	0.1	60	0	432 ± 29	1702 ± 130	3.0 ± 0.8	271.2 ± 90.3	1.7 ± 0.2	470 ± 66	1913 ± 257
UK1	11.4	105	> 18000	576 ± 47	1909 ± 123	3.7 ± 1.0	507.1 ± 81.7	1.8 ± 0.3	1071 ± 131	3966 ± 451
UK2	7.8	81	30	557 ± 51	1756 ± 117	14.6 ± 2.9	809.1 ± 126.4	1.9 ± 0.2	612 ± 52	2286 ± 167
UKC	3.1	30	0	423 ± 49	1668 ± 150	3.3 ± 0.6	468.6 ± 100.3	1.8 ± 0.2	275 ± 25	1321 ± 120

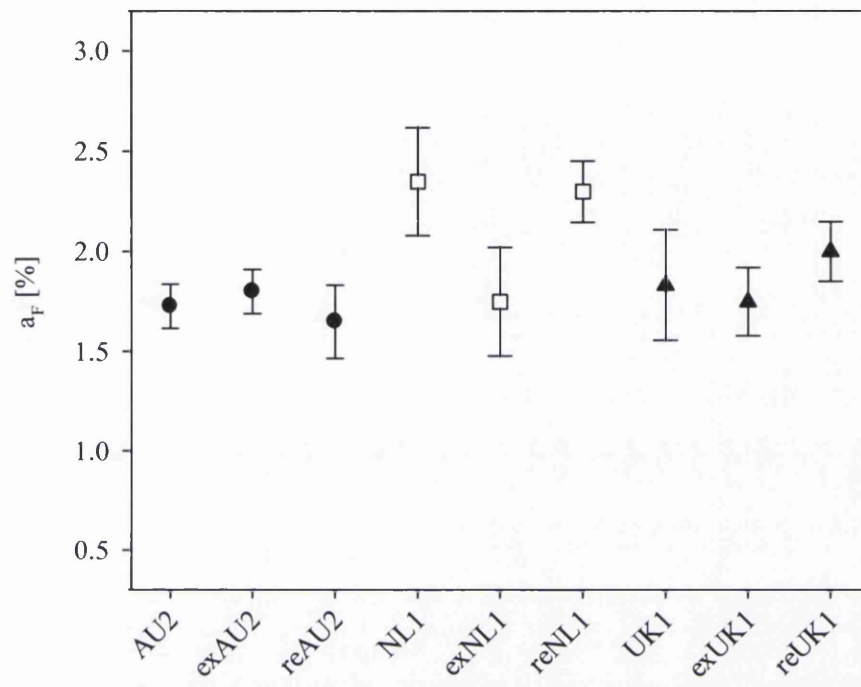


Figure A-5: a_F of original, extracted and re-applied AU2, NL1 and UK samples. Error bars represent the standard error.

Table A. 2: Fluorescence measures C_F , N_F , I_F of individual particles from samples AU1, AU2, AUC, NL1, NL2, NLC, PT1, PT2, PTC, UK1, UK2, UKC.

	C_F	N_F	a_F	$I_{Ar-laser}$	C_F	N_F	a_F	$I_{Ar-laser}$	C_F	N_F	a_F	$I_{Ar-laser}$	C_F	N_F	a_F	$I_{Ar-laser}$			
AU1	2.0	291.0	1.0	621.2	NL1	18.4	391.0	3.0	1554.1	PT1	10.1	1140.0	2.5	643.1	UK1	9.9	847.0	3.0	705.6
	5.8	288.0	1.5	407.8		4.2	461.0	1.5	813.1		10.4	755.0	2.5	638.8		2.7	482.0	3.0	525.6
	14.6	396.0	2.0	271.5		38.7	342.0	3.0	2169.6		7.1	515.0	2.5	759.3		2.3	768.0	1.5	545.7
	12.1	458.0	1.0	269.2		16.5	542.0	2.5	1174.9		14.2	590.0	2.5	n.d.		1.9	797.0	2.0	n.d.
	6.3	431.0	1.5	278.4		8.7	445.0	2.5	550.7		36.3	699.0	3.0	n.d.		2.2	264.0	1.5	681.0
	11.0	237.0	1.5	252.0		4.1	76.0	1.0	195.0		12.2	980.0	3.0	1043.4		0.5	308.0	1.0	401.7
	6.9	411.0	1.0	433.3		18.7	190.0	3.0	234.7		3.0	731.0	2.5	854.1		6.1	193.0	2.5	351.9
	4.5	257.0	1.0	302.9		6.9	302.0	1.0	370.1		10.5	498.0	3.0	770.9		5.3	521.0	1.0	502.2
	2.2	145.0	1.0	362.4		14.7	262.0	3.0	421.3		32.7	558.0	3.0	2299.5		2.5	384.0	1.0	370.0
	4.5	605.0	1.5	386.7		8.7	451.0	3.0	319.4										
AU2	6.3	196.0	1.5	337.4	NL2	1.5	1523.0	1.5	716.8	PT2	9.4	872.0	1.5	619.2	UK2	3.1	865.0	1.0	580.8
	8.0	586.0	2.0	n.d.		1.0	1410.0	1.5	404.0		13.7	783.0	1.0	869.4		1.1	150.0	1.0	174.9
	11.3	375.0	1.5	368.0		5.0	421.0	1.5	213.1		31.1	807.0	3.0	884.1		11.3	875.0	1.5	267.8
	10.0	1659.0	2.0	n.d.		3.4	1574.0	2.0	515.4		12.9	880.0	2.5	793.8		7.3	1071.0	1.5	351.0
	6.8	338.0	2.0	594.0		1.9	346.0	1.5	289.4		11.8	853.0	2.0	649.1		9.9	282.0	2.5	307.8
	7.1	368.0	2.0	341.8		15.0	957.0	1.5	402.5		12.3	1015.0	2.0	526.1		26.6	692.0	2.5	563.7
	4.1	255.0	1.0	237.5		15.8	678.0	1.5	391.6		2.0	534.0	2.0	526.1		20.2	786.0	2.5	737.1
	3.1	159.0	1.5	161.3		16.7	955.0	1.5	658.0		3.2	330.0	2.0			23.6	1105.0	1.5	697.9
	3.1	743.0	1.5	345.4		7.9	736.0	1.0	320.0		12.7	1297.0	2.0			18.3	721.0	2.5	641.1
	2.0	512.0	2.5	292.9							5.2	769.0	3.0			25.0	1544.0	2.5	n.d.
1.9	391.0	1.5	357.2																
AUC	6.3	470.0	1.5	535.1	NLC	0.4	1320.0	1.5	382.5	PTC	1.4	924.0	1.5	n.d.	UKC	4.8	229.0	1.5	763.7
	2.1	282.0	1.5	381.9		0.2	1025.0	1.5	368.9		2.4	279.0	1.5	425.0		5.7	137.0	1.5	427.9
	3.5	240.0	1.5	304.3		0.2	801.0	2.5	321.3		0.1	229.0	2.0	284.1		4.4	699.0	2.0	353.0
	10.2	154.0	2.0	276.9		0.7	619.0	1.5	291.6		10.0	653.0	1.5	606.3		2.1	276.0	2.5	282.1
	5.2	217.0	1.5	186.4		0.5	890.0	1.5	410.5		1.9	128.0	1.0	204.0		1.1	258.0	2.0	285.7
	2.4	203.0	1.5	242.2		0.8	1163.0	1.0	576.6		4.0	668.0	2.5	623.1		3.3	1073.0	2.0	298.7
	2.2	95.0	1.0	155.4		0.3	440.0	1.5	275.5		2.3	122.0	1.5	382.7		1.3	632.0	2.5	610.3
	13.8	189.0	3.0	n.d.		0.5	575.0	3.0	469.4		3.6	474.0	1.5	463.8		5.8	444.0	1.5	397.8
	1.6	591.0	1.5	584.1		1.0	564.0	2.5	447.9		2.3	694.0	1.0	446.0		1.4	144.0	1.0	233.1
						0.6	1033.0	2.0	594.4		2.3	180.0	3.0	364.9		3.6	794.0	1.0	316.6

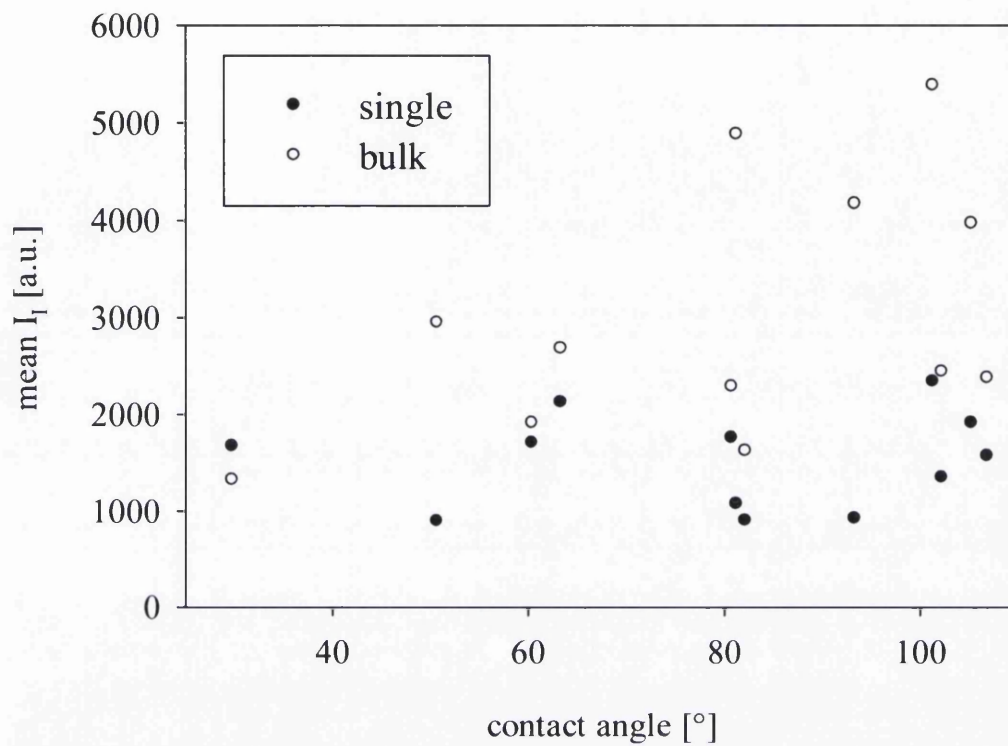


Figure A-6: Mean I_1 of single particle images vs CA; various samples, He/Ne-laser.

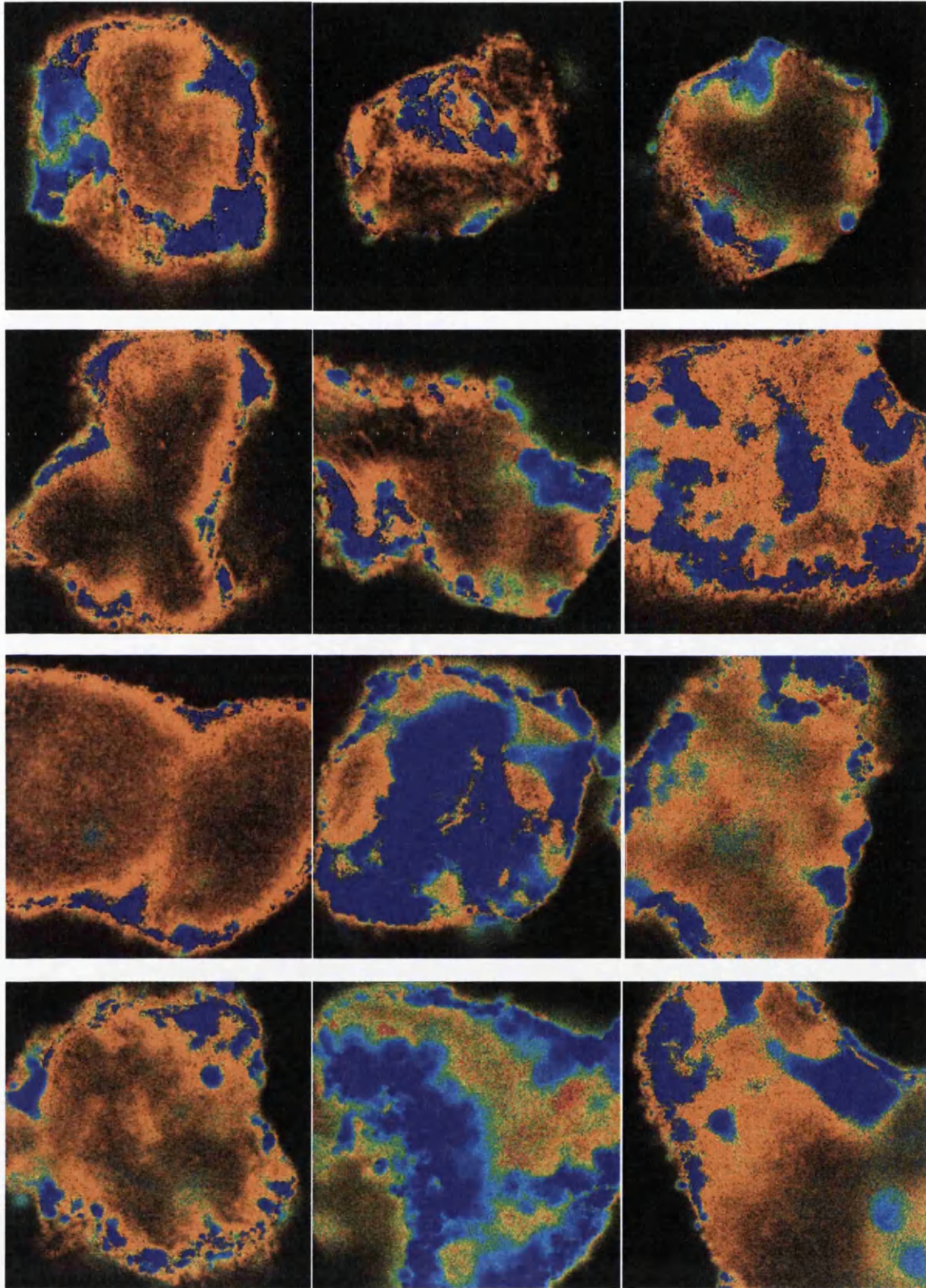


Figure A-7: Colour coded overlays of wavelength distributions. First row: NL1, NL2, NL3, second row: NLC, UK1, UK2, third row: UKC, GK1, GK2, fourth row: GKC, PT1, PT2.

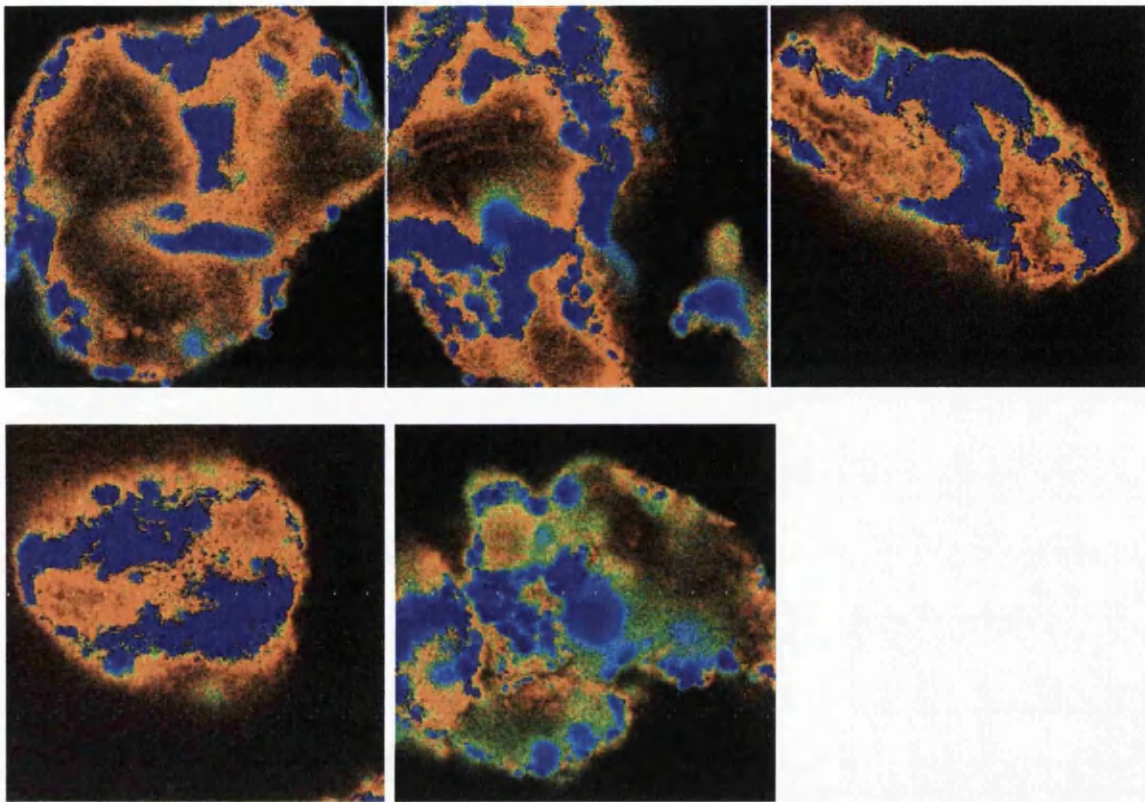


Figure A-8: Colour coded overlays of wavelength distributions. First row: PT3, PTC, AU1, second row: AU2, AU3.

B Appendix to chapter 4

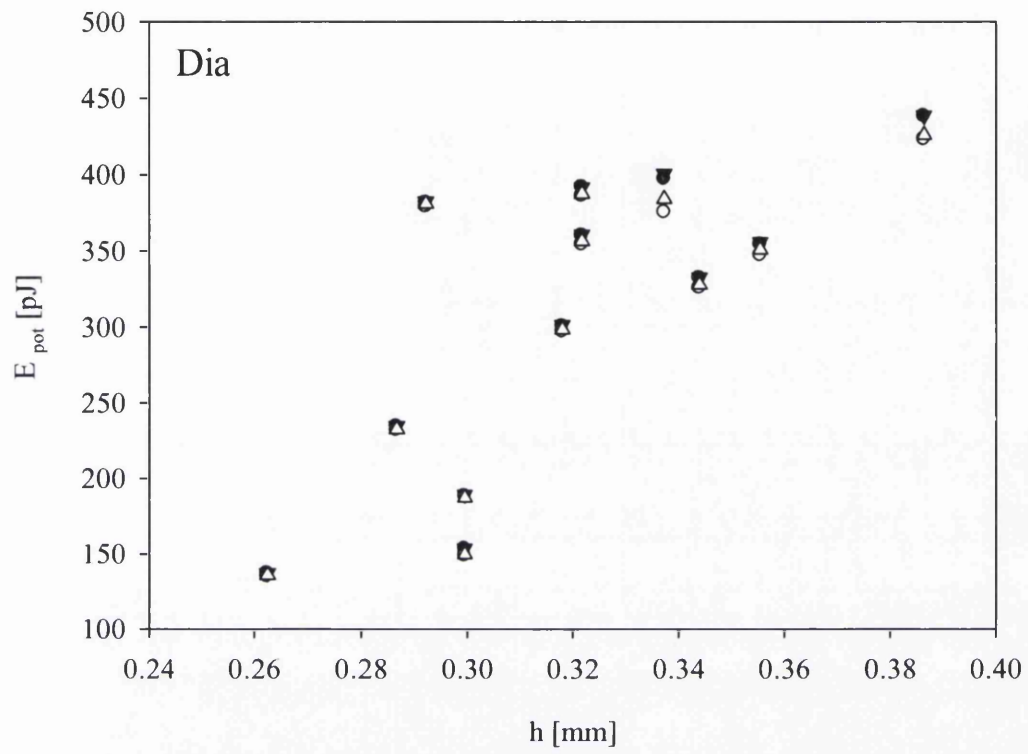


Figure B-1: Mean E_{pot} vs h of sample DIA.

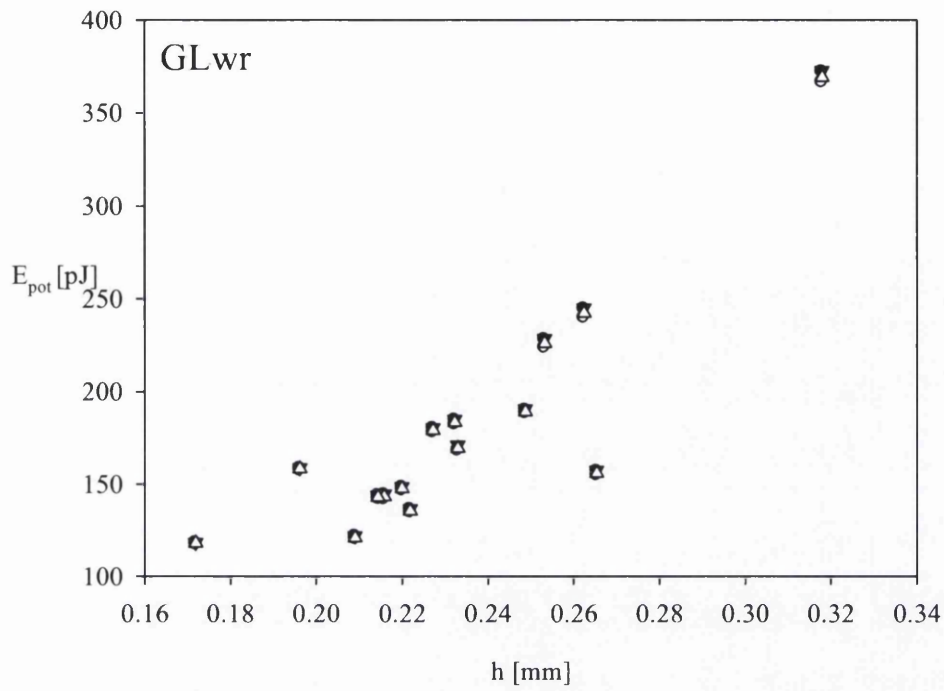


Figure B-2: Mean E_{pot} vs h of sample GLwr.

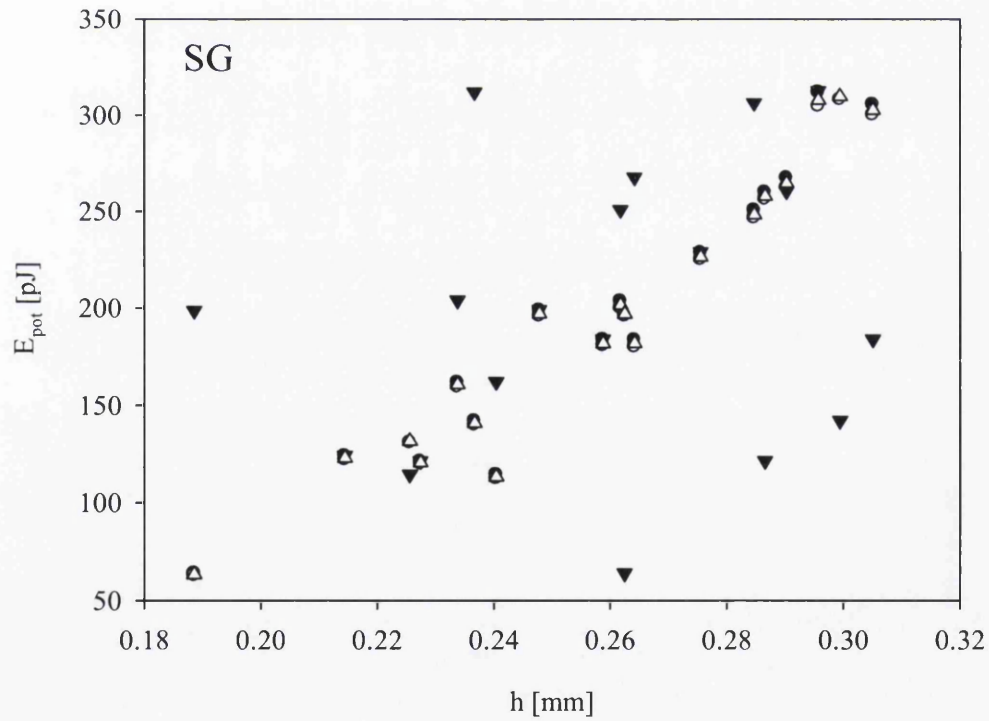


Figure B-3: Mean E_{pot} vs h of sample SG.

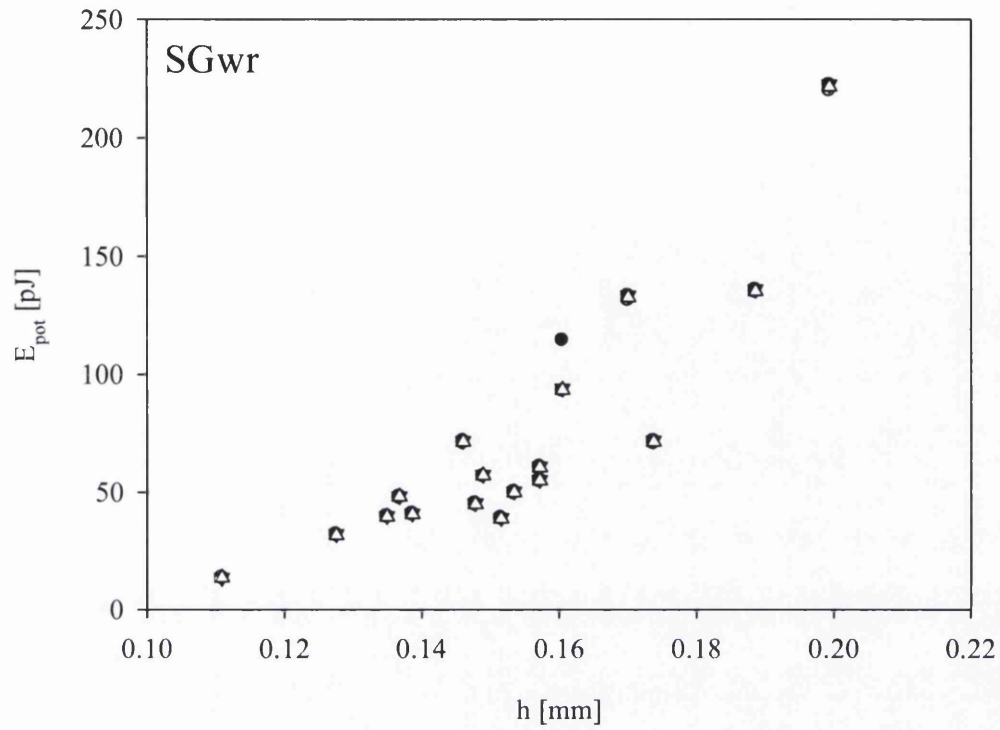


Figure B-4: Mean E_{pot} vs h of sample SGwr.

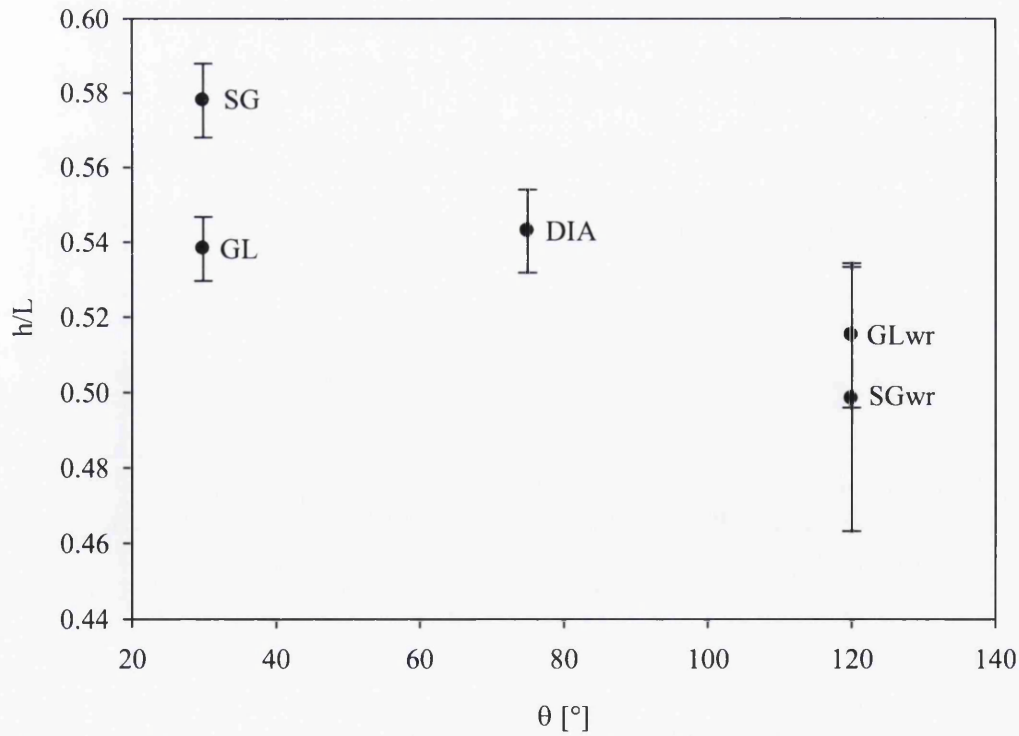


Figure B-5: h/L of individual particles vs θ of the material on a flat surface; measured by o-mWPM.

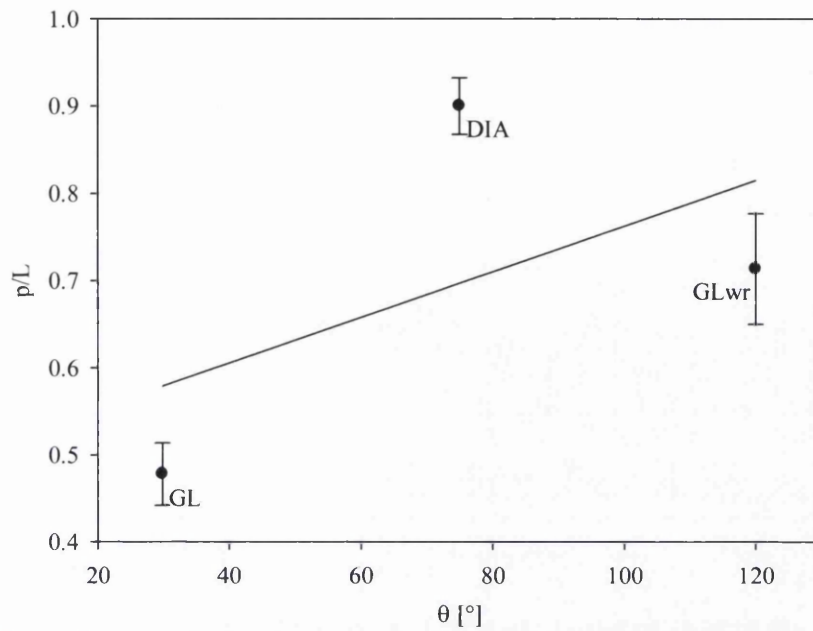


Figure B-6: p/L of individual particles vs θ of the material on a flat surface; measured by g-mWPM.

Table B-1: Mean h of lamella height measurement repetitions of sample UK1 (5 repetitions per sample), standard deviation σ in mm and %.

	mean h [mm]	σ [mm]	σ [%]
A	0.37	0.00	1.22
B	0.36	0.01	2.66
C	0.36	0.00	0.93
D	0.18	0.01	6.81
E	0.19	0.01	6.81
F	0.21	0.00	2.17

1 Reaction of soil water repellency on artificially induced changes in soil pH

2 D. DIEHL¹, J.V. BAYER^{1,2}, S.K. WOCHÉ³, R. BRYANT², S.H. DOERR⁴, G. E. SCHAUMANN¹

3 ¹Universität Koblenz-Landau. Institute for Environmental Sciences, Department of Environmental
4 and Soil Chemistry, Fortstr. 7, D-76829 Landau, Germany

5 ²School of Engineering, Swansea University, Singleton Park, Swansea SA2 8PP, UK

6 ³Universität Hannover. Institut of Soil Sciences. Herrenhäuser Straße 2. 30419 Hannover

7 ⁴School of Environment and Society, Swansea University, Singleton Park, Swansea SA2 8PP, UK.

8 Correspondence: Dörte Diehl. E-mail: diehl@uni-landau.de.

9

10 Abstract

11 Few studies have systematically investigated the relationship between soil water repellency (SWR)
12 and soil *pH*. The hypothesis that the *pH* may control repellency via changes in the variable surface
13 charge of soil material has not yet been tested. Previously it has been shown that it is necessary to
14 eliminate the direct influence of changes in soil moisture content so that the unique relationship
15 between *pH* and SWR can be isolated.

16 A method has been developed which allows adjustment of the *pH* of soils with low moisture
17 content via the gas phase with minimal change in moisture content. The method was applied to 14 soil
18 samples from Germany, Netherlands, the UK and Australia, using the water drop penetration time
19 (*WDPT*) as the indicator of SWR. Sessile drop and Wilhelmy plate contact angles (Θ_{sess} and Θ_{WPM}
20 resp.) were measured on the four samples from Germany and the data correlated with those of *WDPT*.
21 The titratable surface charge of these four soils was measured at selected *pH* values using a particle
22 charge detector (PCD).

23 The comparison of repellency determination by *WDPT*, Θ_{sess} and Θ_{WPM} highlights the advantages
24 and constrains of each individual method.

25 Changes in SWR with soil *pH* were found to be influenced by the density and type of sites able to
26 interact with protons at the available surfaces of organic and mineral materials in soil. The maximum
27 SWR occurred for soil at natural *pH* and where the charge density was minimal. As *pH* increased,
28 negative surface charge increased due to deprotonation of sites and *WDPT* decreased. Two types of
29 behaviour were observed: Those in which (i) *WDPT* shortened with decreasing *pH* and ii) *WDPT* was
30 sensibly constant with decreasing *pH*. The data suggest that the availability and relative abundance of
31 proton active sites at mineral surfaces, and those at organic functional groups influence the behaviour.

32 Keywords:

33 Soil water repellency, *pH*, surface charge

34 Introduction

35 Soil water repellency (SWR) is a world wide phenomenon leading to uneven water distribution in
36 soils, preferential flow and enhanced surface runoff, which in turn may result in a lack of water to
37 support plant growth, accelerated leaching and transport of surface nutrients and contaminants toward
38 groundwater, top soil degradation and erosion. The causes and mechanisms affecting SWR are many
39 fold and not fully understood. Soil wettability was observed to improve following addition of lime,
40 kaolinite clay, ammonia and sodium hydroxide solution (Karnok et al., 1993; Roper, 2005; van't
41 Woudt, 1959) This led to the general acceptance that, among others, soil *pH* influences SWR (Wallis
42 and Horne, 1992). Roberts & Carbon (1971) found that water repellent sandy soils from south-western
43 Australia were more likely to have a lower *pH* than wettable soils. Similar trends were reported for
44 3000 garden and agricultural samples from New York State by Steenhuis et al. (2001) for 66 samples
45 from calcareous forest soils with a generally very narrow range of *pH* (Mataix-Solera et al., 2007) and
46 for soils from ants' nests (Cammeraat et al., 2002). Hurrass & Schaumann (2006) observed that, from
47 a batch of 46 soil samples from an inner city park "Tiergarten" in Berlin, repellency was only detected
48 in those with *pH* below 4.5. However, they did not find any correlation between *pH* and water
49 repellency of samples drawn from a former sewage disposal field in Berlin.

50 Several mechanisms for the *pH* – SWR relationship have been proposed:

51 *I) Changes in the surface charge of organic material:* The hydrophobicity of humic acids (HA) was
52 observed to increase with decreasing *pH* in the ranges $8 < \text{pH} < 11$, caused by protonation of phenolic
53 groups (Duval et al., 2005; MacCarthy et al., 1979) and $4 < \text{pH} < 7$ by protonation of carboxylic

54 groups (Terashima *et al.*, 2004). In these ranges this results in a reduction of negative surface charge
55 which in turn leads to a less polar and, therefore, less wettable surface. Holmes-Farley *et al.* (1985)
56 observed the same *pH* effect on sessile drop contact angle (Θ_{sess}) at a polymer surface (PE) with
57 covalently attached carboxylic acid groups. The same mechanisms could be responsible for a decrease
58 of soil water repellency as observed in field studies after increasing the *pH* via lime addition (Roper,
59 2005; van't Woudt, 1959) or the application of 0.1 M NaOH to repellent soils (Karnok *et al.*, 1993). A
60 further decrease in *pH* may lead to positive charge, e.g. by protonation of amine groups. On
61 heptylamine plasma polymer surfaces this leads to an increasing wettability of the material (Chatelier
62 *et al.*, 1997).

63 *II) Conformational changes in the organic matter:* HA are not completely hydrophobic, but have
64 amphiphilic character, and can render a soil water repellent when orienting the non-polar groups
65 towards the pore space (Tschapek, 1984). Changes in *pH* may result in the rearrangement of moieties,
66 fragments or entire molecules of SOM, which may influence their hydrophobicity (Duval *et al.*, 2005;
67 Ohashi and Nakazawa, 1996; Terashima *et al.*, 2004). Deo *et al* (2005) observed, that at low *pH*,
68 carboxylic groups on organic macromolecules with hydrophobic side chains, were orientated toward
69 the bulk water, protecting the hydrophobic groups by encasing them in the inner part of coiled
70 macromolecules. As *pH* increased and carboxylic groups were deprotonated, electrostatic repulsion
71 was considered responsible for the observed swelling, loosening and/or chain expansion of
72 hydrophobic nano-domains leading to an increased outward orientation of hydrophobic groups.
73 Similar mechanisms were also suggested for water repellent soils (Ma'shum and Farmer, 1985; Valat
74 *et al.*, 1991). A decrease in *pH* from 7 to 5 was found to facilitate a membrane-like aggregation of HA
75 on mineral surfaces by hemimicelle or admicelle-like formations with increasing hydrophobicity of
76 HA (Terashima *et al.*, 2004). This was caused by protonation of carboxylic and phenolic groups
77 leading to a reduction in repulsion forces between these moieties (Ohashi and Nakazawa, 1996) and to
78 the formation of H-bridges and a more compact structure of HA with a maximum compaction around
79 the pK_a of carboxylic sites.

80 *III) Leaching of fulvic acid (FA)s:* The relatively high solubility of FA at low *pH*, in comparison with
81 those of HA, provide opportunities for preferential dissolution and transport that do not arise at higher
82 *pH* (>7). These high solubilities reflect a wettable character to FA so the quantities of FA and HA, and
83 their relative abundances, may influence SWR (Babejova, 2001; Chen and Schnitzer, 1978; Tschapek,
84 1984); high FA/HA may confer wettability and low FA/HA may lead to SWR. Generally, the addition
85 of HA to soil samples has been shown to increase their water repellency, and stable humic acid
86 complexes were identified as an important contribution to water repellency in some sandy soils
87 (Roberts and Carbon, 1972). The contact angle of FA and HA extracts was found to be the inversely
88 related to their *pH*, indicating that *pH* might be an indicator for the hydrophobic potential of these
89 materials (Lin *et al.*, 2006).

90 *IV) Changes in bacterial and fungal communities:* Fungal exudates could be an agent for local *pH*
91 reduction. This could lead to polymerization and/or precipitation of FA and HA and, therefore, be
92 responsible for the resulting SWR observed in areas of high fungal activity (Lin *et al.*, 2006). Liming
93 may increase soil wettability not only by increasing its *pH* directly, but also by promoting microbial
94 activity of wax degrading bacteria (Roper, 2005). However, some studies (Bayer and Schaumann,
95 2007; Hurraß and Schaumann, 2006) did not find increased fungal growth within water repellent areas
96 of soil.

97 Few studies have systematically investigated the influence of *pH* changes on soil sample wettability.
98 Instead of changing the soil *pH* directly, Graber *et al.* (2009) used Na^+ and Ca^{2+} solutions at various
99 *pH*s to measure drop penetration times (a modified form of the *WDPT* test). The maximum time
100 occurred using drops in the range $7 < pH < 9$ near to the original soil *pH* (~7.3 - 7.7) which was not
101 adjusted. Only in the presence of Ca^{2+} did the water repellency of their samples increase with
102 increasing *pH*. This was explained as the complexation of free undissociated fatty acids with the
103 mineral surface via Ca^{2+} bridges leading to a higher density of fatty acid groups on the mineral surface
104 and hydrocarbon tails left to express water repellency above them.

105 Bayer & Schaumann (2007) investigated the change of *pH* and its influence on soil wettability
106 following the addition of aqueous HCl and NaOH solutions to soils. These actions only affected the
107 wettability of samples from "Tiergarten" with a distinct maximum in SWR occurring in the range 4.5
108 $< pH < 6.5$. and a similar wettability when brought to similar *pH* by addition of liquid NaOH.
109 However, they found no such effect on samples from "Buch". As soil moisture content is altered by
110 the addition of aqueous reagents, this approach provides opportunities for partial solvation and re-
111 arrangement of large organic molecules or flexible side-chains, which would not arise in the field
112 where SWR has developed through natural drying. It is, therefore, difficult to resolve the effects of the
113 imposed *pH* change from the impact of the method on soil moisture content on SWR (Bayer and

114 Schaumann, 2007). Differences in repellency following drying have been observed between Buch and
115 Tiergarten soils. Some mechanisms for the influence of water content on repellency in them (such as
116 conformational changes in SOM at the surface, together with water coverage) were suggested by
117 Diehl *et al.* (in press). Diehl & Schaumann (2007) discussed this in the context of several chemical
118 reactions with activation energies of 65 – 94 kJ mol⁻¹, 42 kJ mol⁻¹ and 8 - 20 kJ mol⁻¹ for the wetting
119 process of dried Buch, repellent and wettable Tiergarten samples respectively.

120 This study presents an alternative approach to the investigation of the relationships between soil
121 *pH* and SWR where the soil moisture content is essentially unaffected so that the mobility of organic
122 material is not enhanced by solvation effects. The method involves exposing samples to various
123 concentrations of gaseous hydrogen chloride or ammonia (drawn from the headspace gas above their
124 respective concentrated solutions) for 24 h. The outcomes of the method are compared with those of
125 previous studies (Diehl and Schaumann, 2007; Hurraß and Schaumann, 2006; Täumer *et al.*, 2005)
126 concerning SWR of soils from “Buch” and “Tiergarten” sites, in Berlin, Germany, and the differences
127 between them. The method was also applied to soil samples from the Netherlands, the UK and
128 Australia and correlated with *WDPT* data. The *pH* data, from processed German soils, are compared
129 with those from water drop penetration times (*WDPT*), water contact angles, estimates of both surface
130 charge density and potential cation exchange capacity (*CEC_{pot}*) and an assessment of the influence of
131 interactions between surface sites and protons in relation to *pH* and SWR is presented.

132 **Material and Methods**

133 **Soil samples**

134 German soil samples originate from two strongly anthropogenically influenced sites, a former
135 sewage field in the north east of Berlin “Buch” and an inner city park in Berlin “Tiergarten”. The
136 locations are in a transition zone between temperate oceanic and continental climates with moderate
137 precipitation (< 500 mm a⁻¹) and highest yield in the summer months.

138 At both sites the topsoil consists of medium sized sand with clay content below 5 % and is
139 characterized by high soil organic matter content (*SOM*) between 5 and 20 % (Diehl and Schaumann,
140 2007; Hoffmann, 2002; Schlenker, 1996; Täumer *et al.*, 2005).

141 Samples were collected at the sites in spring 2007. The grass cover was removed (~ 1 m²) and four
142 individual samples taken in a depth of 10-20 cm from visibly distinguishable dry or wet patches
143 known to reflect different SWRs (Hurraß and Schaumann, 2006). The wet and dry soil samples differ
144 strongly in actual wettability (Table 1 and Table 2). Samples are identified by their source locations
145 and SWRs as initially determined in their field moist states: Buch-wettable (BW), Buch- repellent
146 (BR), Tiergarten-wettable (TW) and Tiergarten-repellent (TR).

147 **Table 1**

148 **Table 2**

149 Samples from the Netherlands were obtained from an individual profile (4). Samples of topsoils
150 were collected from the UK (3) and Australia (3) between October 1999 and May 2001. Each set
151 consisted of 2 or 3 water repellent samples (NLR, UKR and AUR) and one wettable sample (NLW,
152 UKW and AUW, respectively). Wettable samples were collected as close as possible to the sites of
153 water repellent soils to eliminate, insofar as possible, variations in soil type and land use. Sample
154 information (Table 1) was obtained from Llewellyn (2004) and Mainwaring (2004) and further details
155 of precise locations are available (Doerr *et al.*, 2002; Doerr *et al.*, 2005a; Doerr *et al.*, 2005b; Douglas
156 and Doerr, 2007; Morley *et al.*, 2005). All samples are sandy soils representing various locations,
157 covering vegetation, and climates (Table 1). The Australian samples (AU) are from a Mediterranean-
158 type climate with long dry periods during the summer, whereas those from the Netherlands (NL) and
159 the United Kingdom (UK) are exposed to oceanic humid-temperate climates with rainfall throughout
160 the year.

161 **Sample preparation and characterization**

162 **Sample storage**

163 The German samples were air dried and then stored (> 8 weeks at 19°C) over saturated CaCl₂-
164 solution at ~ 31% relative humidity (*RH*). The NL, UK and AU samples were dried at 20°C in an oven
165 and then stored in closed bottles at ambient conditions without temperature control. Prior to
166 assessments of SWR these samples were equilibrated at 20°C and *RH* ~ 50% for 24 h.

167 **SOM content**

168 The *SOM* content of the German samples was assessed by loss of ignition (samples sieved
169 < 2 mm, heating at 550°C for 5 h, DIN 18128) and total organic carbon content (*TOC*) estimated by

170 dividing *SOM* by the factor 1.72 (AG Boden, 2005). *TOC* of NL, UK and AU samples was
 171 determined using a Solid Sample TC Analyser (Primacs^{SC}, Skalar, Netherlands) controlled by a PC.
 172 Oxygen was used as the oxidant. Samples were ground, by hand, to improve the rate of combustion
 173 and heated to 1050°C for seven minutes. As samples were free of inorganic carbon, total carbon (*TC*)
 174 content was considered equivalent to *TOC*. The quantity of CO₂ released on combustion was
 175 determined, at a wavelength of 4.2 μm, using an IR detector. The instrument was calibrated using
 176 oxalic acid as a standard.

177 *Water content, soil pH and electrical conductivity*

178 Soil *pH* and electrical conductivity were determined using field moist un-sieved soil (~ 12 g) in
 179 CaCl₂-solution (25 ml, 0.01 M) (DIN ISO 10390) using a *pH*-meter (Qph 70, VWR International).
 180 Similar *pH* determinations were also made using less material (German samples ~ 2g soil and 4 ml
 181 CaCl₂-solution or AU, NL and UK samples ~ 5 g and 11 ml CaCl₂-solution). Soil water content of un-
 182 sieved material (*WC*) was determined gravimetrically by oven drying for 24 h at 105°C (DIN ISO
 183 11465). The values are reported on a dry weight basis.

184 *Potential cation exchange capacity (CEC_{pot})*

185 *CEC_{pot}* was determined by complete displacement of all cations by Ba²⁺ ions at *pH* 8.1 and a
 186 subsequent replacement of Ba²⁺ by Mg²⁺ ions. 8–9 g of air dried soil sample (*m*₀) were placed in a
 187 centrifuge tube (*m*₁) and shaken in an overhead shaker for one hour with 30 mL of a 1:1 mixture of
 188 1 mol L⁻¹ BaCl₂-solution and a triethanolamine solution (9 vol%, adjusted at *pH* 8.1 with HCl). The
 189 samples were then centrifuged for 10 min at 3000 g. Afterwards, the supernatant was decanted. This
 190 procedure was repeated twice. After manual shaking with water and subsequent centrifugation and
 191 decantation, the centrifuge tube was weighted again (*m*₂). Finally, 30 mL of a 0.02 mol L⁻¹ MgSO₄
 192 solution was added and shaken overnight. The concentration (*c*) of Mg ions in the solution was
 193 determined by FAAS (Perkin Elmer) and *CEC_{pot}* calculated as:

$$194 \quad CEC_{pot} = \frac{3000 \left(c_{bl} - c \frac{(30 + m_2 - m_1)}{30} \right)}{m_0} \quad (1)$$

195 *Water drop penetration time*

196 The resistance of soil samples to wetting was determined using water drop penetration time,
 197 *WDPT* (Letey, 1969). Samples were placed in small containers, the surface gently smoothed and the
 198 containers placed in a incubator at 20°C. Three drops (100 μL) of distilled water were placed on each
 199 sample and the period required for complete penetration was determined. When *WDPT* exceeded
 200 1 min, the period was determined from magnified digital photographs (Canon A300) taken
 201 automatically at increasing intervals from 12 s up to 10 min, such that the relative error of *WDPT* did
 202 not exceed 5 % (Diehl and Schaumann, 2007). *WDPT* of UK, NL and AU samples were determined
 203 using drop volumes of 35 μL.

204 *Contact Angle: Wilhelmy Plate Method*

205 Advancing contact angles (Θ_{WPM}) were determined by the Wilhelmy Plate Method using a
 206 Dynamic Contact Angle Meter and Tensiometer (DCAT 21, Data Physics, Filderstadt, Germany).
 207 Half a glass microscope slide (76 x 26 x 1 mm) was covered completely with double sided adhesive
 208 tape and a thin layer of soil attached to it. The Θ_{WPM} of the slide was measured as an advancing
 209 contact angle (Diehl and Schaumann, 2007).

210 *Contact Angle: Sessile Drop Method*

211 A thin layer of the soil sample was attached to one side of a glass microscope slide using double
 212 sided adhesive tape (Bachmann et al., 2000). Three drops of water (100 μl) were placed on the
 213 surface. After one minute a digital image was taken (Canon A300) and the sessile drop contact angle
 214 (Θ_{sess}) was calculated from the tangent to the three-phase contact point associated with the ellipse that
 215 best fitted the drop shape (Diehl and Schaumann, 2007).

216 *Modification of soil pH*

217 Soil samples were exposed to various concentrations of gaseous HCl and NH₃ in air to change
 218 their *pH*.

219
 220 *pH increase*

221 Ammonia solutions 32% and 35% were obtained from Carl Roth and Fisher Scientific Ltd
 222 (Germany and UK, respectively). A known sample volume of ammonia gas (5 - 100 mL) was drawn
 223 from the headspace of an ammonia solution using a glass syringe via a silicone septum fitted in
 224 the screw cap of a containing bottle. The sample was then injected through a similar septum in the cap of
 225 a small bottle containing soil (~10 or 40g) (Figure 1 A). AU, NL, UK soil samples were treated with
 226 ammonia from the 35% solution and those from Germany with that from the 32% solution). After
 227 24 h, the bottle containing the soil was opened and the wettability and then *pH* and of the soil were
 228 determined.

229 *pH reduction*

231 Hydrochloric acid solutions, 37%, and 36%, were obtained from Carl Roth, Germany and 36 %
 232 Fisher Scientific Ltd., UK resp. A known sample volume between (25 - 500 mL) of air was introduced
 233 into a dispersion tube and passed through a gas wash bottle (250 mL) filled with HCl. The air enriched
 234 in HCl was passed through flexible silicone tubes and glass stopcocks into a second wash bottle
 235 (250 mL) containing soil (~10 g) (Figure 1 B). AU, NL and UK soil samples were treated with fumes
 236 from the 36% solution and those from Germany with fumes from the 37% solution. After 24 h, the
 237 bottle containing the soil was opened and the wettability and the *pH* of the soil were determined.

238 *pH range*

240 Both procedures were applied to known masses of soil and various volumes of HCl and NH₃
 241 fumes to determine the range of adjustment possible to soil *pH*.

242 *Surface charge*

243 Particle surface charge of selected soil samples (sieve fraction < 0.063 mm), at native and adjusted
 244 *pH* (as described above), were determined by titration following dispersion of the samples in
 245 laboratory water (prepared by deionisation and reverse osmosis; 5.4 < *pH* < 6.6; specific
 246 conductivity < 2 μS) using a particle charge detector (PCD 02, Müttek company, Germany). Stepwise
 247 additions of cationic polyelectrolyte (polydiallyl-dimethylammonium chloride, 0.01, 0.1 or 1 mmol L⁻¹)
 248 were made in for negatively charged particles, and anionic polyelectrolyte (sodium polyethylene-
 249 sulfonate, 0.1 mmol L⁻¹), for positively charged particles, using an automatic titrator (Mettler Toledo
 250 DL 25) to effect neutralization of electrokinetic charge. The amount of polyelectrolyte of charge (*c*) in
 251 volume (*V*) required to reach the isoelectric point (*IEP*) of a sample mass (*w*), was detected by the
 252 PCD as an electrokinetic potential of zero. The titratable charge (*Q*) of the sample was calculated as:

$$253 \quad Q = \frac{V \cdot q}{w} \quad (2)$$

254 Provided that the PCD signal is only used in combination with polyelectrolyte titration to detect
 255 the sign of particle charge and to indicate the isoelectric point (*IEP*), PCD technique is reported to
 256 produce reasonable results for titratable surface charge (Böckenhoff and Fischer, 2001).

257 **Figure 1**

258 *Long-term investigation of Buch and Tiergarten site*

259 Between spring 2002 and spring 2004, the sample sites Tiergarten and Buch (Germany) were
 260 subjected to a long-term study of seasonal sampling and characterisation of wettable and repellent
 261 samples, amongst others, *pH*, electrical conductivity (*EC*), *C/N* ratio and “Mehlich” extractable iron
 262 (Mehlich, 1984). Some *EC* and *pH* data were presented by Hurraß & Schaumann (2006). *C/N* ratio
 263 was determined by combustion and quantification of CO₂ and N₂ using gas chromatography and
 264 thermal conductivity detector (*C/N* NA 1500 N Carlo Erba).

265 **Results**

266 *General sample characteristics*

267 The long-term investigations showed that repellent samples in Tiergarten were restricted to a range
 268 3.5 < *pH* < 4.5 whereas wettable Tiergarten samples and all Buch samples were found in a range of
 269 3.5 < *pH* < 5.5 (Figure 2A). Wettable samples from both sites had *EC* values < 350 μS cm⁻¹, whereas
 270 repellent samples had maximum *EC* values of < 1300 μS cm⁻¹ and < 550 μS cm⁻¹ for Tiergarten and
 271 Buch sites, respectively (Figure 2 B). Although Tiergarten samples have higher *C/N* ratios than Buch
 272 samples (Figure 2 C), absolute *N* content is comparable in both sites (data not shown). Tiergarten
 273 samples possessed significantly higher contents of “Mehlich” extractable iron than Buch samples, in
 274 absolute values (Figure 2 D) as well as related to SOM content (data not shown).

275 **Figure 2**

276 Water repellency (*WDPT*) of the originally wettable samples from Germany (TW, BW) changed
 277 significantly after drying at 19°C at constant relative humidity of 31%RH. Values for BW samples
 278 increased from 0 s in field moist state up to 1200 s following drying (Table 2). In contrast, values for
 279 TW samples increased from 0 s in field moist state to 5 s following drying and so the soil remained
 280 wettable. The effect of drying on *WDPT* of the repellent samples (TR, BR) was the inverse: After
 281 drying *WDPTs* were shorter than those for field moist samples (Table 2).

282 *CEC_{pot}* was significantly lower (17 cmol_c kg⁻¹) in the TR sample than in the other 3 German
 283 samples (25-37 cmol_c kg⁻¹) which may reflect the low *SOM* content in the TR samples, 26 g kg⁻¹ in
 284 comparison with ~ 50 g kg⁻¹ *TOC* of the others (Table 2). The TR sample also has a noticeably lower
 285 *pH* (4.0) in comparison with the others (4.4 - 4.6) (Table 1).

286 *TOC* in the NL samples decreased with increasing depth from 36 g kg⁻¹ in the topsoil (0-10 cm)
 287 down to 0 (the detection limit) at a depth of 30-40 cm. The *TOC* of UK and AU samples varied
 288 between 2 and 14 g kg⁻¹. Original *pH* values of the samples from vegetated sites ranged between 3.9 in
 289 NLR2 and NLR3 (in a depth of 10-30 cm of the NL soil profile) and 5.1 in sample AUR2. Only the
 290 *pH* of the UKW sample, from a vegetation-free site, was distinctly higher (7.0) than those of the
 291 others (Table 1).

292 *Effects of exposure to gaseous NH₃ and HCl*

293 As the volumes of gaseous ammonia or hydrogen chloride, added to soil samples B and T
 294 increased, the resulting *pH* changes increased and decreased respectively away from the initial value
 295 and form sigmoidal curve (Figure 3 D). The slope of *pH* increase / decrease is steepest around *pH* 4 –
 296 5 (untreated samples) and flattens with increased gas volume. The *pH* approaches a value of 8.8 – 9.3
 297 after addition of 10 mL/g of NH₃-enriched air and to a value of 1.8 – 2.4 after addition of 50 mL/g of
 298 HCl-enriched air.

299 The *pH* of the TR sample was slightly more sensitive to increases in concentration of NH₃ in
 300 comparison with its wettable counterpart (TW). In order to increase *pH* of TW sample from 5.2 to 8.1,
 301 ~ 4 mL/g of NH₃ enriched air is needed, whereas TR sample requires only ~ 3 mL/g to increase *pH*
 302 from 5.3 to 8.3. The difference between *pH* of this pair vanished after the addition of 1 mL/g NH₃
 303 (*pH* 5.3) and reappears clearly inverted after the addition of 4 mL/g NH₃.

304 The initial *pH* of untreated BW and BR were identical, but addition of NH₃ (up to 4 mL/g) resulted
 305 in slightly higher *pH* change for BR than for BW. With further additions of NH₃, the *pH* of the TR-
 306 TW pair converged at 9.3 and at 8.8 – 9.0 (Figure 3 D).

307 The *pH* of the repellent sample TR decreased with a steeper slope, than that of TW after addition
 308 of HCl (up to 15 mL/g). Within this range, the *pH* of the TW sample is higher than that of TR,
 309 whereas the *pH* of BW is slightly lower than that of BR. Only after addition of volumes (20 and
 310 50 mL/g) of HCl enriched air, did the *pH* of all samples converge to specific values of 1.8 for T and
 311 2.4 for B pairs (Figure 3 D). In order to decrease the *pH* of TW from its original value (4.4) to that of
 312 TR (4.0), it was necessary to add ~ 3 mL/g of HCl enriched air. A further reduction to *pH* 3.0 required
 313 additions of ~ 12 mL/g and 7.5 mL/g to TW and TR respectively.

314 Samples from Buch have comparable *TOC* content for the wettable and the repellent sample (50
 315 and 47 g kg⁻¹) respectively). In contrast, *TOC* of the wettable TW sample (48 g kg⁻¹) was almost twice
 316 as high as that of its repellent counterpart TR (26 g kg⁻¹) (Table 1).

317 **Figure 3**

318 Most curves of *pH* as a function of the applied gas volume obtained from NL, UK and AU
 319 samples were sigmoidal in shape, similar to those obtained from the German samples. However, the
 320 limits of the induced *pH* change were narrower than those of the German samples. Most curves have
 321 more than one inflexion point so that in some cases the convergence to a maximum (e.g. NLC, AU1)
 322 and minimum *pH* values (e.g. NL1, AU2) was not readily observed within the range investigated
 323 (Figure 3 NL, UK, AU).

324 In most NL, UK and AU samples, a second inflexion point in the curve shape forming a plateau
 325 like shape is indicated in the range just below the original *pH* of the samples, suggesting a buffering
 326 system in this *pH* range. This buffering zone is most strongly pronounced in the sample AU-R2
 327 (Figure 3).

328 In good accordance to the TW and TR samples, the slope of *pH* as a function of added NH₃
 329 volume seems to be steeper for samples with a lower *TOC* than for samples with a higher *TOC*: As
 330 ammonia was added, the *pH* of NLR2 and NLR3 (with *TOCs* of 6 and 1 g kg⁻¹ resp.) increased with a
 331 steeper slope than that of NLR1 (with a *TOC* of 36 g kg⁻¹), similarly the *pH* of UKW (with a *TOC* of
 332 3 g kg⁻¹) increased with a steeper slope than those of UKR1 and UKR2 (with *TOCs* of 11 and 8 g kg⁻¹
 333 resp.) and the *pH* of AUR2 (with a *TOC* of with 2 g kg⁻¹) increased with a steeper slope than those of
 334 AUR1 and AUW (with *TOCs* of 12 and 14 g kg⁻¹ resp.) (Figure 3 NL, UK and AU).

335 The sparse array of data (3-4 points) available for acidified samples is not sufficient to provide a
 336 detailed description of the behaviour of NL, UK and AU samples. Whilst this method of soil

337 acidification appears useful, the experimental design does not provide a relationship between the
 338 added HCl-enriched air volume and the specific HCl concentration in the wash bottle containing the
 339 soil sample.

340 **Reaction of repellency on changes in soil pH**

341 *WDPT*s of the German samples whose *pH* was adjusted were found to fall in the range
 342 $0 < \text{WDPT} < 14400$ s with increasing maxima (TR 1 h, BW 2 h and BR 3 h) and minima (at 2, 12 and
 343 90 s respectively). Data for TW fell in the range $0 < \text{WDPT} < 5$ s indicating a minimal influence of *pH*
 344 in the range $2 < \text{pH} < 9$. *WDPT* decreased with increasing *pH* for all samples (Figure 4 D). Slopes of
 345 the best fit linear regression lines of $\log \text{WDPT}$ vs *pH* in the alkaline direction were -0.36 ± 0.02 and
 346 -0.42 ± 0.03 ($p < 0.0001$, both) comparable for BW and BR, respectively, but significantly steeper
 347 (-0.66 ± 0.04 , $p < 0.0001$) for the TR. This sample became wettable (*WDPT* < 10 s) above *pH* 8.3,
 348 whereas both Buch samples remain repellent (*WDPT* > 10 s) up to the limit of *pH* 9.3 (Figure 4 D).

349 As *pH* was reduced, *WDPT* behaved in an inconsistent manner: The *WDPT* of TR decreased with
 350 a maximum at the original *pH*. Variations in the relatively short *WDPT*s of TW are probably of little
 351 practical significance (with little net change in relation to the value at the original *pH*). Contact angles
 352 measured either from sessile drops or using the Wilhelmy Plate method decrease with decreasing *pH*
 353 for all Tiergarten samples (Figure 5 B, C). In contrast, *WDPT*s of both Buch samples did not decrease
 354 upon *pH* reduction, but remained within a range of $2 < \text{WDPT} < 4$ h for BR and increased from 0.3 h
 355 to 1 h for BW.

356 **Figure 4**

357 Changes in *WDPT* arising from adjustment of soil *pH* of the repellent NL, UK, and AU samples
 358 follow the trends shown by the repellent German samples (BR and TR): In all cases, *WDPT* decreased
 359 with increasing *pH* (Figure 4).

360 Two types of behaviour were observed as *pH* decreased: I) samples with a maximum *WDPT* in the
 361 region of the original *pH* and *WDPT* decreasing with decreasing *pH* (TR, NLR1, UKR2, AUR1 and
 362 AUR2) and II) samples with constant or increasing *WDPT* (BW, BR and UK-R1) after reduction of
 363 *pH*. Samples NLR2 and NLR3 possessed local maxima in *WDPT* at the original *pH*, and *WDPT*
 364 decreased with *pH*, except for the lowest induced *pH*, where *WDPT* reached a second maximum with
 365 a value comparable with or higher than, that at the original *pH* (Figure 4 NL).

366 In contrast to TW, all wettable NL, UK, and AU sets exhibited instant penetration (*WDPT* ~ 1 s) over
 367 the *pH* range examined. Sample BW became repellent after drying and, suffered a reclassification as
 368 repellent.

369 **Comparison of contact angle and *WDPT* data**

370 Contact angle measurements (Θ_{sess}) made on the German samples show qualitatively comparable
 371 trends with *WDPT*. In principle, all three curves (Figure 5 A, B, C) indicate a decrease in repellency
 372 upon increase from the original *pH* for all samples, and a decrease in repellency upon decrease from
 373 the original *pH* for TW and TR samples and only small or negligible changes in repellency upon
 374 decrease from the original *pH* for BW and BR samples. Correlation of *WDPT* and Θ_{WPM} with Θ_{sess}
 375 (Figure 5 D) shows clustering about a linear regression line of $\log(\text{WDPT})$ data of the form:-

$$376 \log(\text{WDPT}) = 0.038 \Theta_{\text{sess}} - 0.29 \quad (3)$$

377 with a range of ~ 40° over the range $0 < \text{WDPT} < 10$ s.

378 Contact angles Θ_{WPM} cluster in a similar manner to Θ_{sess} only at low values with a significant
 379 departure at high values indicating a relative insensitivity of Θ_{WPM} . These effects can be seen in the
 380 scatter Θ_{WPM} as a function of Θ_{sess} , where Θ_{WPM} data cluster around the line:

$$381 \Theta_{\text{WPM}} = 0.73 \Theta_{\text{sess}} + 80^\circ \quad (4)$$

382 in the range $0^\circ < \Theta_{\text{WPM}} < 120^\circ$, whereas in the range $120^\circ < \Theta_{\text{WPM}} < 130^\circ$, where $\Theta_{\text{sess}} > 60^\circ$ scatter
 383 is random about the horizontal. The regions of low sensitivity of the *WDPT* method and Wilhelmy
 384 plate method, in relation to sessile drop method, are shown shaded in Figure 5 A and C, respectively.

385 The WPM method did not resolve the differences between BW and BR detected in the *WDPT* and
 386 Θ_{sess} data. There is little clustering of data in the vertical direction to suggest regions where Θ_{sess} is
 387 insensitive to *WDPT* or Θ_{WPM} . The boundary between wettable and repellent samples defined as
 388 *WDPT* ~ 5 s (Dekker et al., 1998) correspond with Θ_{sess} of ~ 26° and Θ_{WPM} of ~ 100° using Equation 2
 389 and 3, respectively.

390 **Figure 5**

391 **Surface charge changes of German samples**

392 Negative surface charge (Q) strongly increased with increasing pH in all samples (Figure 6), and
 393 data from repellent and wettable samples from Buch (BW, BR) did not differ significantly from each
 394 other in surface charge over the range of pH investigated. At the lowest investigated pH (1.7 for BW
 395 and 2.3 for BR), both revealed minima in Q of $-0.9 (\pm 0.9) \text{ cmol}_c \text{ kg}^{-1}$ and $-0.5 (\pm 0.6) \text{ cmol}_c \text{ kg}^{-1}$,
 396 respectively. Both samples had maximum Q of $-20 \text{ cmol}_c \text{ kg}^{-1}$ at the highest pH (9.3) (Figure 6). Both
 397 Tiergarten samples had positive Q ($1.1 (\pm 0.2) \text{ cmol}_c \text{ kg}^{-1}$ for TW and $3.5 (\pm 0.4) \text{ cmol}_c \text{ kg}^{-1}$ for TR) at
 398 their lowest pH (1.7 and 1.8, respectively). At their highest pH of 9 and 8.8 (TW and TR,
 399 respectively) both had more negative charge than the Buch samples at similar pH (TW:
 400 $-39 (\pm 4) \text{ cmol}_c \text{ kg}^{-1}$, TR: $-30 (\pm 3) \text{ cmol}_c \text{ kg}^{-1}$, Figure 6). The slope of Q as a function of pH showed a
 401 minimum between $pH \sim 3$ and $pH \sim 6$ for all samples (Figure 6), suggesting the elements of a
 402 sigmoidal shaped curve, with at least one inflexion point, whose detail is not made clear by the sparse
 403 data points. As Q data were available for four only pH values, estimates of Q values at intermediate
 404 pH were made by linear interpolation between these (Figure 6).

405 **Figure 6**

406 The pH of isoelectric point (pH_{iep}), at which negative and positive surface charge are equal,
 407 resulting in a net zero surface charge, was found to be higher for TW and TR ($\sim 2 < pH < \sim 3$) than for
 408 BW and BR ($\sim 1 < pH < \sim 2$), respectively and below the pH region of maximum repellency ($pH_{(max.}$
 409 $_{Repell})$ for TW and TR (Table 3).

410 **Table 3**

411 The relationships between Θ_{sess} (which was the measure of repellency that exhibited the highest
 412 sensitivity to pH) and (measured and estimated values of) Q show maxima ($Q_{(max. Repell)}$) (Figure 7) at
 413 ~ -2 and $\sim -5 \text{ cmol}_c \text{ kg}^{-1}$ for TR and TW, respectively (Table 3). Above $Q_{(max. Repell)}$ Θ_{sess} decreases with
 414 increasing Q . Compared with TW, Q values of TR were found to be shifted to higher Θ_{sess} and less
 415 negative Q values. Θ_{sess} of BW and BR samples decreased with decreasing Q , but remained constant
 416 above $Q \sim -5 \text{ cmol}_c \text{ kg}^{-1}$. Compared with BR, Q values of BW were shifted to lower Θ_{sess} , but Q
 417 values were found to be within a similar range. The differences between Θ_{sess} data of BW and BR are
 418 more pronounced at low Q and tend to converge as electroneutral conditions are approached.

419 **Figure 7**420 **Discussion**421 **Comparison of contact angle and WDPT data**

422 The differences in sensitivity between the various methods for assessment of water repellency
 423 probably arise as a consequence of various factors involved in the measurements and associated
 424 properties of soil. *WDPT* measurements involve the process of infiltration and any time dependent
 425 changes of soil surfaces arising from chemical interaction with water. Penetration depends on surface
 426 characteristics, particle and pore size distributions and the accessibility and continuity of pores. Soil
 427 texture and compaction will, therefore, influence the resistance to flow. At short *WDPT* ($< 10\text{s}$) the
 428 effects of minor changes in the resistance to flow will contribute a large relative error in *WDPT*
 429 reducing the sensitivity to detection of purely surface effects. The contact angle methods should avoid
 430 significant depth penetration of liquid and so avoid this error (see, for example, data for sample TW,
 431 in Figure 5 A-C). At *WDPT* $< 5\text{s}$ the drop penetration in response to the hydrostatic pressure may
 432 form a significant component of the time measurement effected by the texture and compactness of the
 433 soil, and a subjective judgement as to when drop penetration is complete.

434 In the range $\Theta_{WPM} > 90^\circ$, small differences in the surface characteristics of soil particle layers may
 435 enhance hydrophobicity through entrapment of air between particles. At $\Theta_{WPM} < 90^\circ$ this entrapment
 436 is known to be less significant.

437 However, measurements are influenced, for example, by surface roughness, temperature and drop
 438 volume and useful comparisons arise when these are known and/or controlled.

439 **Conformational arrangement of SOM molecules**

440 All samples exhibited maximum repellency at pH 3 - 5, in good agreement with the pK_a of
 441 carboxylic acids in HA from peat (Duval et al., 2005), at which a reduction in repulsion forces
 442 between these moieties may cause micelle-like aggregation or a more compact structure of HA with
 443 outward orientated hydrophobic moieties (Duval et al., 2005; Ohashi and Nakazawa, 1996; Terashima
 444 et al., 2004). However, such conformational changes may arise from changes in surface charge density
 445 likely to occur as soil moisture is gained or lost from soil electrolyte solution. Direct evidence of
 446 changes in conformational arrangement of SOM is not available from macroscopic methods;
 447 molecular scale investigations are required.

448 *pH dependent changes in surface charge*449 *Buffer systems in the German samples*

450 The similarity of titration curves for BR, BW and TW (all with similar TOC contents) and the
 451 greater sensitivity of TR to HCl addition may reflect the significantly lower TOC and an associated
 452 lower buffering capacity of this sample.

453 *Increase in pH*

454 The decrease of soil water repellency with increasing pH may arise from an increased population
 455 of dissociated acidic functional groups associated with conjugate acid (ammonium) ions. NH₃ readily
 456 hydrolyses on contact with soil moisture, forming hydroxyl and ammonia ions. The ionic strength will
 457 increase, favouring further dissociation of carboxylic groups at 4 < pH < 7 (Terashima *et al.*, 2004)
 458 and of phenolic groups at 8 < pH < 11 (Duval *et al.*, 2005; MacCarthy *et al.*, 1979). Our results
 459 suggest that sufficient deprotonated sites became available at the surface, to enhance its affinity for
 460 water, as pH was increased.

461 *Decrease in pH*

462 The decrease in repellency observed with reduction of soil pH, for TW, TR, NLR, UKR2, AUR1
 463 and AUR2 samples, may arise from a surplus of a small quantity of acid, albeit in a concentrated
 464 form, able to maintain local acidic organic functional groups in protonated forms on contact with
 465 water. Basic functional groups such as amine groups, with $pK_a \sim 5$ are protonated with decreasing pH
 466 and rendered positively charged. If C/N data (Figure 2 C) is used as a surrogate measure of the mass
 467 concentration of amine groups, responsible for positive surface charge at low pH, then, the decrease in
 468 wettability with decreasing pH observed for TR and TW but not with BR and BW suggest that amines
 469 were of little influence.

470 Amphoteric mineral sesqui(hydr)oxides, (like iron, aluminium, manganese or silicon (hydr)oxides)
 471 may contribute to both positive and negative surface charge at high and low pH respectively. Samples
 472 from Tiergarten generally have a higher concentration of "Mehlich"-extractable iron than those from
 473 Buch (Figure 2 D). These iron species are neutral at about pH 4 and become positively charged with
 474 decreasing pH. Only in Tiergarten samples may the availability of surface active mineral proton
 475 acceptors (e.g. sesqui(hydr)oxides) be sufficient to achieve a net positive surface charge density with
 476 decreasing pH and, therefore, contribute to the increased wettability of Tiergarten samples at low pH.

477 The development of net positive titratable surface charge in TR and TW (Figure 6) at
 478 2.5 < pH < 3, below the pH where measurements of water repellency reach maxima, suggests that
 479 mineral oxides may be responsible. As samples from Buch, did not develop net positive charge and
 480 exhibited no significant reductions in measurements of water repellency at low pH, perhaps there was
 481 insufficient Fe-oxide available.

482 *Net surface charge and wettability*

483 The close proximity of the maximum WDPTs with the natural pH of the samples suggests that this
 484 coincides with the lowest density of ionisable sites. The presence of pH_{iep} consistently below
 485 $pH_{(max\ Repell)}$ for all B and T samples suggests that both, negatively and positively charged sites are
 486 present and some negative sites may be permanent. The net surface charge is then determined by the
 487 sum of (i) permanent charge ($Q_{perm.}$), (ii) variable charge caused by protonation/deprotonation
 488 reactions of organic functional groups (Q_{SOM}) and (iii) mineral compounds ($Q_{mineral}$) and can be
 489 expressed in a simplified form on the basis of averaged pK_i as follows:

$$490 \quad \sum Q_i (pH) = Q_{perm.} + Q_{SOM} + Q_{mineral}$$

$$= Q_{perm.} + \frac{Q_{max, SOM}}{10^{(pK_{SOM} - pH)} + 1} - \frac{Q_{max, mineral}}{10^{(pK_{1, mineral} - pH)} + 1} + \frac{Q_{max, mineral}}{10^{(pH - pK_{2, mineral})} + 1} \quad (5),$$

491 where $Q_{max, SOM}$ is the maximum negative charge from deprotonation of the organic functional
 492 groups, $Q_{max, mineral}$ is the maximum negative or positive charge from deprotonation or protonation of
 493 mineral compounds, pK_{SOM} is the deprotonation constant of SOM surfaces and $pK_{1, mineral}$ and $pK_{2, mineral}$
 494 are the deprotonation and the protonation constants of mineral surfaces, respectively. At pH_{iep} ,
 495 positive and negative charges have the same value and the net surface charge becomes zero. However,
 496 maximum repellency is probably not related to the zero net surface charge but rather with a minimum

497 of the absolute equivalent number of charged sites ($\sum \sqrt{Q_i^2}$), which is expressed as follows:

$$498 \quad \sum \sqrt{Q_i^2} (pH) = \sqrt{Q_{perm.}^2} + \sqrt{[Q_{SOM}(pH)]^2} + \sqrt{[Q_{mineral}(pH)]^2} \quad (6)$$

499 Equations 5 and 6, and the measured ΣQ_i as a function of pH , allow a search of pH dependent
 500 contributions of Q_{SOM} , $Q_{mineral}$ and Q_{perm} to the net surface charge fulfilling the condition that a
 501 minimum $\Sigma \sqrt{Q_i^2}$ coincides with $pH_{(max\ repell)}$ (Supporting information). This offers the following
 502 hypotheses which are not adequately tested with present data: (i) Wetttable samples have higher Q_{perm}
 503 than the repellent ones, (ii) Tiergarten samples have higher $Q_{max, mineral}$ than Buch samples and (iii) the
 504 values of pK_{SOM} are lower for Tiergarten samples than for Buch samples.

505 More detailed information about the contributions of the various surface species (e.g. weak and
 506 strong acidic carboxylic sites, phenolic sites and the fine mineral component clay minerals and
 507 sesqui(hydr)oxides) is required.

508 The occurrence of the peak in the $\Theta_{sess}-Q$ curve of TR at higher (more positive) Q than that of TW
 509 (Figure 7) may arise from the relatively low CEC_{pos} of the former, which indicates a generally low
 510 negative charge density and, therefore, a generally lower wettability in TR than in TW. The
 511 occurrence of positive charge in the low pH range in T samples coincides with a decrease in
 512 repellency with decreasing pH which indicates a close relation between surface charge and repellency.

513 **Chemical reactions**

514 An alternative explanation for pH dependent changes in repellency is a change of SOM surface
 515 properties caused by chemical reactions. Acidic hydrolysis and condensation reactions as suggested in
 516 earlier studies as mechanisms controlling SWR in Buch samples (Diehl and Schaumann, 2007) are
 517 equilibrium reactions highly related to changes in water content and their influence maybe therefore
 518 minimized in the dried samples of the present study. Irreversible base catalyzed hydrolysis reactions,
 519 however, are less influenced by water content and may therefore be an additional explanation for
 520 decreasing repellency with increasing pH .

521 **Comparison with former studies**

522 In agreement with the results of Graber *et al.* (2009), the maximum of $WDPT$ was found in the
 523 range of the original pH of the soil samples.

524 Previous studies involving adjustment of soil pH by addition of aqueous reagents to samples from
 525 the Buch site (Bayer and Schaumann, 2007) found that, following drying, samples were completely
 526 wetttable over the range $3 < pH < 11$, whereas pronounced repellency occurred in these soils when the
 527 pH was adjusted using gases, with minimal effect on soil moisture content. The observed decrease in
 528 repellency with increasing pH of soils from the Netherlands, UK and Australia indicate that it is a soil
 529 characteristic spanning various locations. However, Tiergarten samples, exhibited a maximum
 530 repellency irrespective of how the pH was adjusted, but the repellency of Buch samples seem to be
 531 influenced by changes in water content resulting from the use of liquid reagents. The maximum
 532 repellency of Tiergarten samples reported by Bayer & Schaumann (2007) was at a higher pH than
 533 found in this study, despite a similar original soil pH . The addition of liquid NaOH may lead to
 534 additional SOM alteration which causes a shift in surface charge (Bayer and Schaumann, 2007)
 535 whereas the use of acidic and basic gases as reagents to modify soil pH without significant impact on
 536 soil moisture content appears to provide a useful route to examine the pH dependency of SWR.

537 Bayer & Schaumann (2007) observed that wetttable and water repellent Tiergarten samples
 538 exhibited similar wettability when brought to similar pH by addition of liquid NaOH. In contrast,
 539 when pH was altered via the gas phase Tiergarten samples kept their original repellency differences,
 540 even at the same pH . The addition of moisture to the soil which accompanies the addition of liquid
 541 NaOH probably caused an equalisation of repellency differences between wetttable and repellent
 542 samples. This indicates that the pH alteration via the gas phase applied in this study provide a new
 543 method with reduced side effects and is, therefore, suitable for changes in soil pH and investigations
 544 of those changes on SWR.

545 **Conclusions**

546 The comparison of 3 different methods for repellency determination showed the advantages and
 547 disadvantages of each method: In the range below ~ 10 s, $WDPT$ showed a reduced sensitivity
 548 compared to the other two methods. In contrast to that, the Wilhelmy plate method seemed to be less
 549 sensitive in the range of very strong repellency ($\Theta_{WPM} > 120^\circ$) compared to $WDPT$ and sessile drop
 550 method. The sessile drop method seemed to have no repellency range with reduced sensitivity, but
 551 revealed higher standard deviation between measurement repetitions compared to the two other
 552 methods.

553 By using a newly developed method to change the pH in soil samples via the gas phase without
 554 changing the moisture status, the influence of changes in soil pH on wettability was related to the
 555 number and type of protonable and de-protonable surface sites of organic and mineral surfaces in

556 soils. The highest level of repellency is reached at the original pH when the number of charged sites is
557 minimal. With increasing pH repellency decreased and negative surface charge increased caused by
558 de-protonation. With respect to the repellency reaction on pH decrease, two types of soil can be
559 distinguished: i) soils, in which repellency decreased with decreasing pH because of a sufficient
560 number of protonable surface sites with a significant amount of positive surface charge and ii) soils,
561 with no or not sufficient protonable surface sites to exhibit significant positive surface charge and,
562 therefore, their repellency did not decrease with decreasing pH . Evidences suggested, that the
563 protonable sites in case of the two Tiergarten samples, which are of the soil type I, were rather
564 presented by mineral surfaces, than by organic functional groups.

565 **Acknowledgments**

566 The study was financed by the German Research Association DFG (research group Interurban,
567 subproject HUMUS; SCHA 849/4-3). We thank Lydiya Shemotyuk for her help with the laboratory
568 work and all members of the research group "U-Chemie" for lively discussions and constructive
569 teamwork. We also want to thank Marta Casimiro for the help with lab work on the NL, UK and AU
570 samples. The data of the long-term study of Buch and Tiergarten site are provided by the subproject
571 SOIL from the Interurban research group and published here by the courtesy of Prof. Dr. Gerd
572 Wessolek. We therefore want to thank him and the laboratory staff of Department of Soil Protection
573 (Technical University Berlin).

574

References

- 575 AG Boden, 2005. *Bodenkundliche Kartieranleitung*. Hannover. 5. Aufl. 438 pp.
- 576 Babejova, N., 2001. An influence of changing the humic acids content on soil water repellency and
577 saturated hydraulic conductivity. *Journal of Hydrology and Hydromechanics*, 49(5): 291-300.
- 578 Bachmann, J., Ellies, A. and Hartge, K.H., 2000. Development and application of a new sessile drop
579 contact angle method to assess soil water repellency. *Journal of Hydrology*, 231-232: 66-75.
- 580 Bayer, J.V. and Schaumann, G.E., 2007. Development of soil water repellency in the course of
581 isothermal drying and upon pH changes in two urban soils. *Hydrological processes*, 21(17): 2266 -
582 2275.
- 583 Böckenhoff, K. and Fischer, W.R., 2001. Determination of electrokinetic charge with a particle-charge
584 detector, and its relationship to the total charge. *Fresenius' Journal of Analytical Chemistry*,
585 371(5): 670-674.
- 586 Cammeraat, L.H., Willott, S.J., Compton, S.G. and Incoll, L.D., 2002. The effects of ants' nests on the
587 physical, chemical and hydrological properties of a rangeland soil in semi-arid Spain. *Geoderma*,
588 105(1-2): 1-20.
- 589 Chatelier, R.C., Hodges, A.M., Drummond, C.J., Chan, D.Y.C. and Griesser, H.J., 1997.
590 Determination of the Intrinsic Acid-Base Dissociation Constant and Site Density of Ionizable
591 Surface Groups by Capillary Rise Measurements. *Langmuir*, 13(11): 3043-3046.
- 592 Chen, Y. and Schnitzer, M., 1978. The surface tension of aqueous solutions of soil humic substances.
593 *Soil Science*, 125(1): 7-15.
- 594 Deo, P., Deo, N., Somasundaran, P., Jockusch, S. and Turro, N.J., 2005. Conformational Changes of
595 Pyrene-Labeled Polyelectrolytes with pH: Effect of Hydrophobic Modifications. *Journal of*
596 *Physical Chemistry B*, 109(44): 20714-20718.
- 597 Diehl, D., Ellerbrock, R.H. and Schaumann, G.E., in press. DRIFT-Spectroscopy of untreated and
598 dried soil samples of different wettability. *European Journal of Soil Science*.
- 599 Diehl, D. and Schaumann, G.E., 2007. Wetting mechanism assessed from time dependent sessile drop
600 shape. *Hydrological Processes*, 21(17): 2255 - 2265.
- 601 Doerr, S.H., Dekker, L.W., Ritsema, C.J., Shakesby, R.A. and Bryant, R., 2002. Water repellency of
602 soils: The influence of ambient relative humidity. *Soil Science Society of America Journal*, 66(2):
603 401-405.
- 604 Doerr, S.H. et al., 2005a. Effects of heating and post-heating equilibration times on soil water
605 repellency. *Australian Journal of Soil Research*, 43(3): 261-267.
- 606 Doerr, S.H. et al., 2005b. Extraction of compounds associated with water repellency in sandy soils of
607 different origin. *Australian Journal of Soil Research*, 43(3): 225-237.
- 608 Douglas, P. and Doerr, K.A.M.C.P.M.S.H., 2007. The kinetics and energetics of transitions between
609 water repellent and wettable soil conditions: a linear free energy analysis of the relationship
610 between WDPT and MED/CST. *Hydrological Processes*, 21(17): 2248-2254.
- 611 Duval, J.F.L., Wilkinson, K.J., Van Leeuwen, H.P. and Buffle, J., 2005. Humic substances are soft
612 and permeable: Evidence from their electrophoretic mobilities. *Environmental Science &*
613 *Technology*, 39(17): 6435-6445.
- 614 Graber, E.R. and S. Taggera, a.R.W., 2009. Role of Divalent Fatty Acid Salts in Soil Water
615 Repellency. *Soil Science Society of America Journal*, 73(2): 541-549.
- 616 Hoffmann, C., 2002. *Schwermetallmobilität und Risikopotential der Rieselfelder Berlin Buch*.
617 *Bodenökologie und Bodengenese*, 35: 226 pp.
- 618 Holmes-Farley, S.R., Reamey, R.H., McCarthy, T.J., Deutch, J. and Whitesides, G.M., 1985. Acid-
619 base behavior of carboxylic acid groups covalently attached at the surface of polyethylene: The
620 usefulness of contact angle in following the ionization of surface functionality. *Langmuir*, 1(6):
621 725-740.
- 622 Hurraß, J. and Schaumann, G.E., 2006. Properties of soil organic matter and aqueous extracts of
623 actually water repellent and wettable soil samples. *Geoderma*, 132(1-2): 222-239.
- 624 Karnok, K.A., Rowland, E.J. and Tan, K.H., 1993. High pH treatments and the alleviation of soil
625 hydrophobicity on golf greens. *Agronomy Journal*, 85(5): 983-986.
- 626 Letey, J., 1969. Measurement of contact angle, water drop penetration time, and critical surface
627 tension., *Water repellent soils - Proceedings of the symposium on water repellent soils*, University
628 of California, Riverside, May 6-10, 1968, pp. 4347.
- 629 Lin, C.Y., Chou, W.C., Tsai, J.S. and Lin, W.T., 2006. Water repellency of *Casuarina* windbreaks
630 (*Casuarina equisetifolia* Forst.) caused by fungi in central Taiwan. *Ecological Engineering*, 26(3):
631 283-292.
- 632 Llewellyn, C.T., 2004. *Studies of the molecular basis of soil water repellency*, Univerisity of Wales,
633 Swansea, 205 pp.

- 634 Ma'shum, M. and Farmer, V.C., 1985. Origin and assessment of water repellency of a sandy South
635 Australian Soil. *Australian Journal of Soil Research*, 23: 623-626.
- 636 MacCarthy, P., Peterson, M.J., Malcolm, R.L. and Thurman, E.M., 1979. Separation of humic
637 substances by pH gradient desorption from a hydrophobic resin. *Analytical Chemistry*, 51(12):
638 2041-3.
- 639 Mainwaring, K.A., 2004. Chemical characterisation and repellency-inducing effects of organic
640 compounds isolated from sandy soils. Department of Chemistry, University of Wales, Swansea,
641 293 pp.
- 642 Mataix-Solera, J. et al., 2007. Water repellency under different plant species in a calcareous forest soil
643 in a semiarid Mediterranean environment. *Hydrological Processes*, 21(17): 2300-2309.
- 644 Mehlich, A., 1984. Mehlich 3 soil test extractant: A modification of Mehlich 2 extractant.
645 *Communications in Soil Science and Plant Analysis*, 15(12): 1409 - 1416.
- 646 Morley, C.P. et al., 2005. Organic compounds at different depths in a sandy soil and their role in water
647 repellency. *Australian Journal of Soil Research*, 43(3): 239-249.
- 648 Ohashi, H. and Nakazawa, H., 1996. The microstructure of Humic Acid-Montmorillonite composites.
649 *Clay Minerals*, 31: 347-354.
- 650 Roberts, F.J. and Carbon, B.A., 1971. Water repellence in sandy soils of south-western Australia.
651 1. Some studies related to field occurrence. *Field station record*, 10: 13-20.
- 652 Roberts, F.J. and Carbon, B.A., 1972. Water repellence in sandy soils of southwestern Australia. II.
653 Some chemical characteristics of the hydrophobic skins. *Australian Journal of Soil Research*,
654 10(1): 35-42.
- 655 Roper, M.M., 2005. Managing soils to enhance the potential for bioremediation of water repellency.
656 *Australian Journal of Soil research*, 43: 803-810.
- 657 Schlenker, L.M., B.; Hoffmann, C.; Renger, M., 1996. Ursachen mangelnder Anwuchserfolge bei der
658 Aufforstung der Rieselfelder in Berlin-Buch. *Verhandlungen der Gesellschaft für Ökologie*, 25:
659 349-359.
- 660 Steenhuis, T.S. et al., 2001. Water Repellency in New York State Soils.
- 661 Täumer, K., Stoffregen, H. and Wessolek, G., 2005. Determination of repellency distribution using
662 soil organic matter and water content. *Geoderma*, 125(1-2): 107-115.
- 663 Terashima, M., Fukushima, M. and Tanaka, S., 2004. Influence of pH on the surface activity of humic
664 acid. Micelle-like aggregate formation and interfacial adsorption. *Colloids and Surfaces, A:
665 Physicochemical and Engineering Aspects*, 247(1-3): 77-83.
- 666 Tschapek, M., 1984. Criteria for determining the hydrophilicity - hydrophobicity of soils. *Zeitschrift
667 für Pflanzenernährung und Bodenkunde*, 147(2): 137-149.
- 668 Valat, B., Jouany, C. and Rivièrè, L.M., 1991. Characterization of the wetting properties of air-dried
669 peats and composts. *Soil Science*, 152: 100-107.
- 670 van't Woudt, B.D., 1959. Particle coatings affecting the wettability of soils. *Journal of Geophysical
671 Research*, 64: 263-267.
- 672 Wallis, M.G. and Horne, D.J., 1992. Soil water repellency. *Advances in Soil Science*, 20: 91-146.
- 673
- 674

686
687
688
689
690
691
692
693
694
695
696
697
698
699
700
701
702
703
704
705
706
707
708
709
710
711
712
713
714
715
716
717
718

Figure Captions

Figure 1: Experimental design of modification of soil-*pH*. **A** Exposition of soil to gaseous ammonia enriched atmosphere. **B** Exposition of soil to HCl enriched atmosphere.

Figure 2: **A** *pH*, **B** electrical conductivity (*EC*), **C** Soil C/N ratio, and **D** “Mehlich”-extractable iron measured in wettable and repellent soil samples from Tiergarten (TW, TR) and from Buch (BW, BR, respectively) from a study of seasonally sampling between spring 2002 and spring 2004.

Figure 3: Artificially induced soil-*pH* as a function of the added volume of HCl- and NH₃-enriched air for **D** samples from Germany, **NL** samples from Netherlands, **UK** samples from the UK, and **AU** samples from Australia.

Figure 4: Water drop penetration time (*WDPT*) as a function of artificially induced *pH* of repellent samples and wettable control samples: **D** from two sites in Germany, **NL** from a profile in the Netherlands, **UK** from two sites in UK, and **AU** from two sites in Australia.

Figure 5: Wettability of the German Tiergarten (TW, TR) and Buch (BW, BR) samples as a function of artificial induced soil *pH*: **A** as contact angle measured by Wilhelmy Plate Method (Θ_{WPM}), **B** as contact angle measured by sessile drop method (Θ_{sess}), and **C** measured as water drop penetration time (*WDPT*). **D** *WDPT* and Θ_{WPM} as a function of the respective Θ_{sess} .

Figure 6: Particle surface charge (*Q*) of soil fraction < 63 μm of selected *pH*-treated sub-samples with highest, lowest and medium artificially induced *pH* from the wettable and repellent Buch samples (BW, BR) and Tiergarten samples (TW, TR, respectively).

Figure 7: Wettability of the German Tiergarten (TW, TR) and Buch (BW, BR) samples as contact angle measured by sessile drop method depicted as a function of particle surface charge (*Q*) of soil fraction < 63 μm . Particle surface charge data are measured at four data points for each sample (indicated by double symbol frame) and linearly interpolated between these four points by their *pH* dependency (Figure 6).

Figures

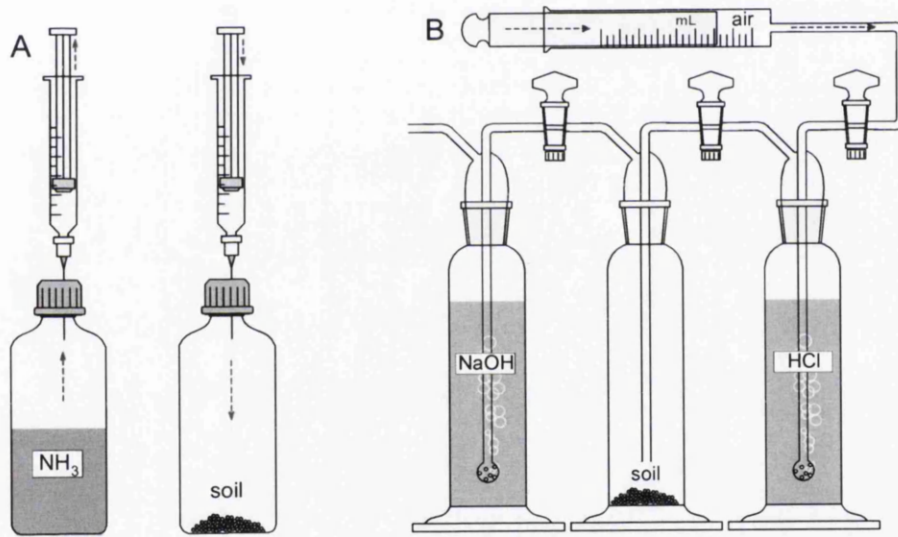


Figure 1

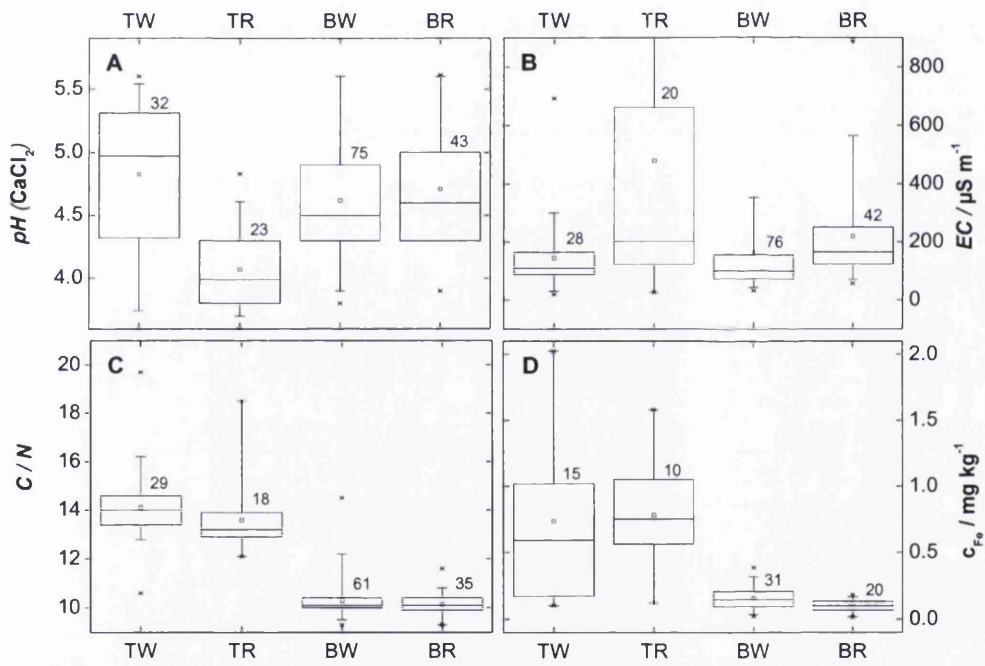


Figure 2

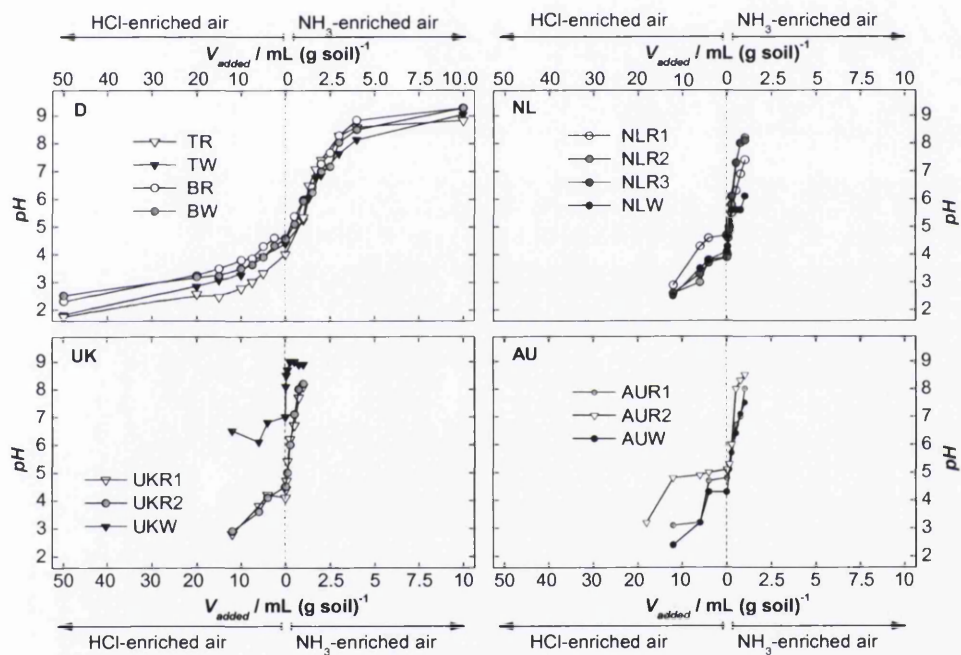


Figure 3

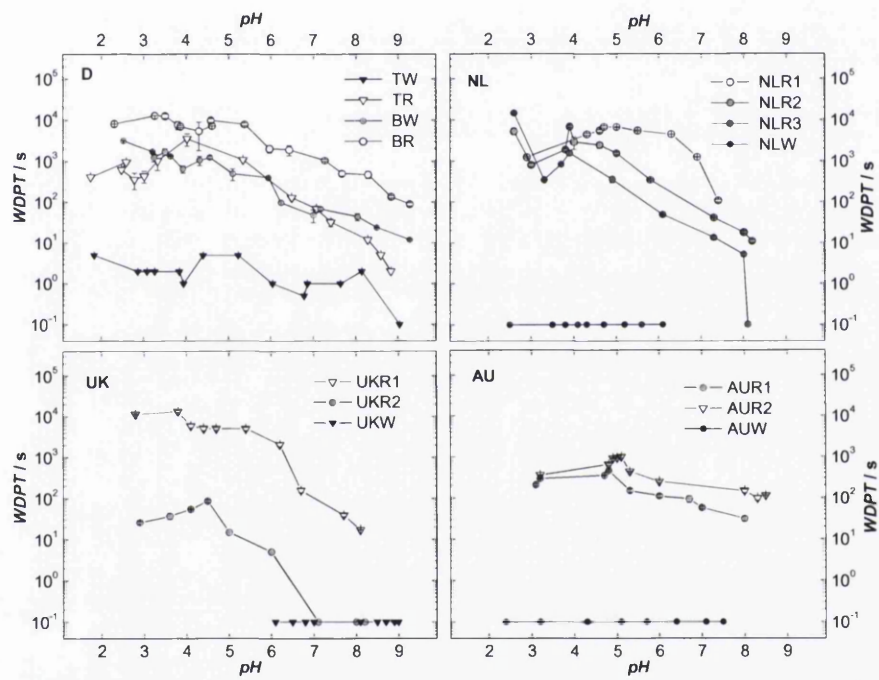


Figure 4

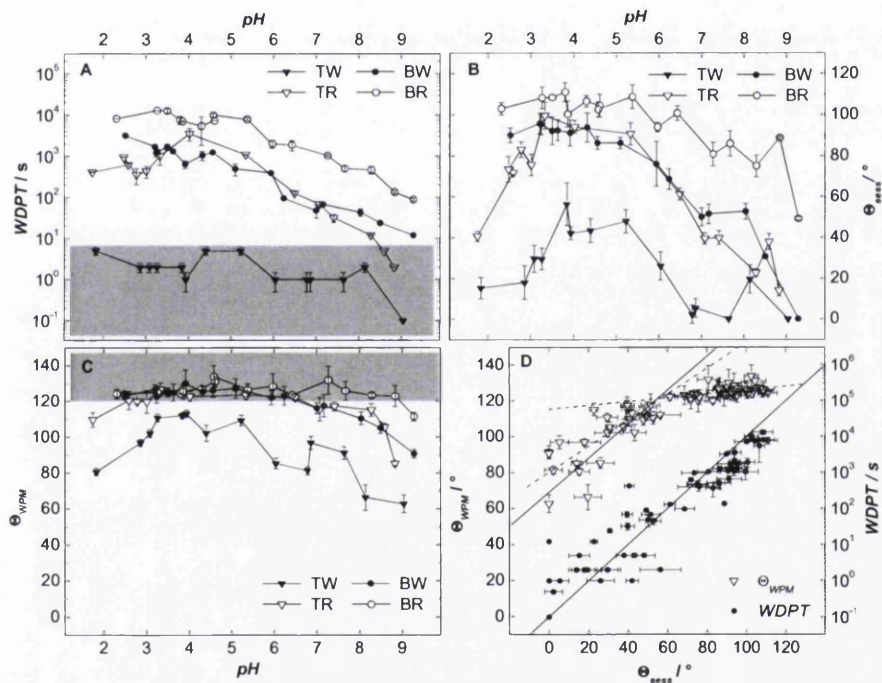


Figure 5

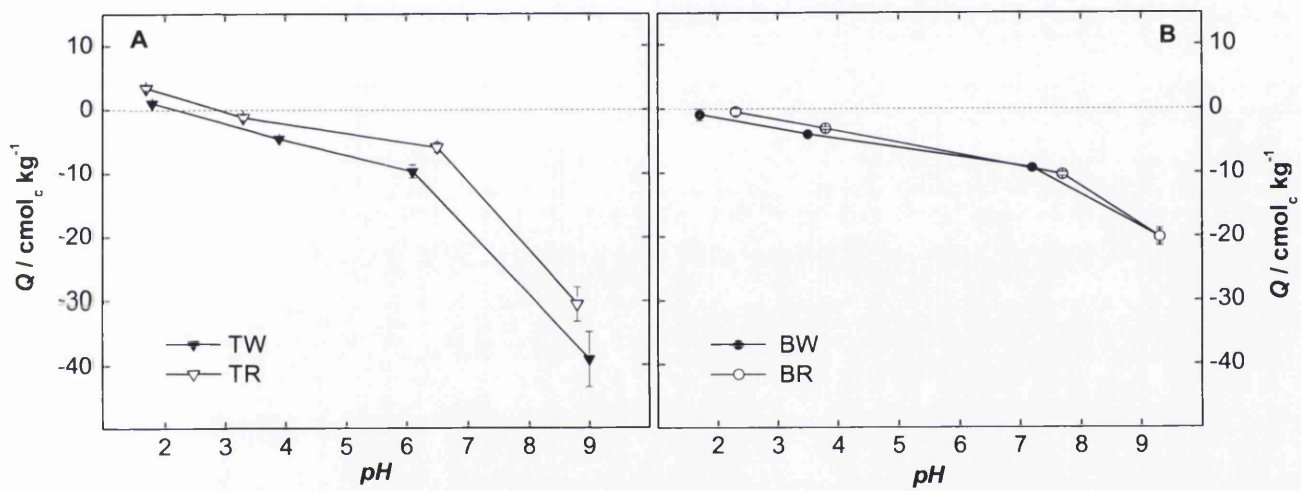


Figure 6

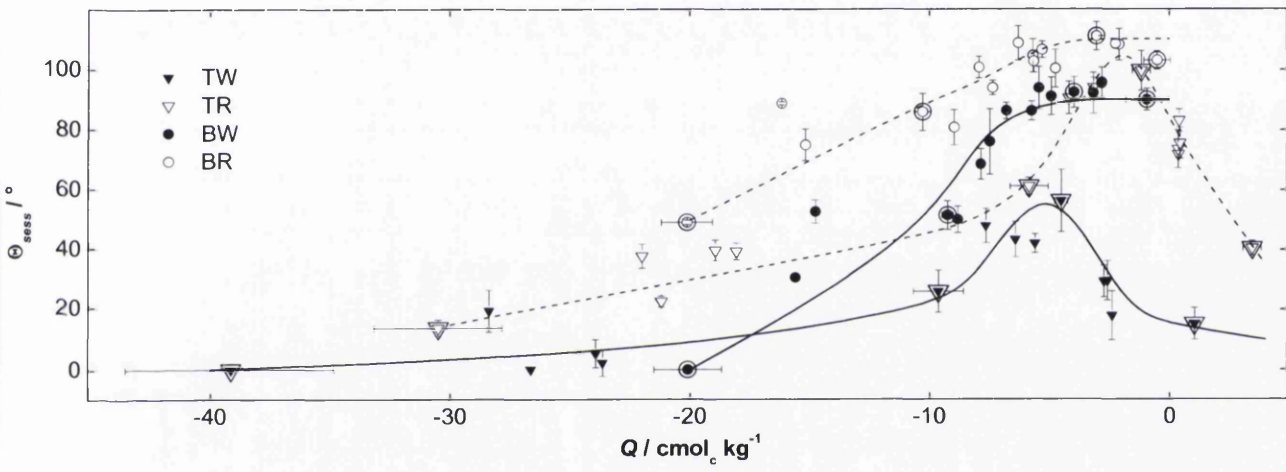


Figure 7

737

Supporting information

738

739

740

741

742

743

744

745

746

747

748

749

Figure 8

750

751

752

753

754

755

756

757

758

759

760

761

762

763

764

765

766

767

768

Table 4

Figure 8 shows a combination of the measured net surface charge values (ΣQ) and a suggestion, how Q_{SOM} and $Q_{mineral}$ may change with pH resulting in a sum of absolute equivalent charge values ($\Sigma\sqrt{Q_i^2}$) which could explain the measured pH dependent wettability. At $pH_{(max\ Repell)}$ the lowest total number of charged sites is reached and at this pH , negatively charged sites dominate in all samples. In Tiergarten samples, below $pH_{(max\ Repell)}$, with the total number of charged sites, wettability increased with increasing Q and decreasing pH (Figure 8 TW, TR). This led to the assumption that in these samples mineral surfaces are probably available, where the positive surface charge increases with decreasing pH , exceeding the negative permanent charge. In contrast, in Buch samples, the lack of changes in wettability in the range of $pH_{(max\ Repell)}$ with < 5 indicates a nearly constant total number of charged sites (Figure 8 BW, BR). The number of protonable mineral surface sites is probably not high enough to increase wettability with decreasing pH .

The parameters of equation 4 and 5 were adapted to create a scenario with minimum $\Sigma\sqrt{Q_i^2}$ at $pH_{(max\ Repell)}$. A ΣQ -curve was laid through the data points of the measured net surface charge of the respective German samples (Figure 8, Table 4). This led to the following hypotheses which need to be tested in further investigations: (i) The wetttable samples have higher Q_{perm} than the repellent samples and (ii) Tiergarten samples have higher $Q_{max, SOM}$ and higher $Q_{max, mineral}$ than Buch samples (Table 4). (iii) The values of pK_{SOM} are with ~ 7 lower for Tiergarten samples than for Buch samples with ~ 8 . Compared to generally postulated pKa values of 3 – 4 for strong acidic carboxylic surface groups, 5 – 6.5 for weak acidic groups and 7 – 8 for phenolic groups (Scheffer and Schachtschabel, 2002), the pK_{SOM} used in the scenario (Table 4) are rather high, which implies high amounts of weaker acidic functional groups and considerable amounts of phenolic groups. The chosen values for $pK_{mineral}$ and the resulting pH_{iep} of $Q_{mineral}$ -curves at pH 4.5 – 5 suggest a higher influence of manganese-(hydr)oxide surface species which reveal a pH_{iep} of 3 – 5, than of silicium-, aluminium- or iron-(hydr)oxide surface species with pH_{iep} of 2 – 3.5, 5 – 9 and 7 – 10, respectively (Scheffer and Schachtschabel, 2002). However, it has to be kept in mind that the parameters in Table 4 are based on only 4 data points of measured surface net charge. Further investigations need to focus on distinguishing between different surface species, e.g. weak and strong acidic carboxylic sites, phenolic sites and the different relevant minerals compounds as clay minerals and sesqui(hydr)oxides and their contribution to the surface charge.

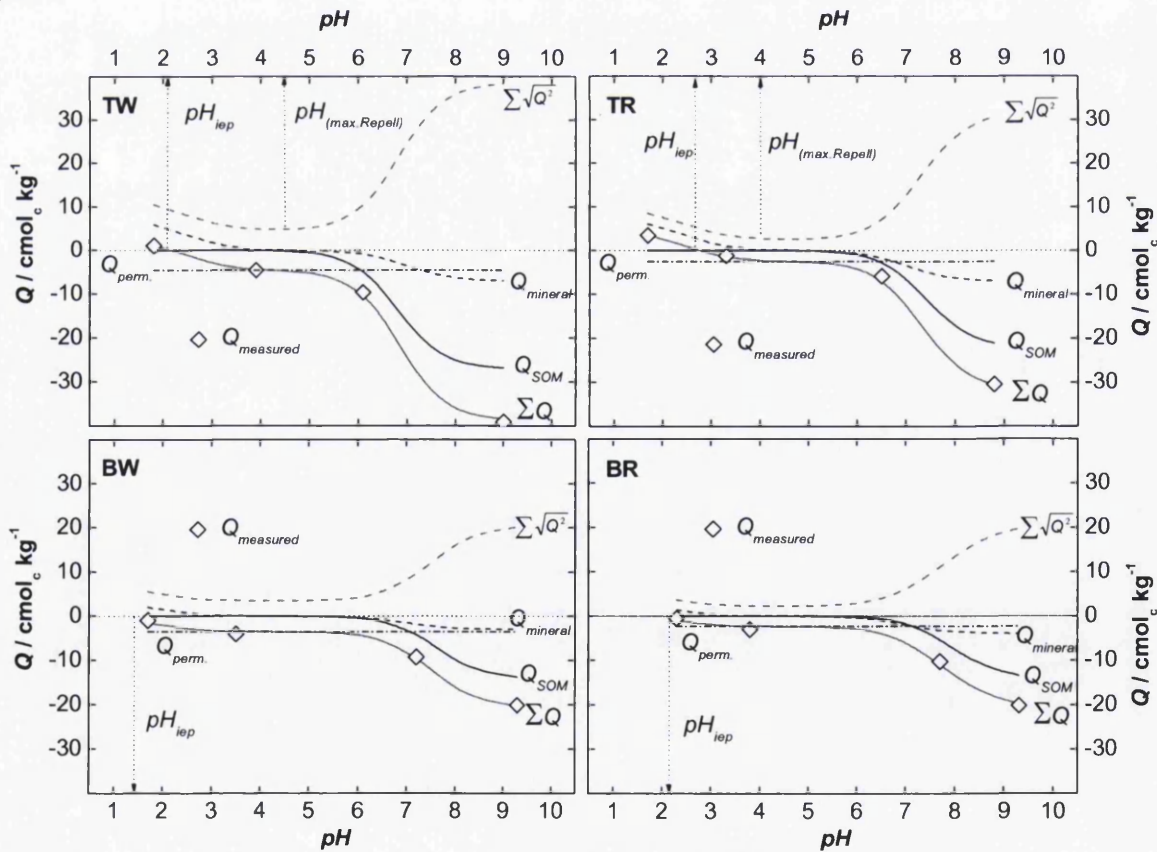
769 Table 4: Parameters chosen in order to create a scenario with minimum $\Sigma\sqrt{Q_i^2}$ at $pH_{(max\ Repell)}$ and a
 770 ΣQ -curve crossing the data points of measured net surface charge of the respective German samples
 771 (Figure 6) using equation 4 and 5: permanent charge ($Q_{perm.}$), maximum negative surface charge
 772 obtainable by deprotonation of SOM ($Q_{max, SOM}$) and the respective deprotonation constant (pK_{SOM}),
 773 maximum negative and positive surface charge obtainable by deprotonation / protonation of mineral
 774 surfaces ($Q_{max, mineral}$) and the respective deprotonation and protonation constants ($pK_{1, mineral} / pK_{2, mineral}$).

	TW	TR	BW	BR
$Q_{perm.}$	-4.6	-2.5	-3.5	-2.3
$Q_{max, SOM}$	-27	-22	-14	-14
pK_{SOM}	6.8	7.4	7.6	7.9
$Q_{max, mineral}$	7	7	3	4
$pK_{1, mineral}$	7	7	7	7
$pK_{2, mineral}$	2.5	2.5	2	2

776
 777
 778
 779
 780
 781
 782
 783
 784

Figure 8: Simplified schematic pH dependent interplay of negative and positive surface charge provided by SOM surfaces (Q_{SOM}), by mineral surfaces ($Q_{mineral}$), and by permanent surface charge ($Q_{perm.}$) using equation 4 and 5 with parameters (Table 4) chosen to create a scenario with minimum $\Sigma\sqrt{Q_i^2}$ at $pH_{(max\ Repell)}$ and a ΣQ -curve crossing the data points of measured net surface charge of the respective German samples.

785 **Figure 8**



786